EXPERIMENTAL STUDY OF SOIL UNDER STATIC AND CYCLIC SHEAR LOADING: A CASE OF AWASH MELKASA TOWN

Tigistu Abu Arficho

A Thesis Submitted to
The department of Civil Engineering
School of Civil Engineering and Architecture

Presented in Partial Fulfillment of the Requirement for the Degree of Master's in Civil Engineering (Specialization in Geotechnical Engineering)

Office of Graduate Studies
Adama Science and Technology University

August, 2021 GC
Adama, Ethiopia

EXPERIMENTAL STUDY OF SOIL UNDER STATIC AND CYCLIC SHEAR LOADING: A CASE OF AWASH MELKASA TOWN

Tigistu Abu Arficho

Advisor: Argaw Asha (Ph.D.)

A Thesis Submitted to
The department of Civil Engineering
School of Civil Engineering and Architecture

Presented in Partial Fulfillment of the Requirement for the Degree of Master's in Civil Engineering (Specialization in Geotechnical Engineering)

Office of Graduate Studies
Adama Science and Technology University

August, 2021 GC
Adama, Ethiopia

APPROVAL SHEET

I, the advisors of the thesis entitled “Experimental Study of Soil Under Static and Cyclic Shear Loading: A Case of Awash Melkasa Town” and developed by Tigistu Abu Arficho, hereby certify that the recommendation and suggestions made by the board of examiners are appropriately incorporated into the final version of the thesis.

Argaw Asha (Ph.D.)	___________________	_________________
Advisor	Signature	Date

We, the undersigned, members of the Board of Examiners of the thesis by Tigistu Abu have read and evaluated the thesis entitled “Experimental Study of Soil Under Static and Cyclic Shear Loading: A Case of Awash Melkasa Town” and examined the candidate during open defense. This is, therefore, to certify that the thesis is accepted for partial fulfillment of the requirement of the degree of Master of Science in Geotechnical Engineering.

Meseret Getnet (Ph.D.)	___________________	_________________
Chairperson	Signature	Date
Yadeta Chimdesa (Ph.D.)	___________________	_________________
Internal Examiner	Signature	Date
Endalu Tadele (Ph.D.)	___________________	_________________
External Examiner	Signature	Date

Finally, approval and acceptance of the thesis is contingent upon submission of its final copy to the Office of Postgraduate Studies (OPGS) through the Department Graduate Council (DGC) and School Graduate Committee (SGC).

Kefale Fufa (M.Sc.)	___________________	_________________
Department head	Signature	Date
Mesfin Benti (Ph.D.)	___________________	_________________
School Dean	Signature	Date
Legesse Lemecha (Ph.D.)	___________________	_________________
Postgraduate Dean	Signature	Date

DECLARATION

I, hereby declare that this Master Thesis entitled "Experimental Study of Soil Under Static and Cyclic Shear Loading: A Case of Awash Melkasa Town" is my original work. That is, it has not been submitted for the award of any academic degree, diploma or certificate in any other university. All sources of materials that are used for this thesis have been duly acknowledged through citation.

Tigistu Abu Arficho	____________	____________
Name of student	Signature	Date

RECOMMENDATION

I, the advisor of this thesis, hereby certify that I have read the revised version of the thesis entitled "Experimental Study of Soil Under Static and Cyclic Shear Loading: A Case of Awash Melkasa Town" prepared under my/our guidance by Tigistu Abu Arficho, submitted in partial fulfillment of the requirements for the degree of Mater's of Science in Geotechnical Engineering. Therefore, I recommend the submission of revised version of the thesis to the department following the applicable procedures.

Argaw Asha (Ph.D.)	___________________	_________________
Advisor	Signature	Date

ACKNOWLEDGEMENT

First and for most, I would like to thank my advisor, Dr. Argaw Asha for encouraging me during the progress of this research and for his unlimited support through supervision and guidance to carry out the research. And I gratefully acknowledge Adama Science and Technology University for providing the scholarship opportunity.

I gratefully acknowledge to Awash Melkasa municipality office for their help during sample collection.

I would like to thank Dr. Tezera Firew for his permission to conduct a cyclic simple shear laboratory test in AAiT and all ASTU and AAiT geotechnical laboratory staff for their enormous help and for making the work environment amiable.

Finally, I am deeply grateful to my parents for their faith, support, sacrifice and motivation throughout this paper.

CONTENTS

LIST OF TABLES

LIST OF FIGURES AND ILLUSTRATIONS

LIST OF ACRONYMS AND ABBREVIATIONS

A: Area of soil sample

AAIT: Addis Ababa Institute of Technology

AASHTO: American Association of State Highway and Transportation Officials

ASTM: American Society of Testing and Materials

C: Clay

CH: Highly plastic clay

CL: Lean clay

CPT: Cone Penetration Test

CSST: Cyclic Simple Shear Test

D: Diameter of soil sample

DMT: Dilatometer test

E: Easting

H: Height of sample

HEP: Hydro Electric Power

G: Gravel

GC: Clayey Gravel

GM: Silty Gravel

GP: Poorly graded gravel

GW: Well graded gravel

L: Length of ellipse

LI: Liquidity Index

LL: Liquid Limit

LVDT: Linear Variable Differential Transformer

M: Silt

MASW: Multi Channel Analysis of Surface Waves

MDD: Maximum Dry Density

MER: Main Ethiopian Rift

MH: Highly plastic silt

ML: Lean silt

N: Northing

O: Organic soil

OCR: Over Consolidation Ratio

OMC: Optimum Moisture Content

P: Primary school

PI: Plasticity Index

PL: Plastic Limit

PMT: Pressure Meter Test

S: Sand

SASW: Spectral Analysis Surface Waves

SC: Sandy Clay

SM: Silty Sand

SP: Poorly graded sand

SW: Well graded sand

SL: Shrinkage Limit

SPT: Standard Penetration Test

TP: Test Pit

USCS: Unified Soil Classification System

W: Well graded

A_{loop}: Area of the stress - strain loop

A_{Δ}: Area of triangle

B: Width of ellipse

C_c: Coefficient of curvature

C_u: Coefficient of uniformity

D_r: Relative density

e: Void ratio

Eq.: Equation

F: Shear force

f: Frequency of cyclic loading

G: Shear modulus

G_{max}: Maximum shear modulus

G/G_{max}: Normalized shear modulus

G_s: Specific gravity

G_{sec}: Secant shear modulus

H_z: Hertz

K:	Dimensionless quantity which is a function of PI
K_0:	Coefficient of lateral earth pressure at rest
M_a:	Mass of glass field with water
M_b:	Mass of glass with soil and water
M_o:	Mass of dry soil
N_c:	Number of cycle
No:	Number
P_c:	Pre-consolidation pressure
P_0:	Present effective vertical pressure
V_s:	Shear wave velocity
W:	Maximum strain energy
ΔW:	Dissipated energy
ρ:	Density of soil
ρ_b:	Bulk density of soil
ρ_d:	Dry density of soil
ρ_w:	Density of water
σ'_o:	Effective confining stress
$\sigma_v{}'$:	Effective vertical stress
τ:	Cyclic shear stress
τ_{max}:	Maximum cyclic shear stress
τ_{min}:	Minimum cyclic shear stress
γ:	Cyclic shear strain
γ_{max}:	Maximum cyclic shear strain
γ_{min}:	Minimum cyclic shear strain
ξ:	Damping ratio

ABSTRACT

The dynamic properties of the soil are widely studied parameters for the analysis and design of geotechnical structures subjected to dynamic loads (such as machine vibration, earthquakes, vehicle traffic, pilings, blasting and nuclear explosions). These loads can cause problems in the geotechnical structure. When structures were subjected to these loads they could stand large strain levels. For all geotechnical problems, the dynamic properties of the soil must be determined, especially in earthquake-prone areas. Awash Merkasa is located in the Great Rift Valley of East Africa. The area is prone to seismic activity and is classified as a magnitude four seismic zone. For earthquake-prone areas; it is important to determine the dynamic characteristics of the soil.

In this study, an attempt was done to determine the dynamic properties of soils found at Awash Melkasa town. The soil samples were collected from Awash Melkasa town at three different locations, namely; Primary School, High School, and Mesino. Some index soil laboratory tests were carried out on the collected samples, and based on the result they were classified according to USCS and AASHTO. The soil from P @ 1.75 m, M @ 2 m and M @ 3 m were classified as elastic silt soil (MH, A-7-5), P @ 3 m was classified as lean clay soil (CL, A-7-6), H @ 1.5 m was classified as lean silt soil (ML, A-5), and H @ 3 m was classified as (none plastic silt soil, A-5). The elastic silt soils dominate the area, having the liquid limit value ranging from 58.73 % to 63.3 % and plasticity index value of 12.77 % to 30.36 %. The specific gravity value ranges from 2.35 to 2.53. The shear modulus and damping ratio values were determined using cyclic simple shear machine. The tests were conducted as a function of cyclic strain amplitude of 0.01 %, 0.1 %, 1 %, 2.5 % and 5 % under axial stress of 150 kPa, 275 kPa and 400 kPa. The value of shear modules was in the ranges of 0.292 MPa to 15.998 MPa and damping ratio values from 0.146% to 30.851%. The normalized shear modulus values of Awash Melkasa soils have good agreement with curve of sand developed by Seed and Idriss. The shear modulus reduction values at high strain values (≥1%) also agree with the curve of saturated clay of Seed and Idriss (1970) and Vucetic and Dobry (1991). But, the damping ratio values of the studied soils are generally lower than the curves developed for saturated clay by Seed and Indriss (1970) and for different PI values by Vucetic and Dobry (1991).

The major influencing factors that affect the dynamic properties of soils are confining pressure, shear strain amplitude and soil plasticity. The method of sample preparation and testing condition also have significant effect on the damping ratio values. To note the effects of method of sample preparation, frequency of cyclic loading, degree of compaction, degree of saturation and particle size; the test needs to be conducted by considering this factors. In order to obtain complete information about the dynamic properties of the soil, it is recommended to conduct both field and laboratory test methods. Further consideration of strain rate other than the strain rate considered in this study are recommended

Key words: *Dynamic properties, Shear modulus, Damping ratio, Normalized shear modulus and Cyclic simple shear test* (*CSST)*

CHAPTER ONE

INTRODUCTION

1.1. Background of the Study

Soil is one of the most valuable resource which is found naturally. It is formed due to the disintegration of rock by chemical and/or physical weathering. The conditions that play important role in the formation of soil are topographic characteristics, geological conditions, and climatic conditions. In general soil is considered as a three-phase system (air, water, and solid) initiating substantial alterations in the system characteristics due to collaboration of these phases under applied static and/or dynamic load (Kumar et al., 2013).

The dynamic characteristics of the soil are the key parameters for the seismic design and performance of the geotechnical system. An accurate estimation of the dynamic properties of soil is essential for the correct assessment of the soil's response to dynamic loads such as earthquakes, explosions, road and rail traffic, wind, pile-driving, blasting and waves (Majid, 2017). These loads differ depending on frequency, amplitude, loading rate, the repetition or number of cycles, the state of stress, stress history, strain levels, void ratio, confining stress, water content, and drainage condition, which causes reduction and increases on the stiffness of the material and damping (Wilson, 2016).

The dynamic properties of soils help to forecast and/or analyze the dynamic behavior. The properties namely modulus reduction and material damping with strain levels, shear wave velocity, and liquefaction susceptible parameters are the key input parameters for numerous dynamic studies and investigations. The determination of dynamic soil properties is an ultimate critical and vital aspect of geotechnical earthquake engineering problems (Kumar et al., 2013).

There are different laboratory and field test methods that can be used to determine the dynamic properties of the soil, but each technique has its own problems and limitations. Laboratory testing usually provides the most direct method of evaluating dynamic soil parameters in seismic analysis. Depending on the amplitude of applied lateral dynamic load exerted, laboratory dynamic soil properties tests are divided into two groups, they are small and large strain ranges. Some laboratory tests that can be used to measure the dynamic characteristics of the soil under different levels of strain include: - resonant Column test, ultrasonic pulse test and the piezoelectric bender element test, cyclic simple shear test, cyclic triaxial test and cyclic torsional test are the commonly employed techniques (Jia, 2018).

The purpose of this study is to determine the dynamic characteristic parameters of the soil using a cyclic simple shear test machine. The cyclic simple shear test is one of the laboratory methods used to obtain dynamic parameters of soils. It is possible to measure stiffness and damping characteristics over a wide range of strain levels by imposing cyclic shear stress on horizontal planes.

1.2. Statement of the Problem

Several problems in engineering practice require an understanding of the dynamic properties of soil and liquefaction. Determining the dynamic properties of the soil is a key task, but it is a very important feature in geotechnical earthquake engineering problems. Problems associated to foundations and retaining structures exposed to dynamic loads were divided into either a small strain amplitude or large strain amplitude response. The dynamic loads that caused problems in engineering practices are earthquakes, vehicular traffic, machine vibration, pile-driving, blasting and nuclear explosions. Structures during earthquakes could stand large strain levels. For all geotechnical problems, the dynamic properties of the soil must be determined, especially in earthquake-prone areas. Awash Merkasa is located in the Great Rift Valley of East Africa. The area is prone to seismic activity and is classified as a magnitude four seismic zone. At this time, the construction of buildings started in Awash Melkasa, so in order to consider the dynamic loading effect of the basic design structure, the dynamic characteristics of the soil must be determined.

1.3. Objectives of the Study

1.3.1. General Objective of the Study

The major objective of this study is to determine the dynamic properties of typical soils found in Awash Melkasa Town.

1.3.2. Specific Objectives of the Study

- ✓ To determine what type of soils are found at Awash Melkasa town
- ✓ To determine the shear modulus and damping ratio of Awash Melkasa soil using a cyclic simple shear test
- ✓ To determine which factor has a significant effect on dynamic properties of soil
- ✓ To determine which type of soil is highly resistant to dynamic load

1.4. Research Questions

At the end of this study, the research will answer the following questions: -

- ✓ What types of soils are found in Awash Melkasa town?
- ✓ What is the shear modulus and damping ratio of the soil?
- ✓ What are the major factors that affect the dynamic properties of soil?
- ✓ Which type of Awash Melkasa soil is highly resistance to dynamic load?

1.5. Significance of the Study

This study will have a valuable significance to provide dynamic soil information for dynamic loading considered foundation designs in Awash Melkasa Town. The outcome of this study will help in a better understanding of the major factors that influencing the dynamic properties of soil. Furthermore, the study can be used as an input for other researchers or institutions as literature.

1.6. Scope of the Study

The study considered quantitative experimental studies and determined the static and dynamic characteristics of soil samples collected from Awash Melkasa town. Soil samples were taken from three different test pits. Generally, the experiment includes tests performed in the field as in-situ density and natural moisture content. The in-situ tests were performed to determine field density and the natural moisture content of the soil. In the laboratory; grain size analysis and consistency tests are conducted for classification purposes. The specific gravity, compaction, 1D - consolidation, and cyclic simple shear tests are conducted to determine the dynamic characteristics of the soil.

1.7. Limitation of the Study

The study is limited to the investigation of some dynamic properties (shear modulus and damping ratio) of soils that were collected from Awash Melkasa Town. The method used in the determination of these parameters is limited to the cyclic simple shear test. The collected samples may not fully represent all the soil profiles in Awash Melkasa Town. Due to the budget constraint, the soil samples collected only from three test pits and the depth of investigation also limited to the maximum depth of three-meter.

1.8. Organization of the Study

This research is organized into five chapters and appendixes. The first chapter gives a brief description of the thesis background, statement of the problem, objectives, research questions, significance of the study, and scope and limitation of the study. The literature review is mainly presented in the second chapter which includes the dynamic properties of soils, method of determining shear modulus and damping characteristics and factors that affect dynamic properties of soils. Chapter three discusses the study area, sample collection, sample preparation, overview of cyclic simple shear apparatus, and experimental program. Chapter four explains the results obtained from the field and laboratory test and discussion on test results and some comparison with the previous study is presented. Chapter five presents the conclusions and recommendations of the study.

CHAPTER TWO

LITERATURE REVIEW

2.1. Introduction

The sophisticated behavior of soils under various types of dynamic loading conditions have been discovered by many researchers. Destruction due to dynamic loadings is affected by the response of soil deposits and the soil response is governed by the soil dynamic properties (Hailemariam, 2017). The mechanical properties of the soil are strongly control the responses of soils subject to dynamic and cyclic loadings. This properties of soils are shear modulus, damping, Poisson's ratio, and density (mass). From these properties, shear modulus and damping are the most important properties of the material, and uses them to characterize the dynamic behavior of the soil. The dynamic properties values of soils; shear modulus and damping ratio are affected by a number of parameters with varying level of importance. These parameters can be divided in to two groups, namely factors related to loading condition (amplitude of cyclic loading, mean effective stress, long term time effect, number of loading cycles, loading frequency, overconsolidation ratio and location of ground water) and factors regarding physical properties of soil (soil type, grain size, shape of grains or void ratio and plasticity index)(Jia, 2018).

In this chapter, some dynamic properties of the soil are reviewed. Shear modulus and damping ratio are the most important dynamic characteristics of the soil, which are used to illustrate the dynamic characteristics of the soil. The methods and factors that influence the dynamic characteristics of the soil are summarized.

2.2. Dynamic Properties Soil

The dynamic properties of the soil control the response of soils subjected to dynamic loads. To determine the dynamic characteristics of the soil, it is necessary to analyze the response of the soil obtained under the application of different loads. When the soil exposed to cyclical loads shows a hysteresis response. The hysteresis loop obtained from the cyclic loading of a given soil can be defined by the path of the loop itself or by two parameters. These paths or parameters describe the general shape of the loop. These parameters are the slope and width of the hysteresis loop, damping ratio and shear modulus. For different strain amplitudes of cyclic load values, loops of different sizes will be produced (Kebede, 2019).

2.2.1. Shear Modulus

The shear modulus of a dynamic load is a significant kinetic parameter of soil. It also an important pointer of the dynamic characteristics of soils. It is an essential parameter for in-situ seismic response analysis calculations. The shear modulus of a dynamic load designate the deformation characteristics of soil subjected to dynamic loading (Qiao et al., 2020). The dynamic shear modulus G is defined as the slope of the line connecting two peak points on the hysteresis loop at a certain shear strain (Figure 2.1). Moreover, G can be defined as the ratio of cyclic shear stress (τ) to the corresponding cyclic strain (γ), it can be calculated by using Eq. (2.1) (Wilson, 2016).

$$G = \frac{\tau}{\gamma} \quad \text{(2.1)}$$

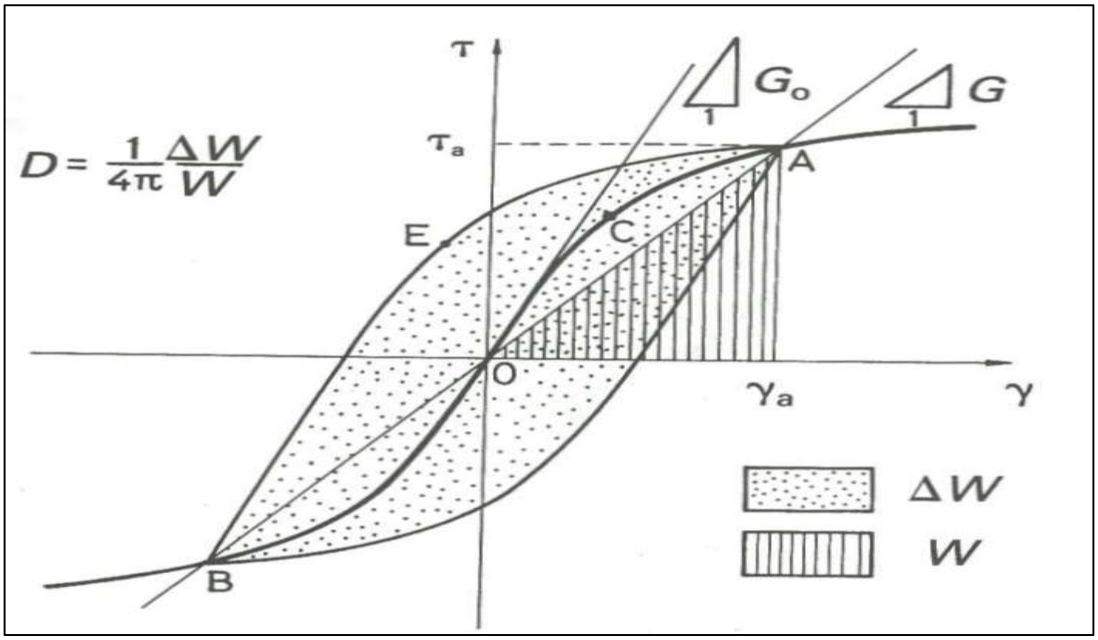

Figure 2.1: Hysteretic loop for one cycle of loading showing G_0 or G_{max}, G, and D or ξ (Kumar et al., 2013)

When the cyclic strain amplitude increases, the secant shear modulus will decrease. For different cyclic loading strain amplitude, different sizes of loops will be developed. The curve obtained by joining the locus of the points corresponding to the tips of these loops is called the skeleton (backbone) curve (Figure. 2.2 a). The modulus reduction curve (Figure. 2.2 b) shows the variation of shear modulus with cyclic strains. This curve represents shear modulus degradation with cyclic strain. The modulus ratio is the normalization of shear modulus (G) to the maximum shear modulus (G_{max}) and it is obtained from the modulus reduction curve (Kumar et al., 2013).

In an equivalent linear model, the modulus ratio G_{sec}/G_{max} often written as G/G_{max}, is commonly accepted to describe the secant shear stiffness degradation of soils. The reduction of secant shear stiffness causes a modulus reduction (also called normalized shear modulus) curve, which gives the similar information as the backbone curve. Additionally, they can be determined from each other. The model of the shear modulus reduction curve for course grained and fine grained soils are usually modeled independently. However, the gradual transition of the modulus reduction curve between plastic fine-grained soils and non-plastic coarse-grained soil cannot be reflected by the backbone curve (Jia, 2018).

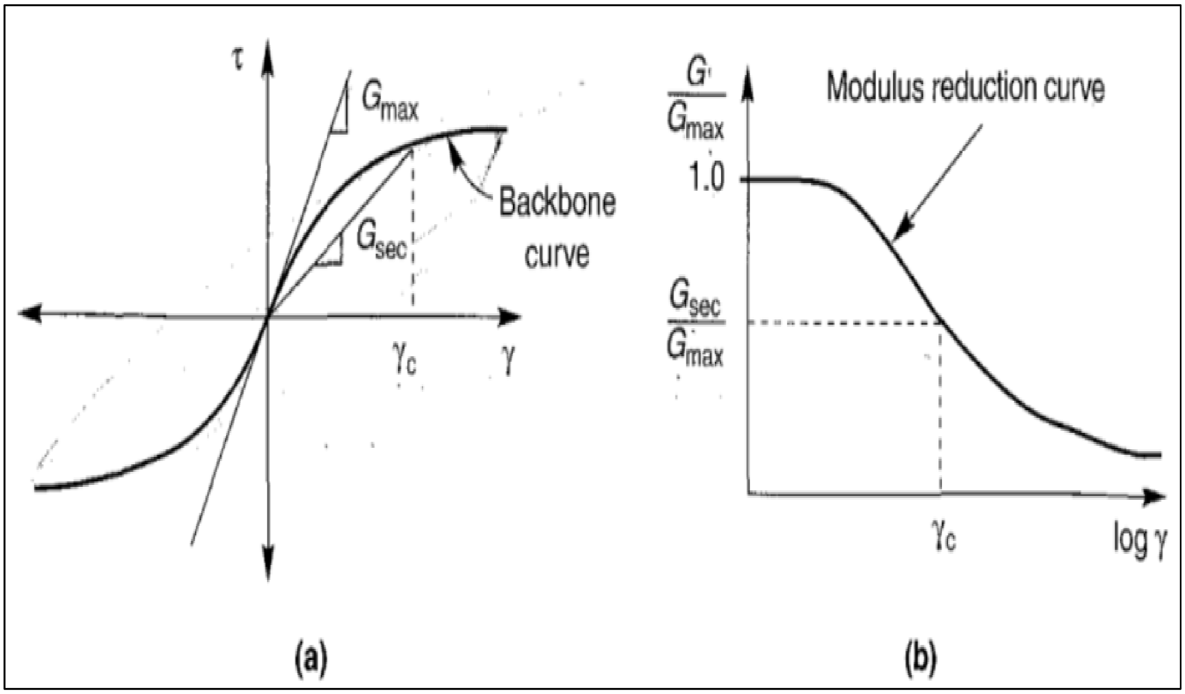

Figure 2.2: (a) Stress-strain curve with variation of shear modulus (b) Modulus reduction curve (Kumar et al., 2013)

2.2.2. Damping Ratio

The dynamic damping ratio is a significant kinetic parameter of soil. It is also an important pointer of the dynamic characteristics of soils. It is an essential parameter for in-situ seismic response analysis calculations. The dynamic damping ratio designates the deformation characteristics of soil subjected to dynamic loading. It increases with increasing shear strain (Feng Qiao e. , 2020).

The dissipated energy due to frictional relative displacements in dynamic problems represents the damping ratio value. The hysteretic damping ratio is calculated from the peak strain energy during one loading cycle and the energy dissipated in the soil sample during this cycle. We can measure the dissipated energy by determining the area of the hysteresis loop, ΔW. Whereas the maximum strain energy is measured by calculating the area under the secant shear modulus line from zero to ultimate strain value, W (Figure 2.1) (Wilson, 2016). Thus, the hysteretic damping ratio, ξ can be obtained by: -

$$\xi = \frac{1}{4\pi}\frac{\Delta W}{W} \qquad (2.2)$$

where: ΔW = dissipated energy

W = maximum strain energy

The shape of the ellipse and that of hysteresis loop is nearly same so we can approximate the area of the hysteresis loop to the area of ellipse. The area of the ellipse (ΔW) can be determined from Eq. (2.3) (Wilson, 2016).

$$\Delta W = \frac{\pi}{4} LB \qquad (2.3)$$

Where: L: Length of ellipse

B: Width of ellipse

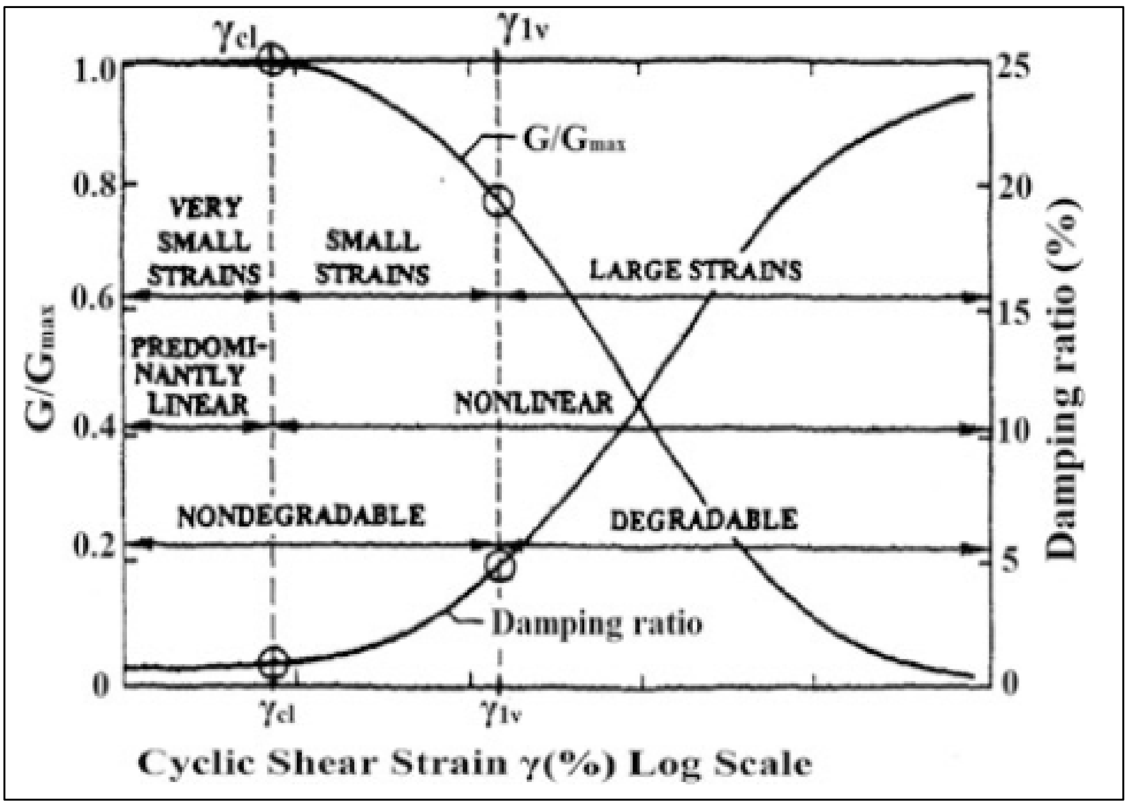

Figure 2.3: Curves of secant modulus reduction (expressed in normalized terms) and damping (expressed in absolute terms) varied with the cyclic shear strain (Jia, 2018)

2.3. Methods of Determining Shear Modulus and Damping Characteristics

Determining the response of the soil under dynamic loads is essential, but requires an accurate estimate of the dynamic shear modulus and damping ratio (Ghayoomi et al., 2017). To determine shear modulus and damping characteristics of soils we can use different procedures, including laboratory and field tests (Das, 2011). The choice of testing techniques, to measure the dynamic soil properties needs careful attention and understanding of the specific problem at hand (Camelo, 2017). The main procedures can be summarized as follows:

2.3.1. Direct Determination of Stress- Strain Relationships

The stress-strain relationship of the hysteresis loop is shown in Figure 2.1. It can be determined in the laboratory by using different cyclical tests; such as cyclic simple shear test, cyclic triaxial compression test or cyclic torsional shear test. The shear modulus and damping factors under moderate to relatively high strains ($0.01 < \gamma < 5$ %) can be measured by using this procedure (H. Bolton Seed I. M. Idriss, 1970).

2.3.2. Forced Vibration Tests

This tests are used to determine both shear modules and damping factors by determining the resonant frequencies and also used for measurement of response with different frequencies. In the laboratory; this test conditions have included the application of torsional vibrations and longitudinal vibrations to cylindrical samples or shear vibrations to layers of soil placed on a shaking table. But in the field, shear vibrations of dams have been induced by large shaking machines; it is difficult to interpret the results of field tests to determine damping factors. In general these procedures are suitable to determine properties at relatively low to moderate strain levels ($10^{-4} < \gamma < 10^{-2}$ %) (H. Bolton Seed I. M. Idriss, 1970).

2.3.3. Free Vibration Tests

Free vibration tests, in which the shear modulus and damping ratio value of a soil is measured from the decay in response of a soil deposit or soil sample. The methods of excitation we apply for this test is same as that of forced vibration tests, but we apply this procedures when we want to determine the characteristics of soil at relatively low to moderately high strain levels ($10^{-3} < \gamma < 1$ %) (H. Bolton Seed I. M. Idriss, 1970).

2.3.4. Field Measurement of Wave Velocities

The velocity propagation of shear waves, compression waves, and Rayleigh waves can be measured at field using different field tests. This tests are used to determine the low strain ($\gamma \leq 10^{-4}$ %) modulus value of soil at field, but can't provide damping ratio value (H. Bolton Seed I. M. Idriss, 1970). A summary of those test conditions, range of applicability, and the parameters obtained are given in Table 2.1.

The procedure we utilized in this study is a direct determination of hysteretic stress-strain relationships. It determines the dynamic properties (shear modulus and damping ratio) of soil under moderate to relatively high strains (0.01 < γ < 5 %). These properties were determined in the laboratory by cyclic simple shear test. The methods used for investigation of dynamic soil properties are shown in the Table 2.2.

Table 2.1: Test procedures for measuring modules and damping characteristics (Das, 2011)

General procedure	Test condition	Approximate strain range	Properties determined
Determination of hysteretic stress - strain relationships	Triaxial compression	10^{-2} to 5%	Modulus; damping
	Simple shear	10^{-2} to 5%	Modulus; damping
	Torsional shear	10^{-2} to 5%	Modulus; damping
Forced vibration tests	Longitudinal vibrations	10^{-4} *to* 10^{-2} %	Modulus; damping
	Torsional vibrations	10^{-4} *to* 10^{-2} %	Modulus; damping
	Shear vibrations - lab	10^{-4} *to* 10^{-2} %	Modulus; damping
	Shear vibrations - field	10^{-4} *to* 10^{-2} %	Modulus
Free vibration tests	Longitudinal vibrations	10^{-3} *to* 1%	Modulus; damping
	Torsional vibrations	10^{-3} *to* 1%	Modulus; damping
	Shear vibrations - lab	10^{-3} *to* 1%	Modulus; damping
	Shear vibrations - field	10^{-3} *to* 1%	Modulus
Field wave velocity Measurements	Comparison waves	$\approx 5 \times 10^{-4}$%	Modulus
	Shear waves	$\approx 5 \times 10^{-4}$%	Modulus
	Rayleigh waves	$\approx 5 \times 10^{-4}$%	Modulus

Table 2.2: Field and laboratory tests employed for dynamic investigation of soil (Kumar et al., 2013)

Field tests		Laboratory tests	
Low strain (< 0.001 %)	High strain (> 0.01 %)	Low strain (< 0.001 %)	High strain (> 0.01 %)
✓ Seismic reflection ✓ Seismic refraction ✓ Steady-state vibration ✓ Spectral analysis of surface waves (SASW) ✓ Multi-channel analysis of surface waves(MASW) ✓ Seismic borehole survey (cross-hole, down-hole and up-hole) ✓ Seismic cone test	✓ Standard penetration test (SPT) ✓ Cone penetration test (CPT) ✓ Dilatometer test(DMT) ✓ Pressuremeter test (PMT)	✓ Resonant column test ✓ Ultrasonic test ✓ Piezoelectric bender element test	✓ Cyclic triaxial test ✓ Cyclic simple shear test ✓ Cyclic torsional test

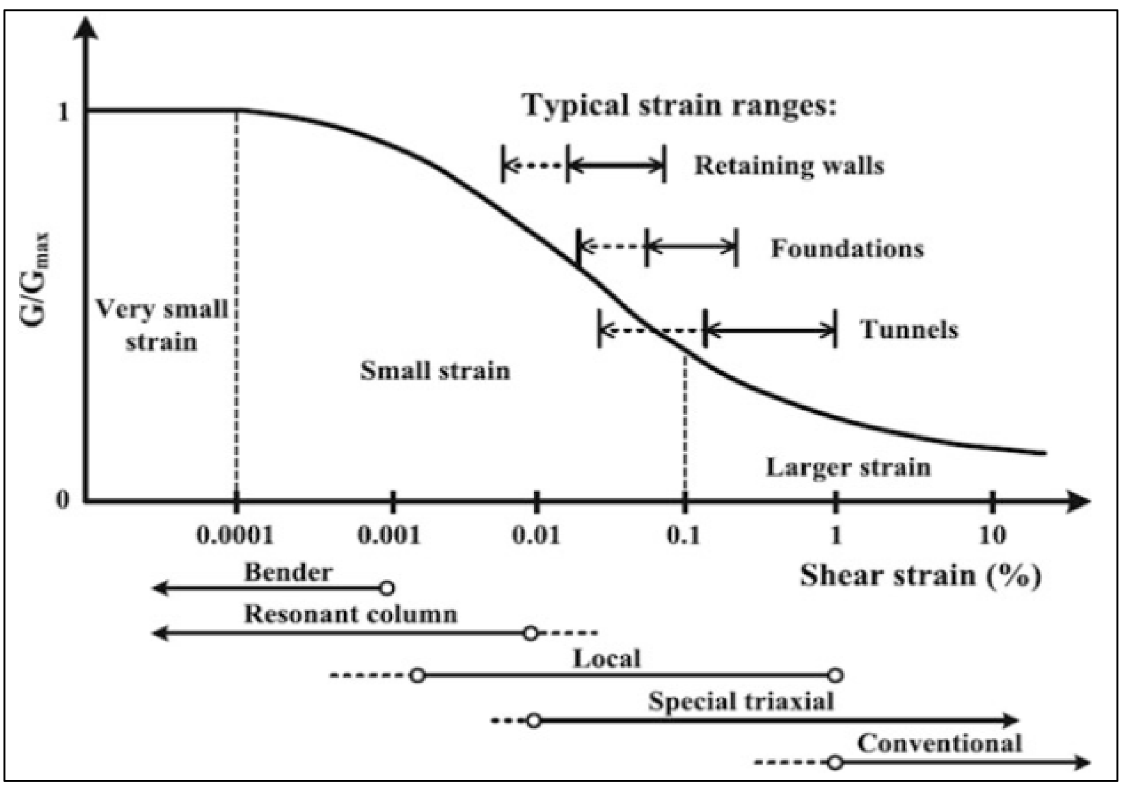

Figure 2 4: Normalized stiffness degradation curve with corresponding geotechnical applications (Jia, 2018)

2.4. Determination of Hysteretic Shear Stress - Shear Strain Relationships

The hysteresis loop is the loop that shows the stress-strain relationship. It is achieved by plotting shear stress against shear strain for values obtained from 50 sample points in a cycle. This loop was used to determine the shear modulus and damping ratio values for each cycle. The equation used to determine shear stress and shear strain is given below: -

$$\text{Shear stress}, \tau = \frac{\text{Lateral force}}{\text{Area of soil sample}} = \frac{F}{A} \quad \text{(2.4)}$$

$$\text{Area of sample}, A = \frac{\pi D^2}{4} \quad \text{(2.5)}$$

$$\text{Shear strain}, \gamma = \frac{\text{Lateral Lvdt}}{H} \quad \text{(2.6)}$$

Where: D is diameter of sample = 70 mm and H = height of sample after consolidation in mm

The equation used in the determination of shear modulus and damping ratios are: -

$$\text{Shear modulus}, (G) = \frac{(\tau_{max} - \tau_{min})}{(\gamma_{max} - \gamma_{min})} \quad \text{(2.7)}$$

$$\text{Damping ratio}, \xi = \frac{1}{4\pi}\frac{\Delta W}{W} = \frac{1}{4\pi}\frac{\text{Area of the hysteresis loop}}{\text{Area of triangle}} = \frac{A_{loop}}{4\pi A_{\Delta}} \quad \text{(2.8)}$$

$$A_{loop} = \frac{1}{2}\sum_{i=1}^{n}(\tau_i - \tau_{i+1}) * (\gamma_i + \gamma_{i+1}) \quad \text{(2.9)}$$

$$A_{\Delta} = \frac{1}{2} * (L * S) \quad \text{(2.10)}$$

Where: τ_{max} = maximum shear stress

τ_{min} = minimum shear stress

γ_{max} = maximum shear strain

γ_{min} = minimum shear strain

A_{loop} = Area of the hysteresis loop

A_{Δ} = Area of triangle as shown in Figure 2.1 with shaded part

L = length of the shaded part

S = height of the shaded part

2.5. Determination of Initial (Maximum) Shear Modulus (G_{max})

Maximum shear modulus is also known as initial shear modulus; it is one of the most important parameters in seismic response analysis of soil. It represents the elastic behavior of the soil at a very low strain($< 3 * 10^{-4}$ %). When the shear strain is smaller than $3 * 10^{-4}$ %, we can measure the maximum shear modulus G_{max} directly by measuring soils' shear wave velocity v_s:

$$G_{max} = \rho {v_s}^2 \quad (2.11)$$

Where: G_{max} = initial shear modulus of soil (Pa)

ρ = Density of soil (kg/m^3) and

v_s = Shear wave velocity (m/s)

The shear wave velocity of soils is increased with the hardness of the soil. The range of shear wave velocity for loose gravel and sand is from 330 to 1200 m/s and the shear wave velocity for firm gravel or soft rock is increases within the range of 1200 – 2300 m/s. For stiff gravel and hard rock, this value increases to the range 2300 - 6600 m/s. The velocity of sound in air is 330 m/s and in water is around 1500 m/s (Jia, 2018).

Table 2.3: Typical ranges of shear wave velocities for various types of soils (Jia, 2018)

Soil type	Shear wave velocity (m/s)
Dry silt, sand, loose gravel, loam, loose rock, moist fine grained top soil	180 - 750
Compact till, gravel below water table, compact clayed gravel, cemented sand, sandy clay	750 - 2250
Weathered rock, partly decomposed rock, fractured rock	600 - 3000
Sound shale	750 - 3300
Sound sandstone	1500 - 4200
Sound limestone and chalk	1800 - 6000
Sound igneous rock (granite, diabase)	3600 - 6000
Sound metamorphic	3000 - 4800

Generally for particular soil deposit, the most reliable in-situ value of G_{max} can be evaluated by using measured shear wave velocity value. The maximum shear modulus, G_{max} can't be determined using cyclic simple shear test because this test is a high strain test, but we can evaluate it by correlating with other soil properties such as plasticity, effective vertical stress, void ratio and over-consolidation ratio (OCR) (Mengistu, 2015). It is an important parameter for computation of normalized shear modulus. Hardin and Drnevich (Hardin, 2016) developed a special relationship with G_{max} for low strain amplitudes in anisotropic stress states:

$$G_{max} = \frac{3230*(2.97-e)^2}{1+e} * (OCR)^K * (\sigma'_\circ)^{0.5} \quad (2.12)$$

$$\sigma'_\circ = {\sigma_v}' * \frac{(1+2K_0)}{3} \quad (2.13)$$

$$e = \frac{G_s \rho_w}{\rho_d} - 1 \quad (2.14)$$

$$OCR = \frac{P_c}{P_o} \quad (2.15)$$

Where:

G_{max} = Maximum shear modulus (kPa)

e = Void ratio

$\sigma'_{\circ}$= Effective confining stress (kPa)

OCR = Overconsolidation ratio

$\sigma_v{}'$or P_o= Effective vertical stress (kPa)

K = Dimensionless quantity which is a function of PI

K_0 = Coefficient of lateral earth pressure at rest ≈ 0.5

G_s = Specific gravity

ρ_w = Density of water

ρ_d = Dry density of soil

P_c = pre-consolidation pressure

Table 2.4: Over-consolidation ratio exponent K varied with PI (Das, 2011)

Plasticity index, PI(%)	K
0	0
20	0.18
40	0.3
60	0.41
80	0.48
≥ 100	0.5

2.6. Factors Influencing Dynamic Properties of Soil

Soils, compares to many structural materials, are extremely nonlinear even at very low strains. This nonlinearity results stiffness reduction of soil (expressed by shear modulus reduction curve) and increasing in damping ratio with increasing in shear strain amplitude (Feyissa, 2011) which is shown in Figure 2.3.

Various researchers have been studying the effects of test procedures and material properties on the cyclic strength and dynamic properties of different soils. From the study they conclude that these properties are influenced by numerous factors such as techniques of sample preparation during a laboratory (whether intact and reconstituted samples), confining pressure, void ratio, water content, methods of loading, overconsolidation ratio, loading frequency, shearing strain amplitude, number of loading cycles, soil plasticity and percentage of fines (Jia, 2018).

2.6.1. Effect of Sample Preparation

There are different methods of soil sample preparation suggested by several investigators. Some of the methods of soil sample preparation are spooning, moist vibration, air-pluviation, wet-tamping, trimming, and raining technique. From these methods of specimen preparation, the loosest specimens were prepared by air-pluviation technique while the densest were prepared by moist-vibration technique. The effect of sample preparation on shear modulus is significant but not for damping ratios (Kumar et al., 2013).

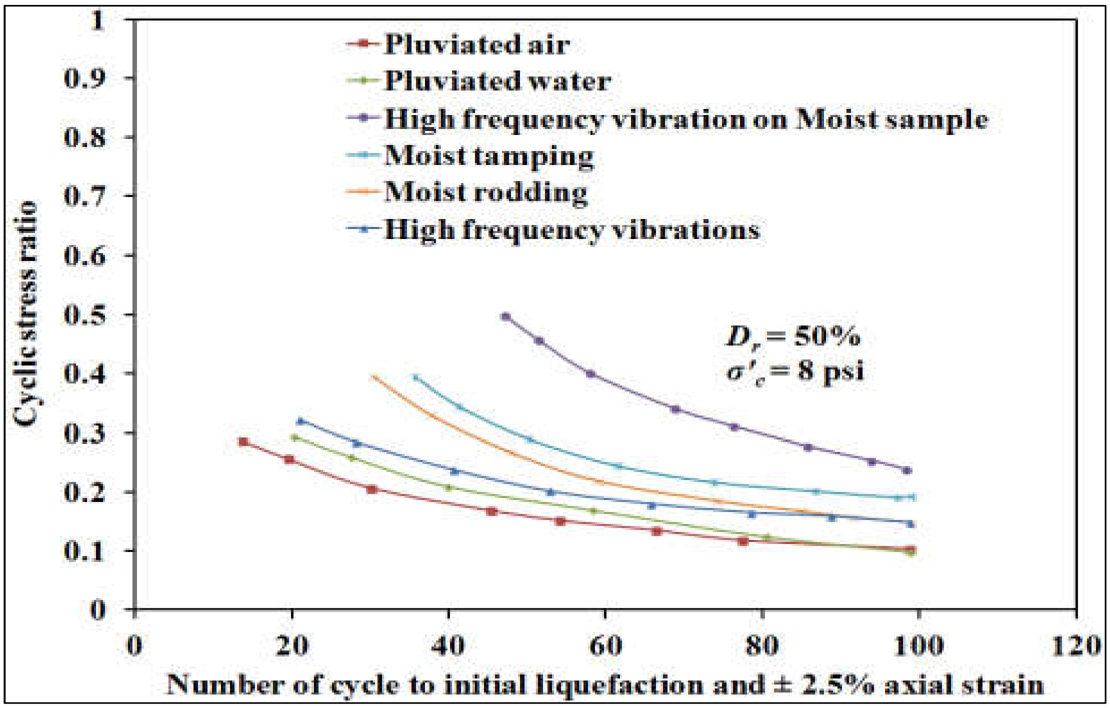

Figure 2.5: Variation of cyclic stress ratio with number of cycles for different compaction procedures (Kumar et al., 2013)

2.6.2. Effect of Confining Pressure

Numerous studies have been made to observe the influence of confining pressure on the dynamic behaviors of soil (Chadi S. El Mohtar, 2014; Feng Qiao a. J., 2020; Jian Li, 2017). The effect of confining pressure on dynamic behaviors is; when we increased the confining pressure, the shear modulus also increased proportionally, but the damping ratio responded oppositely. This is because of the densification/compactness of the soil sample. Compactness of the soil sample causes an increase in the relative density which further results in the increment of the number of cycles required to initiate liquefaction (Lee et al., 2015).

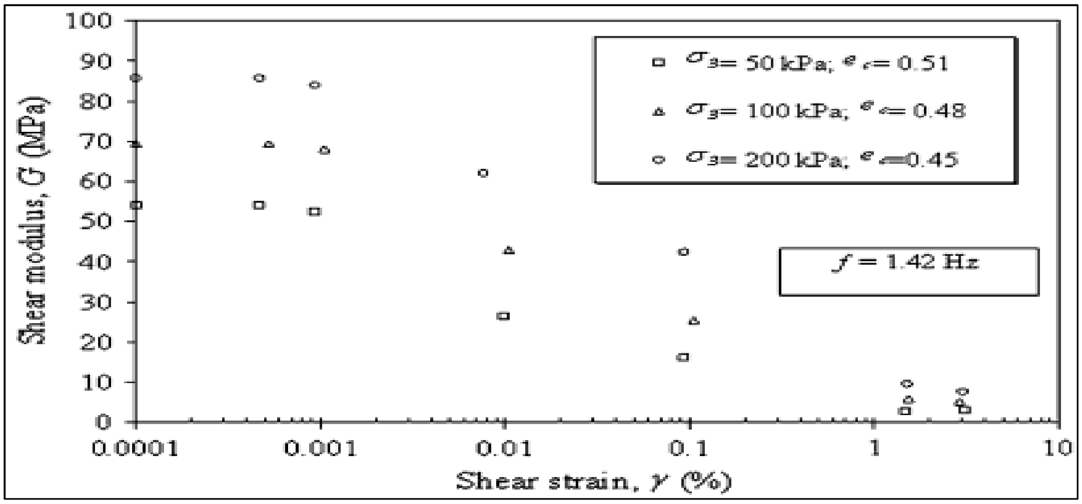

Figure 2.6: Variation of shear modulus with shear strain for different confining pressures (Sitharam & Vinod, 2010)

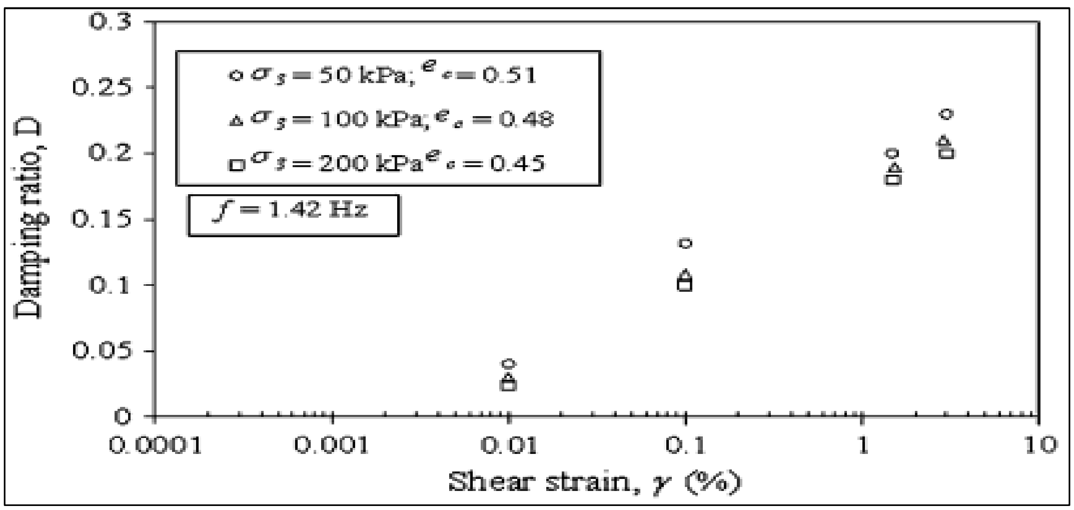

Figure 2.7: Variation of damping ratio with shear strain for different confining pressures (Sitharam & Vinod, 2010)

2.6.3. Effect of Void Ratio

The void ratio of soil is a comparison between saturated or unsaturated soil void volume and soil solid volume. It is one of the mechanical soil properties which is mainly affected by the static/cyclic actions of loading. A larger void ratio means the void in the soil is large, so the presence of large void may decrease the value of dynamic shear wave velocity and shear modulus of the soil. It also reduce the natural frequency of soil that is caused by earthquake load (Munirwansyah, 2020). However, as seen from Figure 2.8, the value of shear modulus decreases with increasing of void ratio. It is evident from Figure 2.9 that the variation of damping ratio with initial void ratio falls in a narrow band showing an insignificant influence of initial void ratio on damping ratio values.

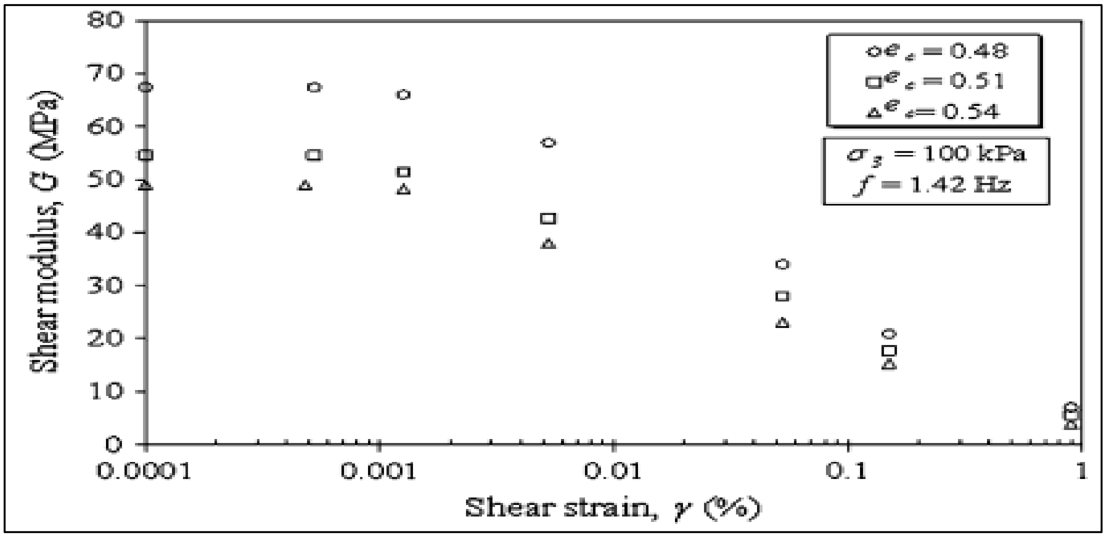

Figure 2.8: Variation of dynamic shear modulus value with void ratio (Sitharam & Vinod, 2010)

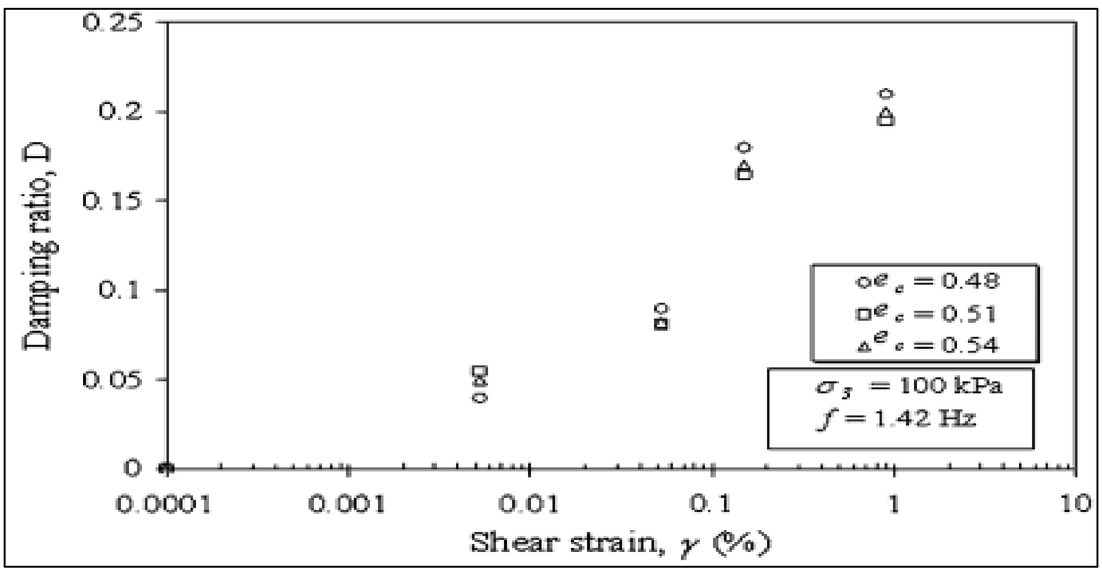

Figure 2.9: Variation of damping ratio value with void ratio (Sitharam & Vinod, 2010)

2.6.4. Effect of Water Content

Shear modulus and damping ratio of partially saturated sand specimens weren't significantly affected by pore water. However, the water content reaches the saturated state the differences are great. For dry sand, the shear modulus is higher as compared to partially saturated and fully saturated sand, but damping ratio increases with water content (Jafarzadeh & Sadeghi, 2009).

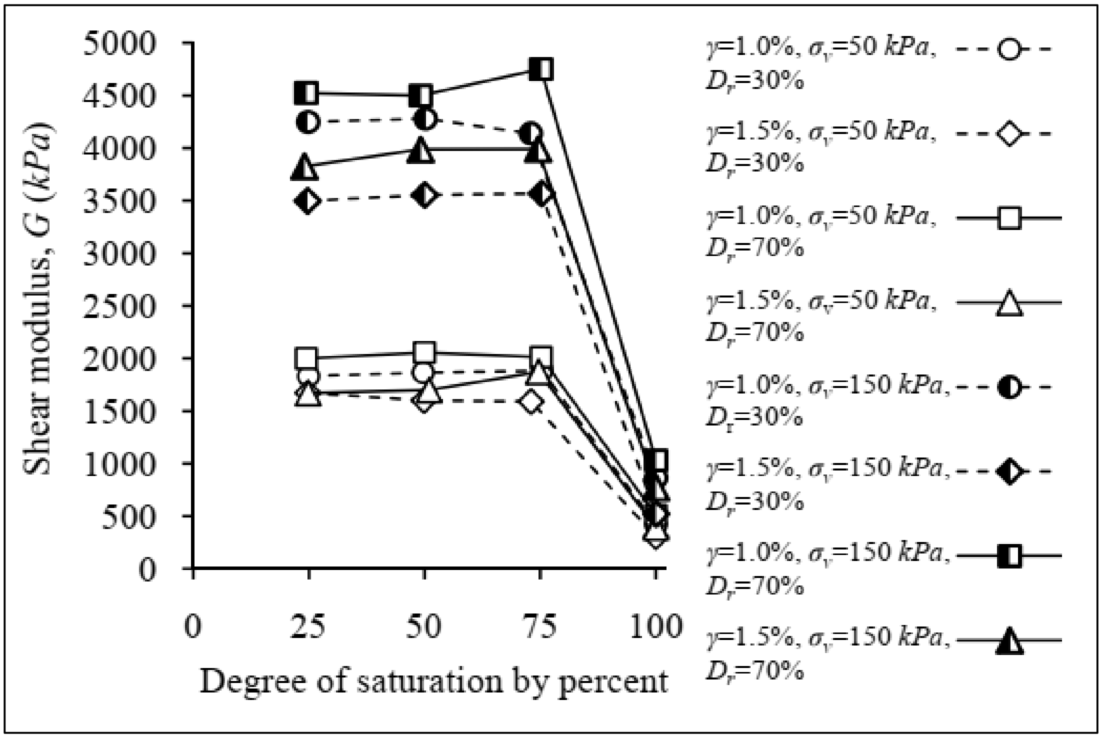

Figure 2.10: Variation of shear modulus values with degree of saturation (Jafarzadeh & Sadeghi, 2009)

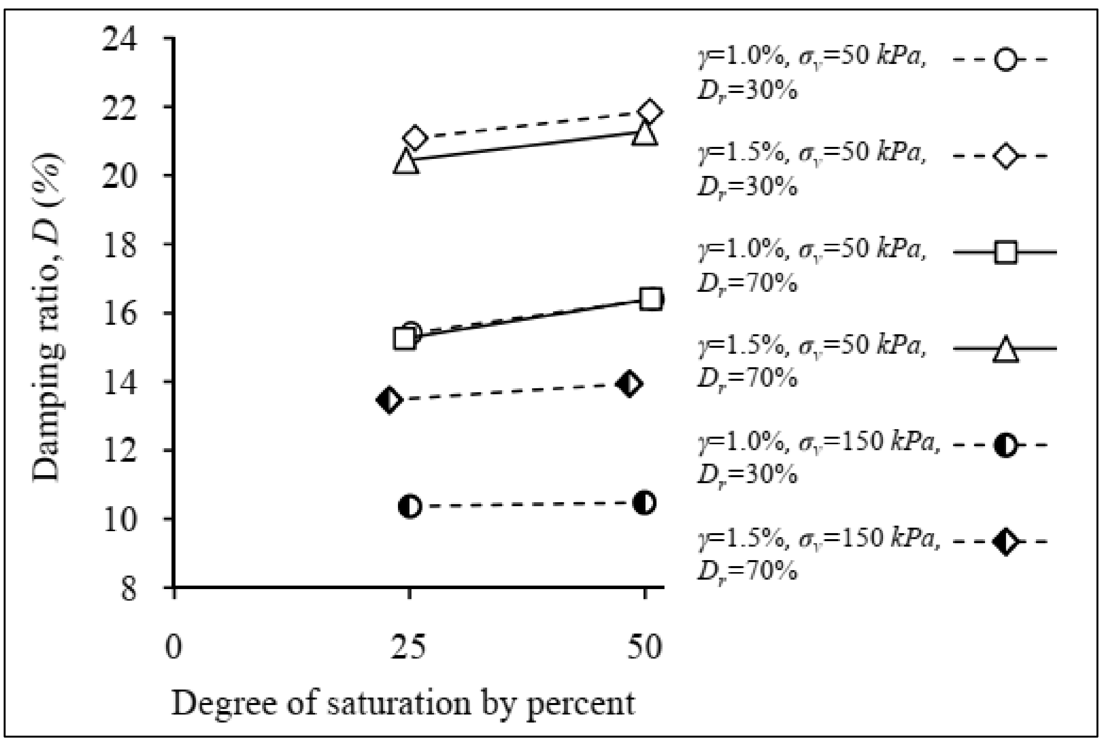

Figure 2.11: Variation of damping ratio values with degree of saturation (Jafarzadeh & Sadeghi, 2009)

2.6.5. Effect of Method of Loading

The dynamic properties and cyclic strength of soil can be evaluated by using different cyclic loading waveforms. Some of the cyclic loading waveforms which used to evaluate dynamic properties and cyclic strength of soils are triangular, rectangular and sinusoidal waves. The rectangular loading waveform gives 5 – 20 % lower strength than the triangular loading waveform, but sine waveform gives approximately 30 % higher cyclic strength than the triangular or rectangular waveforms (Kumar et al., 2013).

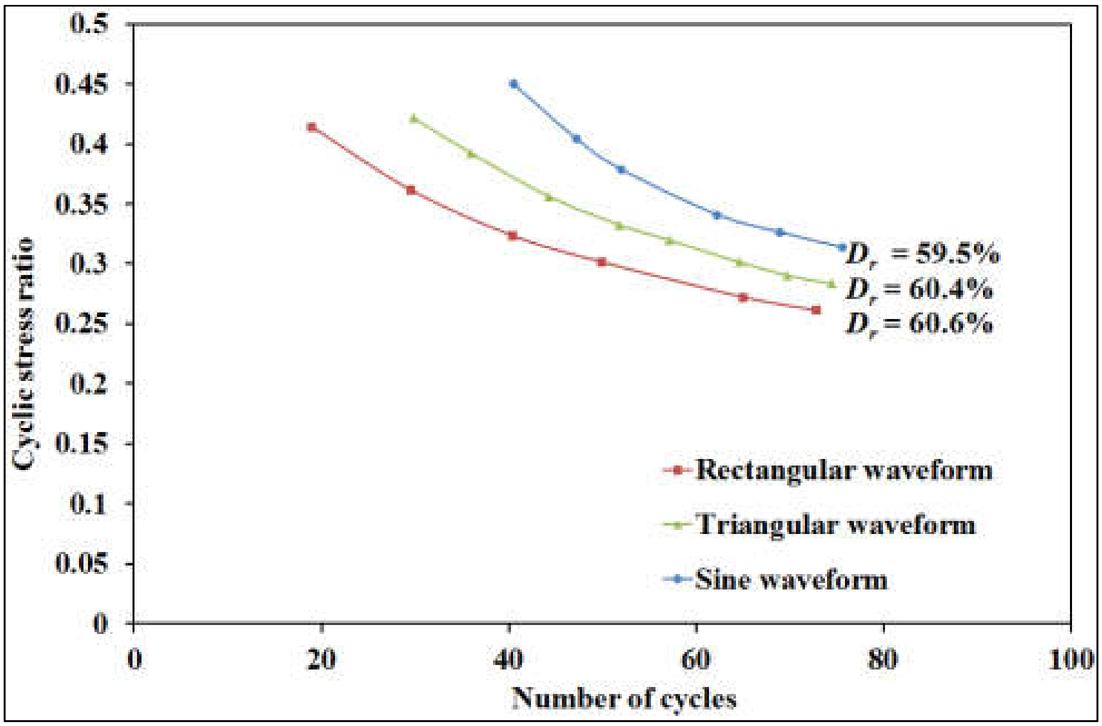

Figure 2.12: Variation of cyclic stress ratio with No. of cycles for different loading waveform (Kumar et al., 2013)

2.6.6. Effect of Overconsolidation Ratio (OCR)

The historical change in state of stress of a subsoil is denotes by one of the geotechnical parameter overconsolidation ratio (OCR). It is one of the most leading factors that affect the engineering behavior of plastic soil. Whilst having no effect for non-plastic soils. For plastic soils, there is an increase in the normalized shear modulus and decrease in damping ratio with increasing overconsolidation ratio. This effect is slightly more significant for higher PI values. Nevertheless, the impact of overconsolidation ratio is minimal at both small and large strains and becomes increasingly less important for higher OCR values (Kontoe & Taborda, 2016).

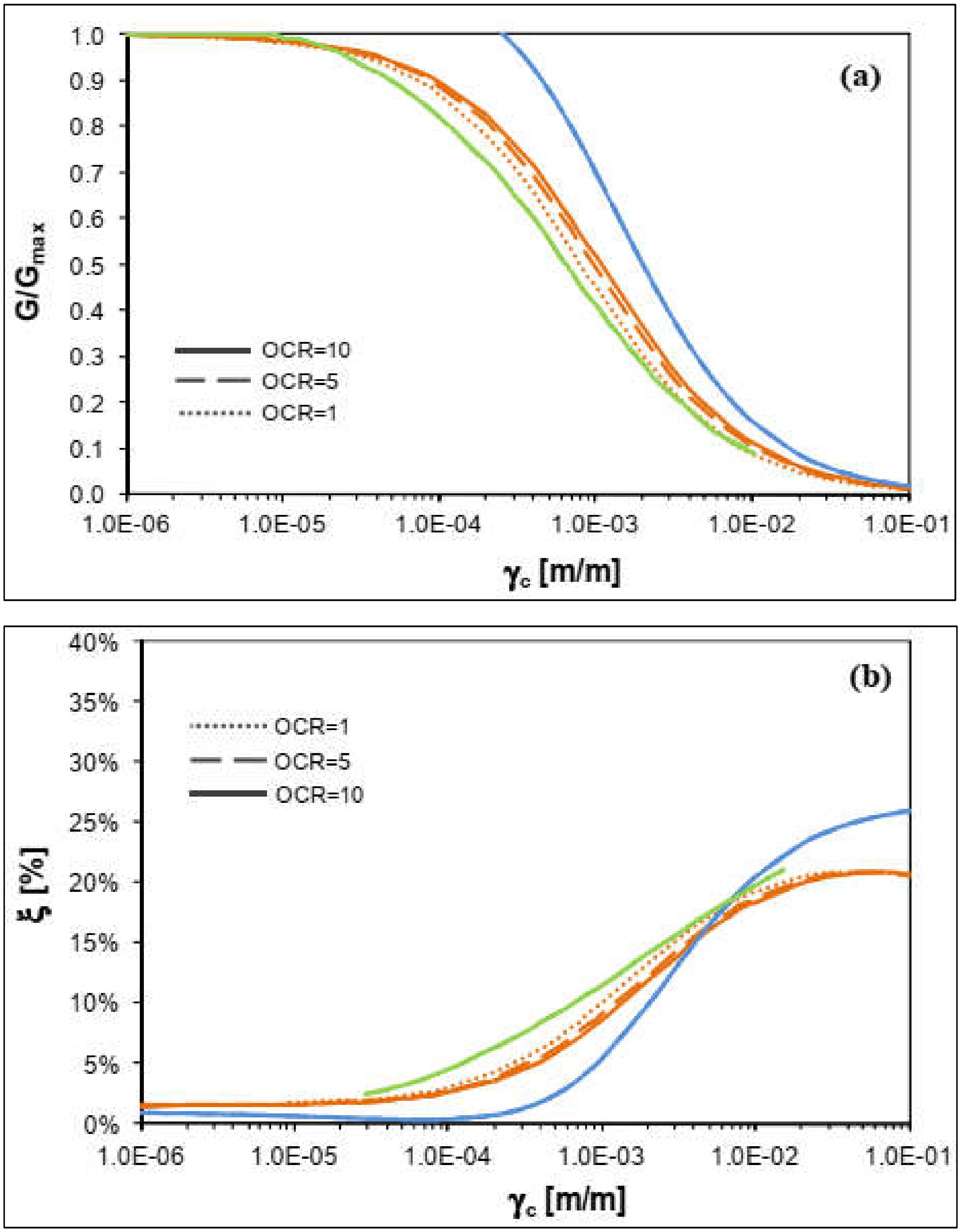

Figure 2.13: Variation of (a) normalized shear modulus and (b) decrease in damping ratio values with OCR (Kontoe & Taborda, 2016)

2.6.7. Effect of Frequency of Cyclic Loading

The frequency of cyclic loading has no effect on the damping properties of dry sand. The frequency of cyclic loading did not significantly affect the shear modulus, but it has significant effect on the damping ratio. The lower loading frequency gives slightly higher strength. (Lee et al., 2015).

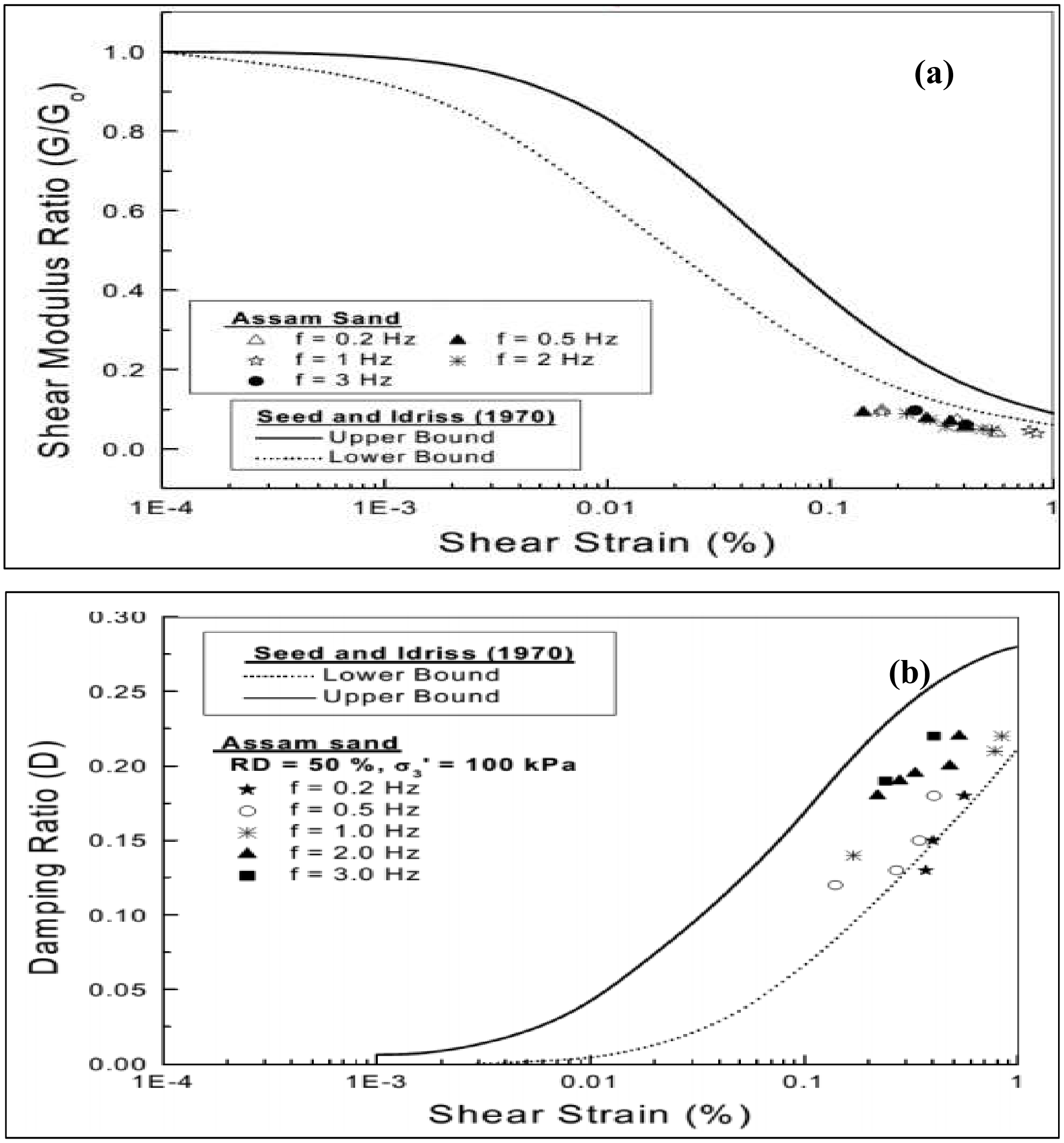

Figure 2.14: Variation of (a) shear modulus and (b) damping ratio values with frequency (Kumar et al., 2013)

2.6.8. Effect of Shearing Strain Amplitude

The most important external variables that influence the soil's dynamic behavior are the magnitude of applied stress or strain. For any small-strain tests, the shearing strain amplitude is controlled under 0.001 % and for higher strain tests, the shearing strain amplitude is controlled higher than 0.1 %. The shearing strain amplitude for the nonlinear dynamic properties tests is increased from possible low level to possible high level, (0.001 % < γ < 0.1 %). At low strain amplitude, the shear modulus is high, but it decreases as the shear strain amplitude increases. At low strain amplitude, the damping ratio is low, but it increase with strain amplitude (Mengistu, 2015).

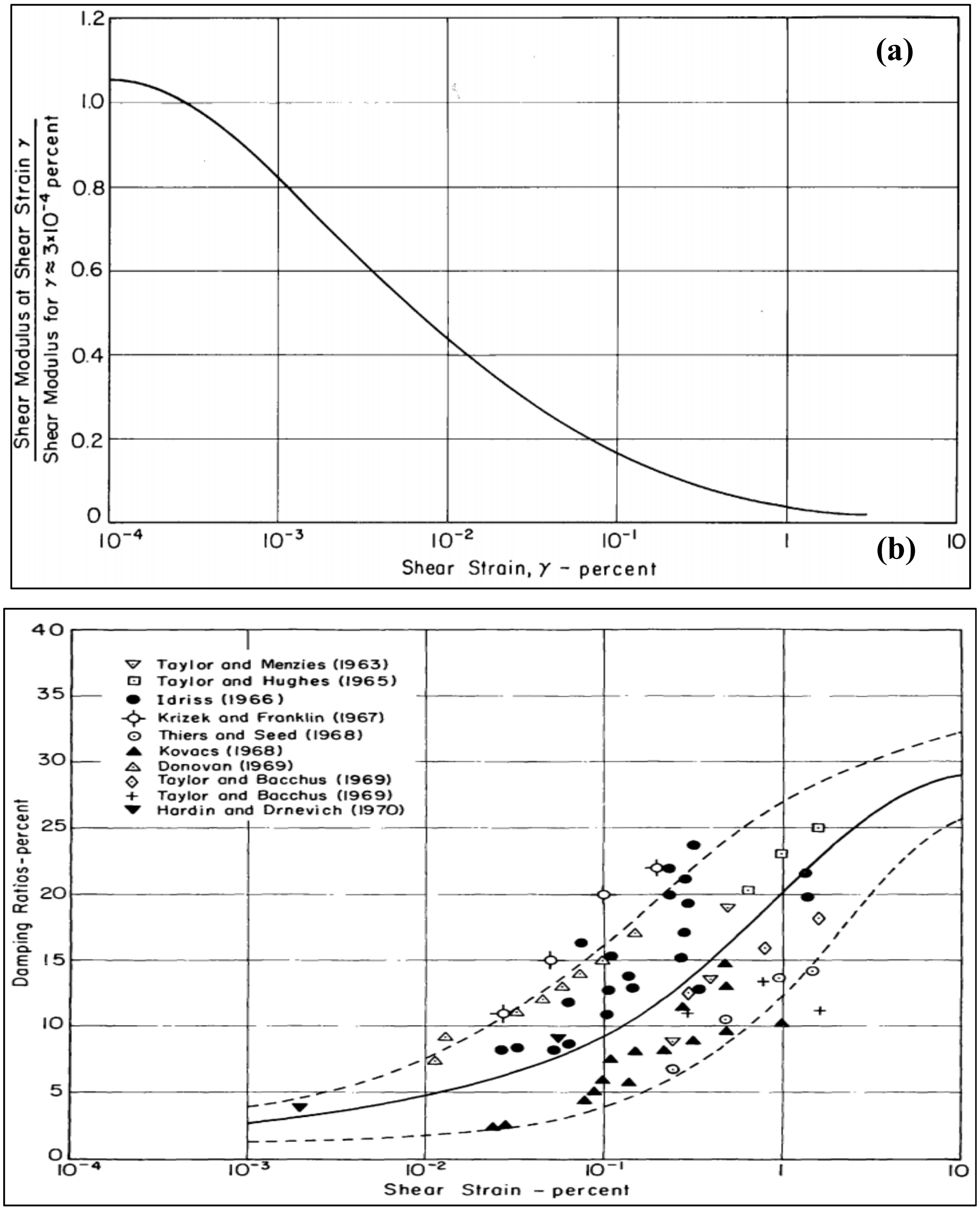

Figure 2.15: Variation of (a) shear modulus and (b) damping ratio with strain amplitude for saturated clay soil (H. Bolton Seed I. M. Idriss, 1970)

2.6.9. Number of Loading Cycles

The number of loading cycles has no significant effect on shear modulus but it has on damping ratio. The shear modulus slightly increases and the damping ratio significantly decreases with an increasing number of loading cycles. In general, the shear modulus increases slightly while the damping ratio significantly decreases with an increasing number of loading cycles (Mengistu, 2015).

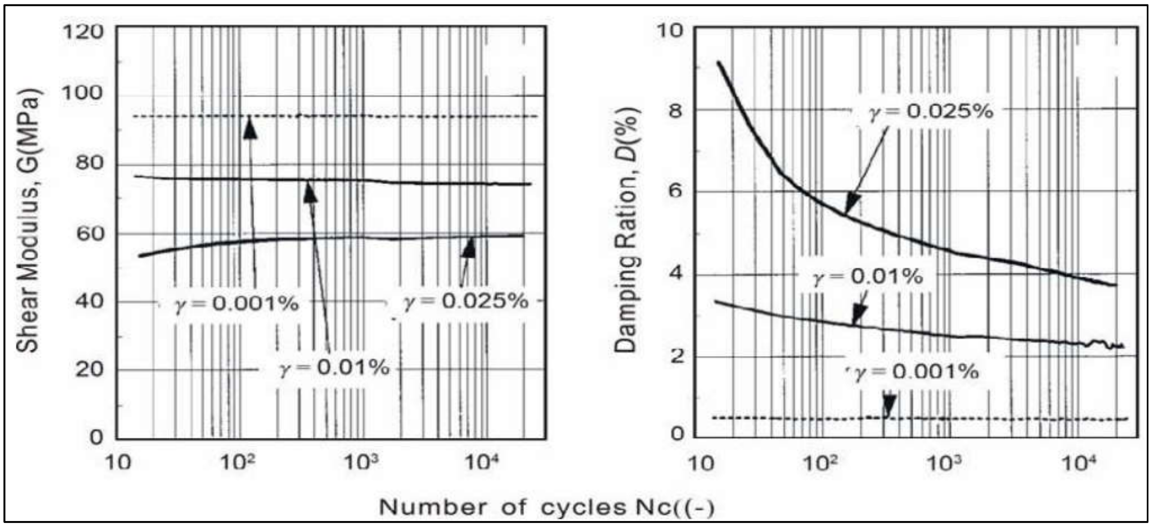

Figure 2.16: Variation of shear modulus and damping ratio with No. of cycles on for dry sand (Mengistu, 2015)

2.6.10. Effect of Soil Plasticity

Highly plastic soils tend to have a more linear cyclic stress-strain response at smaller strains and degrade less at larger shear strain. The cyclic stress ratio causing liquefaction of silty soils at a given number of cycles decreases with the increase in plasticity index. A soil with higher plasticity generally has influences on the G/G_{max} curve and damping ratio curve. For same cyclic strain value, the shear modulus of soil is increases with PI, but damping ratio is decrease with PI. (Kumar et al., 2013).

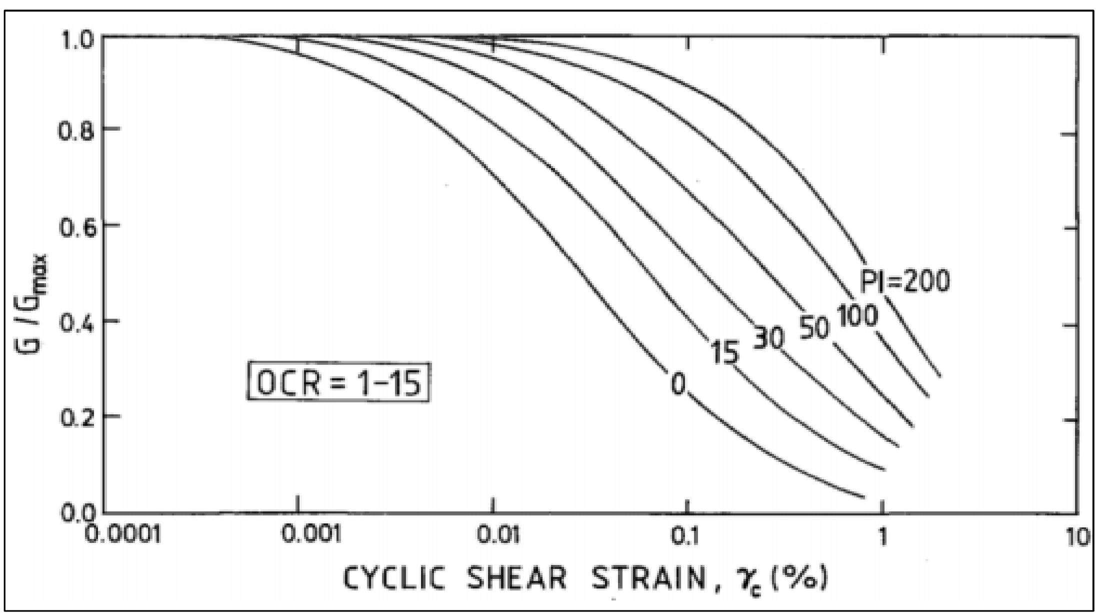

Figure 2.17: Effect of soil plasticity on G_{sec}/G_{max} for normally and overconsolidated soils (Kumar et al., 2013)

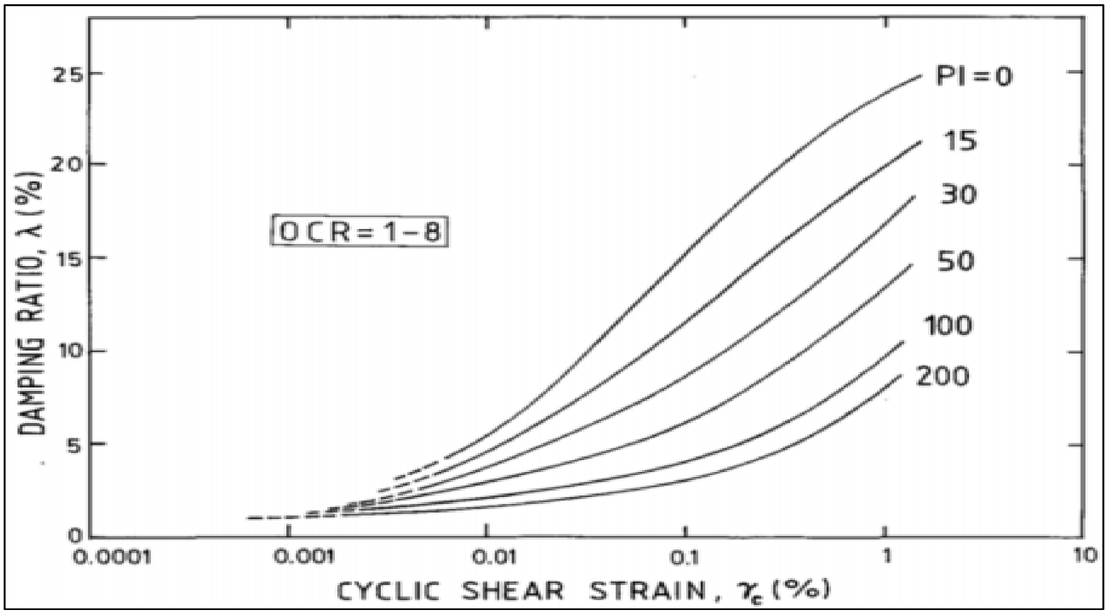

Figure 2.18: Effect of soil plasticity on damping ratio for normally and overconsolidated soils (Kumar et al., 2013).

2.6.11. Effect of Percentage Fines

The pore pressure response and liquefaction behavior of a soil is affected by the percentage of fines in soil. The presence of fines affects the liquefaction resistance of soil, only when the soil contains more than 5 % of fines of the soil. The damping ratio decrease albeit increase in silt content, but it has no significant effect on the shear modulus (Lee et al., 2015).

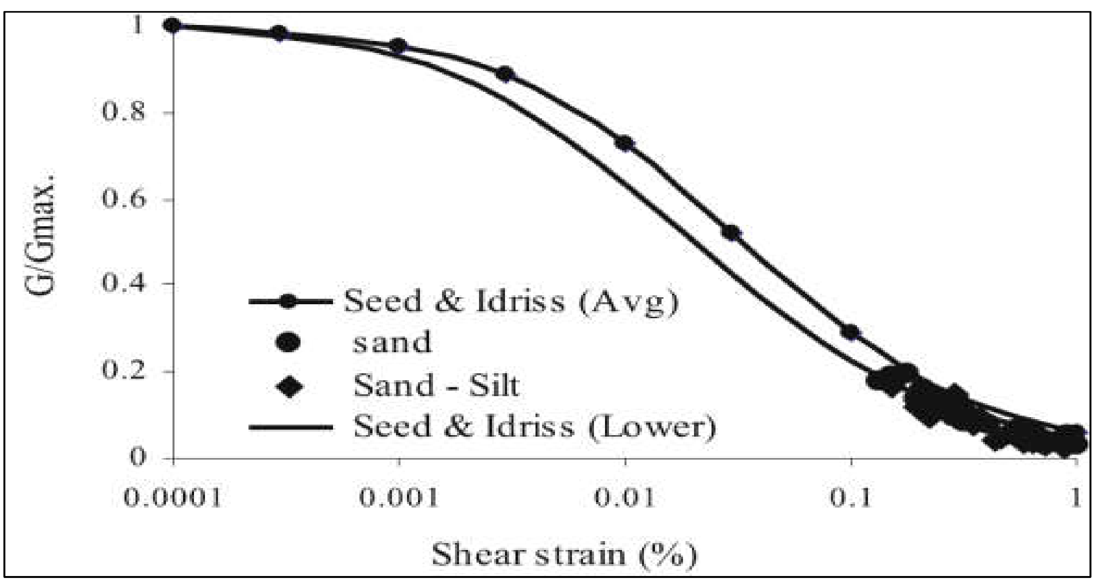

Figure 2.19: Variation of normalized shear modulus values with fines content of soil (Kumar et al., 2013)

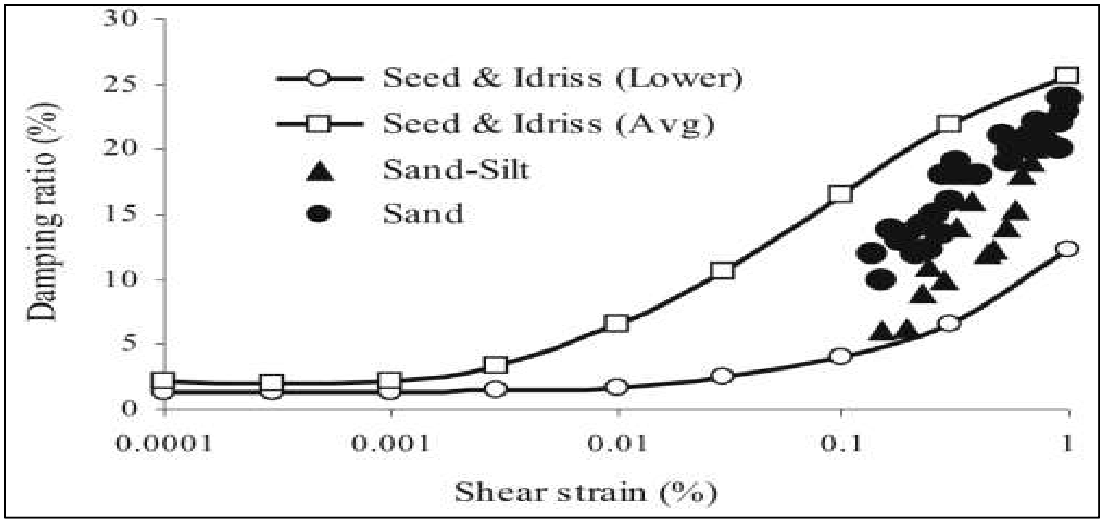

Figure 2.20: Variation of damping ratio values with fines content of soil (Kumar et al., 2013)

2.7. Earthquake Hazard in Ethiopia

Earthquake is one among the dynamic loads that affect the dynamic behaviors of soil. The Ethiopian rift system which is the component of the East African rift system passes through the center of the country making it one among the foremost seismically active regions within the world. Thus, substantial and damaging earthquakes are reported and recorded within the past in this region (Lamessa et al., 2019). A catalog of those damages are presented in Table 2.5 particularly for the time between 1842– 2011.

Table 2.5: List of earthquakes and reported damages between 1842 – 2011

Date	Region	Magnitude	Damages	Reference
08/12/1842	Ankober		Sever	(NGDC, 1972)
02/11/1875	Tigray region	6.2	Sever	(NGDC, 1972)
1906	Langano	6.75	Low	(Herbert, 2013)

14/08/1921	Massawa Subregion	5.9	Sever	(NGDC, 1972)
01/06/1961	Kara Kore	6.5	Moderate (buildings were damaged)	(NGDC, 1972)
29/03/1969	Sardo	6.2	Many houses destroyed	(NGDC, 1972)
28/07/1979	Akaki	4.1	No damage to the Aba Samuel HEP station a few kilometers away. Cracks in poorly built masonry structures	(Kinde et al., 2011)
1983	Hawassa	5.3	Damage to steel frames in Hawassa. Damage to Wetera Abo Church in Wondo Genet (1983 earthquake, masonry building with irregular vertical and horizontal stiffness. Damage seems to occur where there is stiffness discontinuity).	(Kinde et al., 2011)
01/04/1984	Near Lake Hayk	-	High-rise buildings shaken. Mortgage Bank Building in Kazanchis	(Kinde et al., 2011)
1985	Oitu Bay (Langano)	5.1	Strongly felt in Lake Langano camp, central MER. Cracks in buildings in resort area hotels	(Kinde et al., 2011)
1989	Dobi Graben [Afar]	6.2	Several bridges damaged	(Herbert, 2013)

13/04/1989	Mekelle	5.3	Felt by many causing some panic	(Kinde et al., 2011)
20/08/1989	Dichotto	5.8	Dining people thrown-off table, masonry house collapsed, landslides killed 4 people and 300 cattle, 6 bridges destroyed in Dichotto	(Kinde et al., 2011)
08/06/1989	Soddo	5.0	Widespread panic, broken windows and some injured in Soddo.	(Kinde et al., 2011)
1993	Nazareth	5.0	Collapse of several adobe buildings in Nazareth town northern MER. Felt as far as Debre Zeit and Addis Ababa	(Kinde et al., 2011)
01/08/2002	Mekelle	5.2	Buildings shaken in the city of Mekelle.	(Kinde et al., 2011)
26/09/2005	Afar Triangle	-	Fumes as hot as 400 °C shoot up from some of them; the sound of bubbling magma and the smell of sulfur rise from others. The larger crevices are dozens of meters deep and several hundred meters long. Traces of recent volcanic eruptions are also visible. This was followed by a week-long series of earthquakes. During the months that followed, hundreds of further crevices opened up in the ground, spreading across an area of 345 square miles.	(Kinde et al., 2011)
2009/09/19	Ankober	5.0	Earthquake strikes near Ankober Town and was widely felt in Addis specially by residents who live on multistory buildings	(Kinde et al., 2011)

20/12/2010	Hosanna	5.3	Damage sustained by reinforced concrete frame dormitory building at Jimma University with in-filled walls at where as many as 26 students were injured. structural damage to slab and column joint. Damage to many building in Hosanna	(Kinde et al., 2011)
03/03/2011	Ethio-Somali Border	6.1	Buildings shaken in Dire Dawa, Jijiga, and Somalian towns	(Kinde et al., 2011)
09/03/2011	Abosto/ Yirga Alem	5.0	Damage to unreinforced cinder-block cladded timber building. 100 houses were destroyed and 2 people were injured in this earthquake	(Kinde et al., 2011)

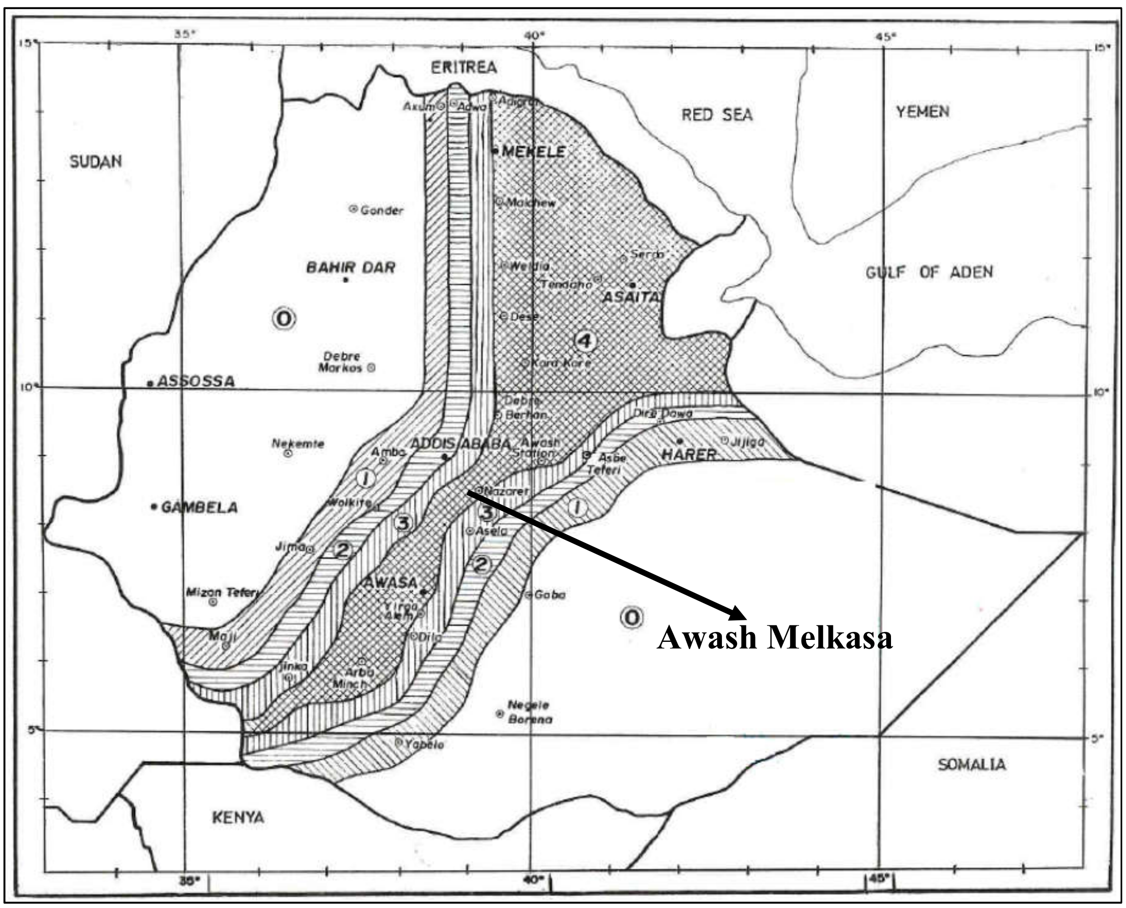

Figure 2.21: Seismic hazard map of Ethiopia for 100 year return period as per EBCS 8: 1995 (Asrat, 2011)

2.8. Summary of Literature Review and Research Gaps

The literatures reviewed in this study have generally show that the behavior of soils subjected to dynamic lading are governed by dynamic soil properties. The most important dynamic properties of soils are shear modulus and damping ratio. These properties are used to characterize the dynamic behavior of soils. These parameters are affected by several factors. Some of the factors are techniques of sample preparation in a laboratory (whether intact and reconstituted samples), confining pressure, void ratio, water content, methods of loading, overconsolidation ratio, loading frequency, shearing strain amplitude, number of loading cycles, soil plasticity and percentage of fines. Among these factors, void ratio and confining pressure are the major parameters affecting small strain shear modulus of soils. Whereas level of strain and confining pressure have a major effect on the magnitude of the damping ratio. Related woks about dynamic properties of soil are summarized in Table 2.6.

Table 2.6: Summary of literature review

Author	Focus area	Major findings
(Qiao et al., 2020)	Study on the dynamic characteristics of soft soil	✓ The G/G_{max} value for σ'_v of 100 kPa for shear strain value of 10^{-3} % is 0.39, but that of 200 kPa is 0.5. the damping ratio value for σ'_v of 100 kPa for shear strain value of 10^{-3} % is 18.5%, but that of 200 kPa is 14%. This shows that the normalized shear modulus increases with the increase of effective confining pressure, but the damping ratio decreases with the increase of effective confining pressure. ✓ The G/G_{max} value for OCR value of 1 at shear strain value of 10^{-3} % is 0.38, but that of 1.5 is 0.48. The damping ratio value for OCR value of 1 at shear strain value of 10^{-3} % is 18.5%, but that of 1.5 is 14 %. This shows that the normalized shear modulus increases with the increase of OCR, but the damping ratio decreases with the increase of OCR. ✓ The G/G_{max} value for consolidation time of 12 hr at shear strain value of 10^{-3} % is 0.47, but that of 24 hr is 0.37. The damping ratio value for consolidation time of 12 hr at shear strain value of 10^{-3} % is 12 %, but that of 24 hr is 19 %. This shows that the normalized shear modulus decreases with the increase of consolidation time, but the damping ratio increases with the increase of consolidation time.

(Kumar et al., 2013)	Review on parameters influencing dynamic soil properties	✓ The cyclic strength of the undisturbed specimens was about 15% greater than that of the reconstituted specimens. This shows that sample preparation method has a significant effect on shear modulus ✓ The G/G_{max} value for PI of 0 at shear strain value of 0.1 % is 0.275, but that of 30 is 0.55. The damping ratio value for PI of 0 at shear strain value of 0.1 % is 15 %, but that of 30 is 8 %. This shows that the normalized shear modulus increases with the increase of PI, but the damping ratio decreases with the increase of PI. ✓ Sine waveform gives approximately 30 % higher cyclic strength than the triangular or rectangular waveforms
(Lee et al., 2015)	Overviews of factors affecting dynamic properties of tropical residual soil	✓ Confining pressure and frequency of cyclic loading are the main extrinsic factors affecting the dynamic properties of soil, while soil plasticity and percentage of fines are identified as the main intrinsic factors of soil ✓ The damping ratio decrease albeit increase in fines content, but does not have a significant effect on shear modulus ✓ The frequency of the cyclic load has no significant effect on the shear modulus, but has a significant effect on the damping ratio
(Munirwansyah et al., 2020)	Void ratio effect on dynamic shear modulus and shear wave velocity	✓ The G_{max} value for e of 1 is 240 MPa, but that of 1.25 is 160 MPa. This shows that the presence of large void may reduce the value of dynamic shear modulus of the soil.
(F. Jafarzadeh & H. Sadeghi, 2009)	Effect of water content on dynamic properties of sand in cyclic simple shear tests	✓ For dry sand, compared to partially saturated and fully saturated sand, the shear modulus is higher, but the damping ratio increases with increasing water content.

(Mengistu, 2015)	Investigation in to some dynamic properties of soils around Ziway	✓ The value of shear modules is in the range of 1.0 to 8 MPa for strain level (0.01 %< γ <0.1 %) and 8.0 to 25 MPa for strain level (γ >0.1 %). ✓ The damping ratio values range between 2.85 to 10 % for strain level (0.01 %< γ <0.1 %) and 10.0 to 27.0 % for strain level (γ >0.1 %). ✓ The specimens having higher void ratio have lower shear modulus ✓ The void ratio has no significant influence on damping ratio at any shearing strain amplitude under all confining pressures
(Hailemariam, 2017)	Investigation of shear modulus and damping ratio of Modjo silt and silty sand soil using cyclic simple shear test	✓ The value of shear modulus is in the range of 0.11 MPa to 22.98 MPa and damping ratio values range between 0.25% and 25.63%. ✓ As number of loading cycles and confining pressure increase, the shear modulus increases and damping ratio decreases. ✓ Shear modulus decreases and damping ratio increases with increase in cyclic shear strain amplitude.
(Kebede, 2019)	Cyclic behaviour and dynamic properties of soils: a case of Jimma town	✓ The value of shear modules found in the laboratory ranges from 0.33 to 7.01 MPa and damping ratio values from 2.03 to 22.98%. ✓ Testing conditions, sample preparation and type of soil sample have significant effect on the shear modulus values and damping characteristics

CHAPTER THREE

MATERIALS AND METHODS

3.1. Description of the Study Area

3.1.1. Location, Topography and Population Size

Awash Melkasa is a town found in the central rift valley of Ethiopia. Located within the East Shewa Zone within the state of Oromia near Adama about 115 km from the capital city Addis Ababa. It has a latitude between 8.18°N and 8.72°N and longitude between 39.09°E and 39.48°E with an elevation between 1500 and 1600 meters.

Based on the 2007 national census conducted by the central statistical agency of Ethiopia Awash Melkasa has an estimated total population of 4225 comprising of 2083 men and 2142 women.

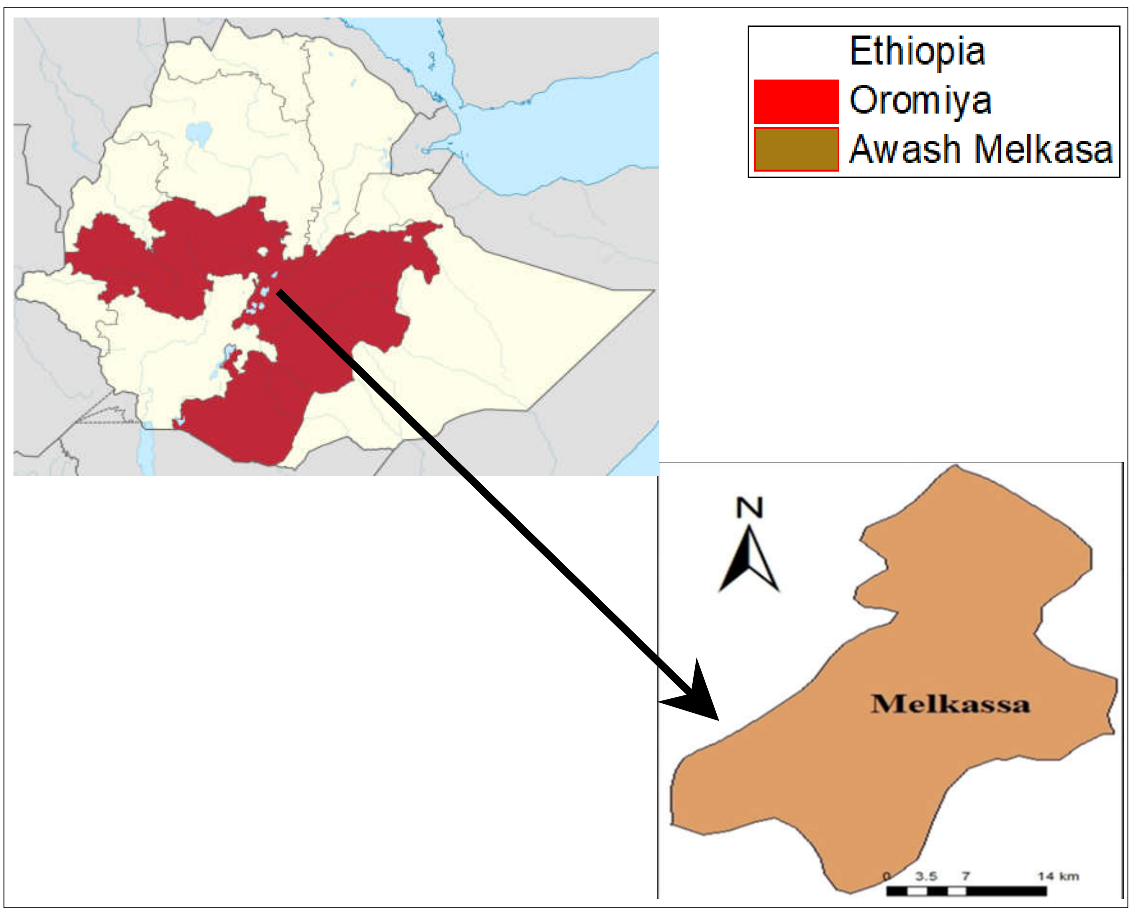

Figure 3.1: Map of the study area

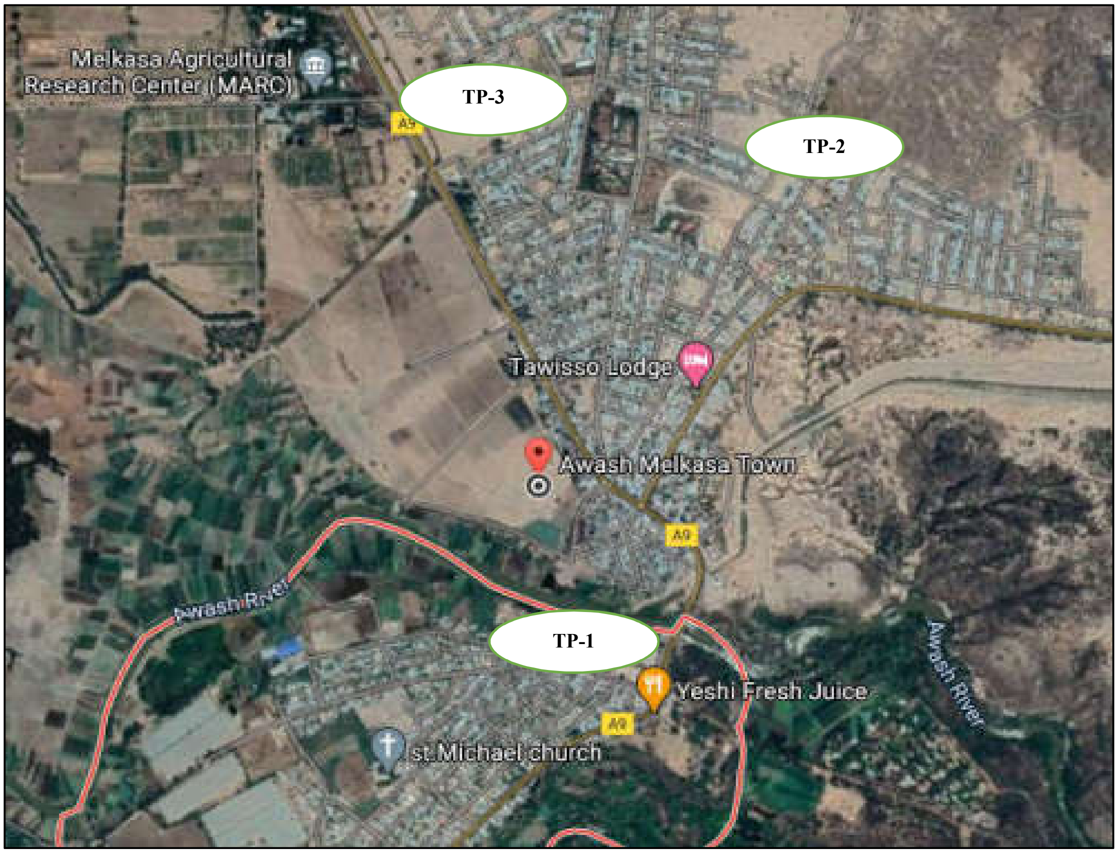

Figure 3.2: Satellite view of the study area with test pit location (Awash Melkasa - Google Maps, 2021.)

3.1.2. Climate Condition

The temperature and rainfall data obtained from World Weather Online.com based on the data between 2010 and 2020 are shown below.

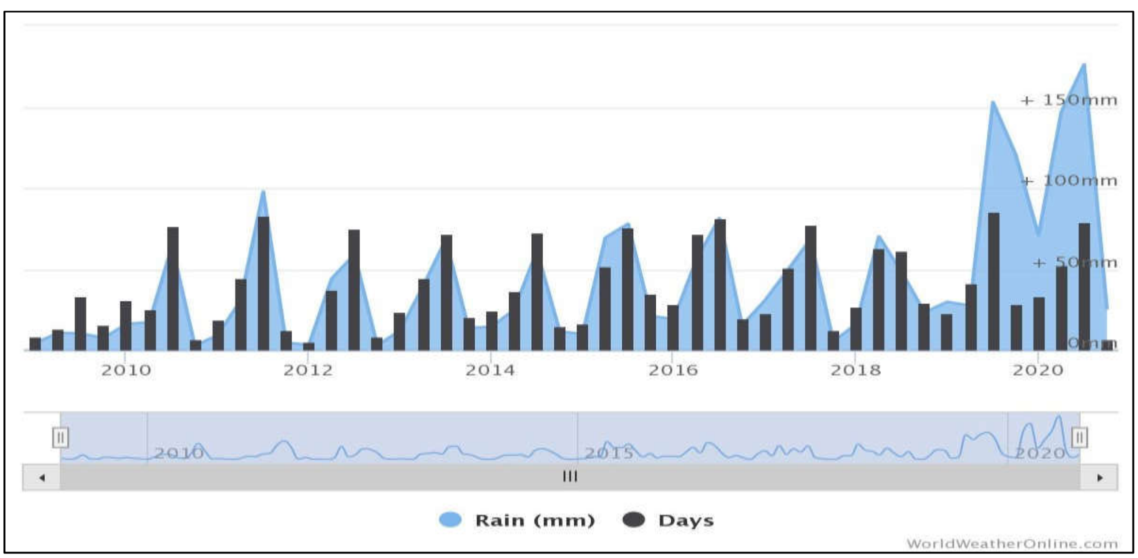

Figure 3.3: Average rainfall amount (mm) and rainy days (Online, 2020.)

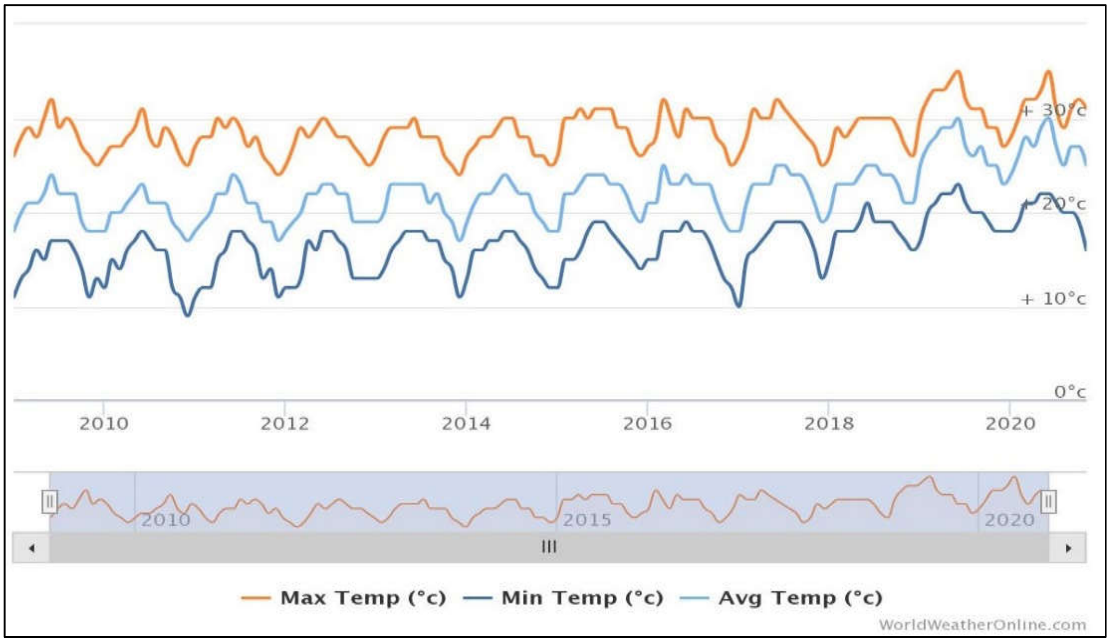

Figure 3.4: Maximum, Minimum, and Average temperature (°C) (Online, 2020.)

3.2. Study Design

This study considered quantitative experimental research because it used systematic random sampling techniques to determine the static and dynamic characteristics of the soil samples collected from Awash Melkasa town. Soil samples were taken from three different test pits at different depths. The field and laboratory experiment program was designed to perform all the basic laboratory tests to study the properties of the soil. The disturbed soil samples were first air dried and then used for various laboratory tests in accordance with the American Society for Testing and Materials (ASTM) soil testing procedures.

3.3. Materials

Before deciding the location of test pit, first visual site surveys were conducted to take soil samples uniformly in the town. From different locations of the town three representative test pit areas were selected, the chosen points were Awash Melkasa Primary School (TP-1), Awash Melkasa High School (TP-2), and Mesino (TP-3) as shown in Figure 3.2. Test pits were excavated to the depth of three meters and two samples were taken from each test pit from different depth wherever there was a change in a soil layer. Due to the nature of the soil and the lack of sampling materials, only disturbed samples were collected. We collected around 30 kg of disturbed soil samples from each layer at different depths for laboratory tests of static and dynamic characteristics. The global coordinates of test pits i.e. Northing, Easting and Elevations were shown in Table 3.1.

Table 3.1: Global coordinates of test pits location

Test pit No.	Test pit location	Northing	Easting	Elevation (m)
TP-1	Elementary School	$8^0 24' 1''$	$39^0 20' 11''$	1537
TP-2	High School	$8^0 24' 45''$	$39^0 20' 24''$	1560
TP-3	Mesino	$8^0 24' 48''$	$39^0 19' 52''$	1535

3.4. Test Programs

In this study, the collected soil samples were tested based on two test methods. The test methods used in this study are field test methods and laboratory test methods. In the field only two tests, the density and natural moisture content of the field soil were conducted. In the laboratory, different laboratory tests were done in two parts static and dynamic property tests. The static property laboratory tests were conducted in Adama Science and Technology University's geotechnical laboratory and the dynamic property laboratory test, the cyclic simple shear test are carried out in Ababa Addis Ababa Institute of Technology's geotechnical laboratory. Figure 3.5 shows the summary of test program utilized in this study.

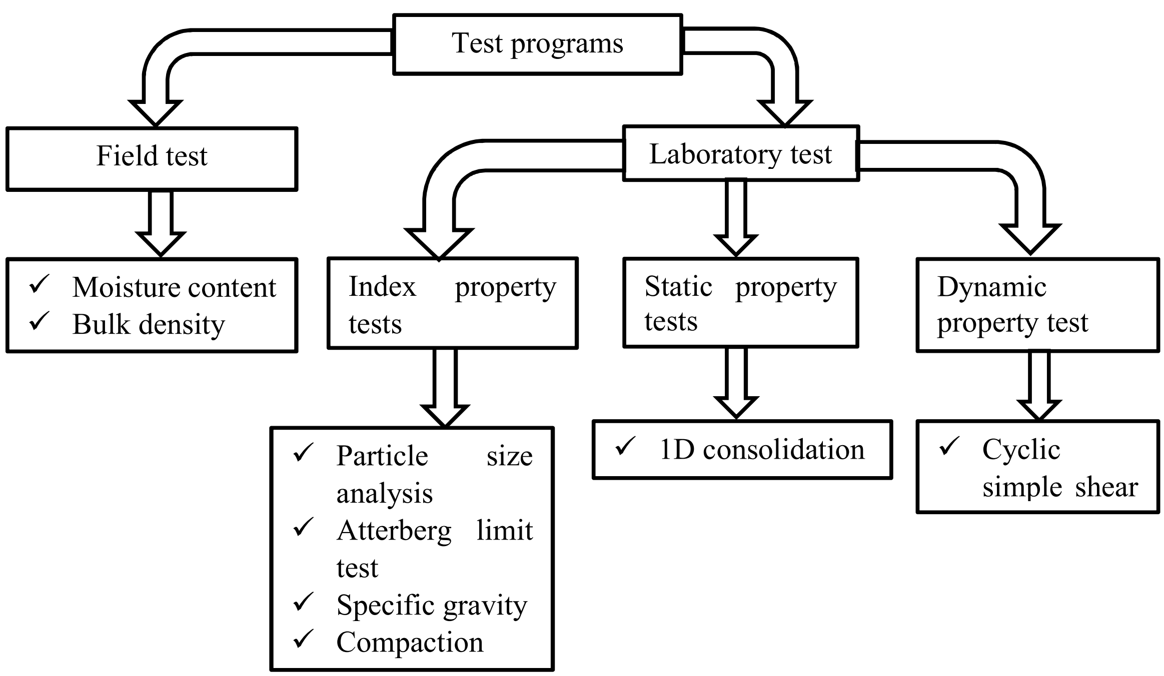

Figure 3.5: Flow chart of test programs

3.5. Methods

The in-situ density and natural moisture content of the collected soil sample were conducted in the field. The laboratory tests including Grain size analysis, Specific gravity, Atterberg limits, Compaction, 1D – Consolidation and Cyclic simple shear test were conducted on the collected soil in order to determine the dynamic properties of soil.

3.5.1. Field Tests

The field soil density and natural moisture content test was carried out at the field according to ASTM D1556: standard test method for density and unit weight of soil in place by the sand-cone method. This method employs the use of poorly graded sand. This test method was used for the determination of the field density and natural moisture content of soils. The reason to conduct this test was the test results were used for sample preparation in consolidation and cyclic simple shear tests.

3.5.2. Index Soil Property Tests

3.5.2.1. Particle Size Analysis

Particle size analysis is widely used in engineering soil classification. It's the quantitative determination of the distribution of particle sizes in soils. The test was conducted in two parts; the first part is conducted according to ASTM D422: standard test method for particle-size analysis of soils (Wet sieve analysis) and then according to ASTM D1140: standard test method for amount of material in soils finer than the No. 200 (75-µm) sieve (Hydrometer analysis).

The hydrometer test is performed using a solution of 40 grams of sodium hexametaphosphate per liter of solution. For hydrometer analysis, place 50 g of soil in a 150 ml beaker. For samples tested with the solution, add 125 ml of sodium hexametaphosphate solution (40 g / L) and stir until the soil is completely wet and soaked for at least 16 hours Then, immediately after dispersion, transfer the suspension of soil water to a glass sedimentation cylinder, add distilled water to a total volume of 1000 ml and read with a 152H hydrometer. Finally, the results of the two methods are combined to obtain the general particle size distribution curve.

To accomplish both wet and hydrometer, oven, balances, deep, sieves, mixing bowl, sink, squeezing bottle, Stirring Apparatus, dispersion cup, hydrometer 152H, sedimentation cylinder, thermometer and water bath for maintaining the soil suspension at a constant temperature during the hydrometer analysis were used. From this test, the grain size distributions and the percentage of fines for a given soil sample were determined.

3.5.2.2. Atterberg Limit Test

Soils have four states: liquid, plastic, semi-solid and solid states. Marginal water contents that separate these states are known as Atterberg limits. The limits of the four states of soils are shrinkage limit (SL), plastic limit (PL), and liquid limit (LL). In this study Liquid Limit (LL), Plastic Limit (PL), and Plasticity Index (PI) are done. The tests were conducted according to ASTM D4318: standard test methods for liquid limit, plastic limit, and plasticity index of soils for soils passing No. 40 (425 µm) sieve. As described in ASTM D4318, LL is the water content of the soil at the arbitrarily defined boundary between the semi-liquid and plastic state, expressed as a percentage. It is obtained by using cup in which a groove is cut in the soil sample and the sample cup is raised and dropped a specified number of times for the groove to barely close. The water content of the soil in which this occurs is called the liquid limit. The relationship between the water content and the number of blow is plotted on the graph. The water content corresponding to the intersection of the line and the abscissa of 25 blow is called the liquid limit of the soil.

The plastic limit is defined as the transition water content value of a soil from semi-solid to plastic state, and it was determined by rolling a soil into a 3 mm diameter thread until its water content is reduced to a point at which the thread crumbles and can no longer be pressed together and re-rolled. The plasticity index (PI) is calculated as the difference between the liquid limit and the plastic limit. In order to perform these tests in the laboratory, a Casagrande liquid limiting device, a flat groove tool, a spatula, a frosted glass plate, an oven, and a moisture content can were used. The reason for conducting Atterberg limit tests are the values obtained from the test were important for soil classification purposes.

3.5.2.3. Specific Gravity Test

In this study the test was done according to ASTM D 854 by means of a water pycnometer. The soil sample used for the test were 15 g oven dried that pass through No. 4 (4.75 mm) sieve. To complete this test, balance capable of measuring to the nearest 0.01 g, 200-ml etched flask, squeeze bottle, thermometer capable of reading to the nearest 0.5 °C, funnel, stopper and tubing for connecting flask to vacuum supply and vacuum supply capable of achieving a gauge vacuum of 660 mm Hg. The typical values of specific gravity are presented in Table 3.2.

Table 3.2: Typical values of specific gravity (Roy & Bhalla, 2019)

Soil type	Specific gravity
Sand	2.65 - 2.67
Silty sand	2.67 - 2.7
Inorganic clay	2.7 - 2.8
Soil with mica or iron	2.75 - 3
Organic soil	1.0 - 2.6

3.5.2.4. Standard Compaction Test

It is performed to determine the relationship between soil maximum dry density and optimum moisture content for a specified compaction energy. The compaction test can be performed by standard or modified procedures. In this study the test was conducted according to ASTM D698: standard test method for laboratory compaction characteristics of soil using standard effort. For one specimen around 2.5 kg air-dried soil passing No. 4 sieve size was used. Equipment used to perform laboratory standard compaction is standard proctor compaction hammer, compaction mold, collar, and stand, large screwdriver, cutting bar, balance capable of measuring to the nearest 0.01 g, drying oven, 3 soil moisture containers and permanent marker.

3.5.3. Static Soil Property Test

3.5.3.1. 1D - Consolidation Test

The Awash Melkasa town soil may have been pre-consolidated during the geologic past either by natural loads or by human-made loads or even by the decrease of the groundwater table. This test was done to get better understanding on stress history of the soil under study. The test was conducted according to ASTM D2435: standard test method for one-dimensional consolidation properties of soils using odometer apparatus for the 3 m depth soil samples. The soil sample were remolded at field density of size 50 mm in diameter and 20 mm high. The main reason for conducting this test is, the test result (pre-consolidation pressure) is mandatory to calculate the maximum shear modulus. Equipment used to perform a one-dimensional consolidation test is soil trimming equipment, consolidation ring, consolidation cell, filter paper, calipers, consolidation load frame, deformation indicator capable of measuring to the nearest 0.001 mm, timer, squeeze bottle, two oven-safe moisture content containers, balance capable of measuring to the nearest 0.01 g; and soil drying oven set at 110° ± 5 °C.

3.5.4. Dynamic Soil Property Test

3.5.4.1. Cyclic Simple Shear Test Machine

In the laboratory, the dynamic properties of soil can be determined from different kinds of machine. These include resonant column, ultrasonic pulse, piezoelectric bender element, cyclic direct simple shear, cyclic triaxial, and cyclic torsional shear (Kumar et al., 2013). From these machines for this study we were utilized cyclic direct simple shear test machines.

The cyclic simple shear machine has a better representation of the idealized field stress conditions, the principal stresses continuously rotate due to the application of shear stress as almost like those imposed on the soil element in the field subjected to vertically propagating shear waves and that we can also directly measure shear stress and shear strain. But it has a limitation on the distribution of stress at the specimen boundaries, shear stress is only applied to the top and bottom surfaces of the specimen, and since no complementary shear stresses are imposed on the vertical sides and therefore the moment caused by the horizontal shear stresses must be balanced by non-uniformly distributed shear and normal stresses (Vos, 2003).

The cyclic simple shear tests can be conducted for a wider range of strain amplitude (10^{-2} % - 5 %). This range is the general range of strain encountered in the ground motion during seismic activities. The pore water pressure can be measured at the boundary (Das, 2011). The cyclic simple shear machine contains either of a rectangle box made of hinged plates or a cylindrical wire-reinforced membrane which surrounds the specimen and confines the specimen from enlarging laterally in all direction for the duration of consolidation stage, but permits the soil specimen to deform horizontally at the time of cyclic loading test (Vos, 2003).

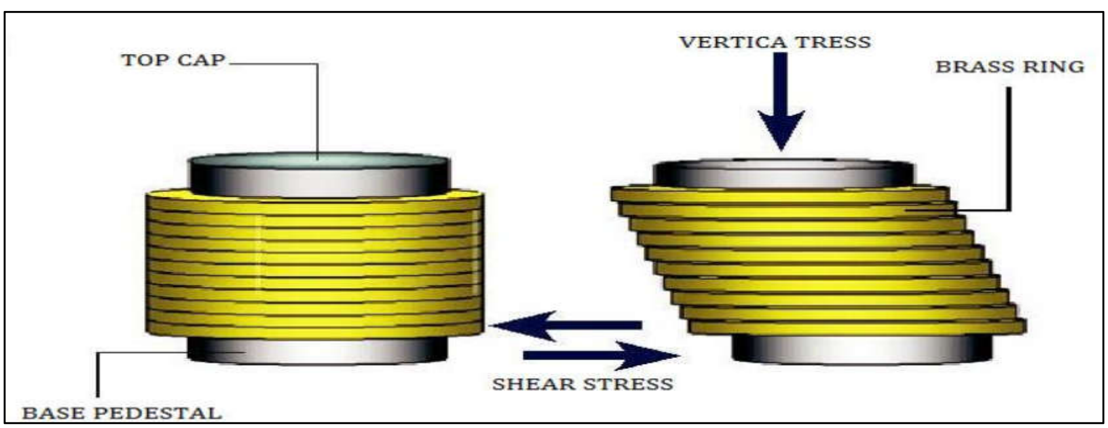

Figure 3.6: Cylindrical soil sample surrounded by wire-reinforced membrane (Mengistu, 2015)

The cyclic direct simple shear machine is linked to an electronic reading system. This reading system records axial displacement and force, lateral displacement and force. This system is governed by the UTS004 software application program that incorporates the functionality to perform consolidation, cyclic simple shear, and linear displacement rate shear. And also, the simple shear machine comprises of the features that is assembled for applying a constant vertical load or for keeping a constant sample height while measuring the vertical load. Figure 3.6 shows a mechanism for applying a horizontal cyclic shear load (Vos, 2003).

The size of specimen used in cyclic simple shear tests, usually 20 – 30 mm high with a side length (or diameter) of 60 - 80 mm (Das, 2011). The effect of non-homogeneity of stress distribution can be minimized by increasing the diameter/height ratio of the specimen: such effects are major at diameter/height ratios smaller than about 8:1. The cyclic simple shear machine present in AAiT has the effect of non-uniformity stress condition because it's diameter/height ratio is 7:2. To control this effect we used rough plate.

The cyclic simple shear is a plane strain machines. The shear strain is induced by horizontal movement at the bottom of the sample relative to the top. The width (or diameter) of the sample remains constant; therefore, any volume change could only be due to vertical movement of the top platen. The system is designed to permit a sample to be consolidated and then sheared under constant volume conditions. We were attained a constant-volume shearing condition by adjusting the vertical load, due to this shearing condition the height of laterally confined cylindrical specimen was constant (Zehtab, 2010). After consolidation was completed, the shear test was performed by applying a horizontal shear strain to the specimen at a predetermined rate.

3.5.4.2. Cyclic Simple Shear Test Procedure

The completion of cyclic simple shear test passes through three stages. The first stage is specimen preparation and setting up the test apparatus. The second stage is the consolidation stage and the final stage is a constant-volume shearing stage. The phases of this test, which are consistent with ASTM D 6528 standard, are explained below.

A. Sample Preparation and Setting Up the Test Machine

The pulverized soil that passes through sieve No.4 (4.75 mm sieve) were remolded cylindrically to the size of 20 mm height and 70 mm diameter at field density and natural moisture content. Then carefully placed the sample on the fixed bottom plate.

Then we placed cylindrical wire-reinforced rings around the specimen that confines the specimen from enlarging laterally in all direction for the duration of consolidation stage, but permits the soil specimen to deform horizontally at the time of cyclic loading test. Then we fix the loading ram on the top of the specimen. Finally, the vertical load cell connected to the top frame to the top plate to complete the test setup.

The axial stresses (pressures) during consolidation maybe 20, 50, 100, 150, 200, 250, 300, 350 and 400 kPa. The strain ranges are between 0.01 % and 5 %. The cyclic behavior of the soil is relatively insensitive to the frequency of the applied cyclic load within the range of 0.5 to 2 Hz (Hailemariam, 2017). In most seismic events, the number of significant cycles is likely to be less than 20. For practical purpose the 5^{th} cycles are likely provide reasonable values (Das, 2011). Sinewave gives approximately 30 % higher cyclic strength than the rectangular or triangular waveforms (Kumar et al., 2013), so for this study we utilize sine waveform of cyclic loading.

The method of sample preparation utilized for this study was the tamping specimen preparation technique and the method of loading was sinusoidal wave with 1Hz frequency, 40 number cycles were used. Axial/normal stresses of 150 kPa, 275 kPa and 400 kPa and shear strain 0.01 %, 0.1 %, 1 %, 2.5 %, and 5 % were also selected. Cyclic simple shear test provides simply raw data from 50 data points and 40 numbers of cycles for single cyclic loading in the form of Microsoft excel. Hence, for a complete test of any selected pressure and amplitude, 2000 data points were recorded.

Table 3.3: Axial stress and shear strain values used for the cyclic simple shear test

<table>
<tr><th>Test pit No.</th><th>Test pit location</th><th>Depth (m)</th><th>Designation</th><th>Sample type</th><th>Axial stress (kPa)</th><th colspan="5">Shear strain γ (%)</th></tr>
<tr><td rowspan="3">TP-1</td><td rowspan="3">Primary school</td><td rowspan="3">3.00</td><td rowspan="3">P @ 3 m</td><td rowspan="3">Remolded to field condition</td><td>150</td><td>0.01</td><td>0.1</td><td>1</td><td>2.5</td><td>5</td></tr>
<tr><td>275</td><td>0.01</td><td>0.1</td><td>1</td><td>2.5</td><td>5</td></tr>
<tr><td>400</td><td>0.01</td><td>0.1</td><td>1</td><td>2.5</td><td>5</td></tr>
<tr><td rowspan="3">TP-2</td><td rowspan="3">High school</td><td rowspan="3">3.00</td><td rowspan="3">H @ 3 m</td><td rowspan="3">Remolded to field condition</td><td>150</td><td>0.01</td><td>0.1</td><td>1</td><td>2.5</td><td>5</td></tr>
<tr><td>275</td><td>0.01</td><td>0.1</td><td>1</td><td>2.5</td><td>5</td></tr>
<tr><td>400</td><td>0.01</td><td>0.1</td><td>1</td><td>2.5</td><td>5</td></tr>
<tr><td rowspan="3">TP-3</td><td rowspan="3">Mesino</td><td rowspan="3">3.00</td><td rowspan="3">M @ 3 m</td><td rowspan="3">Remolded to field condition</td><td>150</td><td>0.01</td><td>0.1</td><td>1</td><td>2.5</td><td>5</td></tr>
<tr><td>275</td><td>0.01</td><td>0.1</td><td>1</td><td>2.5</td><td>5</td></tr>
<tr><td>400</td><td>0.01</td><td>0.1</td><td>1</td><td>2.5</td><td>5</td></tr>
</table>

B. Consolidation Stage

After setting up the test, the consolidation phase of the test was initiated. The normal stress for consolidation was set to a pre-selected value. The consolidation stage is just the application of static axial (vertical) loading stress to the sample while the lateral loading (shear) axis is held stationary. Axial stress and sample displacements (axial and lateral) data are measured over time and logged by the system. Logged data is also showed to the operator in the form of graphs and tables as the test stage proceeds. The consolidation stage was continued until the rate of vertical strain becomes less than 0.05 % per hour. Since the confining pressure is the main factor that affecting the shear modulus of the soil. When the rate of vertical strain reaches this level axial strain against the time curve is closing to be horizontal see Figure 3.7, then the consolidation stage is manually terminated by the operator.

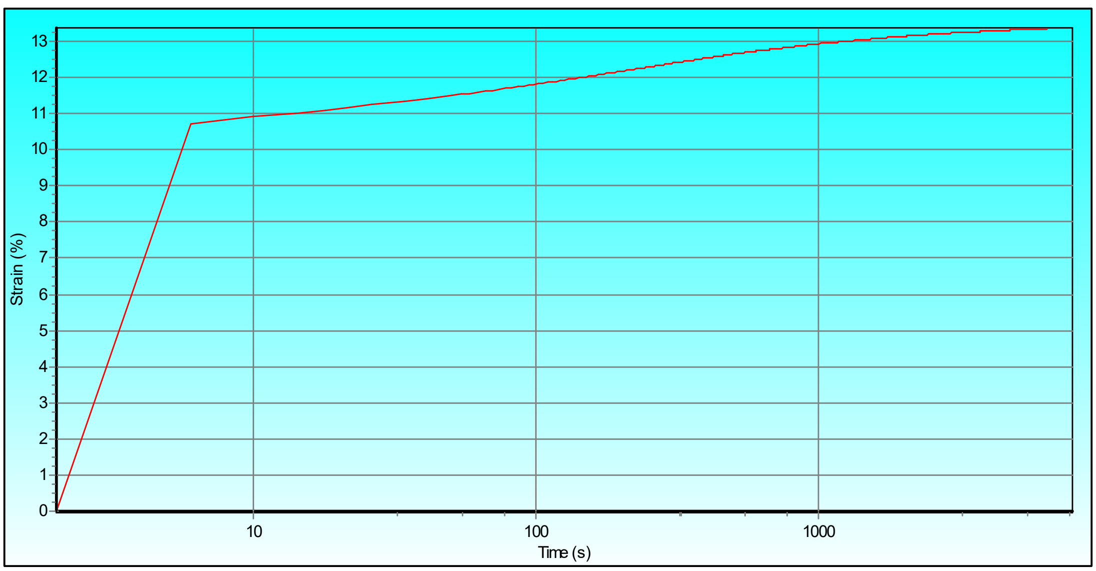

Figure 3.7: Consolidation stage of P @ 3 m under 150 kPa axial stress and 5 % shear strain amplitude

C. Cyclic Simple Shear Stage

After a consolidation phase, constant-volume cyclic shearing of the specimen began. The horizontal load history acting on specimen was considered as a sinusoidal waveform. The frequency of cyclic load, f, was 1.0 Hz. The cyclic shear stage of the test was conducted by applying a lateral cyclic shear force under stated amplitude. Due to the applied lateral shearing force the ring slides over each other, but the sliding couldn't cause any volume change on the specimen. In this stage the constant volume was maintained by keeping the specimen height constant.

The output obtained from cyclic simple shear test, for single cyclic load is series of row data. This row data includes Axial Lvdt, Axial Force, Ext Axial Lvdt, Lateral Lvdt and Lateral Force of 50 data points. These data can be showed in the form of wave shapes, charts and Microsoft excel. From these row data, Lateral Lvdt (specimen displacements) and Lateral force were used to compute the shear stress (τ) and shear strain (γ) values. Also the calculated shear stress (τ) and shear strain (γ) values were used to compute the dynamic soil parameters (shear modulus and damping ratio).

3.6. Soil Classification

The most used soil classification systems are Unified Soil Classification System (USCS) and American Association of State Highway and Transportation Officials (AASHTO). For this study to classify the soil both soil classification systems USCS (ASTM D2487, 2004) and AASHTO (ASTM D 3282 , 2004) were used.

CHAPTER FOUR

RESULTS AND DISCUSSION

4.1. Soil Type Determination

4.1.1. In- Situ Density and Moisture Content Test

From the results, it was observed that the bulk density varies from 1.02 to 1.45 g/cm^3 and moisture content varies from 5.17 to 22.96 %. The test results are shown in Table 4.1. the detailed analysis of the field test result is given in [Appendix-A].

Table 4.1: In-situ test result

Test pit No.	Test pit location	Depth (m)	Designation	In-situ bulk density (g/cm^3)	In-situ dry density (g/cm^3)	Natural moisture content (%)
TP-1	Primary school	1.75	P @ 1.75 m	1.25	1.10	13.01
		3	P @ 3 m	1.45	1.33	9.20
TP-2	High school	1.5	H @ 1.5 m	1.05	0.91	15.00
		3	H @ 3 m	1.02	0.97	5.17
TP-3	Mesino	2	M @ 2 m	1.32	1.08	22.96
		3	M @ 3 m	1.23	1.03	19.61

4.1.2. Particle Size Analysis

Particle size analysis is widely used to classify soil for engineering purposes. In this study the test was conducted according to ASTM D422 (Wet sieve) and ASTM D1140 (Hydrometer test). A summary of particle size distribution curves is shown in Figure 4.1 below. Form the figure we can see that most of the samples are finer than No. 200 (75µm) sieve. This shows that the collected soil samples are fine soil. The sieve analysis result and grain size distribution curve for each test pits depth are given in [Appendix-B].

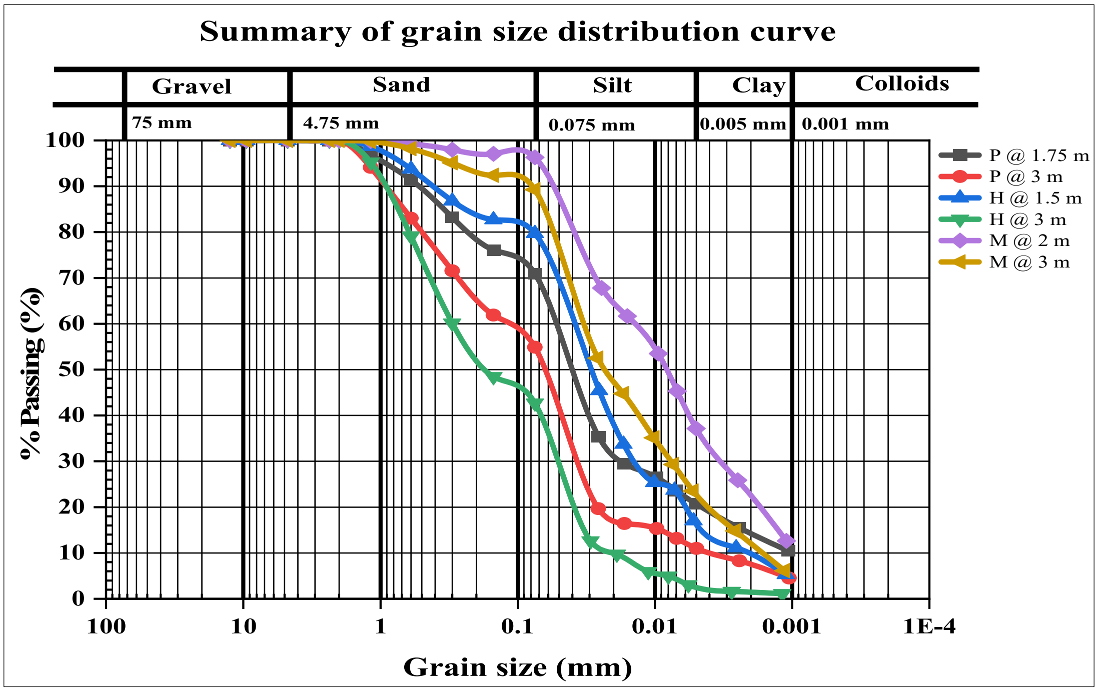

Figure 4.1: Summary of particle size distribution curves

4.1.3. Atterberg Limit Test

The Atterberg limit tests are used to measure the critical water contents of fine-grained soil. The tests were conducted according to ASTM D4318 on soil passing No. 40 (425 µm) sieve. The test result of LL, PL, and PI of this study are summarized in Table 4-2 and also the summary of the liquid limit test graph is shown in Figure 4.2. From the test results the Liquid Limit varies from 32.8 % to 63.3 %, Plastic Limit varies from 19.03 % to 45.96 % and Plasticity Index varies from 3.92 to 30.36 for all the specimens except H @ 3m specimen. The detail test result for each test pits depth are given in [Appendix-C].

Table 4.2: Summary of Atterberg limit tests result

Test pit No.	Test pit location	Depth (m)	Designation	Liquid limit (LL)	Plastic limit (PL)	Natural moisture content	Plasticity index (PI)	Liquidity index (LI)	State of soil
TP-1	Primary school	1.75	P @ 1.75m	63.3	32.94	13.01	30.36	-0.66	Semi solid
		3.00	P @ 3m	48.4	19.03	9.20	29.37	-0.33	Semi solid
TP-2	High school	1.50	H @ 1.5m	42.2	38.28	15.00	3.92	-5.93	Semi solid
		3.00	H @ 3m	32.8	NP	5.17	0	-	-
TP-3	Mesino	2.00	M @ 2m	54.3	37.12	22.96	17.18	-0.82	Semi solid
		3.00	M @ 3m	58.73	45.96	19.61	12.77	-2.06	Semi solid

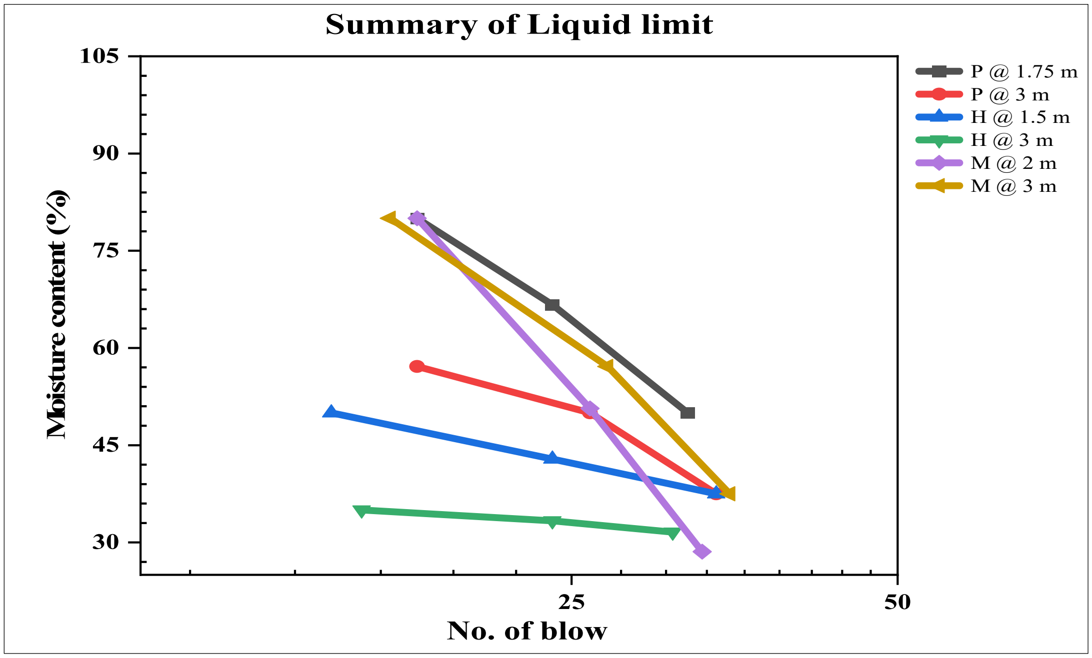

Figure 4.2: Summary of liquid limit curves

4.1.4. Soil Classification According to USCS

This classification system was performed according to ASTM D2487. Based on USCS soil from P @ 1.75 m, M @ 2 m and M @ 3 m are Elastic silt soil (MH), P @ 3 m are Lean clay soil (CL), H @ 1.5 m is Lean silt soil (ML), and H @ 3 m is None plastic silt soil. Table 4.3 shows the classification of soils which is based on a plasticity chart and grain size distribution.

Table 4.3: Classification according to USCS

Test pit location	Depth (m)	% passing #4 (4.75mm) sieve	% passing #200 (0.075mm) sieve	Liquid limit (LL)	Plastic limit (PL)	Plasticity index (PI)	USCS classification	
							Symbol	Name
Primary school	1.75	100	70.92	63.3	32.94	30.36	MH	Elastic silt
	3	100	54.9	48.4	19.03	29.37	CL	Lean clay
High school	1.5	100	79.72	42.2	38.28	3.92	ML	Lean silt
	3	100	42.7	32.8	NP	0	M	None plastic silt
Mesino	2	100	96.3	54.3	37.12	17.18	MH	Elastic silt
	3	100	89.26	58.73	45.96	12.77	MH	Elastic silt

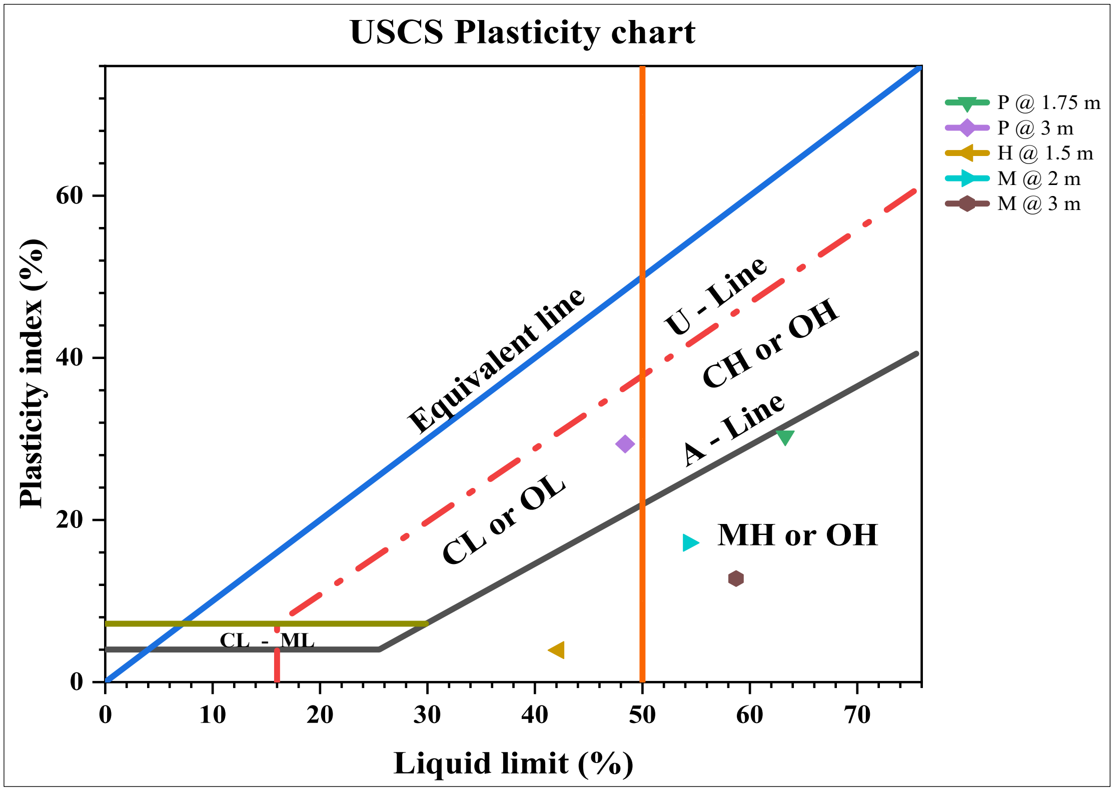

Figure 4.3: USCS soil plasticity chart

4.1.5. Soil Classification According to AASHTO

This classification system was performed according to ASTM D3282. Based on AASHTO soil classification, soil group of P @ 1.75 m, M @ 2 m and M @ 3 m are A-7-5, P @ 3 m is A-7-6, H @ 1.5 m and H @ 3 m are A-5 soil. Table 4.4 shows the classification of soils. which is based on a plasticity chart and grain size distribution.

Table 4.4: Soil classification according to USCS

Test pit location	Depth (m)	% of particles passing #10 (2 mm) sieve	% of particles passing #200 (0.075 mm) sieve	Liquid limit (LL)	Plastic limit (PL)	Plasticity index (PI)	AASHTO classification	
							Group name	Constituent materials
Primary school	1.75	100	70.92	63.3	32.94	30.36	A-7-5 (20)	Clayey soil
	3	100	54.9	48.4	19.03	29.37	A-7-6 (13)	Clayey soil
High school	1.5	100	79.72	42.2	38.28	3.92	A-5 (6)	Silty soil
	3	100	42.7	32.8	NP	0.00	A-5	Silty soil
Mesino	2	100	96.3	54.3	37.12	17.18	A-7-5 (20)	Clayey soil
	3	100	89.26	58.73	45.96	12.77	A-7-5 (18)	Clayey soil

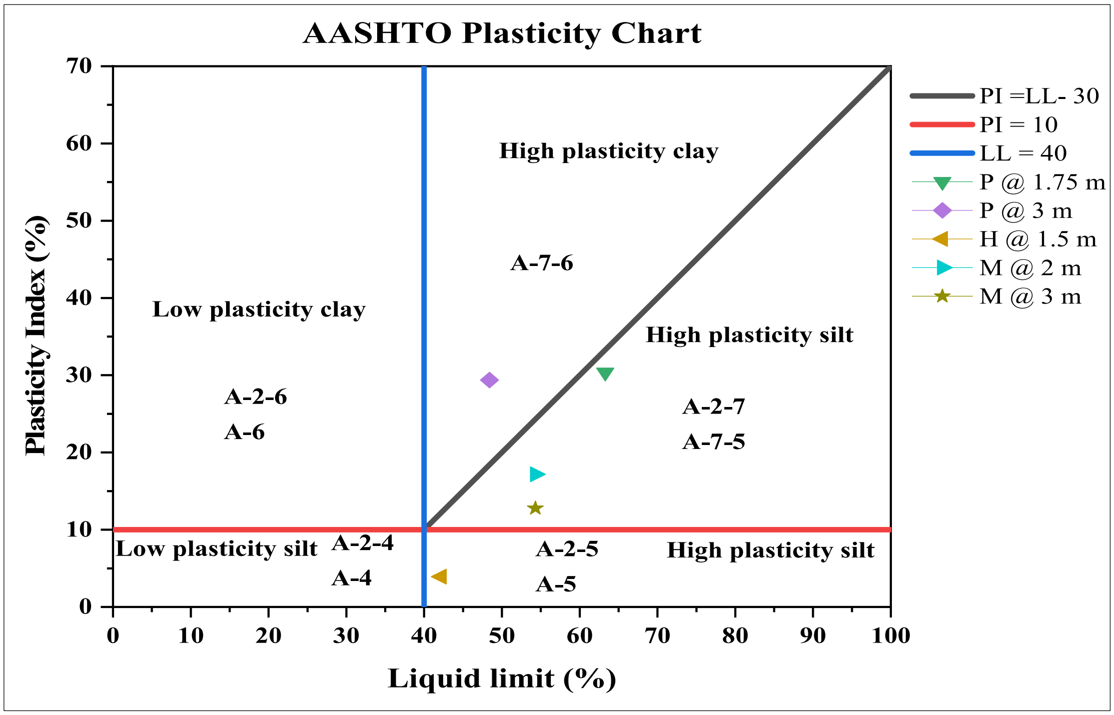

Figure 4.4: AASHTO soil plasticity chart

4.1.6. Specific Gravity Test

Table 4.5 shows the test procedure and test result of P @ 1.75 m soil sample and the remaining specific gravity test results are shown in Table 4.6 below. The specific gravity of the sample is found to vary between 2.25 to 2.72. The remaining samples test data and result are presented in [Appendix-D].

Table 4. 5: Specific Gravity determination for P @ 1.75 m

Specific gravity for P @ 1.75 m		
Determination No.	1	2
Pycnometer No.	P_1	P_2
Mass of pycnometer filled with soil and water, M_b(g)	168.98	171.16
Mass of pycnometer filled with water, M_a (g)	160	162
Mass of pycnometer with dry soil (g)	77	77
Mass of Pycnometer (g)	62	62
Mass of dry soil, Mo (g)	15	15
Specific gravity of soil solids, $G_s = M_o/(M_o + (M_a - M_b))$	2.49	2.57
Average specific gravity	2.53	

Table 4.6: Summary of index properties test result

Test pit location		Primary school		High school		Mesino	
Designation		P @ 1.75 m	P @ 3 m	H @ 1.5 m	H @ 3 m	M @ 2 m	M @ 3 m
Depth (m)		1.75	3	1.5	3	2	3
ρ_b (g/cm^3)		1.25	1.45	1.05	1.02	1.32	1.23
ρ_d (g/cm^3)		1.10	1.33	0.91	0.97	1.08	1.03
G_s		2.53	2.72	2.46	2.25	2.42	2.35
Void ratio (e)		1.29	1.05	1.69	1.33	1.25	1.28
Natural moisture content, w (%)		13.01	9.20	15.00	5.17	22.96	19.61
LL (%)		63.30	48.40	42.20	32.80	54.3	58.73
PL (%)		32.94	19.03	38.28	NP	37.12	45.96
PI (%)		30.36	29.37	3.92	0	24.38	12.77
Percentage of grain	Medium sand (%)	8.58	16.96	6.22	20.88	0.74	1.80
	Fine sand (%)	20.50	28.14	14.06	36.42	2.96	8.94
	Silt (%)	52.48	45.07	65.49	40.48	63.99	70.02
	Clay (%)	7.95	5.32	8.91	1.09	19.69	13.10
	Colloids (%)	10.48	4.52	5.31	1.13	12.62	6.13
Soil classification according to USCS		MH	CL	ML	M	MH	MH
Soil classification according to AASHTO		A-7-5	A-7-6	A-5	A-5	A-7-5	A-7-5

4.1.7. Standard Compaction Test

A compaction test is used to determine the relationship between the dry density and moisture content of the soil. The test was conducted according to ASTM D698 standard method. For one specimen around 2.5 kg air-dried soil passing No. 4 sieve size was used. The summary of test results is shown in Figure.4.5. From the test result, it was observed that P @ 3 m has higher dry density and lower water content. The graph of each sample test result are presented in [Appendix-E].

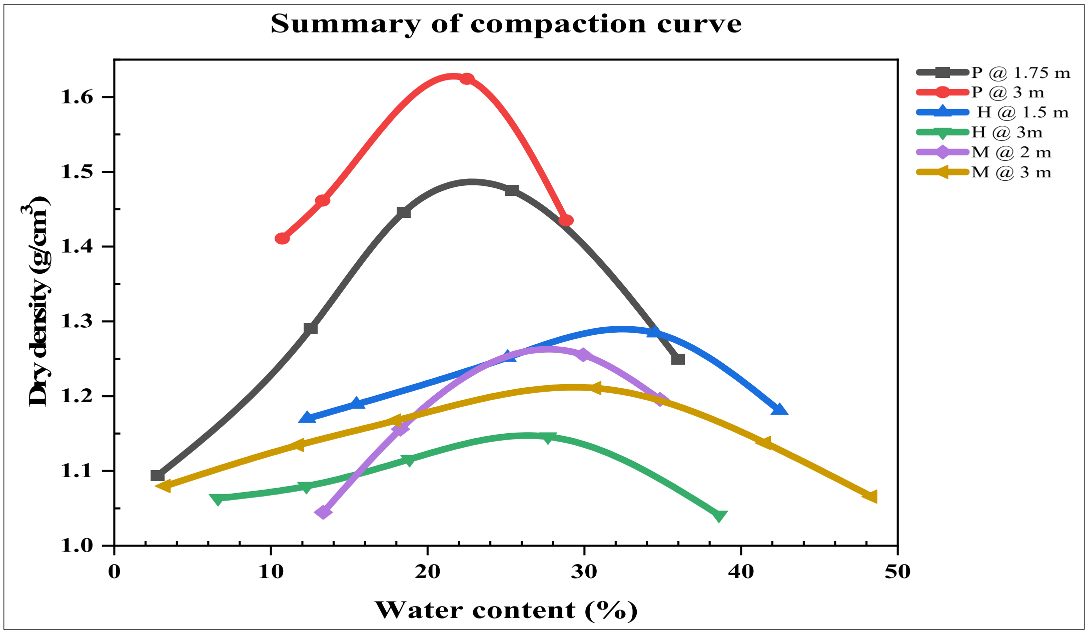

Figure 4.5: Summary of compaction tests result

4.1.8. 1D - Consolidation Test

This test was done to get better understanding on stress history of the soil under investigation. The test was conducted according to ASTM D2435 standard using odometer apparatus. The test was conducted to determine the pre-consolidation pressure. Pre-consolidation pressures of P @ 3 m, H @ 3 m, and M @ 3 m were 129 kPa, 136 kPa, and 166 kPa respectively. The pre-consolidation values of the soils are shown in Figure 4.6, 4.7, and 4.8.

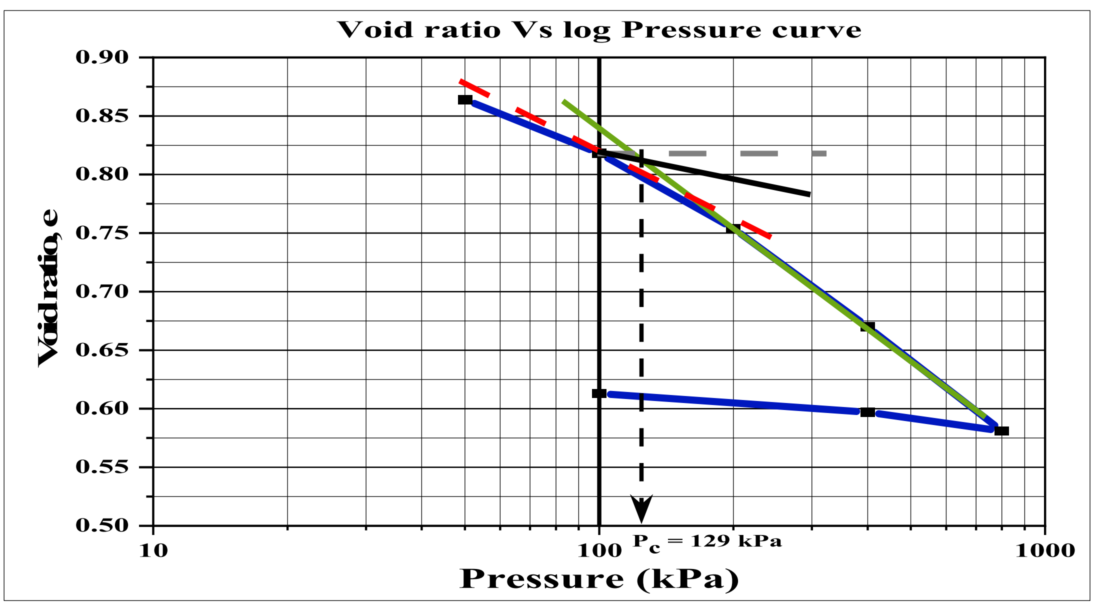

Figure 4.6: Pre-consolidation result of P @ 3 m (Lean clay soil)

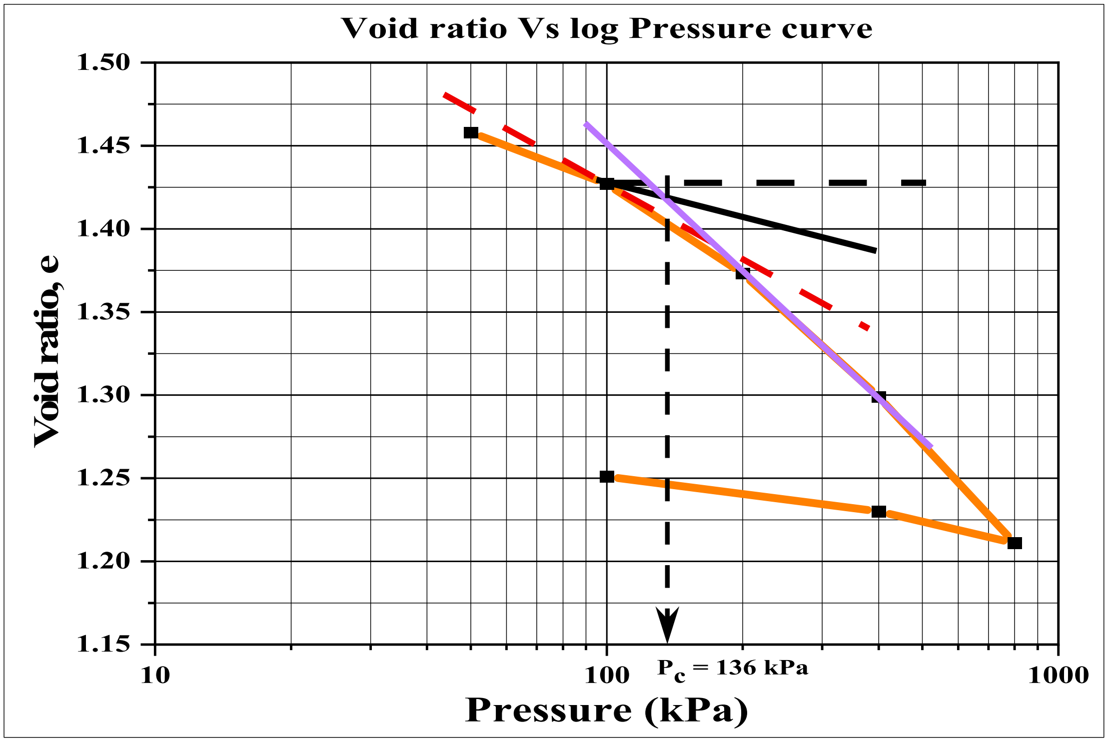

Figure 4.7: Pre-consolidation result of H @ 3 m (None plastic silt soil)

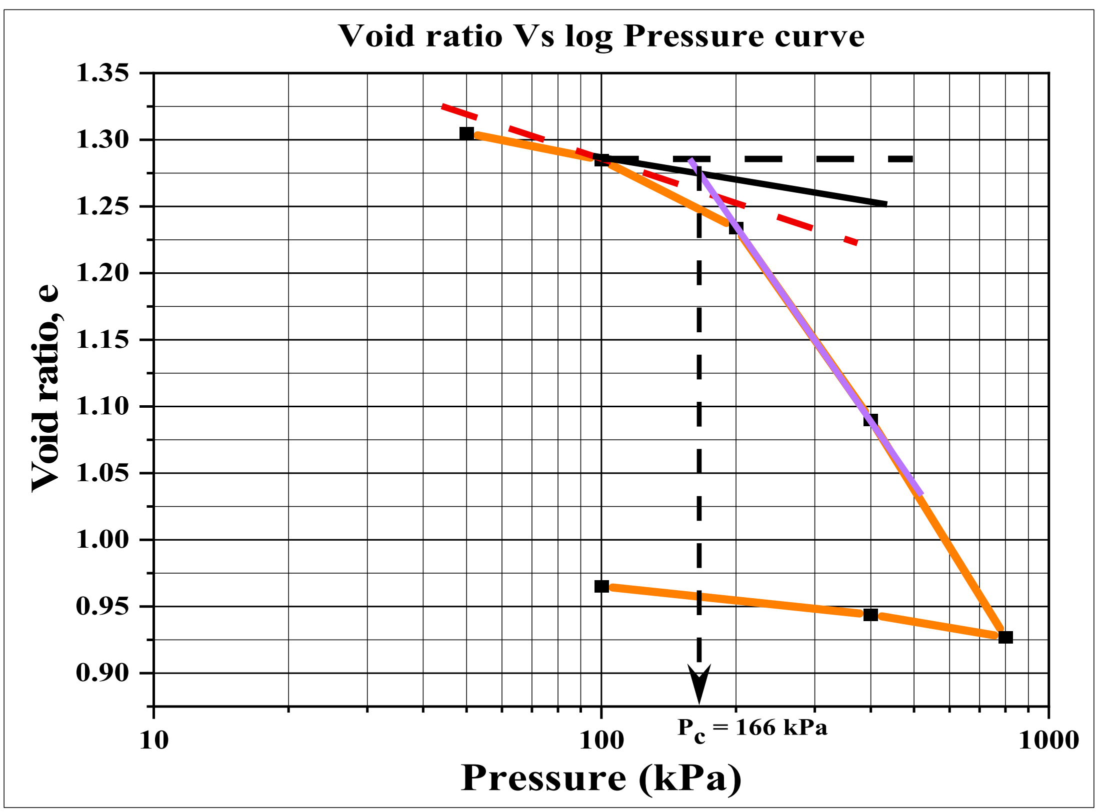

Figure 4. 8: Pre-consolidation result of M @ 3 m (Elastic silt soil)

4.2. Shear Modulus and Damping Ratio Results

The output obtained from cyclic simple shear test, for single cyclic load is series of row data. This row data includes Axial Lvdt, Axial Force, Ext Axial Lvdt, Lateral Lvdt and Lateral Force of 50 data points. Table 4.7 shows output obtained from cyclic simple shear test software, for single cyclic load of P @ 3 m at 5th cycle under 150 kPa axial stress and 5 % shear strain.

Table 4.7: Output obtained from cyclic simple shear test software for P @ 3 m of single cyclic load at 5th cycle under 150 kPa axial stress and 5 % shear strain

Time	Axial Lvdt (mm)	Axial Force (kN)	Ext Axial Lvdt (mm)	Lateral Lvdt (mm)	Lateral Force (kN)
0	-2.78935	-0.08263	-1.02008	-0.11205	-0.01148
0.019	-2.7107	-0.06306	-1.01926	-0.04506	-0.00778
0.038	-2.63016	-0.06594	-1.01877	0.00387	0.00377
0.057	-2.55114	-0.0663	-1.01883	0.06821	0.01402
0.076	-2.51134	-0.02308	-1.01886	0.11937	0.02345
0.095	-2.50302	0.02029	-1.01623	0.17101	0.03611
0.114	-2.49855	0.03463	-1.01354	0.21893	0.04828
0.133	-2.49821	0.03115	-1.01395	0.26751	0.0601
0.152	-2.49778	0.02815	-1.01385	0.30144	0.07254
0.171	-2.49773	0.03144	-1.01344	0.3342	0.08738
0.19	-2.49787	0.02435	-1.01338	0.36084	0.10371
0.209	-2.49878	0.01774	-1.0135	0.38321	0.11975
0.228	-2.50242	-0.00718	-1.0135	0.40112	0.13031
0.247	-2.50777	-0.04405	-1.0139	0.41491	0.13707
0.266	-2.51481	-0.07832	-1.01544	0.42066	0.13912
0.285	-2.54545	-0.07996	-1.01621	0.42283	0.13949
0.304	-2.62538	-0.07944	-1.01655	0.42266	0.13636
0.323	-2.63025	-0.07866	-1.01929	0.40884	0.10473
0.342	-2.60848	-0.06595	-1.02067	0.36604	0.05513
0.361	-2.54691	-0.0666	-1.02056	0.33549	0.02767
0.38	-2.50488	-0.02518	-1.01427	0.29623	-0.00769
0.399	-2.49858	-0.02601	-1.00741	0.23212	-0.02178
0.418	-2.52516	-0.0801	-1.00925	0.19055	-0.03425
0.437	-2.75256	-0.08361	-1.00977	0.11585	-0.03441
0.456	-2.94416	-0.14406	-1.00997	0.08043	-0.04298
0.475	-3.00324	-0.1618	-1.02523	0.00215	-0.05226
0.494	-2.88276	-0.09295	-1.02735	-0.04002	-0.06393
0.513	-2.64215	-0.06466	-1.02788	-0.11763	-0.07395
0.532	-2.4977	0.02124	-1.01428	-0.17145	-0.0719
0.551	-2.49609	0.01169	-1.01003	-0.23058	-0.08097
0.57	-2.49953	-0.01671	-1.01207	-0.27399	-0.1007
0.589	-2.51046	-0.07799	-1.01487	-0.34128	-0.10834

0.608	-2.59609	-0.08011	-1.01625	-0.37338	-0.12386
0.627	-2.62942	-0.07991	-1.0163	-0.43635	-0.1389
0.646	-2.6406	-0.07983	-1.01266	-0.45489	-0.14973
0.665	-2.66864	-0.08033	-1.01402	-0.5089	-0.16846
0.684	-2.69368	-0.07979	-1.01854	-0.51737	-0.17577
0.703	-2.69966	-0.08024	-1.01593	-0.54687	-0.19841
0.722	-2.69903	-0.07995	-1.01612	-0.56218	-0.20868
0.741	-2.69943	-0.07936	-1.01618	-0.56601	-0.21886
0.76	-2.69934	-0.08029	-1.01618	-0.57242	-0.22172
0.779	-2.69908	-0.07957	-1.01647	-0.57694	-0.2118
0.798	-2.6992	-0.07944	-1.01618	-0.57617	-0.22131
0.817	-2.69711	-0.07974	-1.0162	-0.57208	-0.20551
0.836	-2.69185	-0.07828	-1.01523	-0.55797	-0.17111
0.855	-2.69079	-0.07847	-1.01325	-0.52939	-0.12979
0.874	-2.69104	-0.07836	-1.01326	-0.48796	-0.08898
0.893	-2.69734	-0.08024	-1.01286	-0.43337	-0.05648
0.912	-2.77055	-0.08288	-1.01356	-0.36814	-0.03937
0.931	-2.87838	-0.11825	-1.01583	-0.11205	-0.01148

4.2.1. Hysteresis Loop and Values of Shear Stress and Shear Strain

Figure.4.9 shows the shear stress - shear strain hysteretic relationships off P @ 3 m soil under 150 kPa axial pressure and 5 % cyclic shear strain of 40 cycle.

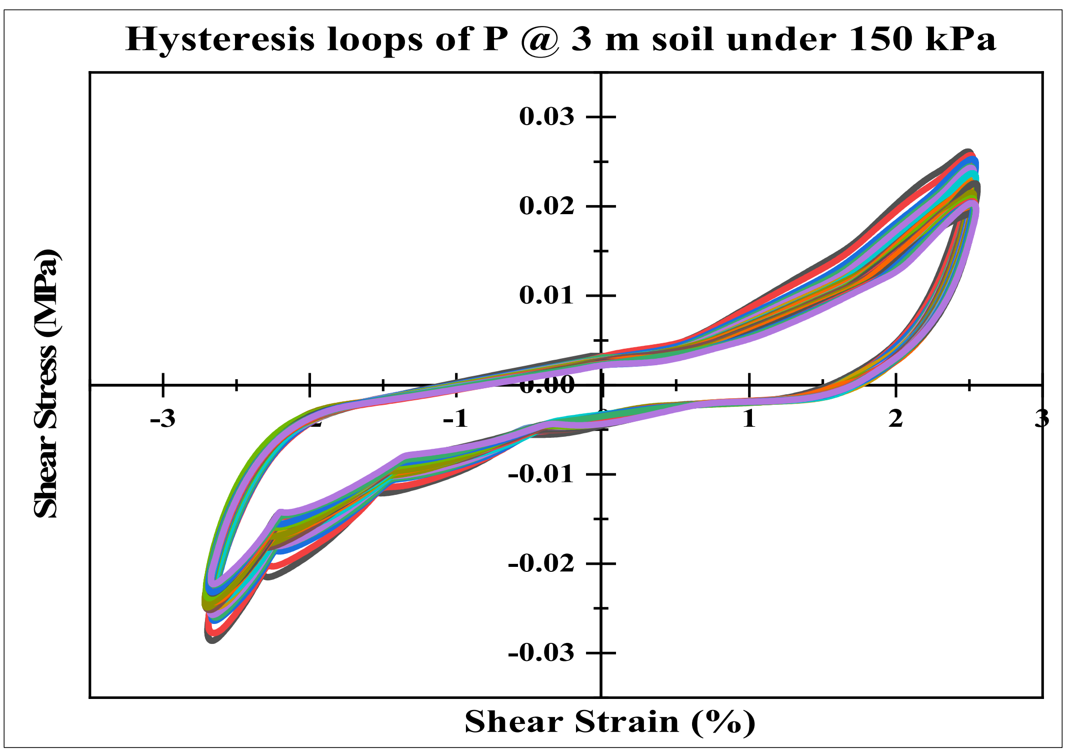

Figure 4.9: Hysteresis loops of P @ 3 m soil under 150 kPa axial pressure and 5 % cyclic shear strain of 40 cycle

The shear stress and shear strain values for single cyclic load of P @ 3 m soil under 150 kPa axial pressure and 5 % cyclic shear strain at the 5th cycle are presented in Table 4.8 and it is determined by using Eq. (2.4) and Eq. (2.6). Figure 4.10 shows the hysteresis loop of P @ 3 m soil under 150 kPa axial pressure and 5 % cyclic shear strain at the 5th cycle.

Table 4.8: Shear stress and shear strain values for single cyclic load of P @ 3 m at 5th cycle under 150 kPa axial stress and 5 % shear strain

Time (Sec.)	Lateral Lvdt (mm)	Lateral Force, F (kN)	Sample Area, A (mm^2)	Shear Stress $(F/A) * 100$ (MPa)	Shear Strain $\frac{Lateral\ Lvdt}{19.195} * 100$ (%)
0	-0.112	-0.011	3848.45	-0.00298	-0.584
0.019	-0.045	-0.008	3848.45	-0.00202	-0.235
0.038	0.004	0.004	3848.45	0.00098	0.020
0.057	0.068	0.014	3848.45	0.00364	0.355
0.076	0.119	0.023	3848.45	0.00609	0.622
0.095	0.171	0.036	3848.45	0.00938	0.891
0.114	0.219	0.048	3848.45	0.01255	1.141
0.133	0.268	0.060	3848.45	0.01562	1.394
0.152	0.301	0.073	3848.45	0.01885	1.570
0.171	0.334	0.087	3848.45	0.02271	1.741
0.19	0.361	0.104	3848.45	0.02695	1.880
0.209	0.383	0.120	3848.45	0.03112	1.996
0.228	0.401	0.130	3848.45	0.03386	2.090
0.247	0.415	0.137	3848.45	0.03562	2.162
0.266	0.421	0.139	3848.45	0.03615	2.192
0.285	0.423	0.139	3848.45	0.03625	2.203
0.304	0.423	0.136	3848.45	0.03543	2.202
0.323	0.409	0.105	3848.45	0.02721	2.130
0.342	0.366	0.055	3848.45	0.01433	1.907
0.361	0.335	0.028	3848.45	0.00719	1.748
0.38	0.296	-0.008	3848.45	-0.00200	1.543
0.399	0.232	-0.022	3848.45	-0.00566	1.209
0.418	0.191	-0.034	3848.45	-0.00890	0.993
0.437	0.116	-0.034	3848.45	-0.00894	0.604
0.456	0.080	-0.043	3848.45	-0.01117	0.419
0.475	0.002	-0.052	3848.45	-0.01358	0.011
0.494	-0.040	-0.064	3848.45	-0.01661	-0.208
0.513	-0.118	-0.074	3848.45	-0.01922	-0.613
0.532	-0.171	-0.072	3848.45	-0.01868	-0.893
0.551	-0.231	-0.081	3848.45	-0.02104	-1.201
0.57	-0.274	-0.101	3848.45	-0.02617	-1.427
0.589	-0.341	-0.108	3848.45	-0.02815	-1.778

0.608	-0.373	-0.124	3848.45	-0.03218	-1.945
0.627	-0.436	-0.139	3848.45	-0.03609	-2.273
0.646	-0.455	-0.150	3848.45	-0.03891	-2.370
0.665	-0.509	-0.168	3848.45	-0.04377	-2.651
0.684	-0.517	-0.176	3848.45	-0.04567	-2.695
0.703	-0.547	-0.198	3848.45	-0.05156	-2.849
0.722	-0.562	-0.209	3848.45	-0.05422	-2.929
0.741	-0.566	-0.219	3848.45	-0.05687	-2.949
0.76	-0.572	-0.222	3848.45	-0.05761	-2.982
0.779	-0.577	-0.212	3848.45	-0.05504	-3.006
0.798	-0.576	-0.221	3848.45	-0.05751	-3.002
0.817	-0.572	-0.206	3848.45	-0.05340	-2.980
0.836	-0.558	-0.171	3848.45	-0.04446	-2.907
0.855	-0.529	-0.130	3848.45	-0.03373	-2.758
0.874	-0.488	-0.089	3848.45	-0.02312	-2.542
0.893	-0.433	-0.056	3848.45	-0.01468	-2.258
0.912	-0.368	-0.039	3848.45	-0.01023	-1.918
0.931	-0.11205	-0.01148	3848.45	-0.00298	-0.584

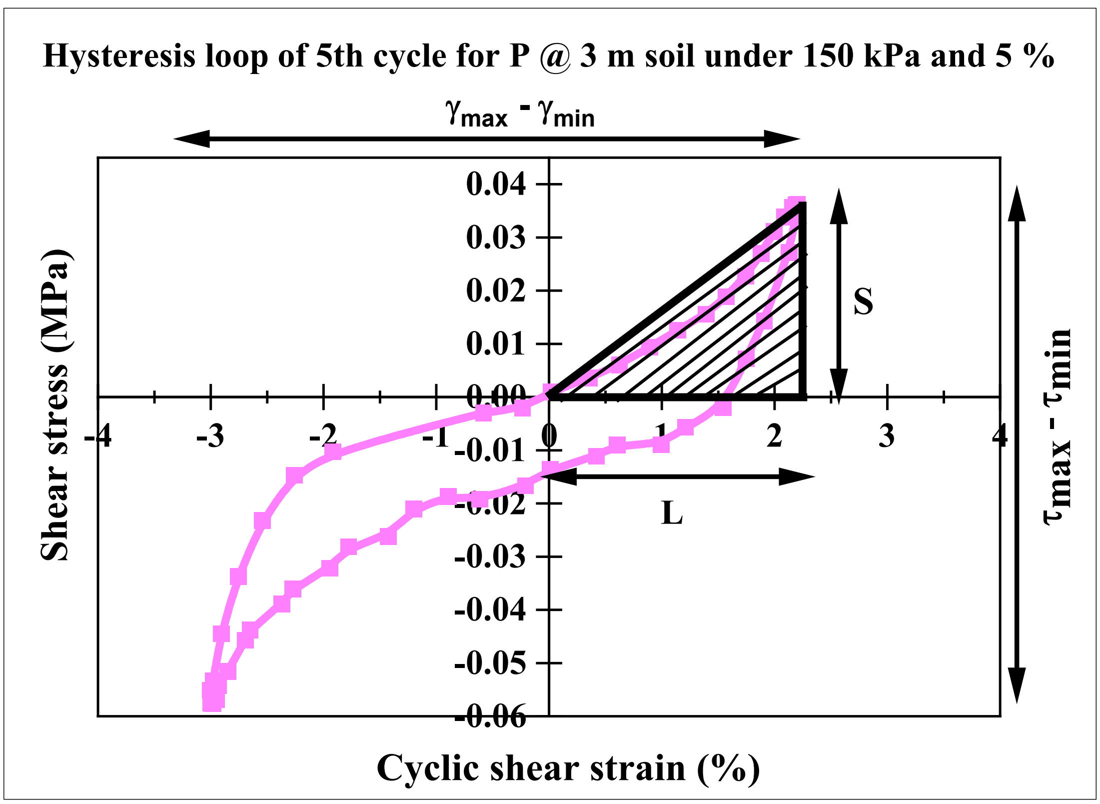

Figure 4.10: Hysteresis loops of P @ 3 m soil under 150 kPa axial pressure and 5 % cyclic shear strain of 5th cycle.

4.2.2. Determination of Shear Modulus and Damping Ratio

The values of shear modulus and damping ratio were determined from shear stress and shear strain value or from the hysteresis loop of P @ 3 m soil under 150 kPa axial pressure and 5 % cyclic shear strain at the 5th cycle and the result is presented in Table 4.10. A typical calculation of shear modulus and damping ratio are presented in Table 4.9.

Table 4.9: Typical calculation of shear modulus and damping ratio of P @ 3 m soil under 150 kPa and 5th cycle

Shear modulus (G)		Damping ratio (ξ)	
$\tau_{max} = S$	0.036246	$A_{loop} = \frac{1}{2}\sum_{i=1}^{n}(\tau_i - \tau_{i+1}) * (\gamma_i + \gamma_{i+1})$	0.000849254
τ_{min}	-0.05761		
$\gamma_{max} = L$	0.022028		
γ_{min}	-0.03006	$A_\Delta = \frac{1}{2} * (L * S)$	0.000399
$\tau_{max} - \tau_{min}$	0.093859		
$\gamma_{max} - \gamma_{min}$	0.052085		
$G\ (MPa) = \frac{(\tau_{max} - \tau_{min})}{(\gamma_{max} - \gamma_{min})}$	1.802	$\xi\ (\%) = \frac{A_{loop}}{4\pi A_\Delta} * 100\%$	16.929

The shear modulus and damping ratio value for the rest cycles are calculated in a similar manner. Table 4.10 shows shear modulus and damping ratio values of each cycle of P @ 3 m soil under 150 kPa axial loads and 0.01 %, 0.1 %, 1 %, 2.5 % and 5 % shear strain determined by using Eq. (2.7) and Eq. (2.8). The shear modulus and damping ratio values of other test pits at respective axial stresses and shear strains are shown under [Appendix - G].

Table 4.10: Shear modulus and damping ratio values for P @ 3 m soil under 150 kPa axial loads

Strain (%)	0.01	0.1	1	2.5	5	0.01	0.1	1	2.5	5
Cycle No.	Shear Modulus, G (MPa)					Damping Ratio, ξ (%)				
1	7.598	5.190	2.606	1.987	1.777	4.889	8.943	13.265	16.982	18.913
2	7.675	5.203	2.865	1.996	1.787	3.524	8.512	12.986	16.832	18.512
3	7.696	5.207	2.914	1.998	1.794	3.136	8.231	12.759	16.882	17.663
4	7.702	5.231	2.972	2.013	1.799	3.065	6.967	12.522	16.853	17.286
5	7.733	5.223	2.993	2.023	**1.802**	2.804	6.184	11.625	15.039	**16.929**
6	7.750	5.239	3.002	2.040	1.810	2.778	6.212	11.601	14.860	16.711
7	7.771	5.246	3.018	2.044	1.817	2.696	6.167	11.590	14.658	16.686
8	7.788	5.258	3.028	2.062	1.821	2.685	5.775	11.570	14.547	16.582

9	7.850	5.263	3.038	2.067	1.825	2.653	6.072	11.537	14.326	16.511
10	7.803	5.266	3.085	2.088	1.839	2.539	5.953	11.493	14.103	16.500
11	7.878	5.292	3.089	2.097	1.857	2.526	5.891	11.459	14.013	16.383
12	7.890	5.304	3.125	2.112	1.858	2.467	5.861	11.401	13.999	16.366
13	7.893	5.307	3.176	2.124	1.862	2.452	5.816	11.360	13.975	16.331
14	7.916	5.336	3.201	2.147	1.873	2.405	5.801	11.334	13.952	15.716
15	7.927	5.340	3.178	2.156	1.898	2.399	5.765	11.013	13.943	16.169
16	7.944	5.352	3.223	2.168	1.911	2.393	5.730	11.285	13.926	16.890
17	7.783	5.363	3.268	2.186	1.930	2.386	5.715	11.219	13.913	16.225
18	7.851	5.391	3.309	2.204	1.940	2.375	5.696	11.186	13.902	16.199
19	7.802	5.395	3.359	2.225	1.980	2.347	5.664	11.102	13.899	16.185
20	8.271	5.598	3.400	2.474	1.981	2.338	5.629	11.021	13.894	16.132
21	7.992	5.436	3.422	2.262	2.012	2.338	5.626	10.986	13.894	16.109
22	8.006	5.449	3.472	2.285	2.036	2.328	5.618	10.925	13.893	16.064
23	8.043	5.475	3.650	2.317	2.063	2.327	5.600	10.902	13.891	16.062
24	8.045	5.496	3.542	2.335	2.107	2.317	5.596	10.888	13.889	16.028
25	7.850	5.519	3.544	2.371	2.136	2.315	5.575	10.637	13.753	15.933
26	8.047	5.533	2.686	2.396	2.158	2.299	5.556	10.542	13.698	15.903
27	8.227	5.557	3.570	2.430	2.172	2.291	5.538	10.451	13.653	15.872
28	8.072	5.588	3.580	2.468	2.206	2.287	5.485	10.696	13.625	15.866
29	7.868	5.688	3.599	2.510	2.239	2.285	5.485	10.946	13.578	15.741
30	8.269	5.617	3.784	2.555	2.306	2.284	5.462	10.855	13.549	15.690
31	7.753	5.631	3.662	2.613	2.350	2.238	4.942	10.916	13.524	15.641
32	8.085	5.704	3.724	2.657	2.405	2.171	4.942	10.767	13.501	15.559
33	8.196	5.750	3.764	2.730	2.082	2.161	5.408	10.602	13.486	15.514
34	8.207	5.783	3.782	2.805	2.466	2.148	5.297	10.317	13.390	15.511
35	8.057	5.816	3.797	2.907	2.542	2.137	5.295	10.305	13.355	15.451
36	8.229	5.877	3.830	3.015	2.633	2.110	5.279	10.127	13.313	15.413
37	8.231	5.924	3.850	3.153	2.779	2.094	5.262	10.585	13.278	15.397
38	8.603	5.935	3.880	3.323	2.799	2.074	5.243	10.478	13.249	14.928
39	8.649	5.965	3.903	3.545	2.812	2.074	5.175	10.425	13.192	14.920
40	8.953	6.022	4.033	3.061	2.833	2.071	5.128	10.412	13.173	14.829

4.3. Determination of Initial (Maximum) Shear Modulus (G_{max})

A typically calculation of initial shear modulus for P @ 3 m soil under 150 kPa axial loads determined using Eq. (2.12) is shown below. From Table 2.4 for P @ 3 m; the value of K for PI value of 29.37 by interpolation is 0.24 and void ratio of 1.05 at the natural state and 150 kPa axial stress. From 1D - consolidation test result pre-consolidation pressure P_c of P @ 3 m was 129 kPa.

$$\text{So, } OCR = \frac{P_c}{P_o} = \frac{129}{150} = 0.860$$

$$\sigma'_{\circ} = \sigma_v{}' * \frac{(1 + 2K_0)}{3} = 150 * \frac{(1 + 2 * 0.5)}{3} = 100\ kPa$$

$$G_{max} = \frac{3230 * (2.97 - e)^2}{1 + e} * (OCR)^K * (\sigma'_{\circ})^{0.5}$$

$$= \frac{3230 * (2.97 - 1.05)^2}{(1 + 1.05)} * (0.860)^{0.24} * (100)^{0.5}$$

Thus, G_{max} = 56,018.406 kPa = 56.018 MPa

With similar manner, G_{max} for each specimen was calculated and the results are presented in Table 4.11 bellow.

Table 4 11: Computation of the initial (maximum) shear modulus (G_{max})

Test pit No.	Designation	Parameters							G_{max} (MPa)
		e	K	P_c (kPa)	P_o or $\sigma_v{}'$ (kPa)	OCR	K_o	$\sigma'_{\circ}$ (kPa)	
TP-1	P @ 3m	1.05	0.24	129	150	0.860	0.5	100	56.018
					275	0.469		183.333	65.580
					400	0.323		266.667	72.291
TP-2	H @ 3m	1.33	0	136	150	0.907	0.5	100	37.285
					275	0.495		183.333	50.484
					400	0.340		266.667	60.886
TP-3	M @ 3m	1.28	0.15	166	150	1.107	0.5	100	41.081
					275	0.604		183.333	50.790
					400	0.415		266.667	57.907

From Table 4.10, the 5th cycle shear modulus of P @ 3 m soil under 150 kPa axial loads and 5 % shear strain was 1.802 MPa.

$$\text{So, } G/G_{max} = 1.80203/56.018$$
$$= 0.032$$

Similarly, the normalized shear modulus value (G/G_{max}) for each specimen was calculated and the results are presented in Table 4.12.

Table 4. 12: Normalized shear modulus values

Test pit No.		TP-1			TP-2			TP-3		
Designation		P @ 3 m			H @ 3 m			M @ 3 m		
Confining pressure (kPa)	Shear strain	G (MPa)	G_{max} (MPa)	G/G_{max}	G (MPa)	G_{max} (MPa)	G/G_{max}	G (MPa)	G_{max} (MPa)	G/G_{max}
150	0.01	7.733	56.018	0.138	1.873	37.285	0.050	4.803	41.081	0.117
	0.1	5.223		0.093	1.076		0.029	3.503		0.085
	1	2.993		0.053	0.661		0.018	2.098		0.051
	2.5	2.023		0.036	0.477		0.013	1.557		0.038
	5	1.802		0.032	0.308		0.008	1.406		0.034
275	0.01	12.812	65.580	0.195	6.695	50.484	0.133	9.711	50.790	0.191
	0.1	10.059		0.153	4.803		0.095	8.402		0.165
	1	7.418		0.113	2.993		0.059	6.672		0.131
	2.5	5.684		0.087	2.183		0.043	5.051		0.099
	5	4.764		0.073	1.771		0.035	4.764		0.094
400	0.01	15.070	72.291	0.208	9.229	60.886	0.152	13.428	57.907	0.232
	0.1	13.423		0.186	7.418		0.122	12.481		0.216
	1	11.023		0.152	5.784		0.095	10.355		0.179
	2.5	9.541		0.132	5.049		0.083	9.440		0.163
	5	9.133		0.126	4.803		0.079	9.007		0.156

4.4. Factors Influencing Shear Modulus and Damping Ratio Value

The dynamic shear modulus and soil damping ratio are affected by many factors. In this study, some of these factors were considered, such as confining pressure, shear strain amplitude, void ratio, No. od loading cycles, and soil plasticity.

4.4.1. Influence of Confining Pressure and Shear Strain On Shear Modulus and Damping Ratio Values

The shear modulus and damping ratio of cyclically loaded soils are highly affected by the confining pressure and shear strain level. But this factors affect the dynamic properties (shear modulus and damping ratio values) oppositely. Which means the shear modulus and damping ratio of the soil increase and decrease with confining pressure respectively. But in case of shear strain amplitude, shear modulus and damping ratio are decrease and increase with shear strain amplitude respectively. From Figure 4.11, Figure 4.13, and Figure 4.15 we observe that the shear modulus increases with confining pressure. This is due to the compactness of the soil grains. For high confining pressure, the shear modulus value also high. We also note that the shear modulus value decrease with shear strain amplitude. When we increase shear strain amplitude, the soil resistance to cyclic load is decrease, this is due to loss of energy.

From Figure 4.12, Figure 4.14 and Figure 4.16 we observe that the damping ratio increases with shear strain amplitude, this is because of energy dissipation during deformation of soil. When we increase the confining pressure, the damping ratio of the soil is decreased, this is because when we increase the confining pressure the soil becomes denser that cause reduction of energy loss. The effect of confining pressure and shear strain amplitude on shear modulus and damping ratio values of the 5th, 20th and 40th cycle and their figures for all test pits are presented here.

Table 4.13: Shear modulus and Damping ratio values of P @ 3m at 5th, 20th and 40th cycle

		P @ 3 m									
		Strain (%)					Strain (%)				
		0.01	0.1	1	2.5	5	0.01	0.1	1	2.5	5
Pressure (kPa)	No. of cycle	Shear Modulus, G (MPa)					Damping Ratio, ξ (%)				
150	5	7.733	5.223	2.993	2.023	1.802	2.804	6.184	11.625	15.039	16.929
	20	8.271	5.598	3.400	2.474	1.981	2.338	5.629	11.021	13.894	16.132
	40	8.953	6.022	4.033	3.061	2.833	2.071	5.128	10.412	13.173	14.829
275	5	12.812	10.059	7.418	5.684	4.764	1.642	4.225	7.732	9.851	12.732
	20	13.388	10.969	8.245	5.863	4.892	1.499	3.871	6.949	9.051	11.374
	40	13.933	12.039	9.780	6.607	5.158	1.178	3.436	6.022	7.726	10.205
400	5	15.070	13.423	11.023	9.541	9.133	0.580	2.119	4.225	5.996	8.253
	20	15.494	13.851	12.063	9.855	9.364	0.289	1.872	3.871	5.096	6.987
	40	15.998	14.326	12.650	10.711	10.244	0.146	1.310	3.197	4.376	5.772

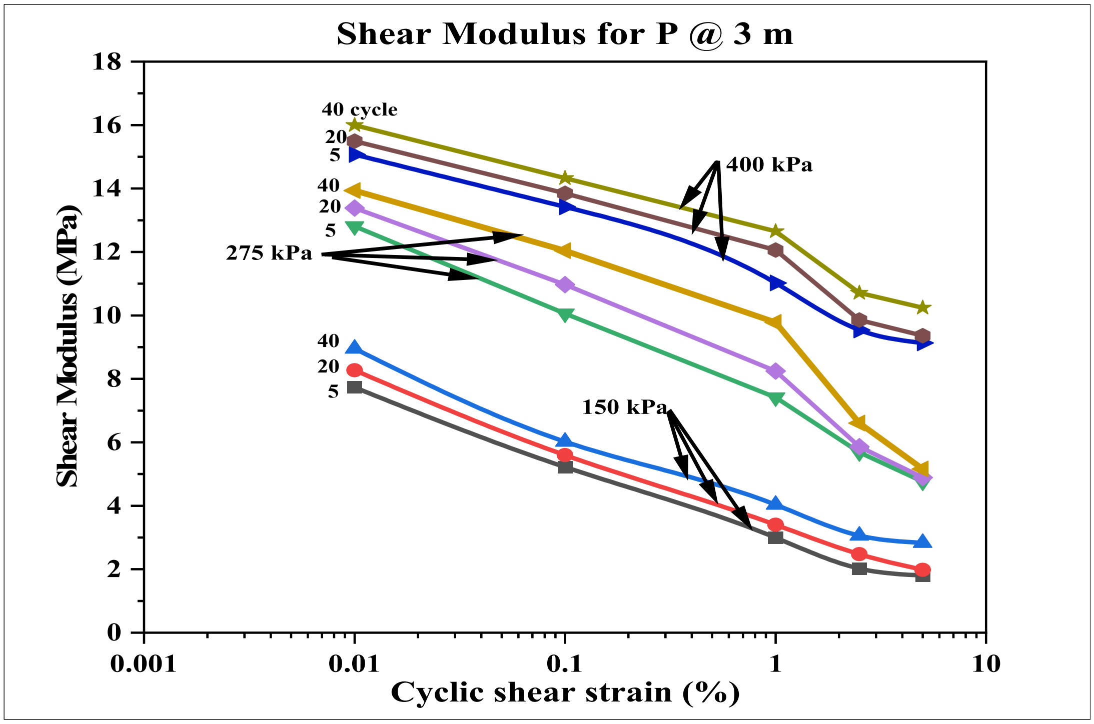

Figure 4.11: Influence of confining pressure and shear strain amplitude on shear modulus values of P @ 3 m

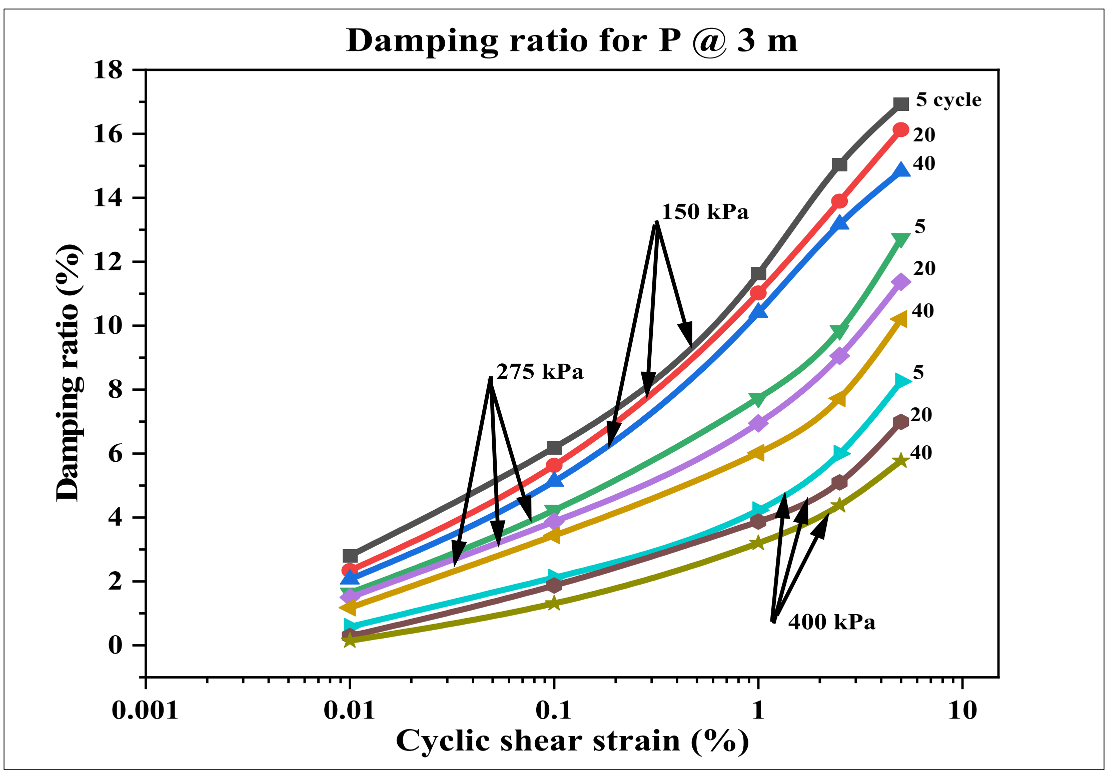

Figure 4.12: Influence of confining pressure and shear strain amplitude on damping ratio values of P @ 3 m

Table 4.14: Shear modulus and Damping ratio values of H @ 3m at 5th, 20th and 40th cycle

		H @ 3 m									
		Strain (%)					Strain (%)				
		0.01	0.1	1	2.5	5	0.01	0.1	1	2.5	5
Pressure (kPa)	No. of cycle	Shear Modulus, G (MPa)					Damping Ratio, ξ (%)				
150	5	1.873	1.076	0.661	0.477	0.308	6.514	11.348	16.942	20.590	28.415
	20	2.177	1.367	0.793	0.529	0.383	5.973	10.526	15.919	19.349	26.049
	40	2.761	2.017	1.232	0.978	0.501	5.600	9.594	15.071	18.359	24.077
275	5	6.695	4.803	2.993	2.183	1.771	3.964	7.593	12.896	16.035	20.590
	20	7.138	5.158	3.393	2.454	1.813	3.297	6.855	11.760	14.973	19.349
	40	7.545	5.524	4.033	2.761	2.199	2.735	6.345	10.962	13.976	18.359
400	5	9.229	7.418	5.784	5.049	4.803	1.999	4.516	8.095	10.972	15.342
	20	9.716	8.245	6.471	5.300	4.868	1.429	3.934	7.358	9.995	13.735
	40	10.605	9.185	7.530	6.240	5.323	0.678	3.049	6.458	8.931	11.182

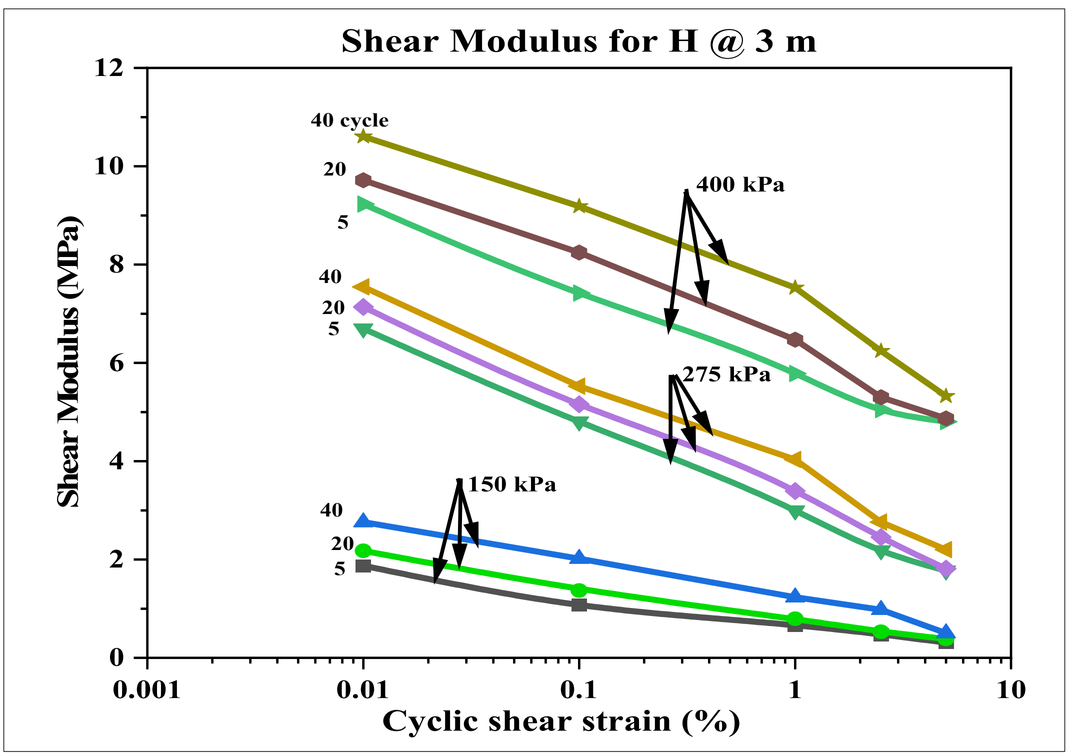

Figure 4.13: Influence of confining pressure and shear strain amplitude on shear modulus values of H @ 3 m

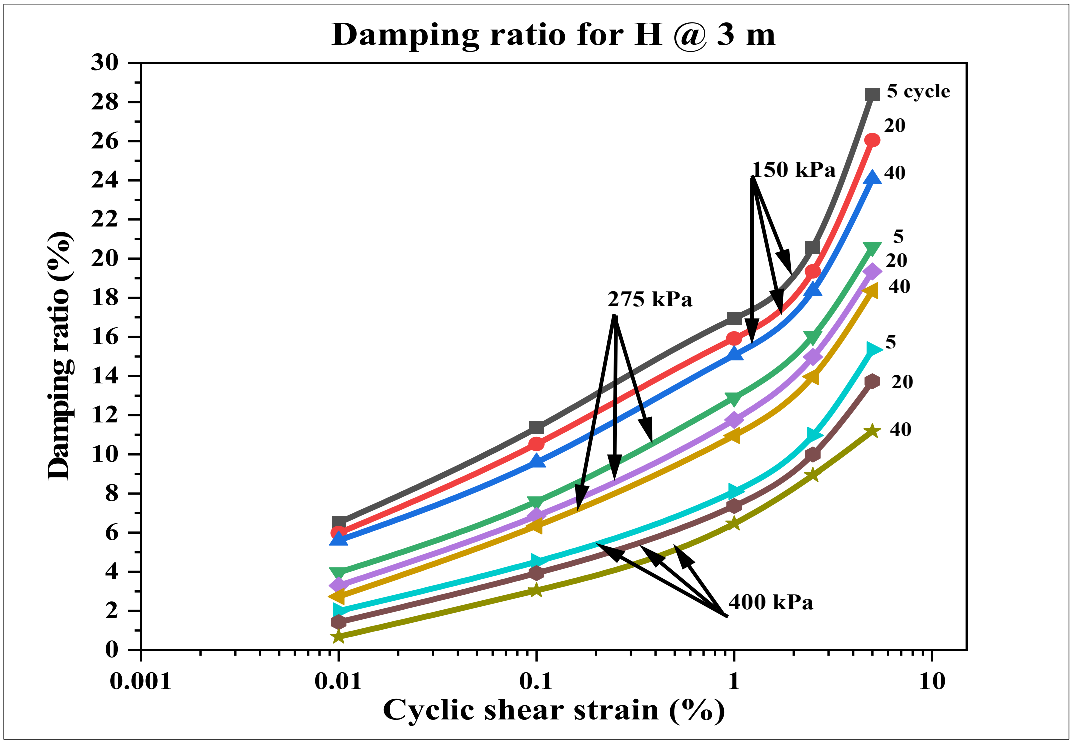

Figure 4.14: Influence of confining pressure and shear strain amplitude on damping ratio values of H @ 3 m

Table 4.15: Shear modulus and Damping ratio values of M @ 3m at 5th, 20th and 40th cycle

		M @ 3 m									
		Strain (%)					Strain (%)				
		0.01	0.1	1	2.5	5	0.01	0.1	1	2.5	5
Pressure (kPa)	No. of cycle	Shear Modulus, G (MPa)					Damping Ratio, ξ (%)				
150	5	4.803	3.503	2.098	1.557	1.406	4.426	7.634	15.342	17.587	20.590
	20	5.213	3.975	2.762	2.161	1.813	4.127	6.996	13.735	16.139	19.349
	40	5.831	4.439	3.315	2.635	2.199	3.787	6.598	12.596	15.052	18.359
275	5	9.711	8.402	6.672	5.051	4.764	3.316	5.573	9.851	13.467	15.978
	20	10.202	8.802	7.366	5.656	4.892	2.689	4.749	9.051	12.524	15.033
	40	10.696	9.305	7.923	6.046	5.158	2.006	3.931	7.726	11.138	13.544
400	5	13.428	12.481	10.355	9.440	9.007	1.201	2.090	6.575	8.937	11.348
	20	13.919	12.851	11.106	9.861	9.324	0.632	1.429	5.624	7.809	9.470
	40	14.578	13.424	11.621	10.388	9.761	0.345	0.858	4.400	6.479	8.696

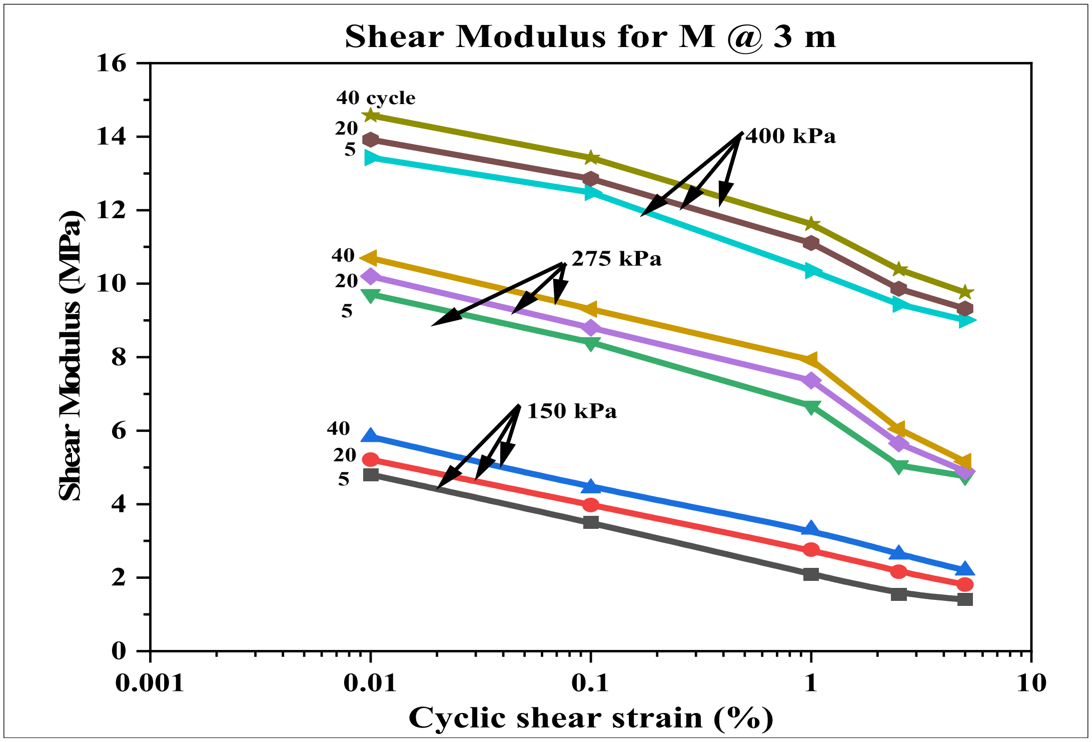

Figure 4.15: Influence of confining pressure and shear strain amplitude on shear modulus values of M @ 3 m

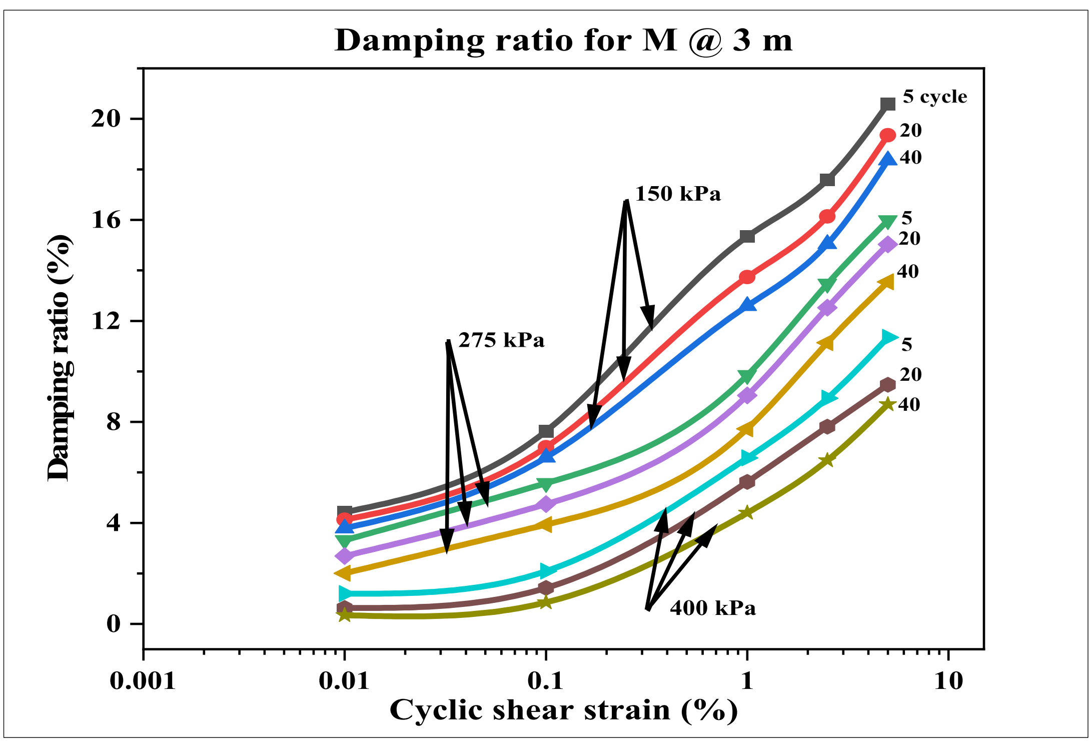

Figure 4.16: Influence of confining pressure and shear strain amplitude on damping ratio values of M @ 3 m

4.4.2. Influence of Void Ratio On Shear Modulus and Damping Ratio Values

The void ratio of the soil has an influence on shear modulus and damping ratio value. For soils which has low value of void ratio; the corresponding shear modulus is high but its damping ratio is low. It is because; when void ratio decreases, the area of contact between soil particles becomes closer. This closeness cause increase in shear modulus and decrease in damping ratio. When the void ratio increases, the area of contact between soil particles becomes far apart this cause increase in damping ratio and reduction of shear modulus. The influence of void ratio on the shear modulus and damping ratio was presented in Figure 4.17 and Figure 4.18 respectively. It can be observed from Figure 4.17 that shear modulus is influenced by initial void ratio. The shear modulus increases with decrease in void ratio. It is evident from Figure 4.18 that the variation of ξ with void ratio falls in a narrow band showing an insignificant influence of void ratio on damping ratio.

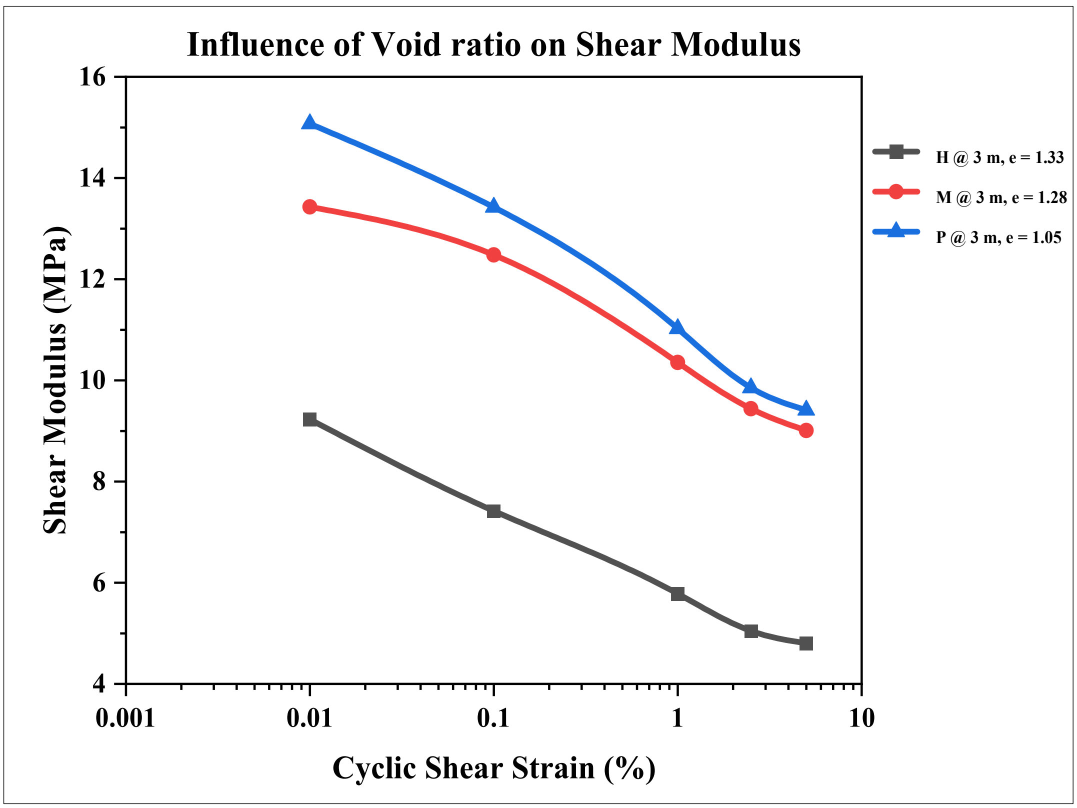

Figure 4.17: Influence of void ratio on shear modulus values at 5th cycle and 400 kPa

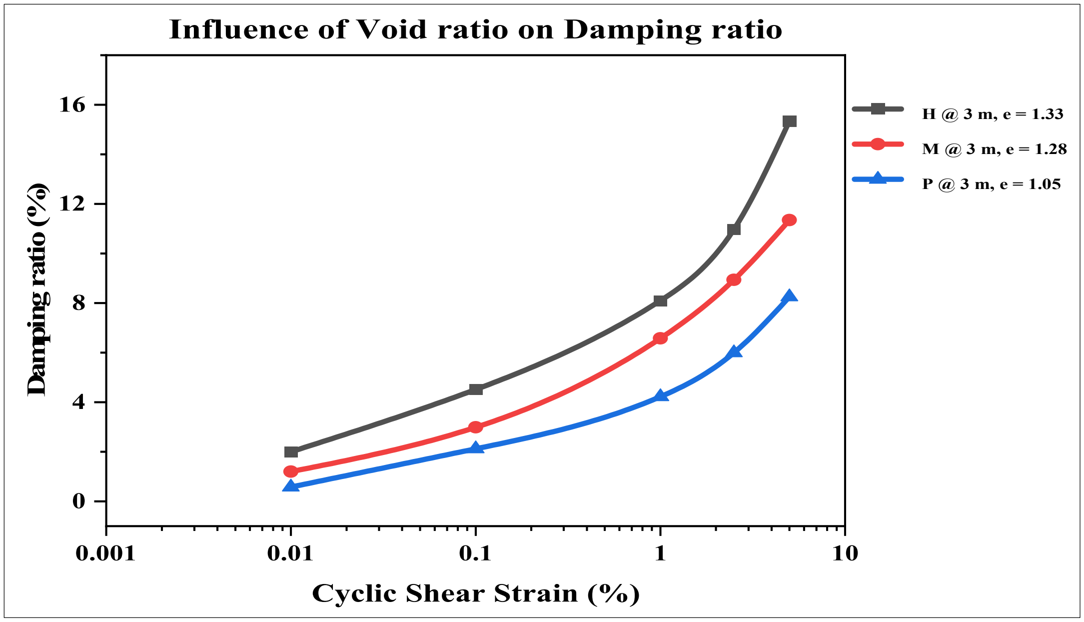

Figure 4.18: Influence of void ratio on damping ratio values at 5th cycle and 400 kPa

4.4.3. Influence of No. Of Loading Cycles On Shear Modulus and Damping Ratio Values

The number of loading cycles has no significant effect on shear modulus but it has on damping ratio. The shear modulus slightly increases and the damping ratio significantly decreases with an increasing number of loading cycles. From Figure 4.19 and Figure 4.20 we observed that, the shear modulus increases and the damping ratio decreases with number of cycles.

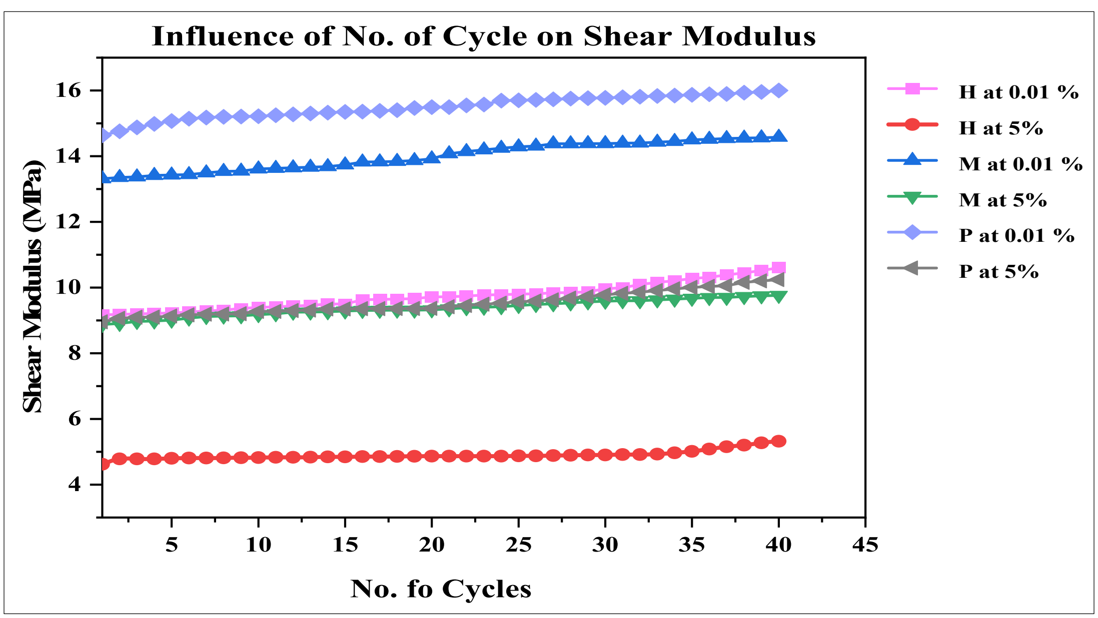

Figure 4.19: Influence of No. of loading cycles on shear modulus values at 400 kPa

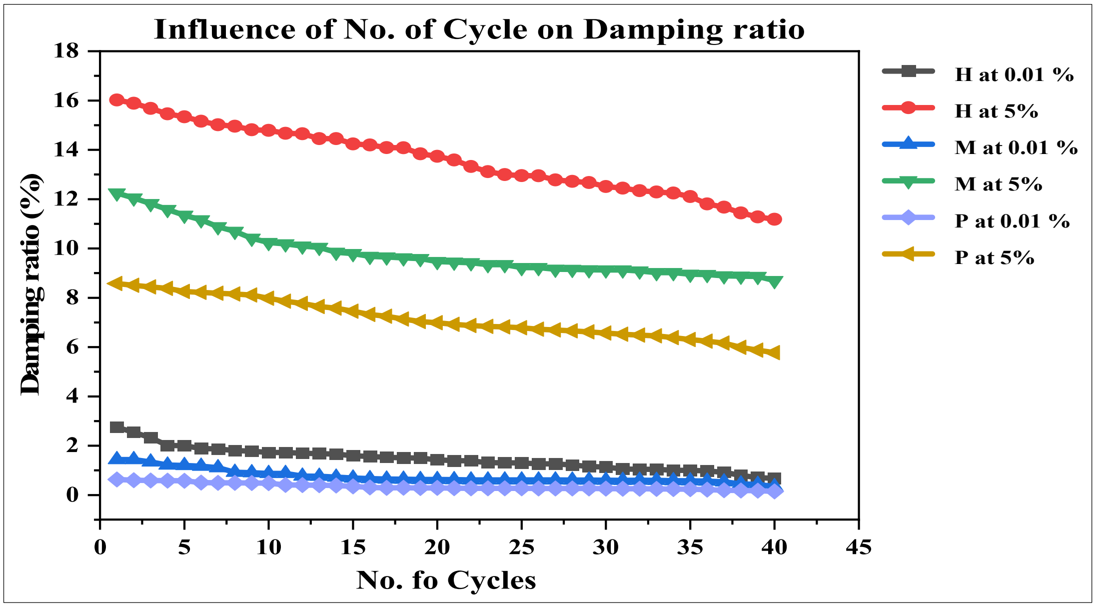

Figure 4.20: Influence of No. of loading cycles on damping ratio values at 400 kPa

4.4.4. Influence of soil plasticity on shear modulus and damping ratio values

Soil plasticity has an influence on both the shear modulus and damping ratio values of soil. The influence of soil plasticity on shear modulus and damping ratio values are presented in Figure 4.21 and Figure 4.22. From these figures we observed that for same confining pressure and No. of loading cycle the shear modulus increases and damping ratio decreases with increasing soil plasticity. It is also observed that the soil has a lower shear modulus at higher strains. Therefore, when strains increases, the influence of the plasticity of the soil on the shear modulus is not significant.

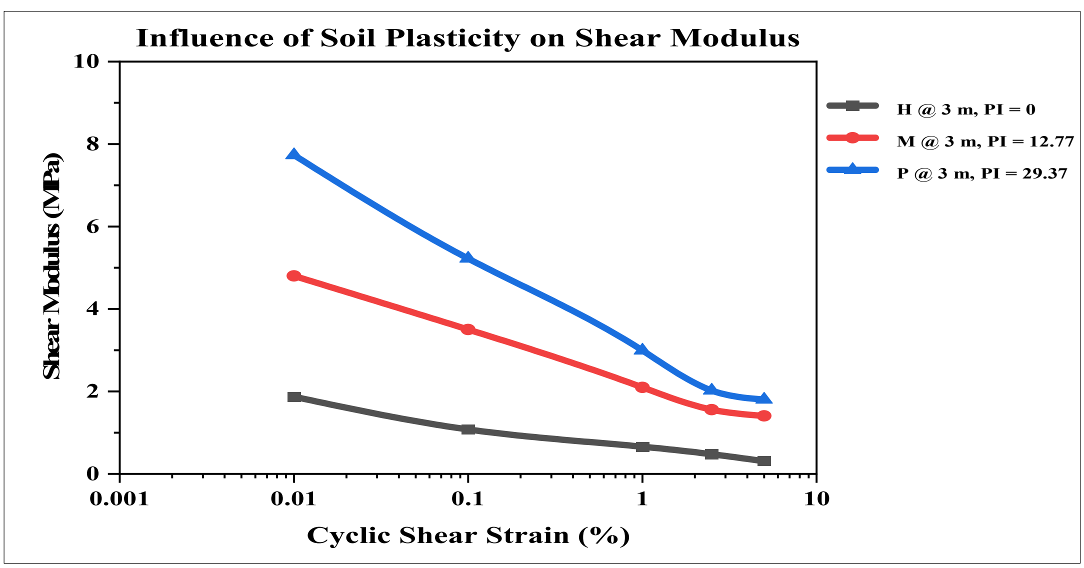

Figure 4.21: Influence of soil plasticity on shear modulus values at 5th cycle and 150 kPa

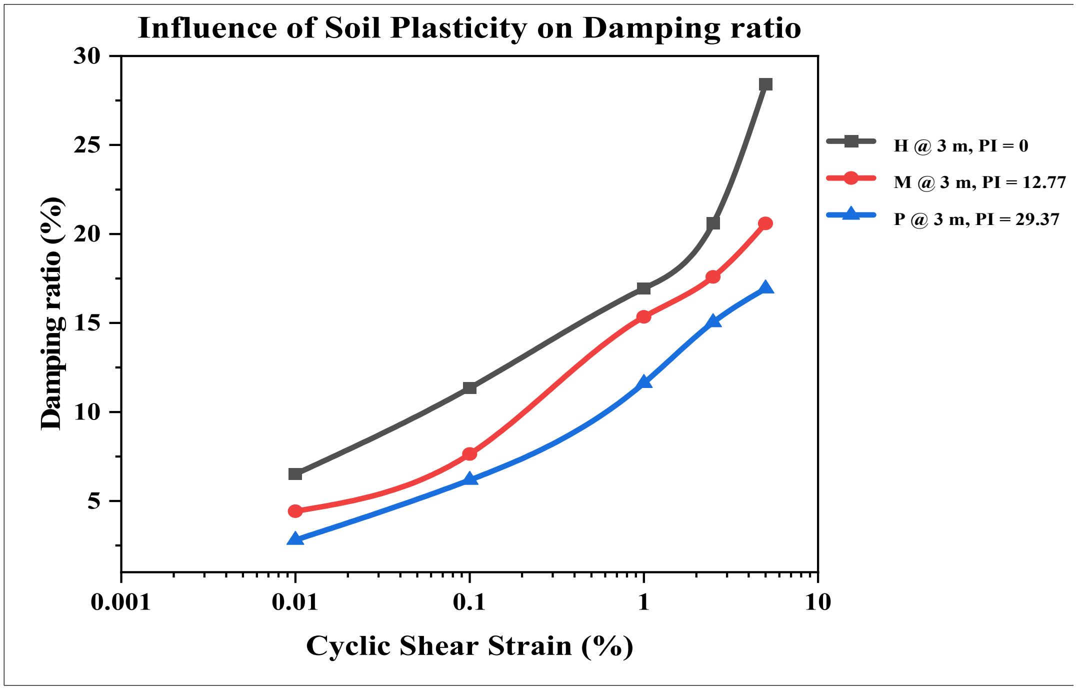

Figure 4.22: Influence of soil plasticity on damping ratio values at 5th cycle and 150 kPa

4.5. Discussion of Findings

Under this section, the experimental result values of the study were compared with previously published literature data. Previously, different researchers developed different modulus reduction (Normalized shear modulus) and damping ratio curves for different soils. From previously developed modulus reductions and damping ratio curves; the curve developed for saturated clay and sand by H.B. Seed and I.M. Idriss (H. Bolton Seed I. M. Idriss, 1970) and the curve developed for different soil plasticity value by Vucetic and Dobry (Vucetic & Dobry, 1991) were used for comparison, because these curves are well-developed curves for different types of soil. For silty soil, the range of normalized shear modulus and damping ratio value is between saturated clay and sand, so for comparison, the curve developed by H.B. Seed and I.M. Idriss was used. From Vucetic and Dobry curves; the selected curve of PI values for comparison was PI = 0, 10 and 30. And also the experimental result of this study were compared with local available modulus reduction and damping ratio curves of silt soil developed by different local researchers. Figure 4.23, Figure 4.24 and Figure 4.25 shows the plot of normalized shear modulus (G/G_{max}) values against cyclic shear strain on the sand and saturated clay curves of H.B. Seed and I.M. Idriss (H. Bolton Seed I. M. Idriss, 1970) and on curve developed for different soil plasticity value by Vucetic and Dobry (Vucetic & Dobry, 1991).

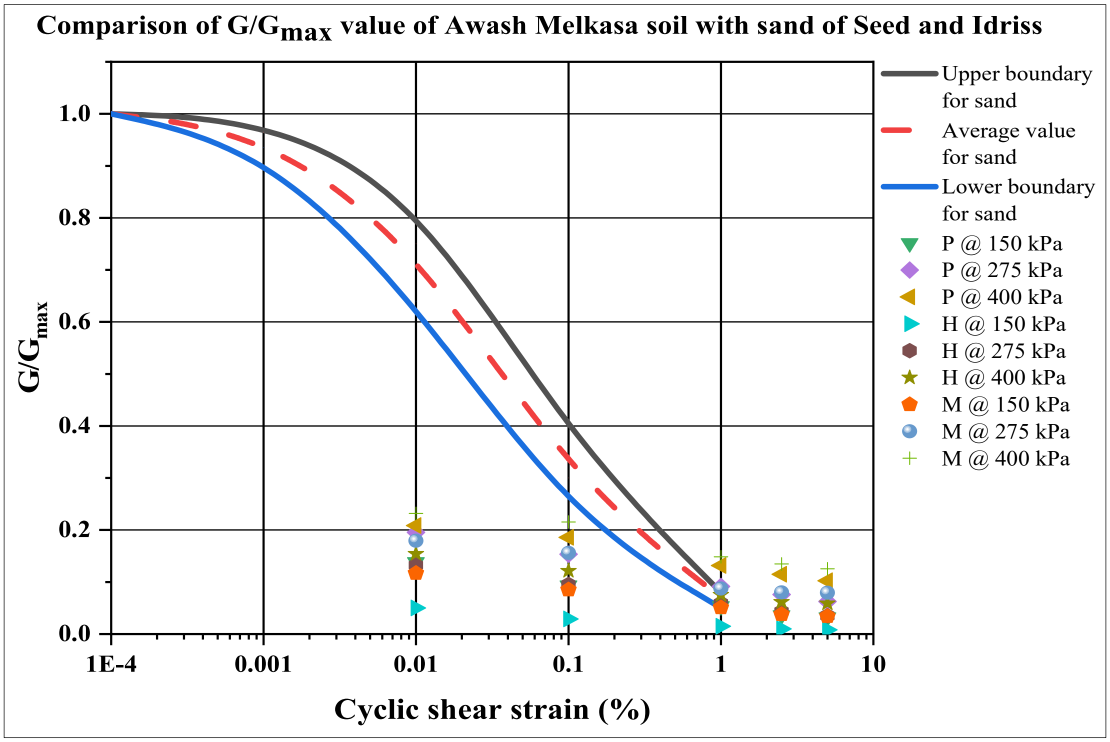

Figure 4.23: Comparison of G/G_{max} values of Awash Melkasa soils with the curve developed for sand by Seed and Idriss (H. Bolton Seed I. M. Idriss, 1970)

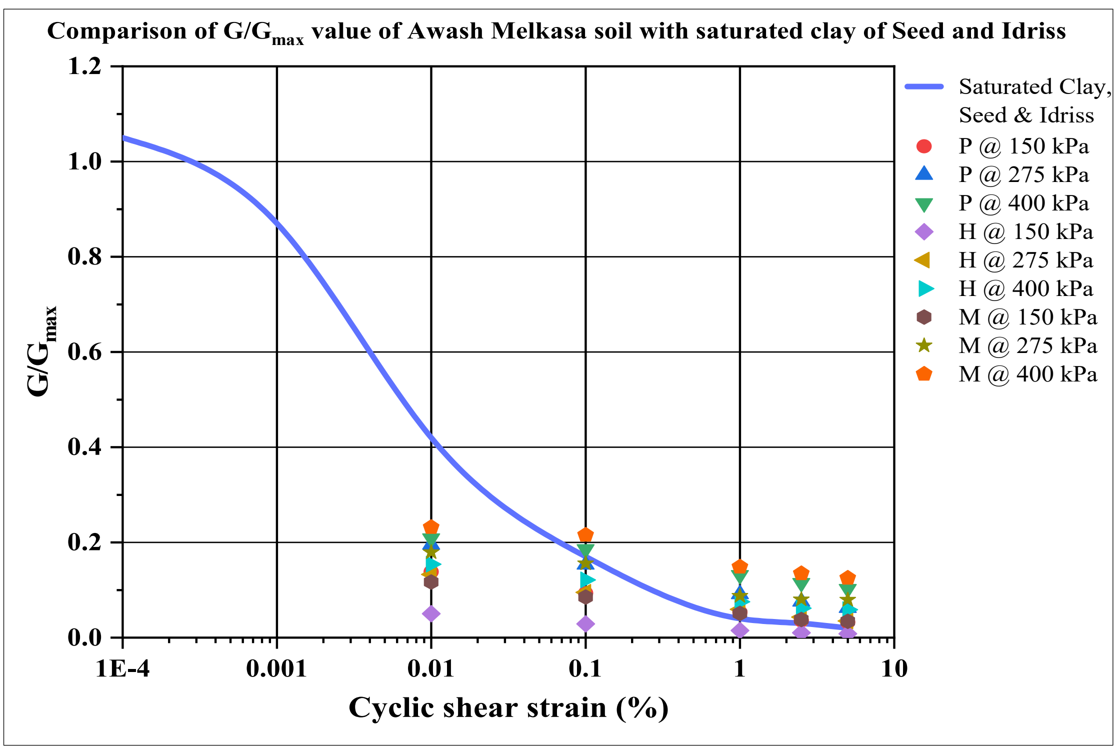

Figure 4.24: Comparison of G/G_{max} values of Awash Melkasa soils with the curve developed for saturated clay by Seed and Idriss (H. Bolton Seed I. M. Idriss, 1970)

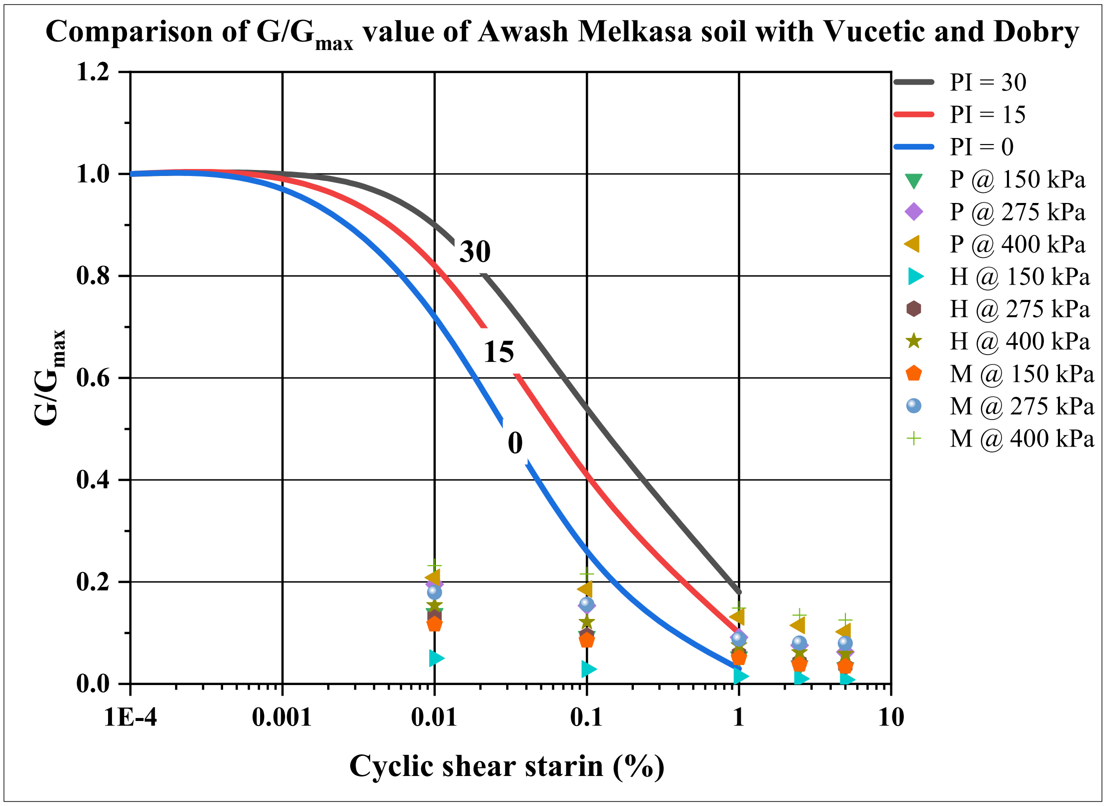

Figure 4.25: Comparison of G/G_{max} values of Awash Melkasa soil with curves developed for plastic soils by Vucetic and Dobry (Vucetic & Dobry, 1991)

From Figure 4.23, we have seen that most of G/G_{max} values of Awash Melkasa soils were lower and some of are within the range of sand values except for the value of P and M @ 400 kPa for strain greater than 1%. Generally, it can be said that the results of G/G_{max} values of Awash Melkasa soils were comparable with sand value of Seed and Idriss (1970). From Figure 4.24 and Figure 4.25, we have seen that; the computed G/G_{max} values of Awash Melkasa soils at lower strains ($\leq 0.1\%$) almost all measured G/G_{max} values were lower than the curves developed for saturated clays by Seed and Idriss (1970) and Vucetic and Dobry (1991). This reduction value at strains ($\leq 0.1\%$) is likely due to the sample preparation method and test conditions. On the other hand, the G/G_{max} values of Awash Melkasa soils at higher strains were agreed with the curves developed for saturated clays by Seed and Idriss (1970) and Vucetic and Dobry (1991).

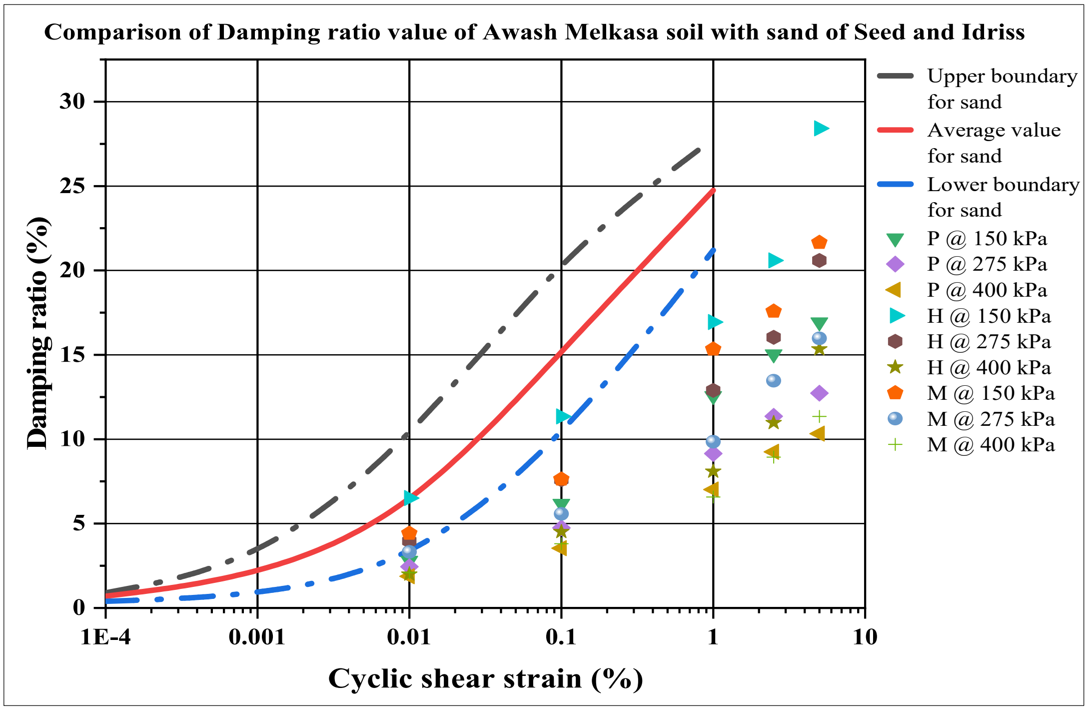

Figure 4.26: Comparison of Damping ratio values of Awash Melkasa soils with the curves developed for sand by Seed and Idriss (H. Bolton Seed I. M. Idriss, 1970)

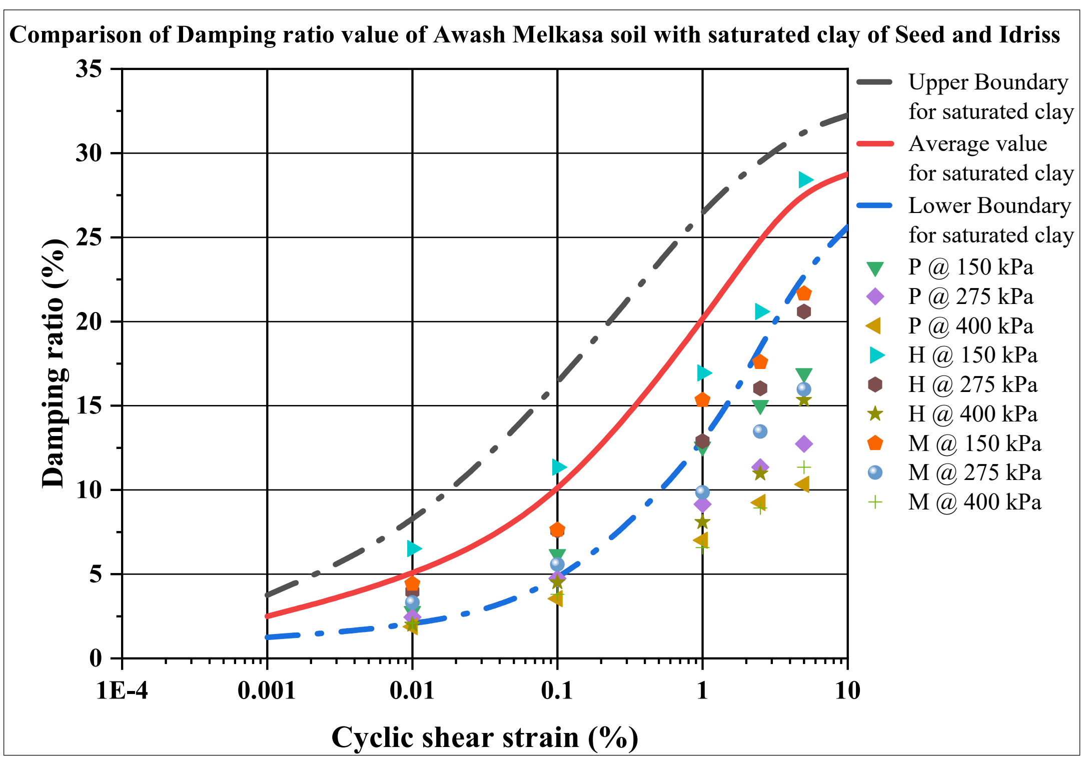

Figure 4.27: Comparison of Damping ratio values of Awash Melkasa soils with the curve developed for saturated clay by Seed and Idriss (H. Bolton Seed I. M. Idriss, 1970)

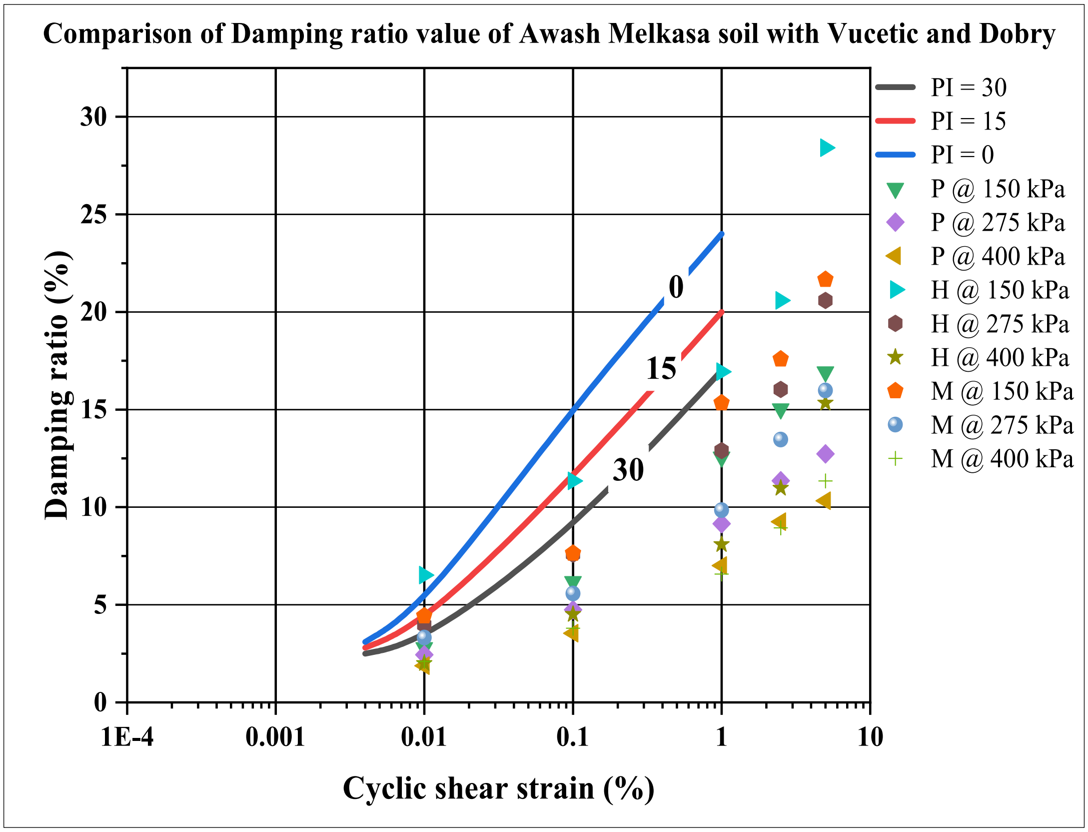

Figure 4.28: Comparison of Damping ratio values of Awash Melkasa soil with curves developed for plastic soils by Vucetic and Dobry (Vucetic & Dobry, 1991)

From Figure 4.26, it is observed that all damping ratio values of Awash Melkasa soil were located below the range of curves given for sand. This values have good agreement with the sand value of Seed and Idriss (1970). From Figure 4.27 and Figure 4.28, it can be observed that the damping ratio values of Awash Melkasa soils at high strains (≥ 1%) almost all measured damping ratio values were lower than the curves developed for saturated clays by Seed and Idriss (1970) and Vucetic and Dobry (1991). This variation on some measured points from the range occurred may be due to:

- The difference in the testing condition and the testing method.
- Differences in sampling and sample preparation methods (samples considered in this study are remolded). Disturbance caused by sampling and sample preparation alters soil properties such as fabric and structures, stress history, strain history, density and degree of saturation. All of these adversely affect the ability of laboratory tests to accurately measure dynamic soil properties. The

cyclic strength of the undisturbed specimens was about 15% greater than that of reconstituted specimens.

- Different types of testing machines (Most of the previous research tests were done through the resonance column and cyclic triaxial testing machine).
- Limitations of the machine to accurately reproduce real field conditions (stress, chemical, thermal and structural).
- Operator experience also affect the shear modulus and damping ratio value
- Using an empirical relationship to estimate the maximum shear modulus results in a deviation of the normalized shear modulus value from the trend in the previous literature.

The effect of confining pressure and shear strain on shear modulus values of Awash Melkasa elastic silt soil at confining pressure of 400 kPa is compared with the shear modulus and damping ratio values of same soil type and confining pressure determined by different local researches. Figure 4.29, shows the comparison of shear modulus and damping ratio values of Awash Melkasa elastic silt soil with Adama (Feyissa, 2011), Hawassa (Gashaw, 2012), Ziway (Mengistu, 2015), Modjjo (Asfaw, 2015), Jimma (Kebede, 2019) and Yeka subcity around Adiss Ababa (Bekele, 2020) silt soil.

From Figure 4.29, it is observed that the shear modulus values have good agreement with all curves at high strain values ($\geq$ 1%); but the values at lower strain is lower than the curves of Yeka, Ziway and Hawasa. From Figure 4.29, 4.30 and 4.31, it can be seen that, when the shear strain value increases the effect of confining pressure on shear modulus and damping ratio decrease. From Figure 4.30 and 4.31, it can be observing that the shear modulus and damping ratio value of Awash Melkasa silt soil shows good agreement with shear modulus and damping ratio values of local silt soils.

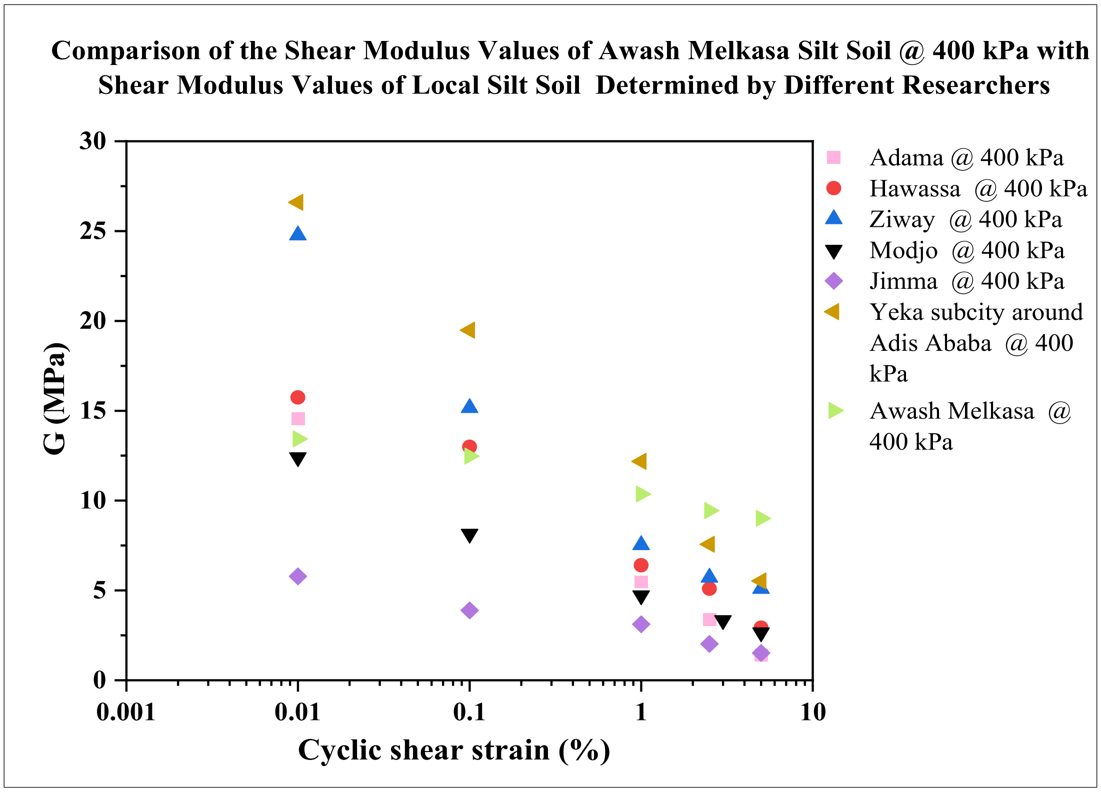

Figure 4.29: Comparison of the shear modulus values of Awash Melkasa silt soil @ 400 kPa with shear modulus values of local silt soil determined by different researchers

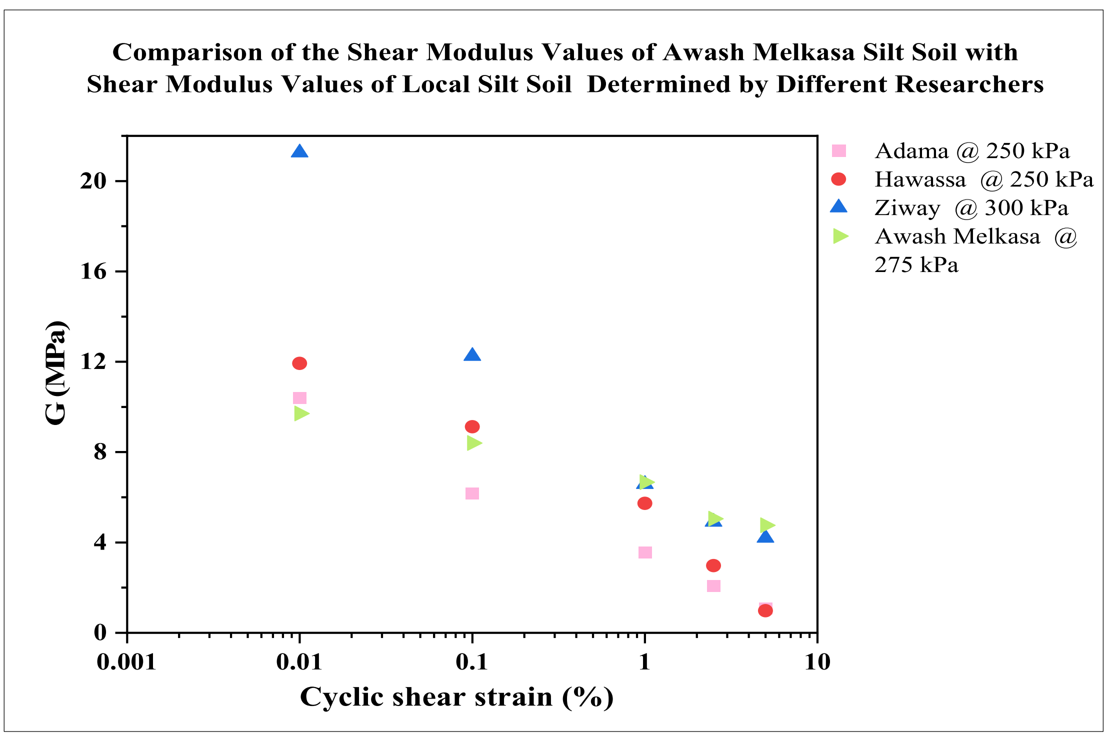

Figure 4.30: Comparison of the shear modulus values of Awash Melkasa silt soil with shear modulus values of local silt soil determined by different researchers

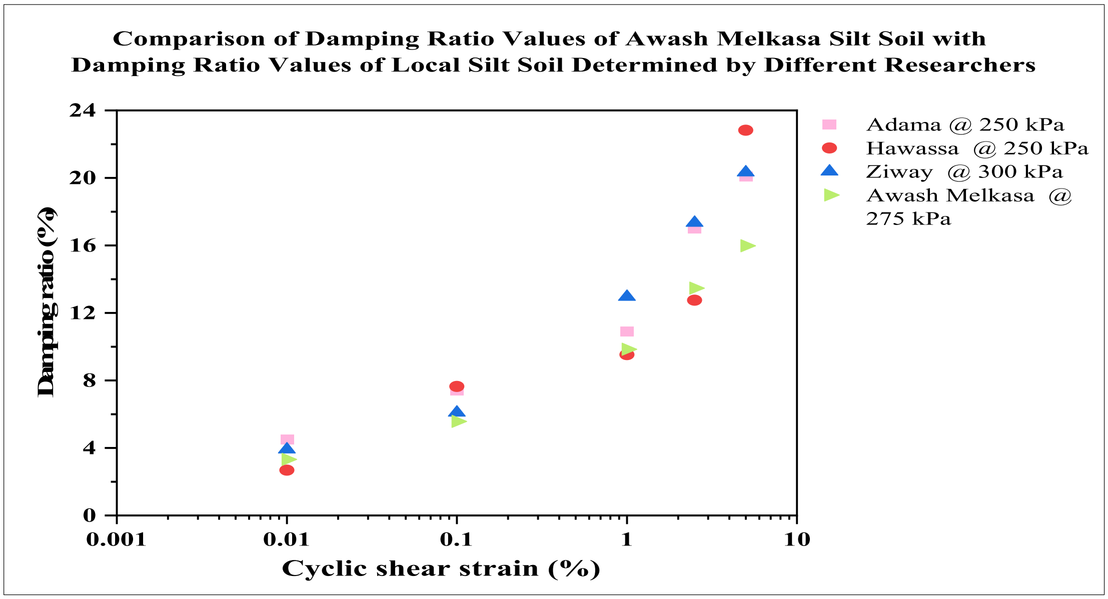

Figure 4.31: Comparison of damping ratio values of Awash Melkasa silt soil with damping ratio values of local silt soil determined by different researchers

The normalized shear modulus and damping ratio of Awash Melkasa elastic silt soil at confining pressure of 400 kPa is compared with the curve developed for same soil type and confining pressure by different local researches. Figure 4.32 and Figure 4.33, shows the comparison of G/G_{max} and damping ratio values of Awash Melkasa elastic silt soil with Adama (Feyissa, 2011), Hawassa (Gashaw, 2012), Ziway (Mengistu, 2015), Modjjo (Asfaw, 2015), Jimma (Kebede, 2019) and Yeka subcity around Adiss Ababa (Bekele, 2020) silt soil.

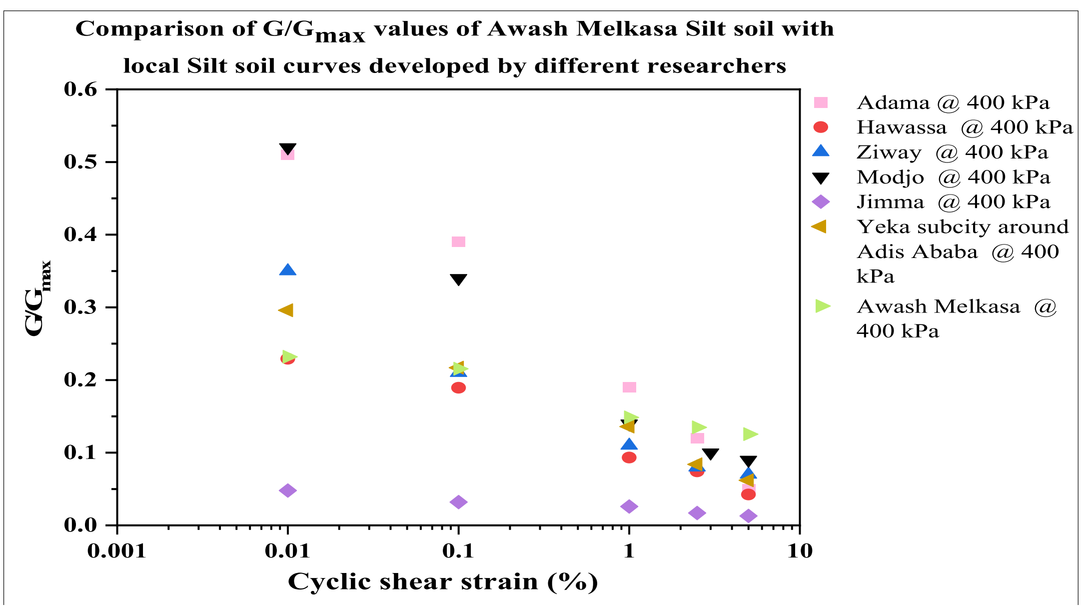

Figure 4.32: Comparison of G/G_{max} values of Awash Melkasa Silt soil with local Silt soil curves developed by different local researchers

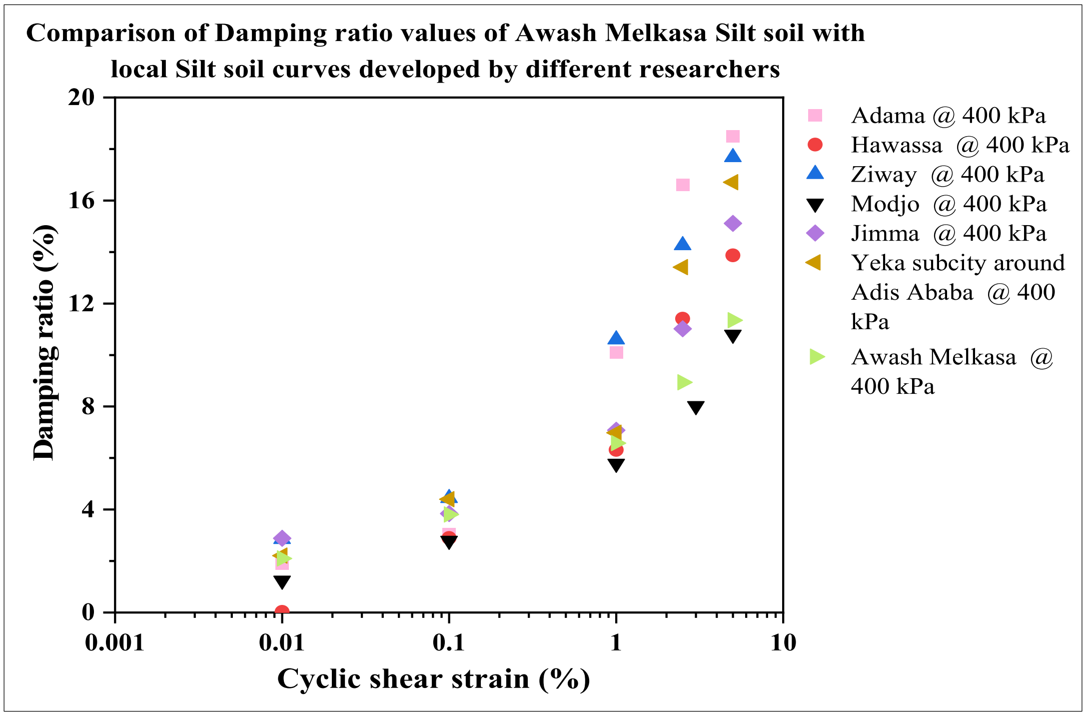

Figure 4.33: Comparison of Damping ratio values of Awash Melkasa Silt soil with local Silt soil curves developed by different local researchers

From Figure 4.32, it is observed that the values of G/G_{max} have good agreement with all curves at high strain values (≥ 1%); but the values at lower strain is lower than the curves of Adama and Modjo. From Figure 4.33, it can be seen that for strain ≤ 1%, the damping ratio is in good agreement with all curves, but it is not consistent with the case of strain > 1%.

CHAPTER FIVE

CONCLUSIONS AND RECOMMENDATIONS

5.1. Conclusions

For effective analysis of geotechnical problems such as seismic design and machine foundations; reliable measurement of dynamic soil properties is important. In this study, the results of an experimental investigation were presented. This study has investigated the dynamic properties of soil, namely the shear modulus (G) and damping ratio (ξ) values of soils found in Awash Melkasa town using cyclic simple shear testing machine. Strain controlled cyclic simple shear tests were performed on remolded samples from 3 test pits for strain values of 0.01 %, 0.1 %, 1 %, 2.5 %, 5 % under axial pressure of 150 kPa, 275 kPa and 400 kPa. In addition, for the classification purpose index property of the soils were determined and based on these properties the soils are classified into lean clay, elastic silt and none plastic silt soils. From the result of this study the following conclusions are drawn:

- ✓ The range of shear modulus values of Awash Melkasa lean clay soil is between 1.777 MPa and 15.998 MPa, and the damping ratio is between 0.146 % and 18.913 %.
- ✓ The range of shear modulus values of Awash Melkasa none plastic silt soil is between 0.292 MPa and 10.605 MPa, and the damping ratio is between 0.678 % and 30.851%.
- ✓ The range of shear modulus values of Awash Melkasa elastic silt soil is between 1.285 MPa and 14.578 MPa, and the damping ratio is between 0.345 % and 21.689%.
- ✓ The range of maximum shear modulus values of Awash Melksa lean clay, none plastic silt, and elastic silt soil is between 56.018 MPa and 72.291 MPa, 37.285 MPa and 60.886 MPa, and 41.081 MPa and 57.907 MPa respectively.
- ✓ The lean clay soil has high dynamic load resistance capacity than elastic silt and none plastic silt soil.
- ✓ The shear modulus values of the soils are increases with confining pressure and soil plasticity and decreases with increase of shear strain amplitude and void ratio. Conversely, the damping ratio increases with shear strain amplitude and decrease with increasing number of cycles, confining pressure and soil plasticity.
- ✓ The normalized shear modulus of the studied soil is consistent with all local curves of high strain values (≥1%), but the low strain normalized shear modulus of the studied soil is smaller than the Adama and Modjo curve. The damping ratio values

agree with all curves for strains ≤ 1%; but it is not consistent with the case of strain > 1%.

- ✓ The shear modulus reduction and damping ratio values of the studied soils were in good agreement with curve of sand developed by Seed and Idriss and shear modulus reduction values at high strain values (≥ 1%) also agree with the curve of saturated clay of Seed and Idriss (1970) and Vucetic and Dobry (1991).
- ✓ The location of the damping ratio values of Awash Melkasa soils are generally lower than the curves developed for saturated clay by Seed and Indriss (1970), and for different PI values by Vucetic and Dobry (1991). This shows that method of sample preparation and testing condition have significant effect on the damping ratio values.

5.2. Recommendations

The objective this study was to determine the shear modulus and material damping of Awash Melkasa soil using cyclic simple shear machine. The following recommendations can be drawn from the findings:

- ✓ Other than cyclic simple shear machine; the tests are needs to be conducted by resonant column devices because the resonant column test results are independent from methods of sample preparation.
- ✓ Further consideration of strain rate other than the strain rate considered in this study are recommended
- ✓ To note the effects of other factors such as method of sample preparation, degree of saturation, frequency of cyclic loading, degree of compaction, degree of saturation and particle size; the test needs to be conducted by considering this factors.
- ✓ Due to budget and time constraints, samples for this study were collected only from three test pits at a depth of 3 m. For better results, need to test more samples at deeper depths (> 3m).
- ✓ In order to obtain complete information about the dynamic properties of the soil, it is recommended to conduct both field and laboratory test methods. This is because field test methods tell us about the properties of soil in its in-situ state and laboratory test allow us to measure all of the dynamic properties of soil.
- ✓ The result of the study could be used for the design of dynamic load resistant structure in Awash Melkasa Town.
- ✓ The study could be used as an input for other researchers or institutions as literature.

REFERENCES

Asfaw, Y. H. (2015). Investigation of Shear Modulus and Damping Ratio of Modjo Silt and Silty Sand Soil Using Cyclic Simple Shear Test.

ASTM, "American Society for Testing and Materials", Annual Book of ASTM Standards, 1998.

Awash Melkasa - Google Maps. Retrieved April 6, 2021, from https://www.google.com/maps/place/Awash+Melkasa/@8.410236,39.3359274,14z/data

Bekele, N. (2020). A Study of Dynamic Properties of Soils Found in Yeka subcity Area of Addis Ababa (Issue January).

Camelo, C. S. (2017). Dynamic Soil Properties. Rio de Janeiro: Federal University of Rio de Janeiro. 1–44.

Chadi S. El Mohtar, 1. V. (2014). Combined Resonant Column and Cyclic Triaxial Tests for Measuring Undrained Shear Modulus Reduction of Sand With Plastic Fines. Geotechnical Testing Journal, 1-9.

Das, B. M. (2011). Principles of Soil Dynamics, Second Edition. United States of America: Cengage Learning.

Dimer, M. (2013). Investigation of Dynamic Property of Soil commonly found in Arba Minch Town.

EBCS- 8 Part 1. (2015). Design of Structures for Earthquake Resistance (Issue December).

Feng Qiao, a. J. (2020). Study on the dynamic characteristics of soft soil. The Royal Society of Chemistry, 4630-4639

Feyissa, A. G. (2011). Shear Modulus and Damping Ratio values of Soils found in Adama.

Gashaw, A. (2012). Hawassa Shear Modulus and Damping Ratio values of Soils (Issue January).

Ghayoomi, M., Ph, D., Asce, A. M., Suprunenko, G., Mirshekari, M., & Asce, S. M. (2017). Cyclic Triaxial Test to Measure Strain-Dependent Shear Modulus of Unsaturated Sand. 1–11. https://doi.org/10.1061/(ASCE)GM.1943-5622.0000917.

H. Bolton Seed I. M. Idriss. (1970). Soil Moduli and Damping factors for Dynamic Response Analyses. In Earthquake Engineering Research Center (Issue December).

Hailemariam, A. Y. (2017). Investigation to Dynamic Properties of Modjo Town Soils Using Cyclic Simple Shear Machine. International Journal of Scientific & Engineering

Research, 8(7), 1–13.

Hardin, B. O. (2016). Shear Modulus and Damping in Soils : Design Equations and Curves. July 1972. https://doi.org/10.1061/JSFEAQ.0001760

Herbert, S. (2013). Assessing seismic risk in Ethiopia. 1–12.

Jafarzadeh, F., & Sadeghi, H. (2009). Effect of water content on dynamic properties of sand in cyclic simple shear tests. Proceedings of the International Conference on Performance-Based Design in Earthquake Geotechnical Engineering, mm.

Jia, J. (2018). Dynamic and Cyclic Properties of Soils. Springer International Publishing.

Jian Li, S.-X. C.-F. (2017). Test study on the influences of dynamic stress and load history to the dynamic properties of the remolded red clay. EARTH SCIENCES RESEARCH JOURNAL, 1--8.

Kebede, T. B. (2019). Cyclic Behaviour and Dynamic Properties of Soils : A Case of Jimma Town (Issue January).

Kinde, S., Engeda, S., Kebede, A., & Tessema, E. (2011). Technical notes and Proposed Guidelines on Updated Seismic Codes in Ethiopia Implication for Large-Scale Infrastructures. Journal of EEA, 28, 1–20.

Kontoe, S., & Taborda, D. M. G. (2016). Comparative Study Of Stiffness Reduction And Damping Curves. February.

Kumar, S. S., Krishna, A. M., & Dey, A. (2013). Parameters Influencing Dynamic Soil Properties : A Review Treatise. National Conference on Recent Advances in Civil Engineering, 1–10.

Lamessa, G., Mammo, T., & Raghuvanshi, T. K. (2019). Homogenized earthquake catalog and b- value mapping for Ethiopia and its adjoining regions.

Lee, L. M., Jianjun, Z., Yong, K. K., & Li, Y. C. (2015). Overviews of Factors Affecting Dynamic Properties of Tropical Residual Soil. The Third Intl. Conf. on Advances in Civil, Structural and Environmental Engineering, 17–20.

Mengistu, A. (2015). Investigation into Some Dynamic Properties of Soils around Ziway.

Munirwansyah, M. (2020). Void ratio effect on dynamic shear modulus and shear wave velocity for soil stiffness in Banda Aceh and Aceh Besar. Journal of Physics, 1–6. https://doi.org/10.1088/1742-6596/1572/1/012090

Online, W. W. (2020). Awash, Ethiopia Weather Averages | Monthly Average High and Low Temperature | Average Precipitation and Rainfall days | World Weather Online. Retrieved March 31, 2021, from https://www.worldweatheronline.com/awash-weather-averages/et.aspx

Roy, S., & Bhalla, S. K. (2019). Role of Geotechnical Properties of Soil on Civil Engineering Structures. March. https://doi.org/10.5923/j.re.20170704.03

Sitharam, T. G., & Vinod, J. S. (2010). Evaluation of Shear Modulus and Damping Ratio of Granular Materials Using Discrete Element Approach. 591–601. https://doi.org/10.1007/s10706-010-9317-5

Vos, K. d. (2003). UTS004 Simple Shear Test Software Reference.

Vucetic, M., & Dobry, R. (1991). Effect of Soil Plasticity on Cyclic Response. Journal of Geotechnical Engineering, 117(1), 89–107. https://doi.org/10.1061/(ASCE)0733-9410(1991)117:1(89)

Wilson, J. F. (2016). Numerical Modelling of the Cyclic Torsional Shear Test on Granular Media. August.

Xhaxhiu, K., & Adam, V. (2015). Particle size distribution analyses. August.

Yimer, Y. M. (2017). Investigations on Index Properties and Maximum Dry Density of Soils Found in Kemise Town. ISSN, 9(11), 1–6.

Zehtab, K. H. (2010). An Assessment of the Dynamic Properties of Adapazari Soils by Cyclic Direct Simple Shear Tests (Issue July).

APPENDIXES

Appendix – A

In-Situ Index Soil Properties Tests

Table A-1: Field density and water content determination

Test pit location	Primary school		High school		Mesino	
Designation	P @ 1.75 m	P @ 3 m	H @ 1.5 m	H @ 3 m	M @ 2 m	M @ 3 m
Depth (m)	1.75	3	1.5	3	2	3
Mass of wet soil from test hole, M_w(g)	2285	2660	1495	1710	1880	1885
Mass of sand cone with sand before filling the hole, M_1 (g)	13140	13065	11638	13045	12860	12745
Mass of sand in the base plate and funnel, M_2 (g)	1002	1002	1002	1002	1002	1002
Mass of sand cone with remaining sand after filling the hole, base plate and funnel, M_3 (g)	9885	9810	8888	9975	10110	9860
Mass of sand used to fill the test hole, base plate and funnel, $M_4(g) = M_1(g) - M_3(g)$	3255	3255	2750	3070	2750	2885
Mass of sand in the test hole, $M_5(g) = M_4(g) - M_2(g)$	2253	2253	1748	2068	1748	1883
Volume of test hole, $V\ (cm^3) = \frac{M_5}{\rho_{sand}}$	1833.198	1833.198	1422.295	1682.669	1422.295	1532.140
Bulk density of soil, $\boldsymbol{\rho_b\ (g/cm^3) = \frac{M_w}{V}}$	**1.246**	**1.451**	**1.051**	**1.016**	**1.322**	**1.230**
Mass of test hole soil after oven dry, $M_d(g)$	2022	2436	1300	1626	1529	1576
Water content, $\boldsymbol{w(\%) = (\frac{M_w - M_d}{M_d})*100\%}$	**13.01**	**9.20**	**15.00**	**5.17**	**22.96**	**19.61**
Dry density of soil, $\boldsymbol{\rho_d\ (g/cm^3) = \frac{\rho_b}{(1+w)}}$	**1.103**	**1.329**	**0.914**	**0.966**	**1.075**	**1.029**

Appendix – B

Sieve Analysis

Table B-1: Grain size analysis for P @ 1.75 m

P @ 1.75 m							
A. Wet sieve analysis							
Sieve size (mm)	Mass of sieve (g)	Mass of sieve with soil retained (g)	Mass retained (g)	Cumulative mass retained (g)	Percentage retained (%)	Cumulative percent retained (%)	Percent passing (%)
12.5	439	439	0.00	0.00	0.00	0.00	100.00
9.5	442	442	0.00	0.00	0.00	0.00	100.00
4.75	440	440	0.00	0.00	0.00	0.00	100.00
2.36	405	405	0.00	0.00	0.00	0.00	100.00
2	383	383	0.00	0.00	0.00	0.00	100.00
1.18	359	360.56	1.56	1.56	3.12	3.12	96.88
0.6	329	331.73	2.73	4.29	5.46	8.58	91.42
0.3	294	298.1	4.10	8.39	8.20	16.78	83.22
0.15	278	281.57	3.57	11.96	7.14	23.92	76.08
0.075	272	274.58	2.58	14.54	5.16	29.08	70.92
pan	252	287.46	35.46	50.00	70.92	100.00	
Total weight (g)	2167	2217	50.00		100.00		

B. Hydrometer analysis									
Elapsed time, t (min)	Actual hydrometer reading, Ra	Temp. (°C)	Effective depth, L (mm)	K From table	Temp. correction factor, Ct	Modified hydrometer reading R = Ra – Cz + Ct	Particle diameter, D (mm)	% finer than D, P (%)	Corrected % finer than D, P (%)
2	30	21	11.18	0.01088	0.176	24.176	0.026	49.80	35.32
5	26	21	11.84	0.01088	0.176	20.176	0.017	41.56	29.48
15	24	21	12.17	0.01088	0.176	18.176	0.010	37.44	26.55
30	22	21	12.5	0.01088	0.176	16.176	0.007	33.32	23.63
60	20	21	12.83	0.01088	0.176	14.176	0.005	29.20	20.71
250	16	23	13.49	0.01062	0.664	10.664	0.002	21.97	15.58
1440	13	21	13.99	0.01088	0.176	7.176	0.001	14.78	10.48

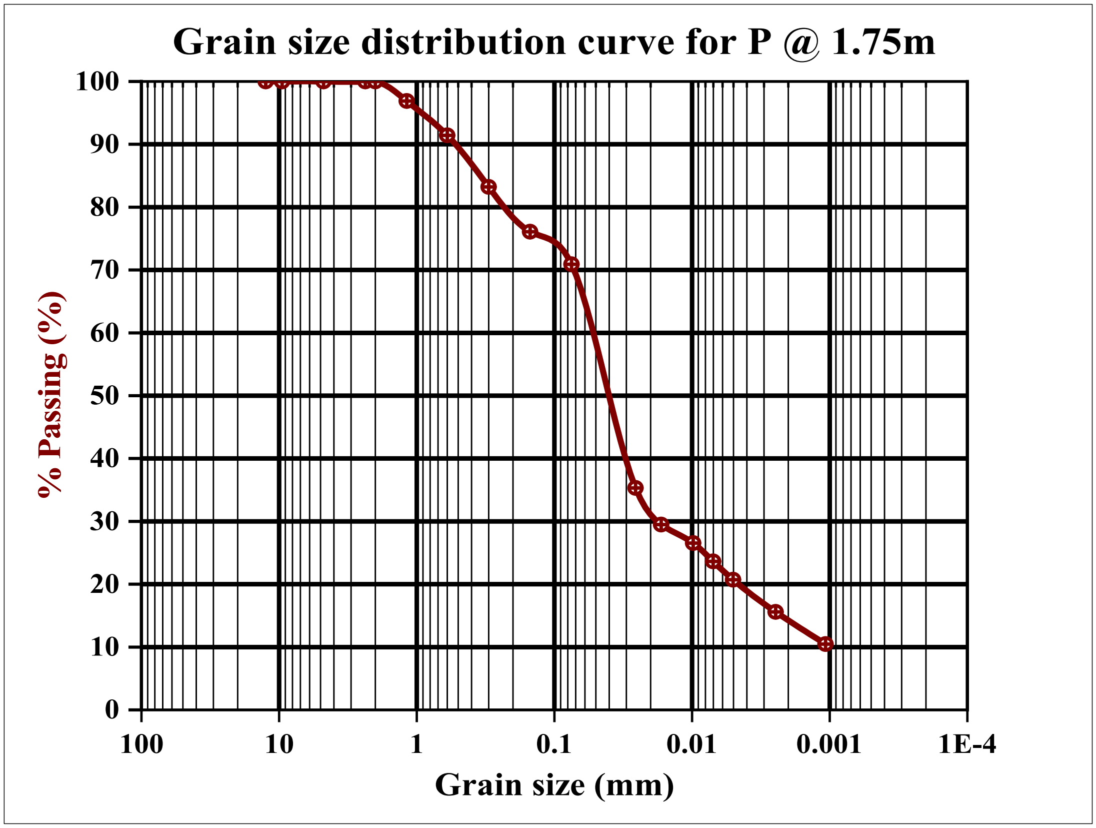

Figure B-1: Graph of grain size distribution curve for P @ 1.75 m

Table B-2: Grain size analysis for P @ 3 m

P @ 3 m							
A. Wet sieve analysis							
Sieve size (mm)	Mass of sieve (g)	Mass of sieve with soil retained (g)	Mass retained (g)	Cumulative mass retained (g)	Percentage retained (%)	Cumulative percent retained (%)	Percent passing (%)
12.5	439	439	0.00	0.00	0.00	0.00	100.00
9.5	442	442	0.00	0.00	0.00	0.00	100.00
4.75	440	440	0.00	0.00	0.00	0.00	100.00
2.36	405	405	0.00	0.00	0.00	0.00	100.00
2	383	383	0.00	0.00	0.00	0.00	100.00
1.18	359	361.94	2.94	2.94	5.88	5.88	94.12
0.6	329	334.54	5.54	8.48	11.08	16.96	83.04
0.3	294	299.74	5.74	14.22	11.48	28.44	71.56
0.15	278	282.84	4.84	19.06	9.68	38.12	61.88
0.075	272	275.49	3.49	22.55	6.98	45.10	54.90
pan	252	279.45	27.45	50.00	54.90	100.00	
Total weight (g)	2167	2217	50.00		100.00		

B. Hydrometer analysis									
Elapsed time, t (min)	Actual hydrometer reading, Ra	Temp. (°C)	Effective depth, L (mm)	K From table	Temp. correction factor, Ct	Modified hydrometer reading R = Ra – Cz + Ct	Particle diameter, D (mm)	% finer than D, P (%)	Corrected % finer than D, P (%)
2	24	21	12.17	0.01049	0.176	18.176	0.026	35.81	19.66
5	21	21	12.67	0.01049	0.176	15.176	0.017	29.90	16.41
15	20	21	12.83	0.01049	0.176	14.176	0.010	27.93	15.33
30	18	21	13.16	0.01049	0.176	12.176	0.007	23.99	13.17
60	16	21	13.49	0.01049	0.176	10.176	0.005	20.05	11.01
250	13	23	13.99	0.01024	0.664	7.664	0.002	15.10	8.29
1440	10	21	14.48	0.01049	0.176	4.176	0.001	8.23	4.52

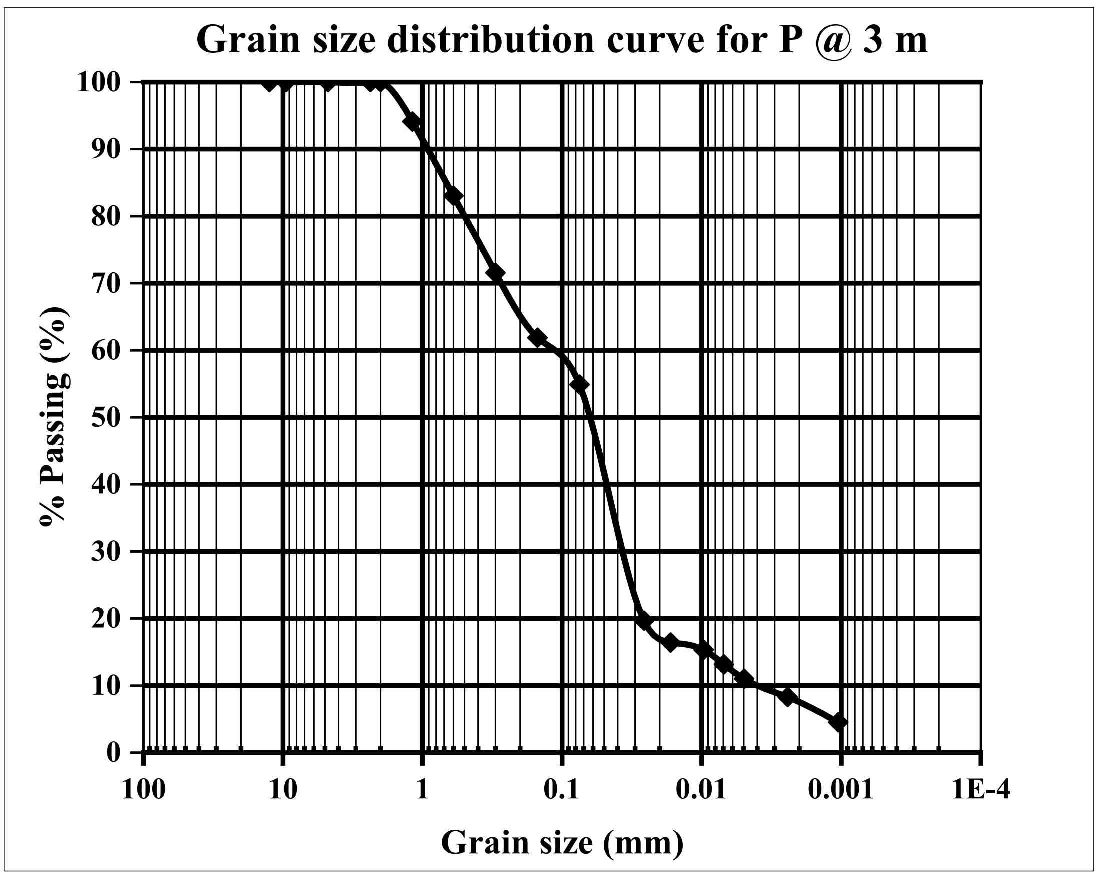

Figure B-2: Graph of grain size distribution curve for P @ 3 m

Table B-3: Grain size analysis for H @ 1.5 m

H @ 1.5 m							
A. Wet sieve analysis							
Sieve size (mm)	Mass of sieve (g)	Mass of sieve with soil retained (g)	Mass retained (g)	Cumulative mass retained (g)	Percentage retained (%)	Cumulative percent retained (%)	Percent passing (%)
12.5	439	439	0.00	0.00	0.00	0.00	100.00
9.5	442	442	0.00	0.00	0.00	0.00	100.00
4.75	440	440	0.00	0.00	0.00	0.00	100.00
2.36	405	405	0.00	0.00	0.00	0.00	100.00
2	383	383	0.00	0.00	0.00	0.00	100.00
1.18	359	359.64	0.64	0.64	1.28	1.28	98.72
0.6	329	331.47	2.47	3.11	4.94	6.22	93.78
0.3	294	297.5	3.50	6.61	7.00	13.22	86.78
0.15	278	280.03	2.03	8.64	4.06	17.28	82.72
0.075	272	273.5	1.50	10.14	3.00	20.28	79.72
Pan	252	291.86	39.86	50.00	79.72	100.00	
Total weight (g)	2167	2217	50.00		100.00		

B. Hydrometer analysis									
Elapsed time, t (min)	Actual hydrometer reading, Ra	Temp. (°C)	Effective depth, L (mm)	K From table	Temp. correction factor, Ct	Modified hydrometer reading R = Ra – Cz + Ct	Particle diameter, D (mm)	% finer than D, P (%)	Corrected % finer than D, P (%)
2	33	21	10.69	0.01102	0.176	27.176	0.025	57.02	45.45
5	26	21	11.84	0.01102	0.176	20.176	0.017	42.33	33.74
15	21	21	12.67	0.01102	0.176	15.176	0.010	31.84	25.38
30	20	21	12.83	0.01102	0.176	14.176	0.007	29.74	23.71
60	16	21	13.49	0.01102	0.176	10.176	0.005	21.35	17.02
250	12	23	14.15	0.01076	0.664	6.664	0.003	13.98	11.15
1440	9	21	14.65	0.01102	0.176	3.176	0.001	6.66	5.31

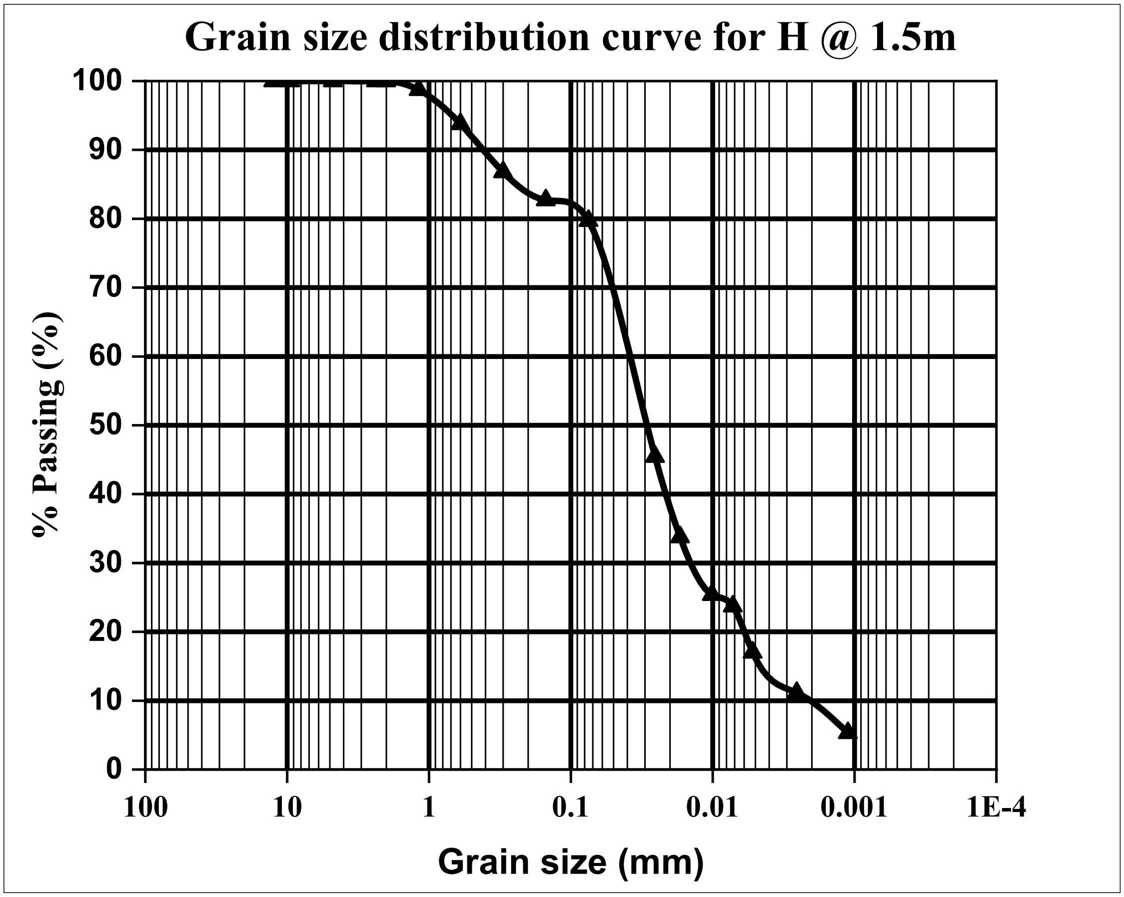

Figure B-3: Graph of grain size distribution curve for H @ 1.5 m

Table B-4: Grain size analysis for H @ 3 m

H @ 3m							
A. Wet sieve analysis							
Sieve size (mm)	Mass of sieve (g)	Mass of sieve with soil retained (g)	Mass retained (g)	Cumulative mass retained (g)	Percentage retained (%)	Cumulative percent retained (%)	Percent passing (%)
12.5	439	439	0.00	0.00	0.00	0.00	100.00
9.5	442	442	0.00	0.00	0.00	0.00	100.00
4.75	440	440	0.00	0.00	0.00	0.00	100.00
2.36	405	405	0.00	0.00	0.00	0.00	100.00
2	383	383	0.00	0.00	0.00	0.00	100.00
1.18	359	361.36	2.36	2.36	4.72	4.72	95.28
0.6	329	337.08	8.08	10.44	16.16	20.88	79.12
0.3	294	303.48	9.48	19.92	18.96	39.84	60.16
0.15	278	283.85	5.85	25.77	11.70	51.54	48.46
0.075	272	274.88	2.88	28.65	5.76	57.30	42.70
Pan	252	273.35	21.35	50.00	42.70	100.00	
Total weight (g)	2167	2217	50.00		100.00		

B. Hydrometer analysis									
Elapsed time, t (min)	Actual hydrometer reading, Ra	Temp. (°C)	Effective depth, L (mm)	K From table	Temp. correction factor, Ct	Modified hydrometer reading R = Ra – Cz + Ct	Particle diameter, D (mm)	% finer than D, P (%)	Corrected % finer than D, P (%)
2	19	21	13	0.01154	0.176	13.176	0.029	29.57	12.63
5	16	21	13.49	0.01154	0.176	10.176	0.019	22.83	9.75
15	12	21	14.15	0.01154	0.176	6.176	0.011	13.86	5.92
30	11	21	14.32	0.01154	0.176	5.176	0.008	11.61	4.96
60	9	21	14.65	0.01154	0.176	3.176	0.006	7.13	3.04
250	7	23	14.98	0.01126	0.664	1.664	0.003	3.73	1.59
1440	7	21	14.98	0.01154	0.176	1.176	0.001	2.64	1.13

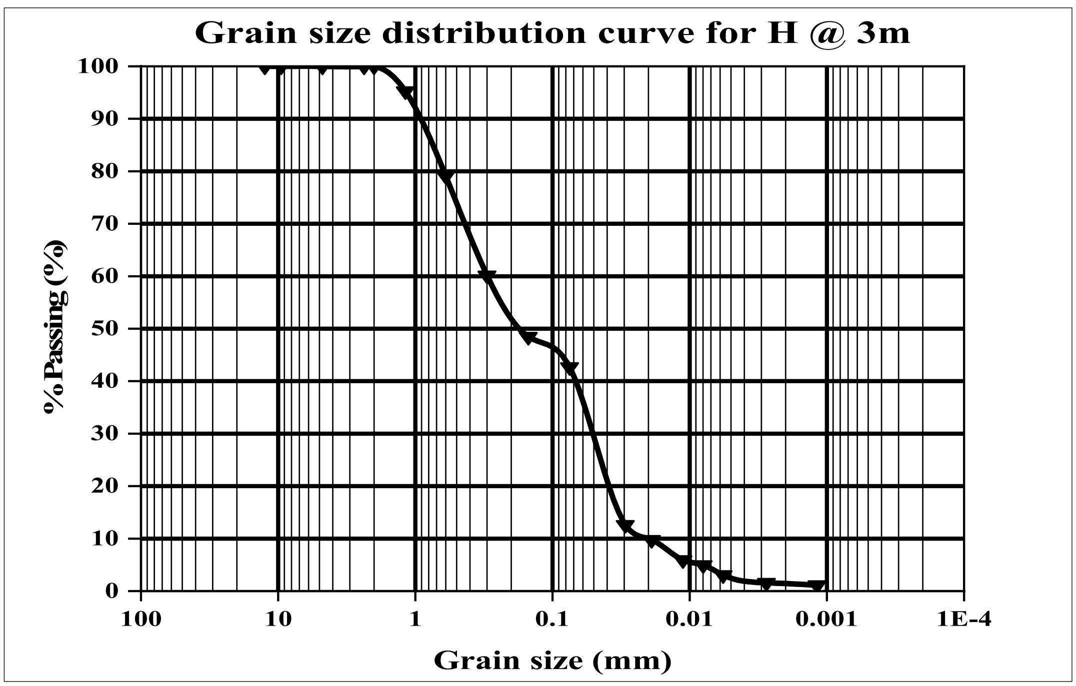

Figure B-4: Graph of grain size distribution curve for H @ 3 m

Table B-5: Grain size analysis for M @ 2 m

M @ 2 m							
A. Wet sieve analysis							
Sieve size (mm)	Mass of sieve (g)	Mass of sieve with soil retained (g)	Mass retained (g)	Cumulative mass retained (g)	Percentage retained (%)	Cumulative percent retained (%)	Percent passing (%)
12.5	439	439	0.00	0.00	0.00	0.00	100.00
9.5	442	442	0.00	0.00	0.00	0.00	100.00
4.75	440	440	0.00	0.00	0.00	0.00	100.00

2.36	405	405	0.00	0.00	0.00	0.00	100.00
2	383	383	0.00	0.00	0.00	0.00	100.00
1.18	359	359.07	0.07	0.07	0.14	0.14	99.86
0.6	329	329.3	0.30	0.37	0.60	0.74	99.26
0.3	294	294.65	0.65	1.02	1.30	2.04	97.96
0.15	278	278.45	0.45	1.47	0.90	2.94	97.06
0.075	272	272.38	0.38	1.85	0.76	3.70	96.30
Pan	252	300.15	48.15	50.00	96.30	100.00	
Total weight (g)	2167	2217	50.00		100.00		

B. Hydrometer analysis

Elapsed time, t (min)	Actual hydrometer reading, Ra	Temp. (°C)	Effective depth, L (mm)	K From table	Temp. correction factor, Ct	Modified hydrometer reading R = Ra – Cz + Ct	Particle diameter, D (mm)	% finer than D, P (%)	Corrected % finer than D, P (%)
2	39	21	9.7	0.01112	0.176	33.176	0.024	70.40	67.79
5	36	21	10.19	0.01112	0.176	30.176	0.016	64.03	61.66
15	32	21	10.85	0.01112	0.176	26.176	0.009	55.55	53.49
30	28	21	11.51	0.01112	0.176	22.176	0.007	47.06	45.32
60	24	21	12.17	0.01112	0.176	18.176	0.005	38.57	37.14
250	18	23	13.16	0.01085	0.664	12.664	0.002	26.87	25.88
1440	12	21	14.15	0.01112	0.176	6.176	0.001	13.11	12.62

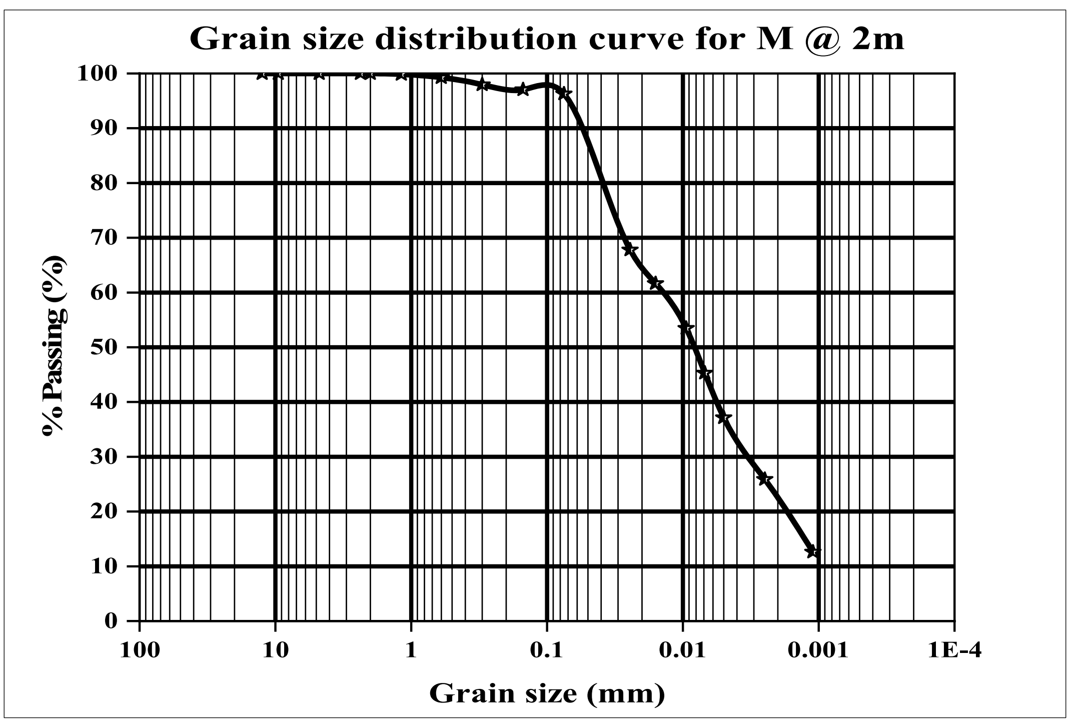

Figure B-5: Graph of grain size distribution curve for M @ 2 m

Table B-6: Grain size analysis for M @ 3 m

M @ 3 m

A. Wet sieve analysis

Sieve size (mm)	Mass of sieve (g)	Mass of sieve with soil retained (g)	Mass retained (g)	Cumulative mass retained (g)	Percentage retained (%)	Cumulative percent retained (%)	Percent passing (%)
12.5	439	439	0.00	0.00	0.00	0.00	100.00
9.5	442	442	0.00	0.00	0.00	0.00	100.00
4.75	440	440	0.00	0.00	0.00	0.00	100.00
2.36	405	405	0.00	0.00	0.00	0.00	100.00
2	383	383	0.00	0.00	0.00	0.00	100.00
1.18	359	359.11	0.11	0.11	0.22	0.22	99.78
0.6	329	329.79	0.79	0.90	1.58	1.80	98.20
0.3	294	295.54	1.54	2.44	3.08	4.88	95.12
0.15	278	279.36	1.36	3.80	2.72	7.60	92.40
0.075	272	273.57	1.57	5.37	3.14	10.74	89.26
Pan	252	296.63	44.63	50.00	89.26	100.00	
Total weight (g)	2167	2217	50.00		100.00		

B. Hydrometer analysis

Elapsed time, t (min)	Actual hydrometer reading, Ra	Temp. (°C)	Effective depth, L (mm)	K From table	Temp. correction factor, Ct	Modified hydrometer reading R = Ra – Cz + Ct	Particle diameter, D (mm)	% finer than D, P (%)	Corrected % finer than D, P (%)
2	33	21	10.69	0.01127	0.176	27.176	0.026	58.81	52.49
5	29	21	11.35	0.01127	0.176	23.176	0.017	50.15	44.77
15	24	21	12.17	0.01127	0.176	18.176	0.010	39.33	35.11
30	21	21	12.67	0.01127	0.176	15.176	0.007	32.84	29.31
60	18	21	13.16	0.01127	0.176	12.176	0.005	26.35	23.52
250	13	23	13.99	0.011	0.664	7.664	0.003	16.58	14.80
1440	9	21	14.65	0.01127	0.176	3.176	0.001	6.87	6.13

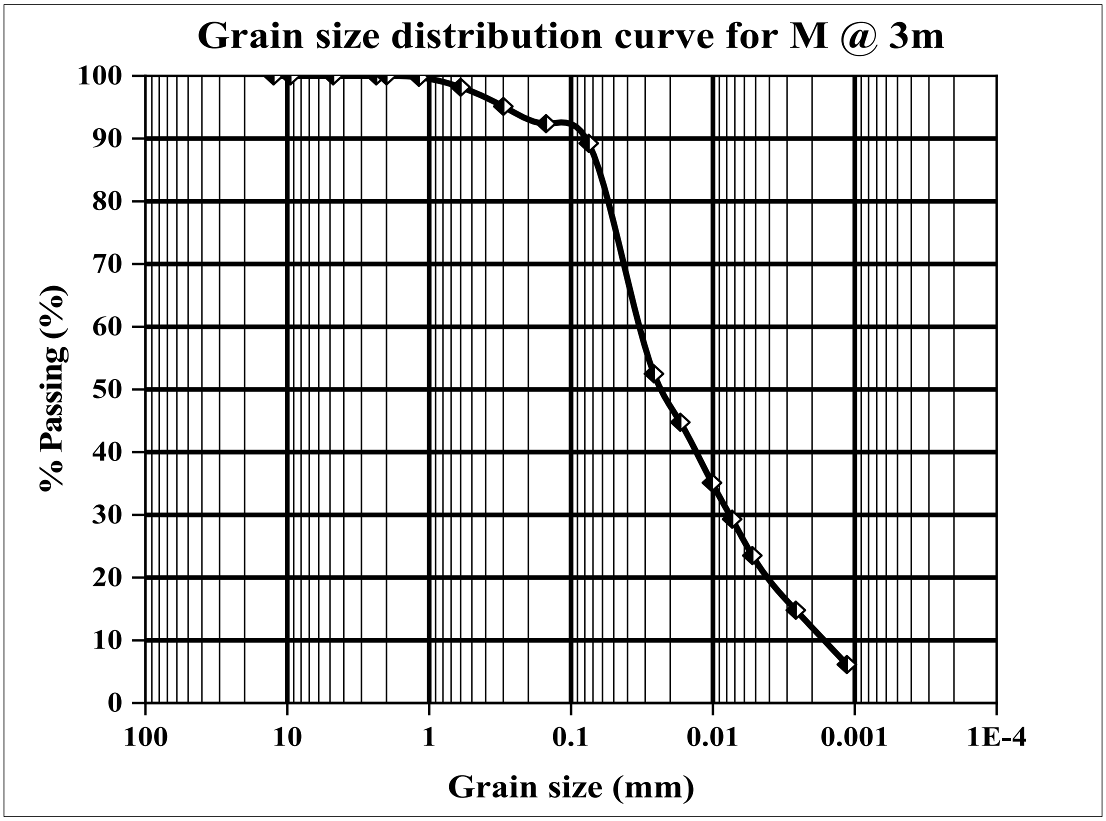

Figure B-6: Graph of grain size distribution curve for M @ 3 m

Appendix – C

Atterberg Limit Tests

Table C-1: Determination of Liquid Limit, Plastic Limit and Plastic Index for P @ 1.75 m

P @ 1.75 m						
	Liquid limit (LL)			Plastic limit (PL)		
Trial No.	1	2	3	1	2	3
Can No.	$P_{1.75}L_1$	$P_{1.75}L_2$	$P_{1.75}L_3$	$P_{1.75}P_1$	$P_{1.75}P_2$	$P_{1.75}P_3$
Mass of can (g)	20	18	20	20	19	19
Mass of wet soil + can (g)	29	28	29	37	37	37
Mass of dry soil + can (g)	26	24	25	32	33	33
Mass of dry soil (g)	6	6	5	12	14	14
Mass of moisture (g)	3	4	4	5	4	4
Water content w (%)	50	66.67	80	41.67	28.57	28.57
Number of blow	32	24	18	Avg. PL	32.94	
LL (%) = 63.3		PL (%) = 32.94			PI (%) = 31.65	

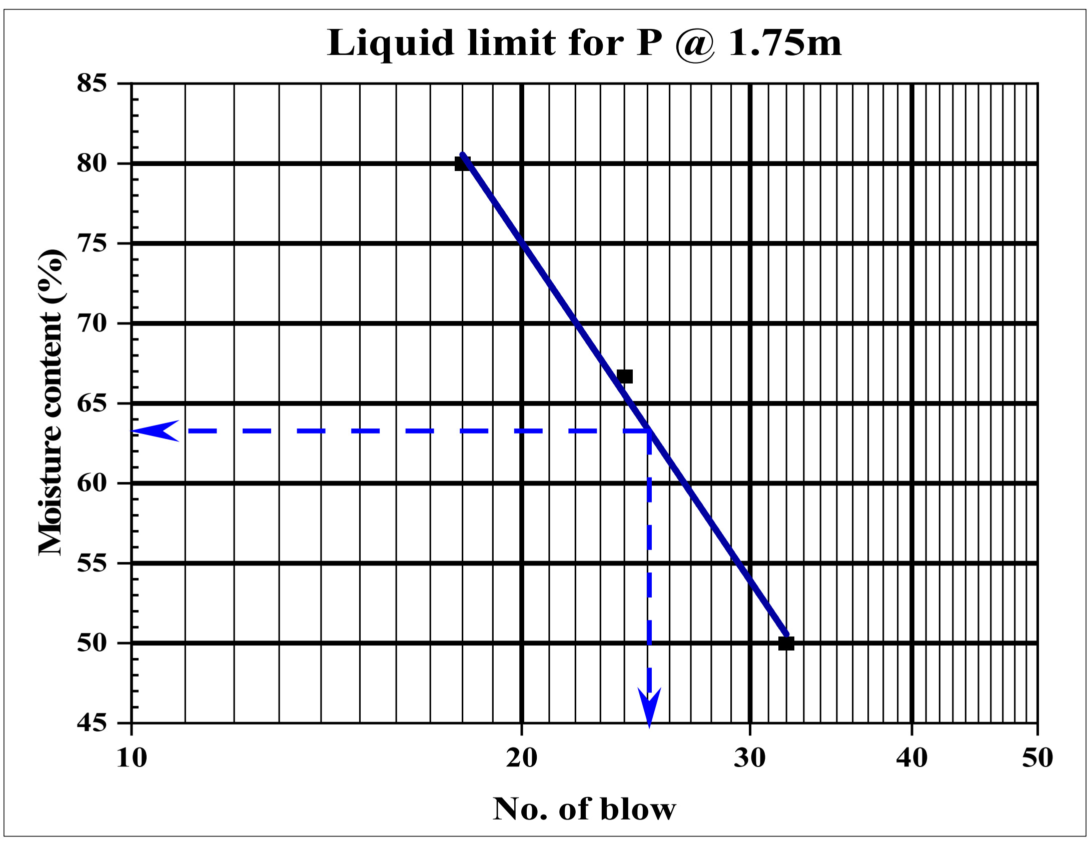

Figure C-1: Graph of Water Content Vs No. of blows for P @ 1.75 m

Table C-2: Determination of Liquid Limit, Plastic Limit and Plastic Index for P @ 3 m

P @ 3 m						
Trial No.	Liquid limit (LL)			Plastic limit (PL)		
	1	2	3	1	2	3
Can No.	P_3L_1	P_3L_2	P_3L_3	P_3P_1	P_3P_2	P_3P_2
Mass of can (g)	19	18	20	19	19	19
Mass of wet soil + can (g)	30	30	31	39	38	36
Mass of dry soil + can (g)	27	26	27	35	35	34
Mass of dry soil (g)	8	8	7	16	16	15
Mass of moisture (g)	3	4	4	4	3	2
Water content w (%)	37.5	50	57.14	25	18.75	13.33
Number of blow	34	26	18	Avg. PL	19.03	
LL (%) = 48.4		PL (%) = 19.03			PI (%) = 31.86	

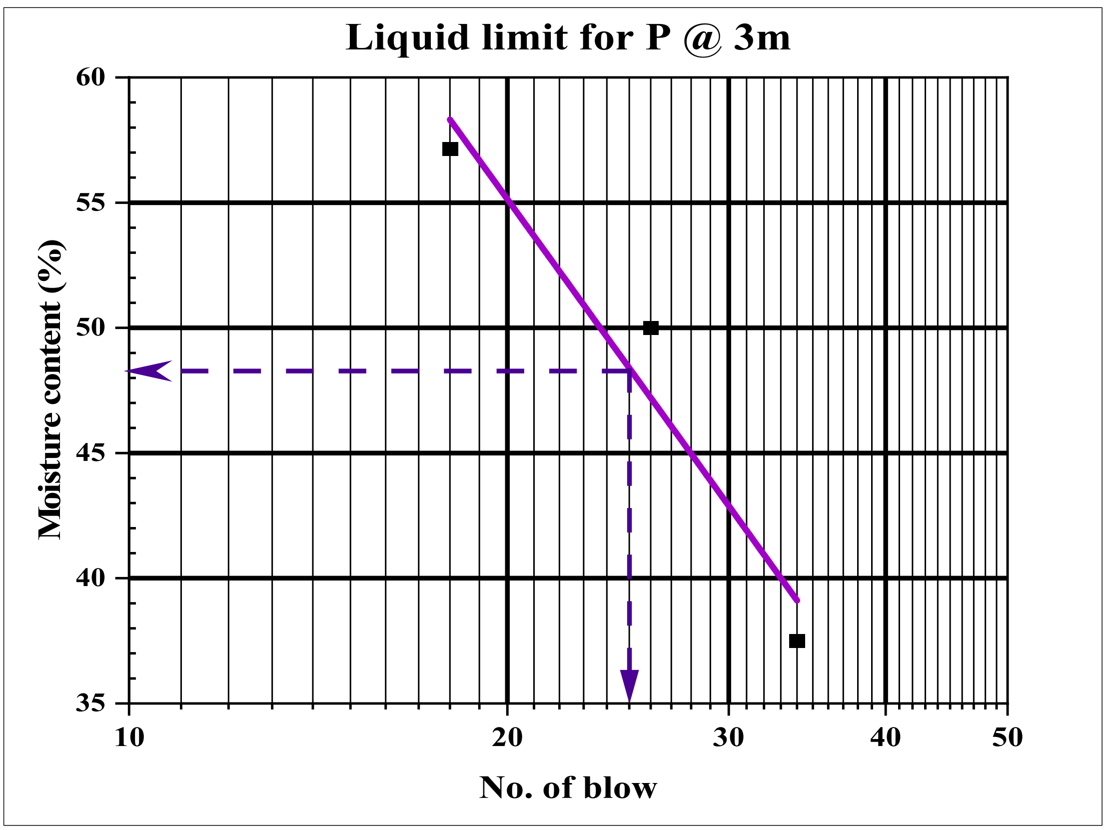

Figure C-2: Graph of Water Content Vs No. of blows for P @ 3 m

Table C-3: Determination of Liquid Limit, Plastic Limit and Plastic Index for H @ 1.5 m

H @ 1.5 m						
Trial No.	Liquid limit (LL)			Plastic limit (PL)		
	1	2	3	1	2	3
Can No.	$H_{1.5}L_1$	$H_{1.5}L_2$	$H_{1.5}L_3$	$H_{1.5}P_1$	$H_{1.5}P_2$	$H_{1.5}P_3$
Mass of can (g)	18	19	19	20	19	20
Mass of wet soil + can (g)	30	30	29	34	37	35
Mass of dry soil + can (g)	26	27	26	30	32	31
Mass of dry soil (g)	8	8	7	10	13	11
Mass of moisture (g)	4	3	3	4	5	4
Water content w (%)	50	37.5	42.86	40	38.46	36.36
Number of blow	15	34	24	Avg. PL	38.28	
LL (%) = 42.2		PL (%) = 38.28			PI (%) = 4.04	

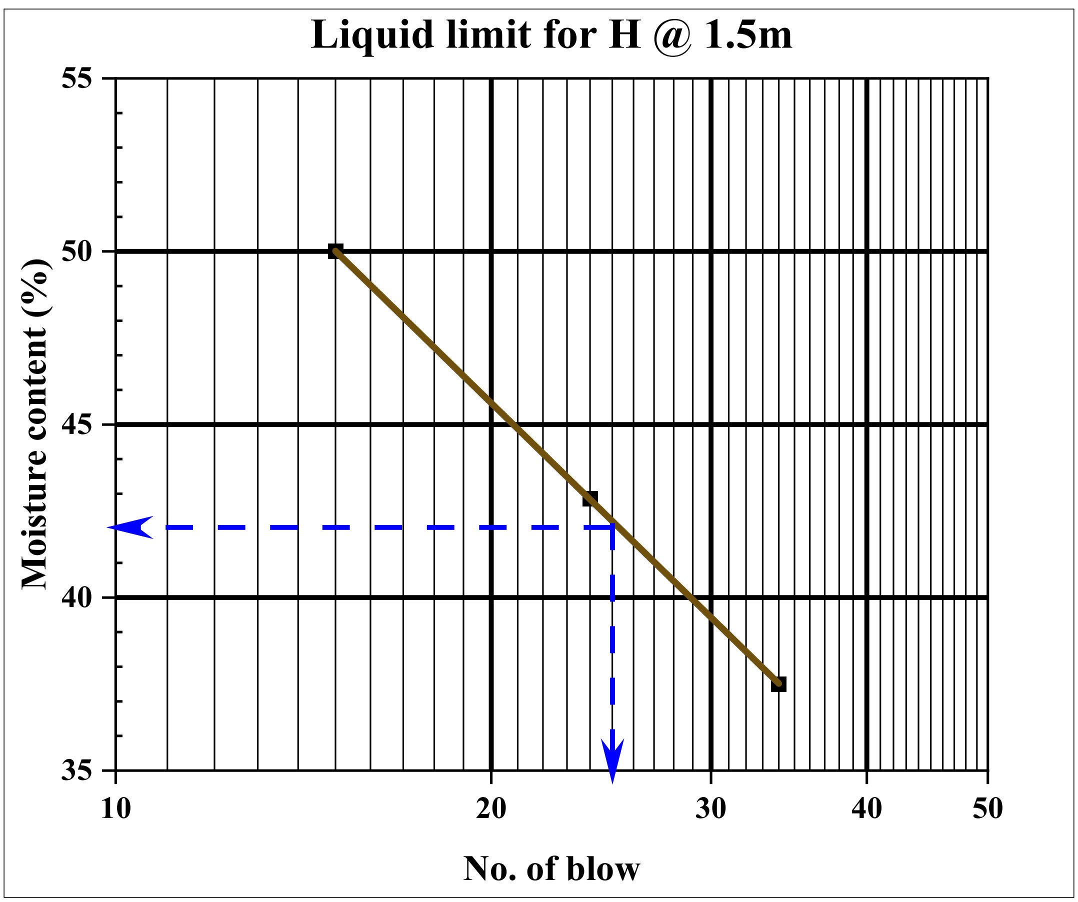

Figure C-3: Graph of Water Content Vs No. of blows for H @ 1.5 m

Table C-4: Determination of Liquid Limit, Plastic Limit and Plastic Index for H @ 3 m

H @ 3 m						
Trial No.	Liquid limit (LL)			Plastic limit (PL)		
	1	2	3	1	2	3
Can No.	H_3L_1	H_3L_2	H_3L_3	H_3P_1	H_3P_2	H_3P_3
Mass of can (g)	18	19	19	-	-	-
Mass of wet soil + can (g)	43	47	56	-	-	-
Mass of dry soil + can (g)	37	40	46	-	-	-
Mass of dry soil (g)	19	21	27	-	-	-
Mass of moisture (g)	6	7	10	-	-	-
Water content w (%)	31.58	33.33	37.04	-	-	-
Number of blow	16	24	31	-		
LL (%) = 32.8		PL (%) = NP			PI (%) = 0	

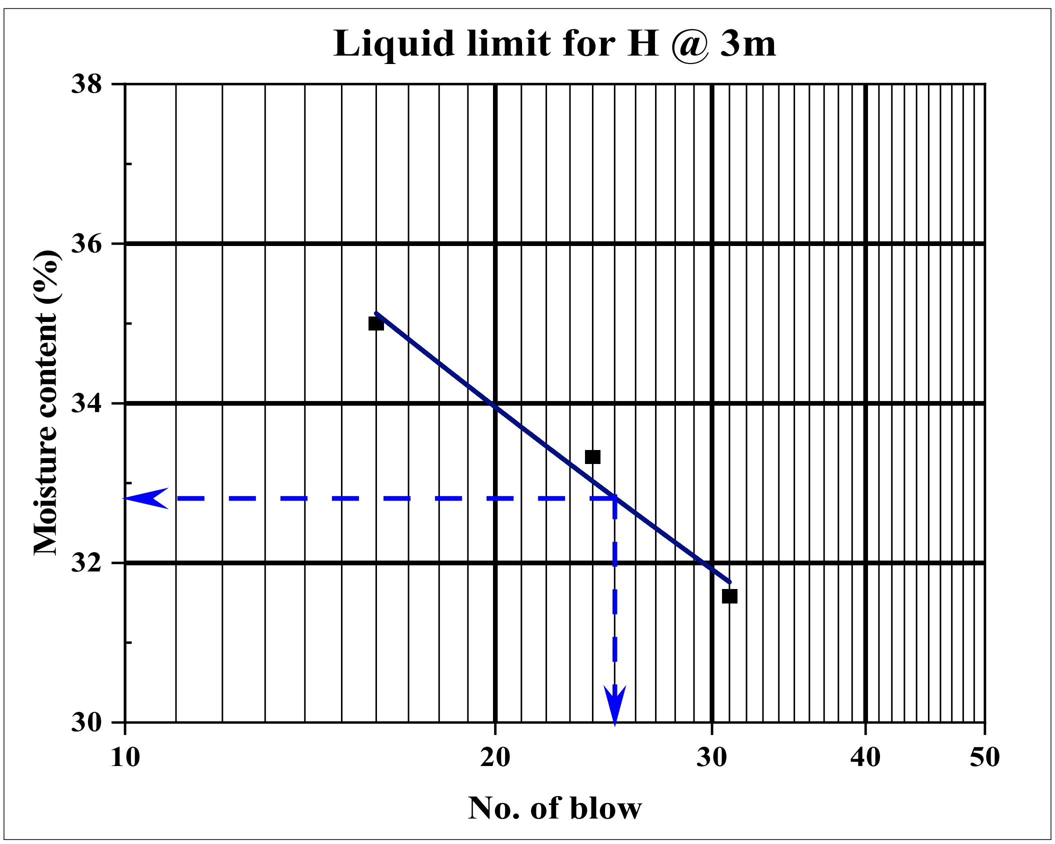

Figure C-4: Graph of Water Content Vs No. of blows for H @ 3 m

Table C-5: Determination of Liquid Limit, Plastic Limit and Plastic Index for M @ 2 m

M @ 2 m						
	Liquid limit (LL)			Plastic limit (PL)		
Trial No.	1	2	3	1	2	3
Can No.	M_2L_1	M_2L_2	M_2L_3	M_2P_1	M_2P_2	M_2P_3
Mass of can (g)	20	20	20	19	19	18
Mass of wet soil + can (g)	29	31	29	35	36	33
Mass of dry soil + can (g)	27	27	25	31	31	29
Mass of dry soil (g)	7	7	5	12	12	11
Mass of moisture (g)	2	4	4	4	5	4
Water content w (%)	28.57	50.68	80	33.33	41.67	36.36
Number of blow	33	26	18	Avg. PL	37.12	
LL (%) = 54.3		PL (%) = 37.12			PI (%) = 17.18	

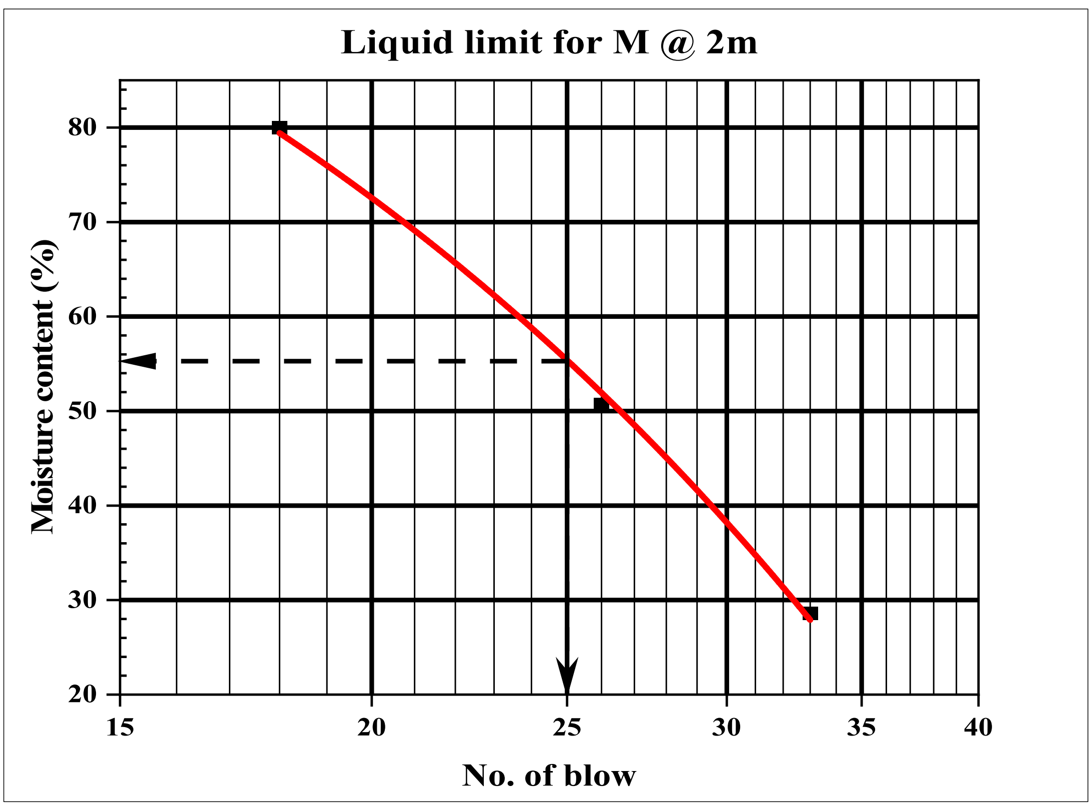

Figure C-5: Graph of Water Content Vs No. of blows for M @ 2 m

Table C-6: Determination of Liquid Limit, Plastic Limit and Plastic Index for M @ 3 m

M @ 3 m						
Trial No.	Liquid limit (LL)			Plastic limit (PL)		
	1	2	3	1	2	3
Can No.	M_3L_1	M_3L_2	M_3L_3	M_3P_1	M_3P_2	M_3P_3
Mass of can (g)	30	31	30	20	18	20
Mass of wet soil + can (g)	39	42	41	37	34	35
Mass of dry soil + can (g)	35	38	38	31	30	30
Mass of dry soil (g)	5	7	8	11	12	10
Mass of moisture (g)	4	4	3	6	4	5
Water content w (%)	80	57.14	37.5	54.55	33.33	50
Number of blow	17	27	35	Avg. PL	45.96	
LL (%) = 58.73		PL (%) = 45.96			PI (%) = 15.75	

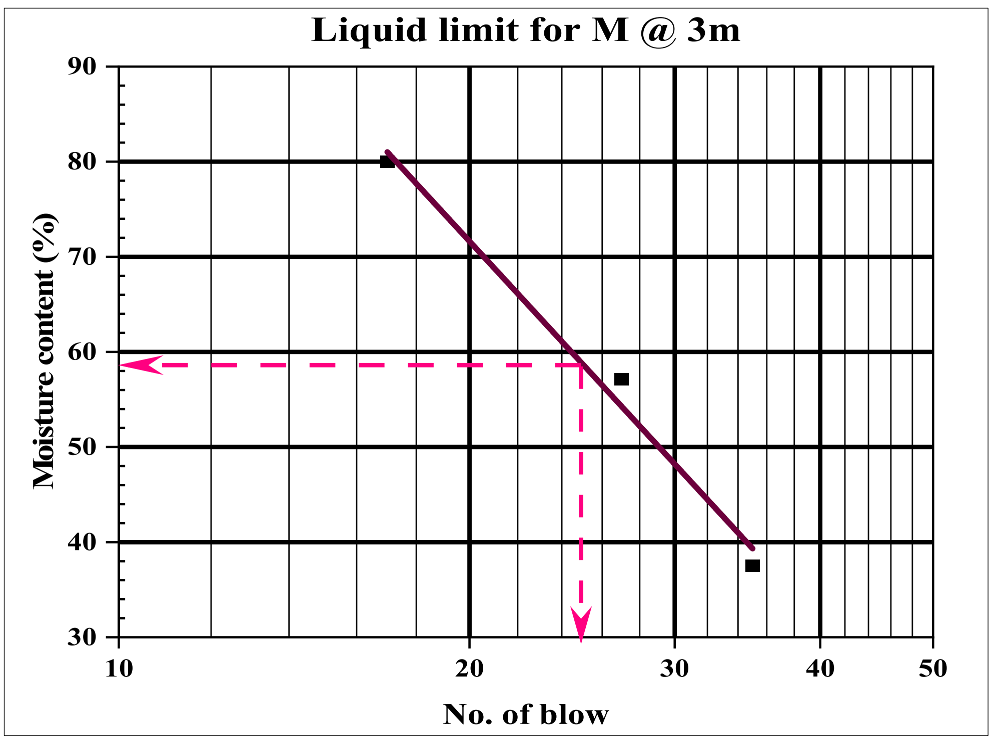

Figure C-6: Graph of Water Content Vs No. of blows for M @ 3 m

Appendix - D

Specific Gravity Test

Table D-1: Specific Gravity Determination for P @ 1.75 m

Specific gravity for P @ 1.75 m		
Determination No.	1	2
Pycnometer No.	P_1	P_2
Mass of Pycnometer filled with soil and water, M_b(g)	168.98	171.16
Mass of Pycnometer filled with water, M_a (g)	160	162
Mass of Pycnometer with dry soil (g)	77	77
Mass of Pycnometer (g)	62	62
Mass of dry soil, Mo (g)	15	15
Specific gravity of soil solids, G_s	2.49	2.57
Average specific gravity	2.53	

Table D-2: Specific Gravity Determination for P @ 3 m

Specific gravity for P @ 3 m		
Determination No.	1	2
Pycnometer No.	P_1	P_2
Mass of Pycnometer filled with soil and water, M_b(g)	161.79	163.14
Mass of Pycnometer filled with water, M_a (g)	152	154
Mass of Pycnometer with dry soil (g)	77	77
Mass of Pycnometer (g)	62	62
Mass of dry soil, Mo (g)	15	15
Specific gravity of soil solids, G_s	2.88	2.56
Average specific gravity	2.72	

Table D-3: Specific Gravity Determination for H @ 1.5 m

Specific gravity for H @ 1.5 m		
Determination No.	1	2
Pycnometer No.	P_1	P_2
Mass of Pycnometer filled with soil and water, M_b(g)	174.14	175.64
Mass of Pycnometer filled with water, M_a (g)	165	167
Mass of Pycnometer with dry soil (g)	77	77
Mass of Pycnometer (g)	62	62
Mass of dry soil, Mo (g)	15	15
Specific gravity of soil solids, G_s	2.56	2.36
Average specific gravity	2.46	

Table D-4: Specific Gravity Determination for H @ 3 m

Specific gravity for H @ 3 m		
Determination No.	1	2
Pycnometer No.	P_1	P_2
Mass of Pycnometer filled with soil and water, M_b(g)	177.67	177.96
Mass of Pycnometer filled with water, M_a (g)	169	170
Mass of Pycnometer with dry soil (g)	77	77
Mass of Pycnometer (g)	62	62
Mass of dry soil, Mo (g)	15	15
Specific gravity of soil solids, G_s	2.37	2.13
Average specific gravity	2.25	

Table D-5: Specific Gravity Determination for M @ 2 m

Specific gravity for M @ 2 m		
Determination No.	1	2
Pycnometer No.	P_1	P_2
Mass of Pycnometer filled with soil and water, M_b(g)	175.07	175.51
Mass of Pycnometer filled with water, M_a (g)	166	167
Mass of Pycnometer with dry soil (g)	77	77
Mass of Pycnometer (g)	62	62
Mass of dry soil, Mo (g)	15	15
Specific gravity of soil solids, G_s	2.53	2.31
Average specific gravity	2.42	

Table D-6: Specific Gravity Determination for M @ 3 m

Specific gravity for M @ 3 m		
Determination No.	1	2
Pycnometer No.	P_1	P_2
Mass of Pycnometer filled with soil and water, M_b(g)	175.39	176.83
Mass of Pycnometer filled with water, M_a (g)	167	168
Mass of Pycnometer with dry soil (g)	77	77
Mass of Pycnometer (g)	62	62
Mass of dry soil, Mo (g)	15	15
Specific gravity of soil solids, G_s	2.27	2.43
Average specific gravity	2.35	

Appendix - E

Compaction Test

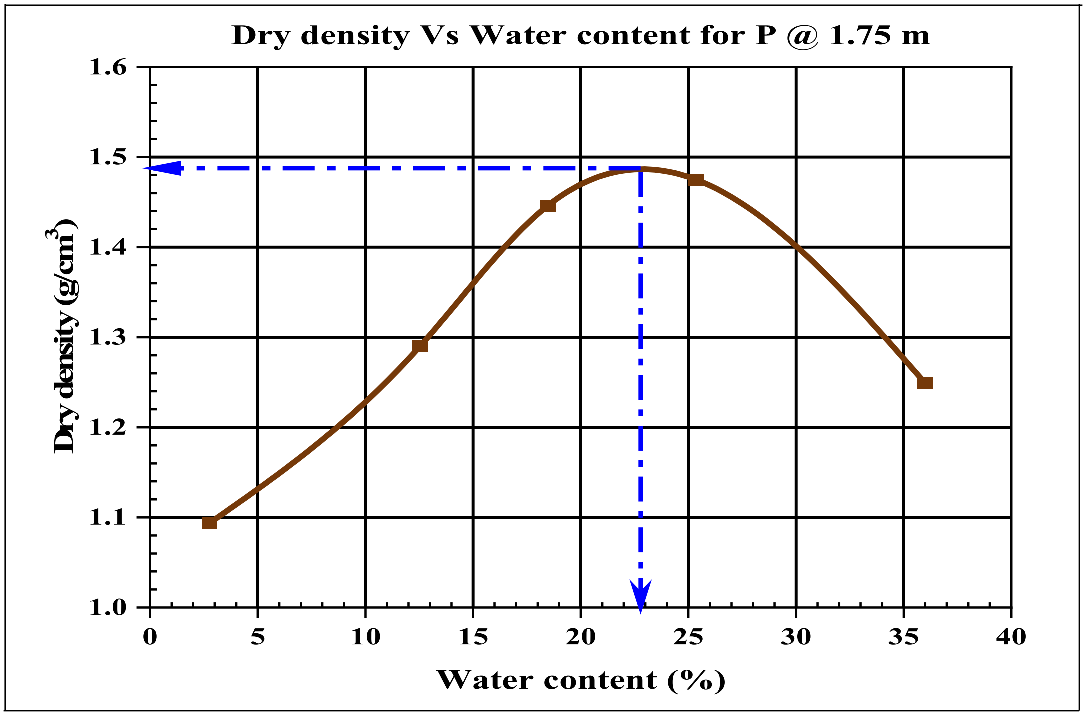

Figure E-1: Graph of Dry density Vs Water content for P @ 1.75 m

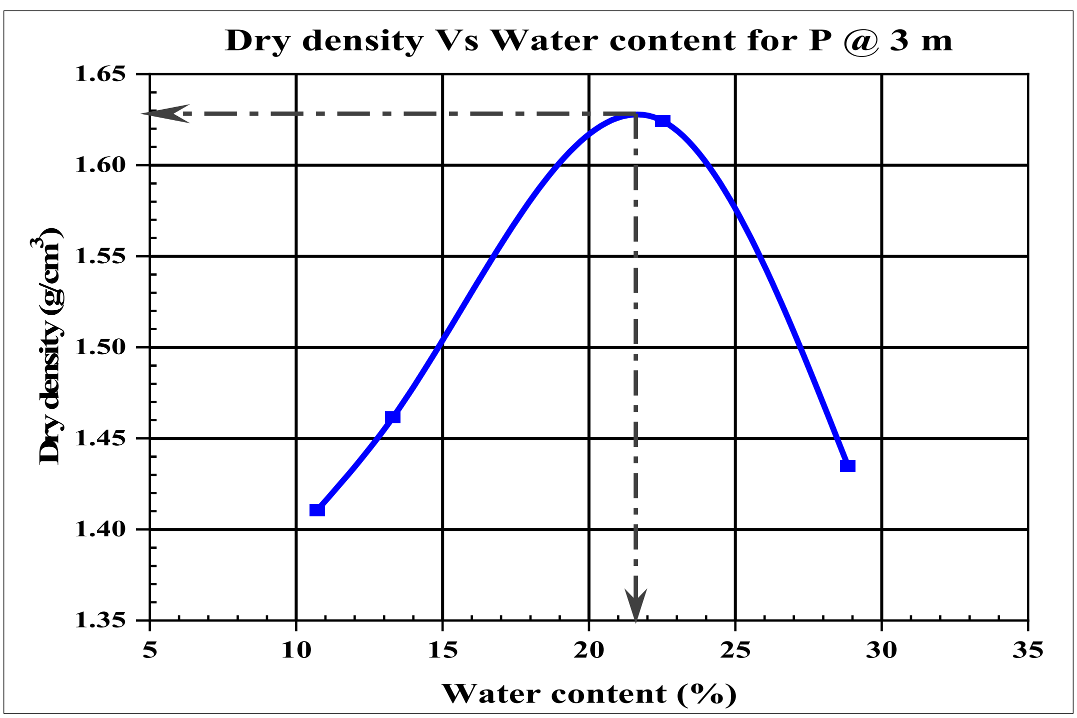

Figure E-2: Graph of Dry density Vs Water content for P @ 3 m

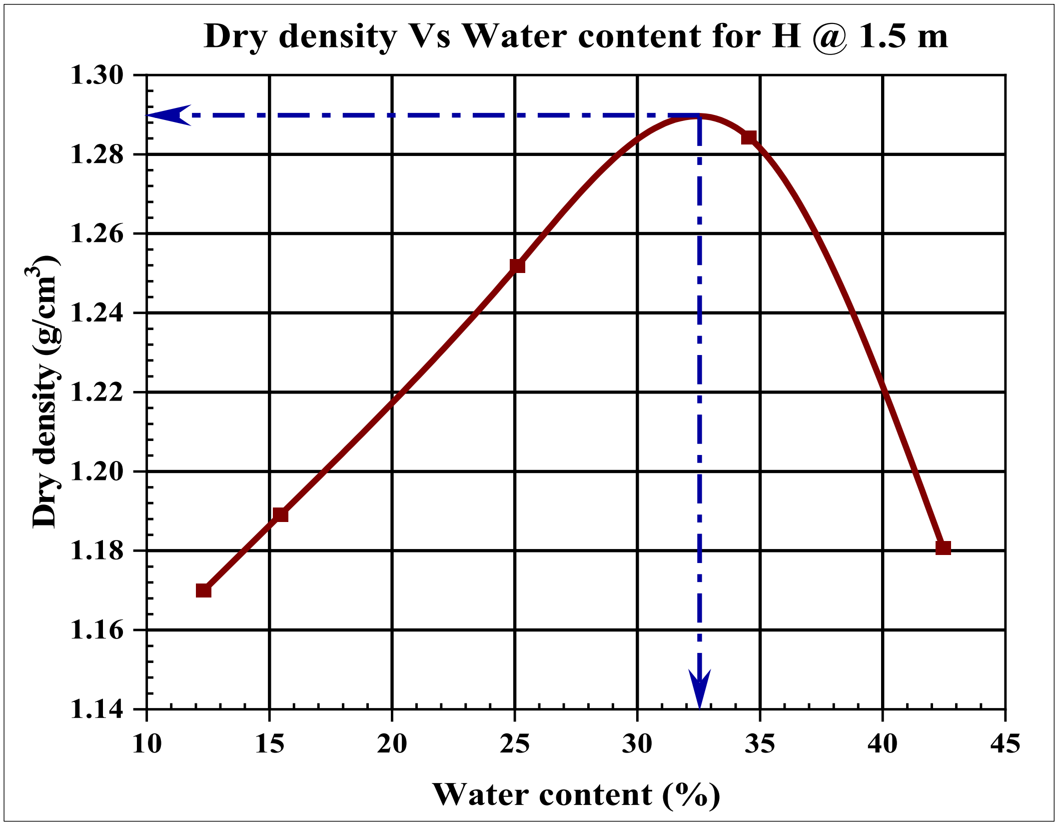

Figure E-3: Graph of Dry density Vs Water content for H @ 1.5 m

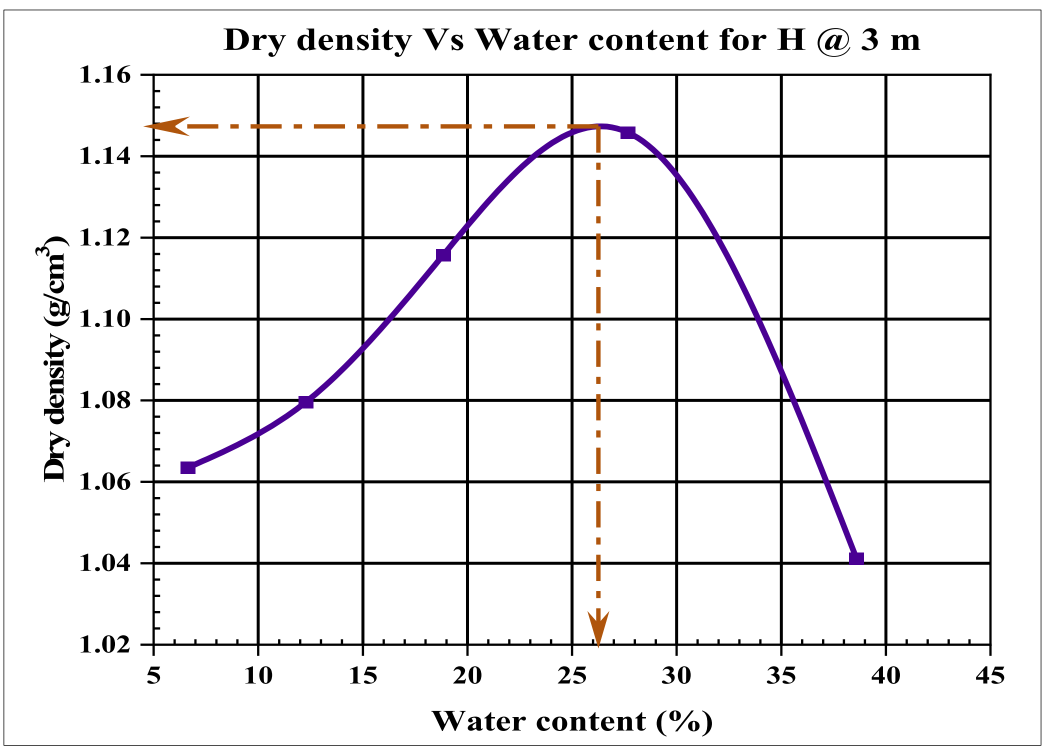

Figure E-4: Graph of Dry density Vs Water content for H @ 3 m

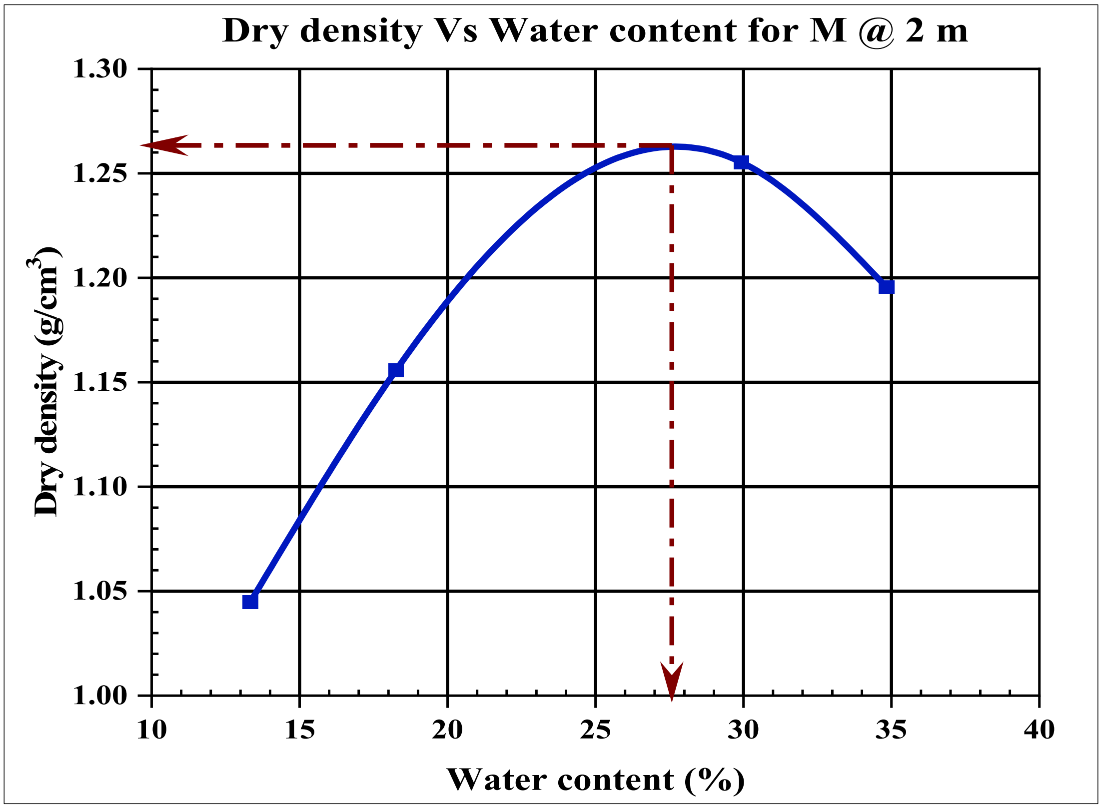

Figure E-5: Graph of Dry density Vs Water content for M @ 2 m

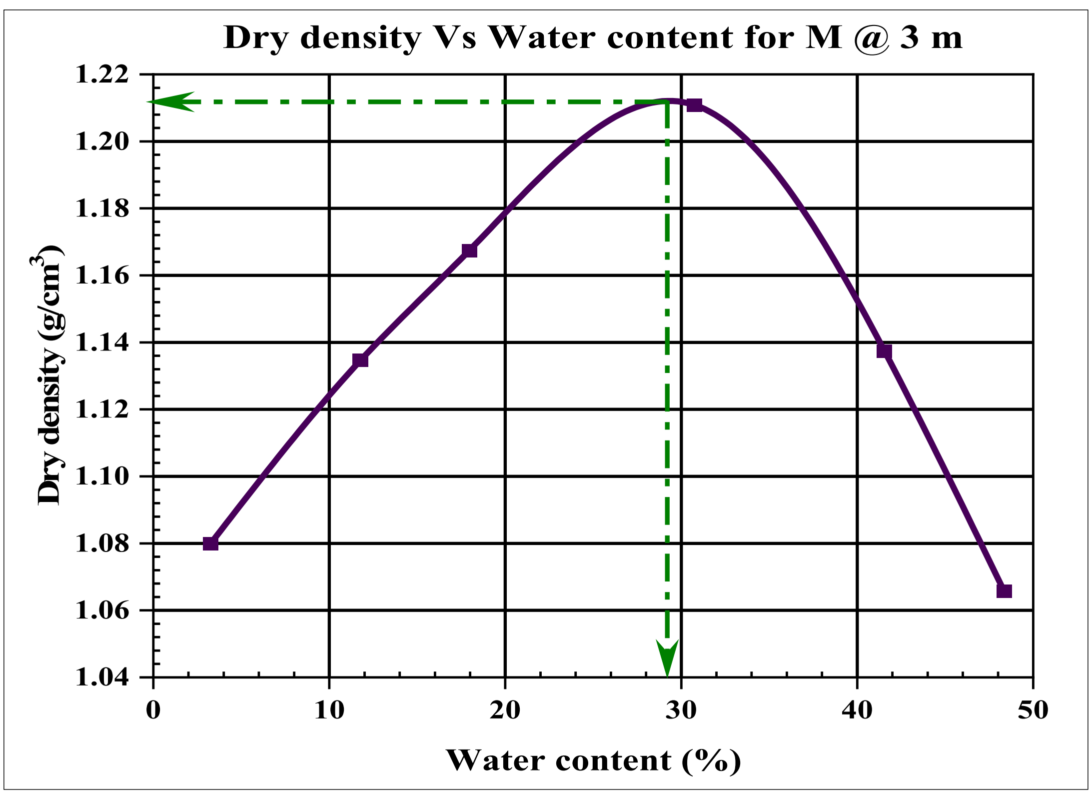

Figure E-6: Graph of Dry density Vs Water content for M @ 3 m

Appendix - F

1D - Consolidation Test

Table F-1: Determination of Pre-consolidation pressure for P @ 3 m

Specimen data			
Before test			
Weight of sample & ring (g)	260.40	Specific gravity, G_s	2.72
Weight of ring (g)	110.90	sample diameter, D (mm)	75.00
Weight of sample (g)	149.50	Sample thickness, H_o (mm)	20.00
Weight of dry sample (g)	124.70	Area, A (cm^2)	44.18
Weight of initial moisture (g)	24.80	Volume, V (cm^3)	88.37
Initial moisture content, w_o	19.89	Bulk density, ρ_b (g/cm^3)	1.69
Initial void ratio, $e_o = \frac{G_s}{\rho_d} - 1$	0.93	Dry density, ρ_d (g/cm^3)	1.41
Height of solids: $H_s = \frac{H_o}{1+e_o}$ (mm)	10.38		
Initial saturation, $S_o = \frac{w_o * G_S}{e_o}$	58.32		
After test			
Weight of sample + ring (g)	265.30	Overall settlement (mm)	3.26
Weight of dry sample + ring + can (g)	235.60	Volume change (cm^3)	14.40
Weight of ring + can (g)	110.90	Final volume (cm^3)	73.97
Weight of wet sample (g)	154.40	Final bulk density (g/cm^3)	2.09
Weight of dry sample (g)	124.70	Final dry density (g/cm^3)	1.69
Weight of final moisture (g)	29.70	final void ratio: (e_f)	0.61
Final moisture content, w_f (%)	23.82		

One-Dimensional Consolidation Test Calculation Sheet										
Voids Ratio					Compressibility			Coefficient of consolidation		
Increment No	Pressure (kPa)	Cumulative compression, ΔH (mm)	Consolidated height, $H_1 = H_o - \Delta H$ (mm)	Voids ratio $e = e_o - \frac{\Delta H}{H_s}$	Incremental Height change, dH (mm)	Incremental Pressure change, dp (kPa)	$m_v = (\frac{dH}{H_1} * \frac{1000}{dp})$ (m^2/MN)	t_{90} (min)	H = $\frac{1}{2}(H_i - H_{i+1})$ (mm)	$C_v = \frac{0.848 * H^2}{t_{90}}$ $(m^2/year)$
1	0	0.000	20.000	0.928						
					0.662	50	0.662			
2	50	0.662	19.338	0.864				0.9	0.331	0.103
					0.474	50	0.490			
3	100	1.136	18.864	0.818				0.9	0.237	0.053
					0.660	100	0.350			

4	200	1.796	18.204	0.754				0.72	0.33	0.128
					0.878	200	0.241			
5	400	2.674	17.326	0.670				1.32	0.439	0.124
					0.920	400	0.133			
6	800	3.594	16.406	0.581				0.9	0.46	0.199
					0.160	400	0.024			
7	400	3.434	16.566	0.597					-0.08	
					0.174	300	0.035			
8	100	3.260	16.740	0.613						

Table F-2: Determination of Pre-consolidation pressure for H @ 3 m

Specimen data			
Before test			
Weight of sample & ring (g)	195.60	Specific gravity, G_s	2.25
Weight of ring (g)	109.40	sample diameter, D (mm)	75.00
Weight of sample (g)	86.20	Sample thickness, H_o (mm)	20.00
Weight of dry sample (g)	78.00	Area, A (cm^2)	44.18
Weight of initial moisture (g)	8.20	Volume, V (cm^3)	88.37
Initial moisture content, w_o	10.51	Bulk density, ρ_b (g/cm^3)	0.98
Initial void ratio, $e_o = \frac{G_s}{\rho_d} - 1$	1.55	Dry density, ρ_d (g/cm^3)	0.88
Height of solids: $H_s = \frac{H_o}{1 + e_o}$ (mm)	7.85		
Initial saturation, $S_o = \frac{w_o * G_S}{e_o}$	15.27		
After test			
Weight of sample + ring (g)	221.70	Overall settlement (mm)	2.34
Weight of dry sample + ring + can (g)	187.40	Volume change (cm^3)	10.35
Weight of ring + can (g)	109.40	Final volume (cm^3)	78.02
Weight of wet sample (g)	112.30	Final bulk density (g/cm^3)	1.44
Weight of dry sample (g)	78.00	Final dry density (g/cm^3)	1.00
Weight of final moisture (g)	34.30	final void ratio: (e_f)	1.25
Final moisture content, w_f (%)	43.97		

One-Dimensional Consolidation Test Calculation Sheet										
Voids Ratio					Compressibility			Coefficient of consolidation		
Increment No	Pressure (kPa)	Cumulative compression, ΔH (mm)	Consolidated height, $H_1 = H_o - \Delta H$ (mm)	Voids ratio $e = e_o - \frac{\Delta H}{H_s}$	Incremental Height change, dH (mm)	Incremental Pressure change, dp (kPa)	$m_v = (\frac{dH}{H_1} * \frac{1000}{dp})$ (m^2/MN)	t_{90} (min)	H = $\frac{1}{2}(H_i - H_{i+1})$ (mm)	$C_v = \frac{0.848 * H^2}{t_{90}}$ $(m^2/year)$
1	0	0.000	20.000	1.549						
					0.716	50	0.716			
2	50	0.716	19.284	1.458				0.9	0.358	0.121
					0.246	50	0.255			
3	100	0.962	19.038	1.427				0.9	0.123	0.014
					0.422	100	0.222			
4	200	1.384	18.616	1.373				0.64	0.211	0.059
					0.580	200	0.156			
5	400	1.964	18.036	1.299				1	0.29	0.071
					0.690	400	0.096			
6	800	2.654	17.346	1.211				0.9	0.345	0.112
					0.150	400	0.022			
7	400	2.504	17.496	1.230					-0.075	
					0.162	300	0.031			
8	100	2.342	17.658	1.251						

Table F-3: Determination of Pre-consolidation pressure for M @ 3 m

Specimen data			
Before test			
Weight of sample & ring (g)	231.70	Specific gravity, G_s	2.35
Weight of ring (g)	114.50	sample diameter, D (mm)	75.00
Weight of sample (g)	117.20	Sample thickness, H_o (mm)	20.00
Weight of dry sample (g)	87.40	Area, A (cm^2)	44.18
Weight of initial moisture (g)	29.80	Volume, V (cm^3)	88.37
Initial moisture content, w_o	34.10	Bulk density, ρ_b (g/cm^3)	1.33
Initial void ratio, $e_o = \frac{G_s}{\rho_d} - 1$	1.38	Dry density, ρ_d (g/cm^3)	0.99
Height of solids: $H_s = \frac{H_o}{1 + e_o}$(mm)	8.42		
Initial saturation, $S_o = \frac{w_o * G_S}{e_o}$	58.23		

After test			
Weight of sample + ring (g)	236.60	Overall settlement (mm)	3.46
Weight of dry sample + ring + can (g)	201.90	Volume change (cm^3)	15.28
Weight of ring + can (g)	114.50	Final volume (cm^3)	73.09
Weight of wet sample (g)	122.10	Final bulk density (g/cm^3)	1.67
Weight of dry sample (g)	87.40	Final dry density (g/cm^3)	1.20
Weight of final moisture (g)	34.70	Final void ratio: (e_f)	0.97
Final moisture content, w_f (%)	39.70		

One-Dimensional Consolidation Test Calculation Sheet

Voids Ratio					Compressibility			Coefficient of consolidation		
Increment No	Pressure (kPa)	Cumulative compression, ΔH (mm)	Consolidated height, $H_1 = H_o - \Delta H$ (mm)	Voids ratio $e = e_o - \frac{\Delta H}{H_s}$	Incremental Height change, dH (mm)	Incremental Pressure change, dp (kPa)	$m_v = (\frac{dH}{H_1} * \frac{1000}{dp})$ (m^2/MN)	t_{90} (min)	H = $\frac{1}{2}(H_i - H_{i+1})$ (mm)	$C_v = \frac{0.848 * H^2}{t_{90}}$ $(m^2/year)$
1	0	0.000	20.000	1.376						
					0.534	50	0.534			
2	50	0.534	19.466	1.313				1	0.267	0.06
					0.300	50	0.308			
3	100	0.834	19.166	1.277				1.69	0.15	0.01
					0.360	100	0.188			
4	200	1.194	18.806	1.234				3.06	0.18	0.01
					1.646	200	0.438			
5	400	2.840	17.160	1.039				1	0.823	0.57
					0.936	400	0.136			
6	800	3.776	16.224	0.927				1	0.468	0.19
					0.142	400	0.022			
7	400	3.634	16.366	0.944					-0.071	
					0.176	300	0.036			
8	100	3.458	16.542	0.965						

Appendix - G

Cyclic Simple Shear Test

A. Shear Modulus and Damping Ratio Values

Table G-1: Shear modulus and damping ration values of H @ 150 kPa

Strain (%)	0.01	0.1	1	2.5	5	0.01	0.1	1	2.5	5
Cycle No.	Shear Modulus, G (MPa)					Damping Ratio, ξ (%)				
1	1.761	0.975	0.591	0.469	0.292	8.332	12.953	19.312	22.419	30.851
2	1.781	0.999	0.612	0.474	0.302	7.755	12.596	18.499	21.818	30.167
3	1.813	1.033	0.635	0.475	0.304	7.241	11.819	17.651	20.792	29.647
4	1.843	1.061	0.641	0.477	0.304	6.633	11.382	17.217	20.790	29.022
5	1.873	1.076	0.661	0.477	0.308	6.514	11.348	16.942	20.590	28.415
6	1.881	1.079	0.664	0.478	0.308	6.457	11.060	16.649	20.365	27.960
7	1.895	1.082	0.698	0.483	0.310	6.426	10.767	16.485	20.265	27.781
8	1.902	1.083	0.704	0.485	0.313	6.401	10.694	16.314	20.242	27.472
9	1.935	1.110	0.710	0.485	0.321	6.399	10.684	16.215	20.233	27.050
10	1.945	1.115	0.725	0.486	0.328	6.378	10.674	16.189	20.197	26.476
11	1.960	1.121	0.726	0.488	0.329	6.343	10.664	16.110	20.193	26.375
12	1.995	1.127	0.730	0.488	0.340	6.314	10.651	16.082	20.189	26.346
13	2.016	1.149	0.735	0.498	0.343	6.285	10.630	16.061	20.151	26.315
14	2.037	1.163	0.738	0.498	0.349	6.259	10.625	16.042	20.077	26.302
15	2.054	1.187	0.741	0.499	0.354	6.214	10.601	15.994	20.026	26.296
16	2.080	1.210	0.752	0.504	0.358	6.176	10.599	15.985	19.676	26.275
17	2.100	1.236	0.774	0.511	0.366	6.149	10.569	15.975	19.655	26.255
18	2.115	1.277	0.781	0.516	0.369	6.103	10.548	15.946	19.473	26.146
19	2.145	1.302	0.793	0.522	0.373	6.013	10.535	15.933	19.406	26.125
20	2.177	1.367	0.793	0.529	0.383	5.973	10.526	15.919	19.349	26.049
21	2.206	1.372	0.804	0.539	0.387	5.955	10.499	15.902	19.254	25.902
22	2.236	1.399	0.809	0.549	0.393	5.935	10.475	15.855	19.204	25.853
23	2.258	1.404	0.819	0.557	0.401	5.933	10.436	15.836	19.136	25.749
24	2.276	1.450	0.828	0.565	0.409	5.925	10.401	15.813	19.112	25.690
25	2.294	1.463	0.832	0.576	0.419	5.902	10.386	15.802	18.943	25.590
26	2.301	1.495	0.853	0.581	0.433	5.899	10.346	15.755	18.928	25.547
27	2.336	1.546	0.873	0.593	0.437	5.875	10.310	15.702	18.911	25.487
28	2.385	1.602	0.894	0.611	0.442	5.855	10.286	15.685	18.862	25.355
29	2.390	1.631	0.908	0.621	0.460	5.796	10.249	15.541	18.842	25.286
30	2.420	1.667	0.929	0.636	0.469	5.746	10.210	15.478	18.797	25.178
31	2.463	1.685	0.955	0.655	0.470	5.737	10.175	15.422	18.752	25.155
32	2.506	1.710	0.965	0.671	0.476	5.712	10.025	15.399	18.747	25.143
33	2.536	1.730	0.987	0.693	0.479	5.702	9.954	15.366	18.678	25.033
34	2.543	1.731	0.999	0.719	0.482	5.696	9.933	15.320	18.606	24.987
35	2.568	1.769	1.098	0.760	0.485	5.675	9.874	15.315	18.559	24.857
36	2.596	1.796	1.120	0.797	0.489	5.666	9.826	15.255	18.557	24.759
37	2.632	1.830	1.169	0.832	0.490	5.649	9.755	15.214	18.538	24.569
38	2.683	1.874	1.195	0.875	0.492	5.632	9.715	15.155	18.504	24.357
39	2.713	1.949	1.220	0.905	0.501	5.610	9.655	15.102	18.431	24.103
40	2.761	2.017	1.232	0.978	0.501	5.600	9.594	15.071	18.359	24.077

Table G-2: Shear modulus and damping ration values of H @ 275 kPa

Strain (%)	0.01	0.1	1	2.5	5	0.01	0.1	1	2.5	5
Cycle No.	Shear Modulus, G (MPa)					Damping Ratio, ξ (%)				
1	6.591	4.692	2.606	1.959	1.757	5.025	8.332	13.859	18.062	22.419
2	6.605	4.782	2.865	2.015	1.764	4.734	7.755	13.543	17.351	21.818
3	6.632	4.786	2.914	2.102	1.774	4.374	7.652	13.255	16.972	20.792
4	6.673	4.786	2.972	2.163	1.767	4.029	7.602	13.026	16.518	20.790
5	6.695	4.803	2.993	2.183	1.771	3.964	7.593	12.896	16.035	20.590
6	6.739	4.810	3.002	2.255	1.774	3.928	7.476	12.862	15.972	20.365
7	6.780	4.811	3.018	2.278	1.775	3.924	7.399	12.833	15.955	20.265
8	6.810	4.816	3.028	2.299	1.776	3.827	7.362	12.786	15.927	20.242
9	6.850	4.819	3.038	2.302	1.776	3.818	7.302	12.754	15.901	20.233
10	6.890	4.820	3.085	2.316	1.783	3.788	7.255	12.733	15.896	20.197
11	6.924	4.825	3.089	2.336	1.788	3.672	7.190	12.710	15.875	20.193
12	6.964	4.829	3.125	2.354	1.788	3.641	7.125	12.692	15.855	20.189
13	6.994	4.848	3.176	2.376	1.788	3.518	6.985	12.675	15.773	20.151
14	7.015	4.886	3.201	2.395	1.789	3.457	6.961	12.635	15.610	20.077
15	7.047	4.918	3.178	2.402	1.792	3.447	6.953	12.585	15.605	20.026
16	7.070	4.953	3.223	2.412	1.795	3.401	6.925	12.482	15.466	19.676
17	7.091	4.986	3.268	2.425	1.798	3.396	6.905	12.255	15.454	19.655
18	7.122	5.060	3.309	2.436	1.800	3.370	6.895	11.986	15.179	19.473
19	7.123	5.109	3.321	2.440	1.802	3.315	6.875	11.875	15.090	19.406
20	7.138	5.158	3.393	2.454	1.813	3.297	6.855	11.760	14.973	19.349
21	7.142	5.154	3.422	2.494	1.814	3.249	6.835	11.733	14.777	19.254
22	7.144	5.230	3.472	2.537	1.816	3.222	6.799	11.699	14.769	19.204
23	7.146	5.269	3.537	2.589	1.820	3.191	6.758	11.658	14.746	19.136
24	7.147	5.276	3.542	2.621	1.833	3.190	6.725	11.578	14.736	19.112
25	7.148	5.289	3.544	2.677	1.837	3.188	6.702	11.535	14.722	18.943
26	7.152	5.295	3.549	2.716	1.846	3.188	6.699	11.502	14.702	18.928
27	7.156	5.321	3.570	2.725	1.849	3.117	6.678	11.499	14.699	18.911
28	7.180	5.372	3.580	2.727	1.852	3.097	6.669	11.475	14.685	18.862
29	7.181	5.401	3.599	2.732	1.894	3.052	6.658	11.422	14.578	18.842
30	7.202	5.412	3.601	2.733	1.901	3.040	6.632	11.395	14.486	18.797
31	7.204	5.429	3.662	2.737	1.913	3.034	6.613	11.368	14.427	18.752
32	7.214	5.438	3.676	2.739	1.932	3.020	6.591	11.321	14.399	18.747
33	7.230	5.478	3.764	2.749	1.968	2.988	6.585	11.285	14.357	18.678
34	7.238	5.498	3.782	2.750	1.986	2.872	6.575	11.255	14.255	18.606
35	7.259	5.518	3.797	2.751	2.005	2.837	6.533	11.236	14.201	18.559
36	7.285	5.519	3.830	2.754	2.035	2.802	6.501	11.175	14.124	18.557
37	7.306	5.519	3.850	2.755	2.118	2.796	6.453	11.125	14.103	18.538
38	7.356	5.521	3.880	2.757	2.141	2.769	6.402	11.075	14.013	18.504
39	7.486	5.522	3.903	2.759	2.178	2.751	6.375	11.022	13.996	18.431
40	7.545	5.524	4.033	2.761	2.199	2.735	6.345	10.962	13.976	18.359

Table G-3: Shear modulus and damping ration values of H @ 400 kPa

Strain (%)	0.01	0.1	1	2.5	5	0.01	0.1	1	2.5	5
Cycle No.	Shear Modulus, G (MPa)					Damping Ratio, ξ (%)				
1	9.166	7.304	5.701	4.936	4.622	2.749	4.986	9.127	11.910	16.022
2	9.185	7.321	5.720	4.978	4.782	2.548	4.846	8.854	11.808	15.888
3	9.199	7.339	5.749	4.996	4.786	2.326	4.785	8.530	11.703	15.679
4	9.210	7.343	5.763	5.030	4.786	2.014	4.688	8.335	11.520	15.461
5	9.229	7.418	5.784	5.049	4.803	1.999	4.516	8.095	10.972	15.342
6	9.255	7.456	5.821	5.074	4.810	1.890	4.502	8.061	10.802	15.162
7	9.285	7.517	5.900	5.128	4.811	1.870	4.499	7.864	10.785	15.018
8	9.315	7.573	5.940	5.130	4.816	1.802	4.476	7.780	10.702	14.956
9	9.366	7.637	6.058	5.142	4.819	1.777	4.468	7.738	10.658	14.811
10	9.395	7.686	6.185	5.173	4.822	1.728	4.458	7.735	10.588	14.791
11	9.413	7.739	6.202	5.200	4.832	1.724	4.398	7.717	10.476	14.668
12	9.436	7.791	6.249	5.211	4.834	1.695	4.328	7.672	10.386	14.652
13	9.458	7.848	6.275	5.215	4.838	1.680	4.201	7.684	10.302	14.455
14	9.499	7.898	6.322	5.219	4.844	1.659	4.168	7.590	10.286	14.455
15	9.503	7.950	6.358	5.240	4.847	1.594	4.165	7.642	10.256	14.240
16	9.627	8.023	6.376	5.246	4.853	1.565	4.155	7.627	10.155	14.195
17	9.644	8.084	6.402	5.269	4.856	1.526	4.136	7.491	10.125	14.090
18	9.649	8.133	6.416	5.281	4.860	1.509	4.128	7.479	10.102	14.084
19	9.664	8.185	6.457	5.291	4.862	1.497	4.000	7.427	10.024	13.841
20	9.716	8.245	6.471	5.300	4.868	1.429	3.934	7.358	9.995	13.735
21	9.724	8.295	6.524	5.307	4.868	1.397	3.822	7.223	9.843	13.590
22	9.740	8.348	6.567	5.352	4.868	1.385	3.587	7.155	9.839	13.328
23	9.777	8.381	6.625	5.394	4.869	1.314	3.504	7.149	9.710	13.117
24	9.784	8.431	6.648	5.434	4.870	1.308	3.391	7.126	9.670	12.996
25	9.803	8.498	6.678	5.474	4.877	1.301	3.342	7.111	9.586	12.951
26	9.813	8.566	6.695	5.524	4.879	1.266	3.314	7.048	9.505	12.948
27	9.841	8.611	6.735	5.584	4.886	1.265	3.291	7.015	9.481	12.781
28	9.846	8.672	6.798	5.614	4.893	1.218	3.258	7.014	9.424	12.721
29	9.873	8.739	6.855	5.644	4.904	1.156	3.245	7.002	9.365	12.672
30	9.965	8.795	6.901	5.685	4.905	1.134	3.236	6.971	9.345	12.509
31	9.998	8.848	6.959	5.715	4.916	1.056	3.231	6.930	9.344	12.448
32	10.094	8.892	7.055	5.745	4.917	1.046	3.230	6.877	9.290	12.345
33	10.157	8.951	7.153	5.951	4.929	1.045	3.225	6.811	9.214	12.288
34	10.206	9.012	7.186	6.004	4.970	1.003	3.201	6.760	9.194	12.248
35	10.278	9.071	7.236	6.046	5.012	1.002	3.199	6.697	9.191	12.107
36	10.311	9.114	7.275	6.098	5.085	0.977	3.178	6.647	9.131	11.806
37	10.389	9.157	7.360	6.131	5.155	0.922	3.155	6.597	9.102	11.675
38	10.443	9.169	7.402	6.181	5.201	0.800	3.102	6.569	8.985	11.439
39	10.520	9.180	7.496	6.218	5.275	0.701	3.085	6.498	8.951	11.281
40	10.605	9.185	7.530	6.240	5.323	0.678	3.049	6.458	8.931	11.182

Table G-4: Shear modulus and damping ration values of M @ 150 kPa

Strain (%)	0.01	0.1	1	2.5	5	0.01	0.1	1	2.5	5
Cycle No.	Shear Modulus, G (MPa)					Damping Ratio, ξ (%)				
1	4.692	3.360	1.912	1.426	1.285	4.987	8.521	16.402	18.293	21.689
2	4.782	3.397	1.955	1.458	1.301	4.678	8.325	16.098	17.903	21.318
3	4.786	3.440	1.975	1.486	1.355	4.577	8.098	15.979	17.789	20.953
4	4.786	3.485	1.985	1.501	1.395	4.551	7.847	15.605	17.631	20.746
5	4.803	3.503	2.098	1.557	1.406	4.426	7.634	15.342	17.587	20.590
6	4.810	3.539	2.157	1.602	1.427	4.386	7.601	15.162	17.578	20.513
7	4.811	3.579	2.186	1.648	1.457	4.382	7.599	15.018	17.432	20.355
8	4.816	3.593	2.215	1.707	1.472	4.382	7.558	14.956	17.308	20.290
9	4.819	3.636	2.289	1.740	1.518	4.371	7.525	14.811	17.161	20.246
10	4.832	3.654	2.361	1.783	1.548	4.351	7.499	14.791	17.106	20.197
11	4.843	3.695	2.396	1.818	1.588	4.308	7.460	14.668	16.984	20.193
12	4.873	3.730	2.456	1.846	1.609	4.230	7.458	14.652	16.961	19.999
13	4.898	3.770	2.486	1.875	1.638	4.208	7.422	14.455	16.868	19.942
14	4.934	3.800	2.527	1.895	1.649	4.202	7.402	14.455	16.688	19.818
15	4.965	3.830	2.577	1.922	1.672	4.178	7.387	14.240	16.566	19.738
16	4.985	3.866	2.609	1.955	1.698	4.174	7.359	14.195	16.477	19.676
17	5.109	3.898	2.640	1.995	1.720	4.169	7.258	14.090	16.397	19.655
18	5.149	3.921	2.697	2.058	1.758	4.143	7.215	14.084	16.300	19.473
19	5.199	3.954	2.736	2.110	1.788	4.137	7.103	13.841	16.176	19.406
20	5.213	3.975	2.762	2.161	1.813	4.127	6.996	13.735	16.139	19.349
21	5.287	4.006	2.782	2.218	1.814	4.124	6.965	13.390	16.008	19.254
22	5.349	4.013	2.808	2.252	1.816	4.117	6.935	13.128	15.893	19.204
23	5.377	4.017	2.830	2.305	1.820	4.117	6.903	13.117	15.864	19.136
24	5.389	4.029	2.855	2.349	1.833	4.083	6.897	12.996	15.631	19.112
25	5.409	4.029	2.884	2.379	1.837	4.043	6.853	12.951	15.528	18.943
26	5.469	4.043	2.915	2.388	1.846	4.043	6.755	12.948	15.459	18.928
27	5.499	4.061	2.952	2.415	1.849	4.038	6.859	12.943	15.320	18.911
28	5.529	4.080	2.984	2.452	1.852	4.038	6.835	12.939	15.310	18.862
29	5.544	4.099	3.021	2.479	1.894	4.031	6.821	12.938	15.302	18.842
30	5.571	4.108	3.066	2.510	1.901	4.026	6.802	12.936	15.299	18.797
31	5.592	4.121	3.111	2.521	1.913	3.941	6.798	12.936	15.295	18.752
32	5.625	4.152	3.161	2.535	1.932	3.937	6.789	12.936	15.275	18.747
33	5.669	4.185	3.194	2.548	1.968	3.909	6.758	12.902	15.265	18.678
34	5.680	4.219	3.201	2.555	1.986	3.898	6.732	12.854	15.245	18.606
35	5.690	4.242	3.215	2.588	2.005	3.872	6.712	12.754	15.210	18.559
36	5.721	4.286	3.234	2.597	2.035	3.864	6.702	12.722	15.199	18.557
37	5.751	4.313	3.242	2.602	2.118	3.854	6.685	12.685	15.175	18.538
38	5.781	4.359	3.275	2.608	2.141	3.840	6.657	12.654	15.149	18.504
39	5.801	4.398	3.297	2.619	2.175	3.795	6.621	12.632	15.102	18.431
40	5.831	4.439	3.315	2.635	2.199	3.787	6.598	12.596	15.052	18.359

Table G-5: Shear modulus and damping ration values of M @ 275 kPa

Strain (%)	0.01	0.1	1	2.5	5	0.01	0.1	1	2.5	5
Cycle No.	Shear Modulus, G (MPa)					Damping Ratio, ξ (%)				
1	9.662	8.269	6.613	4.875	4.740	3.784	6.353	11.025	13.852	17.201
2	9.675	8.288	6.644	4.959	4.751	3.546	6.013	10.578	13.763	16.855
3	9.685	8.328	6.654	4.975	4.752	3.445	5.896	10.209	13.685	16.450
4	9.690	8.370	6.669	4.986	4.762	3.402	5.685	10.066	13.609	16.105
5	9.711	8.402	6.672	5.051	4.764	3.316	5.573	9.851	13.467	15.978
6	9.721	8.431	6.686	5.102	4.775	3.283	5.559	9.760	13.461	15.896
7	9.724	8.469	6.703	5.186	4.779	3.270	5.536	9.694	13.448	15.852
8	9.742	8.499	6.755	5.215	4.787	3.243	5.521	9.653	13.435	15.801
9	9.752	8.521	6.859	5.285	4.794	3.209	5.502	9.639	13.363	15.755
10	9.783	8.559	6.910	5.302	4.801	3.196	5.488	9.637	13.294	15.702
11	9.803	8.589	6.955	5.355	4.807	3.130	5.458	9.510	13.241	15.690
12	9.851	8.609	6.973	5.424	4.847	3.129	5.396	9.456	13.164	15.624
13	9.922	8.639	7.036	5.466	4.860	3.117	5.363	9.379	13.099	15.521
14	9.984	8.679	7.104	5.486	4.866	3.045	5.299	9.296	13.039	15.422
15	10.089	8.692	7.154	5.513	4.878	2.902	5.290	9.238	12.925	15.375
16	10.118	8.719	7.174	5.549	4.881	2.901	5.255	9.212	12.841	15.286
17	10.138	8.749	7.225	5.586	4.885	2.862	4.999	9.195	12.759	15.201
18	10.150	8.779	7.270	5.602	4.889	2.845	4.946	9.190	12.674	15.199
19	10.188	8.799	7.315	5.635	4.891	2.801	4.895	9.109	12.608	15.102
20	10.202	8.802	7.366	5.656	4.892	2.689	4.749	9.051	12.524	15.033
21	10.224	8.869	7.405	5.669	4.906	2.673	4.733	8.985	12.516	15.012
22	10.254	8.904	7.449	5.685	4.918	2.632	4.722	8.939	12.374	14.936
23	10.279	8.934	7.498	5.686	4.931	2.617	4.713	8.812	12.333	14.843
24	10.288	8.955	7.530	5.725	4.939	2.575	4.699	8.783	12.205	14.693
25	10.302	8.957	7.582	5.746	4.947	2.540	4.685	8.659	12.186	14.609
26	10.323	8.960	7.638	5.763	4.959	2.528	4.675	8.656	12.143	14.532
27	10.343	8.960	7.678	5.785	4.977	2.446	4.658	8.573	12.077	14.490
28	10.372	8.963	7.695	5.795	5.008	2.431	4.636	8.542	12.040	14.440
29	10.382	8.967	7.701	5.805	5.015	2.414	4.625	8.472	12.034	14.379
30	10.407	8.977	7.710	5.838	5.030	2.369	4.619	8.463	11.975	14.319
31	10.420	8.985	7.735	5.855	5.041	2.322	4.603	8.397	11.742	14.248
32	10.469	8.993	7.765	5.875	5.061	2.315	4.568	8.305	11.640	14.173
33	10.490	9.048	7.783	5.887	5.077	2.311	4.547	8.174	11.630	14.098
34	10.528	9.077	7.786	5.918	5.100	2.276	4.498	8.093	11.568	13.938
35	10.550	9.081	7.812	5.936	5.102	2.269	4.477	8.066	11.553	13.880
36	10.596	9.109	7.833	5.966	5.117	2.188	4.475	7.995	11.542	13.785
37	10.607	9.165	7.866	5.975	5.126	2.137	4.305	7.962	11.502	13.702
38	10.644	9.215	7.896	5.985	5.142	2.112	4.259	7.798	11.270	13.690
39	10.662	9.269	7.901	6.014	5.156	2.097	4.102	7.754	11.138	13.658
40	10.696	9.305	7.923	6.046	5.158	2.006	3.931	7.726	11.138	13.544

Table G-6: Shear modulus and damping ration values of M @ 400 kPa

Strain (%)	0.01	0.1	1	2.5	5	0.01	0.1	1	2.5	5
Cycle No.	Shear Modulus, G (MPa)					Damping Ratio, ξ (%)				
1	13.311	12.306	10.096	9.274	8.875	1.440	2.291	7.826	9.726	12.246
2	13.352	12.340	10.143	9.310	8.909	1.437	2.240	7.356	9.416	12.043
3	13.369	12.351	10.199	9.380	8.968	1.343	2.198	7.013	9.265	11.819
4	13.415	12.415	10.240	9.419	8.985	1.218	2.150	6.875	9.020	11.582
5	13.428	12.481	10.355	9.440	9.007	1.201	2.090	6.575	8.937	11.348
6	13.441	12.545	10.403	9.512	9.071	1.169	1.973	6.548	8.752	11.160
7	13.494	12.598	10.486	9.561	9.121	1.111	1.870	6.501	8.608	10.877
8	13.539	12.642	10.578	9.578	9.131	0.926	1.802	6.499	8.534	10.694
9	13.544	12.677	10.642	9.686	9.140	0.905	1.777	6.484	8.492	10.411
10	13.612	12.704	10.655	9.712	9.175	0.879	1.728	6.344	8.483	10.239
11	13.629	12.738	10.710	9.733	9.201	0.876	1.724	6.209	8.467	10.184
12	13.648	12.769	10.733	9.751	9.253	0.772	1.695	6.050	8.355	10.099
13	13.665	12.786	10.755	9.771	9.255	0.763	1.680	6.043	8.321	10.041
14	13.683	12.795	10.786	9.802	9.265	0.728	1.659	5.970	8.294	9.846
15	13.737	12.803	10.813	9.814	9.285	0.692	1.594	5.960	8.288	9.791
16	13.822	12.806	10.843	9.845	9.306	0.665	1.565	5.835	8.222	9.680
17	13.829	12.816	10.876	9.847	9.309	0.649	1.526	5.761	8.076	9.657
18	13.840	12.846	10.912	9.855	9.311	0.646	1.509	5.727	7.882	9.617
19	13.868	12.847	10.957	9.859	9.314	0.631	1.497	5.705	7.852	9.591
20	13.919	12.851	11.106	9.861	9.324	0.632	1.429	5.624	7.809	9.470
21	14.074	12.867	11.152	9.897	9.353	0.625	1.397	5.621	7.774	9.442
22	14.141	12.879	11.178	9.917	9.385	0.616	1.385	5.566	7.612	9.419
23	14.192	12.910	11.205	9.938	9.401	0.614	1.314	5.550	7.500	9.343
24	14.241	12.929	11.275	9.958	9.419	0.616	1.308	5.483	7.417	9.341
25	14.285	12.933	11.295	9.980	9.454	0.616	1.301	5.397	7.391	9.223
26	14.309	12.951	11.302	10.024	9.486	0.613	1.266	5.329	7.172	9.221
27	14.380	13.003	11.346	10.047	9.508	0.612	1.265	5.249	7.087	9.156
28	14.380	13.017	11.378	10.080	9.531	0.611	1.218	5.198	7.021	9.150
29	14.381	13.034	11.395	10.102	9.564	0.610	1.156	4.982	6.901	9.131
30	14.385	13.063	11.413	10.137	9.587	0.602	1.134	4.872	6.852	9.130
31	14.399	13.067	11.436	10.166	9.597	0.598	1.056	4.680	6.785	9.128
32	14.401	13.091	11.473	10.175	9.601	0.599	1.046	4.568	6.702	9.085
33	14.426	13.104	11.496	10.199	9.625	0.593	1.045	4.547	6.698	9.021
34	14.449	13.110	11.501	10.238	9.649	0.584	1.003	4.498	6.675	9.019
35	14.499	13.185	11.549	10.266	9.673	0.579	1.002	4.477	6.621	8.952
36	14.518	13.233	11.562	10.285	9.695	0.566	0.977	4.475	6.590	8.943
37	14.536	13.246	11.575	10.301	9.701	0.536	0.922	4.475	6.533	8.888
38	14.551	13.338	11.603	10.347	9.725	0.451	0.910	4.459	6.521	8.875
39	14.561	13.395	11.613	10.366	9.749	0.438	0.877	4.453	6.499	8.863
40	14.578	13.424	11.621	10.388	9.761	0.345	0.858	4.400	6.479	8.696

Table G-7: Shear modulus and damping ration values of P @ 150 kPa

Strain (%)	0.01	0.1	1	2.5	5	0.01	0.1	1	2.5	5
Cycle No.	Shear Modulus, G (MPa)					Damping Ratio, ξ (%)				
1	7.630	5.190	2.761	1.987	1.777	3.159	6.943	12.465	15.610	18.913
2	7.675	5.203	2.865	1.996	1.787	3.024	6.587	12.286	15.528	18.512
3	7.696	5.207	2.914	1.998	1.794	2.976	6.306	12.059	15.488	17.663
4	7.702	5.231	2.972	2.013	1.799	2.927	6.267	11.822	15.285	17.286
5	7.733	5.223	2.993	2.023	1.802	2.804	6.184	11.625	15.039	16.929
6	7.750	5.239	3.002	2.040	1.810	2.778	6.172	11.601	14.860	16.711
7	7.771	5.246	3.018	2.044	1.817	2.696	6.167	11.590	14.658	16.686
8	7.788	5.258	3.028	2.062	1.821	2.685	6.105	11.570	14.547	16.582
9	7.850	5.263	3.038	2.067	1.825	2.653	6.072	11.537	14.326	16.511
10	7.866	5.266	3.085	2.098	1.839	2.539	5.953	11.493	14.103	16.500
11	7.898	5.292	3.089	2.150	1.857	2.526	5.891	11.459	14.013	16.383
12	7.950	5.314	3.125	2.171	1.858	2.467	5.861	11.401	13.999	16.366
13	7.989	5.337	3.176	2.204	1.862	2.452	5.816	11.360	13.975	16.331
14	8.039	5.357	3.201	2.246	1.873	2.405	5.801	11.334	13.952	16.327
15	8.093	5.384	3.178	2.286	1.898	2.399	5.765	11.301	13.943	16.317
16	8.149	5.424	3.223	2.321	1.911	2.393	5.730	11.285	13.926	16.309
17	8.178	5.484	3.268	2.369	1.930	2.386	5.715	11.219	13.913	16.225
18	8.209	5.514	3.309	2.398	1.940	2.375	5.696	11.186	13.902	16.199
19	8.250	5.565	3.359	2.433	1.980	2.347	5.664	11.102	13.899	16.185
20	8.271	5.598	3.400	2.474	1.981	2.338	5.629	11.021	13.894	16.132
21	8.319	5.604	3.422	2.486	2.012	2.338	5.626	10.986	13.894	16.109
22	8.358	5.624	3.472	2.493	2.036	2.328	5.618	10.925	13.893	16.064
23	8.427	5.638	3.515	2.513	2.063	2.327	5.600	10.902	13.891	16.062
24	8.450	5.657	3.542	2.533	2.107	2.317	5.596	10.839	13.889	16.028
25	8.550	5.662	3.544	2.607	2.136	2.315	5.575	10.784	13.753	15.933
26	8.659	5.685	3.556	2.652	2.158	2.299	5.556	10.715	13.698	15.903
27	8.689	5.696	3.570	2.724	2.172	2.291	5.538	10.695	13.653	15.872
28	8.721	5.716	3.580	2.768	2.206	2.287	5.485	10.680	13.625	15.866
29	8.749	5.719	3.599	2.785	2.239	2.285	5.485	10.639	13.578	15.741
30	8.763	5.737	3.608	2.806	2.306	2.284	5.462	10.609	13.549	15.690
31	8.785	5.739	3.626	2.856	2.350	2.238	5.444	10.592	13.524	15.564
32	8.809	5.740	3.657	2.897	2.405	2.171	5.425	10.577	13.501	15.459
33	8.816	5.750	3.706	2.947	2.438	2.161	5.408	10.560	13.486	15.381
34	8.837	5.783	3.758	2.968	2.466	2.148	5.297	10.532	13.390	15.311
35	8.857	5.816	3.797	2.971	2.542	2.137	5.295	10.531	13.355	15.251
36	8.863	5.877	3.830	2.980	2.596	2.110	5.279	10.507	13.313	15.192
37	8.877	5.924	3.850	3.015	2.628	2.094	5.262	10.485	13.278	15.140
38	8.906	5.935	3.880	3.032	2.680	2.074	5.243	10.458	13.249	14.928
39	8.926	5.965	3.903	3.055	2.751	2.074	5.175	10.425	13.192	14.920
40	8.953	6.022	4.033	3.061	2.833	2.071	5.128	10.412	13.173	14.829

Table G-8: Shear modulus and damping ration values of P @ 275 kPa

Strain (%)	0.01	0.1	1	2.5	5	0.01	0.1	1	2.5	5
Cycle No.	Shear Modulus, G (MPa)					Damping Ratio, ξ (%)				
1	12.655	9.652	7.195	5.395	4.740	2.549	4.952	8.754	10.427	13.388
2	12.705	9.696	7.218	5.484	4.751	2.214	4.535	8.496	10.358	13.235
3	12.768	9.873	7.339	5.570	4.752	1.848	4.391	8.252	10.209	13.185
4	12.790	9.935	7.343	5.613	4.762	1.725	4.258	8.022	10.066	13.015
5	12.812	10.059	7.418	5.684	4.764	1.642	4.225	7.732	9.851	12.732
6	12.854	10.125	7.564	5.718	4.775	1.586	4.221	7.695	9.760	12.517
7	12.875	10.176	7.709	5.756	4.779	1.583	4.218	7.612	9.694	12.467
8	12.895	10.199	7.726	5.730	4.787	1.554	4.209	7.548	9.653	12.416
9	12.901	10.205	7.747	5.731	4.794	1.534	4.202	7.479	9.639	12.356
10	12.908	10.234	7.864	5.753	4.801	1.533	4.197	7.413	9.637	12.236
11	12.914	10.368	7.891	5.763	4.807	1.532	4.185	7.383	9.510	12.176
12	13.026	10.422	7.914	5.781	4.847	1.530	4.171	7.359	9.456	12.125
13	13.125	10.425	7.955	5.790	4.860	1.527	4.168	7.286	9.379	11.957
14	13.205	10.426	7.978	5.802	4.866	1.523	4.157	7.215	9.314	11.754
15	13.255	10.439	8.000	5.821	4.878	1.520	4.125	7.185	9.258	11.699
16	13.276	10.568	8.023	5.836	4.813	1.519	4.022	7.125	9.215	11.652
17	13.295	10.732	8.084	5.851	4.824	1.517	3.951	7.085	9.195	11.575
18	13.303	10.766	8.113	5.837	4.828	1.514	3.916	7.013	9.190	11.505
19	13.320	10.901	8.125	5.894	4.841	1.501	3.884	6.995	9.109	11.465
20	13.388	10.969	8.245	5.863	4.892	1.499	3.871	6.949	9.051	11.374
21	13.503	11.006	8.325	5.870	4.906	1.478	3.747	6.912	8.985	11.304
22	13.552	11.059	8.348	5.794	4.918	1.401	3.758	6.857	8.939	11.251
23	13.594	11.085	8.381	5.858	4.931	1.415	3.802	6.824	8.812	11.242
24	13.624	11.244	8.491	5.879	4.989	1.380	3.794	6.785	8.783	11.237
25	13.655	11.274	8.498	5.887	4.947	1.371	3.777	6.712	8.659	11.224
26	13.685	11.372	8.566	5.880	4.959	1.345	3.727	6.697	8.656	11.201
27	13.699	11.449	8.681	5.901	4.977	1.304	3.701	6.665	8.573	11.172
28	13.715	11.547	8.721	5.929	5.008	1.296	3.691	6.621	8.542	11.113
29	13.749	11.713	9.032	5.985	5.015	1.276	3.685	6.599	8.472	11.104
30	13.758	11.807	9.054	5.980	5.030	1.244	3.681	6.533	8.463	11.029
31	13.775	11.815	9.095	6.141	5.041	1.244	3.675	6.473	8.397	10.916
32	13.799	11.820	9.208	6.143	5.061	1.241	3.652	6.451	8.305	10.767
33	13.814	11.835	9.254	6.159	5.077	1.236	3.622	6.385	8.174	10.602
34	13.833	11.872	9.261	6.270	5.100	1.235	3.602	6.302	8.093	10.576
35	13.855	11.910	9.399	6.272	5.102	1.212	3.599	6.285	8.066	10.521
36	13.875	11.946	9.625	6.318	5.117	1.209	3.586	6.249	7.995	10.457
37	13.895	11.967	9.667	6.334	5.126	1.206	3.533	6.175	7.962	10.358
38	13.915	11.983	9.683	6.363	5.142	1.203	3.516	6.143	7.798	10.314
39	13.921	12.025	9.714	6.450	5.156	1.180	3.468	6.085	7.754	10.285
40	13.933	12.039	9.780	6.607	5.158	1.178	3.436	6.022	7.726	10.205

Table G-9: Shear modulus and damping ration values of P @ 400 kPa

Strain (%)	0.01	0.1	1	2.5	5	0.01	0.1	1	2.5	5
Cycle No.	Shear Modulus, G (MPa)					Damping Ratio, ξ (%)				
1	14.633	13.062	10.878	9.490	8.955	0.632	2.315	4.580	6.450	8.579
2	14.759	13.131	10.891	9.515	9.063	0.603	2.280	4.535	6.218	8.508
3	14.875	13.283	10.922	9.536	9.098	0.589	2.237	4.391	6.148	8.437
4	14.985	13.330	10.971	9.539	9.102	0.583	2.178	4.258	6.006	8.380
5	15.070	13.423	11.023	9.541	9.133	0.580	2.119	4.225	5.996	8.253
6	15.143	13.432	11.106	9.546	9.168	0.507	2.069	4.224	5.962	8.219
7	15.175	13.438	11.151	9.568	9.187	0.492	2.025	4.223	5.915	8.181
8	15.198	13.451	11.209	9.587	9.192	0.497	1.999	4.220	5.872	8.151
9	15.205	13.453	11.274	9.616	9.202	0.487	1.986	4.217	5.822	8.110
10	15.214	13.453	11.325	9.649	9.274	0.481	1.975	4.213	5.784	7.982
11	15.249	13.464	11.389	9.669	9.275	0.410	1.966	4.205	5.725	7.860
12	15.275	13.481	11.436	9.689	9.299	0.404	1.952	4.201	5.654	7.769
13	15.301	13.527	11.486	9.706	9.314	0.400	1.942	4.175	5.584	7.644
14	15.325	13.579	11.527	9.747	9.348	0.385	1.938	4.123	5.544	7.579
15	15.349	13.620	11.576	9.762	9.350	0.349	1.925	4.075	5.513	7.453
16	15.359	13.674	11.638	9.796	9.357	0.312	1.910	4.015	5.463	7.324
17	15.378	13.717	11.730	9.812	9.358	0.294	1.895	3.951	5.428	7.248
18	15.402	13.770	11.800	9.833	9.360	0.299	1.880	3.916	5.372	7.136
19	15.468	13.809	11.951	9.848	9.361	0.288	1.880	3.884	5.244	7.038
20	15.494	13.851	12.063	9.855	9.364	0.289	1.872	3.871	5.096	6.987
21	15.494	13.880	12.109	9.859	9.415	0.282	1.849	3.845	4.997	6.923
22	15.548	13.909	12.138	9.902	9.455	0.273	1.809	3.828	4.966	6.877
23	15.575	13.927	12.158	9.941	9.493	0.271	1.763	3.802	4.934	6.836
24	15.690	13.935	12.304	9.956	9.524	0.273	1.706	3.794	4.909	6.822
25	15.701	13.956	12.338	9.979	9.570	0.273	1.646	3.777	4.845	6.782
26	15.715	13.959	12.383	9.996	9.591	0.270	1.585	3.727	4.821	6.726
27	15.733	13.961	12.408	10.063	9.626	0.269	1.505	3.701	4.813	6.692
28	15.751	13.963	12.441	10.105	9.678	0.268	1.463	3.691	4.657	6.657
29	15.765	13.964	12.474	10.140	9.726	0.267	1.426	3.643	4.563	6.614
30	15.775	13.968	12.509	10.171	9.779	0.259	1.424	3.596	4.563	6.570
31	15.792	13.970	12.545	10.181	9.825	0.255	1.428	3.564	4.496	6.522
32	15.812	13.977	12.594	10.208	9.858	0.256	1.422	3.540	4.479	6.484
33	15.835	14.102	12.608	10.281	9.908	0.250	1.419	3.509	4.469	6.457
34	15.847	14.142	12.618	10.362	9.958	0.241	1.401	3.469	4.458	6.381
35	15.869	14.185	12.628	10.412	10.003	0.236	1.392	3.406	4.432	6.305
36	15.885	14.206	12.630	10.471	10.036	0.223	1.378	3.368	4.420	6.242
37	15.896	14.248	12.633	10.523	10.058	0.193	1.363	3.298	4.413	6.163
38	15.932	14.298	12.647	10.593	10.157	0.185	1.358	3.245	4.402	5.988
39	15.956	14.308	12.648	10.653	10.201	0.175	1.333	3.217	4.395	5.877
40	15.998	14.326	12.650	10.711	10.244	0.146	1.310	3.197	4.376	5.772

B. Influence of number of cycles on shear modulus and damping ratio values

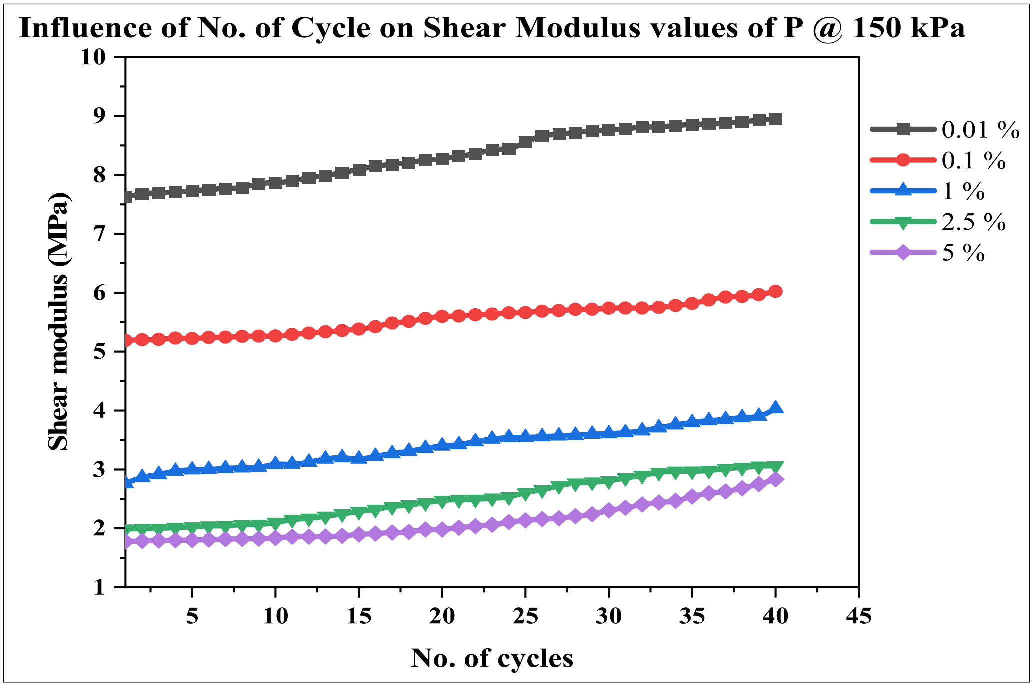

Figure G-1: Influence of number of cycles on shear modulus value of P @ 150 kPa

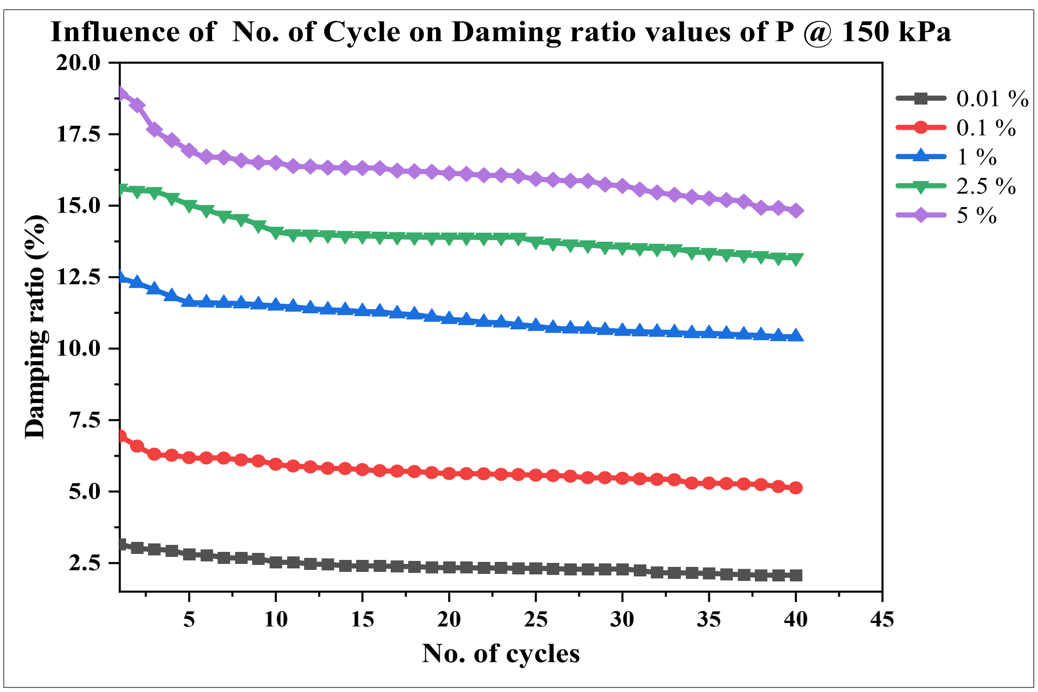

Figure G-2: Influence of number of cycles on damping ratio value of P @ 150 kPa

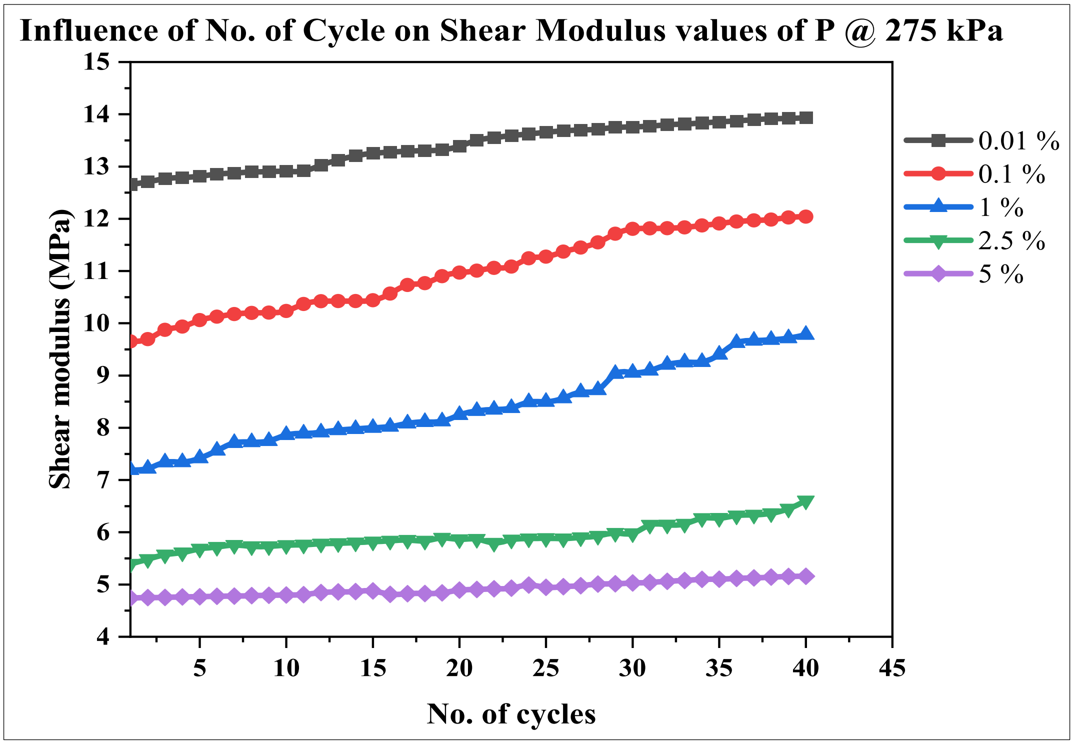

Figure G-3: Influence of number of cycles on shear modulus value of P @ 275 kPa

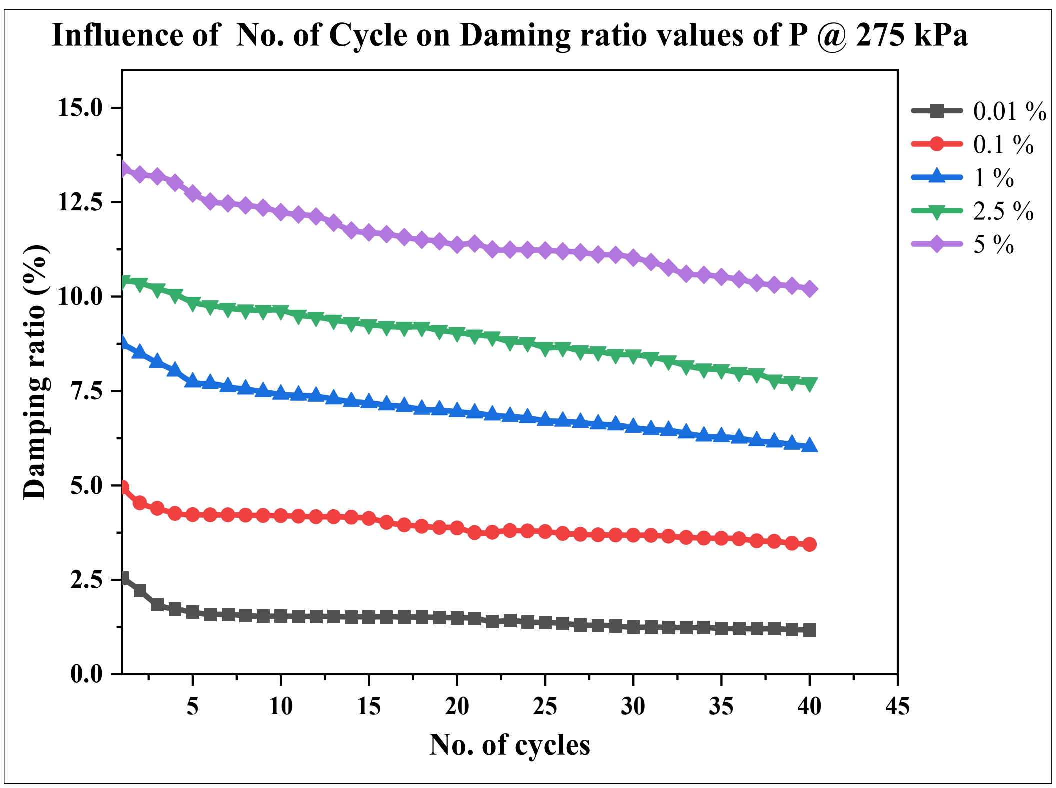

Figure G-4: Influence of number of cycles on damping ratio value of P @ 275 kPa

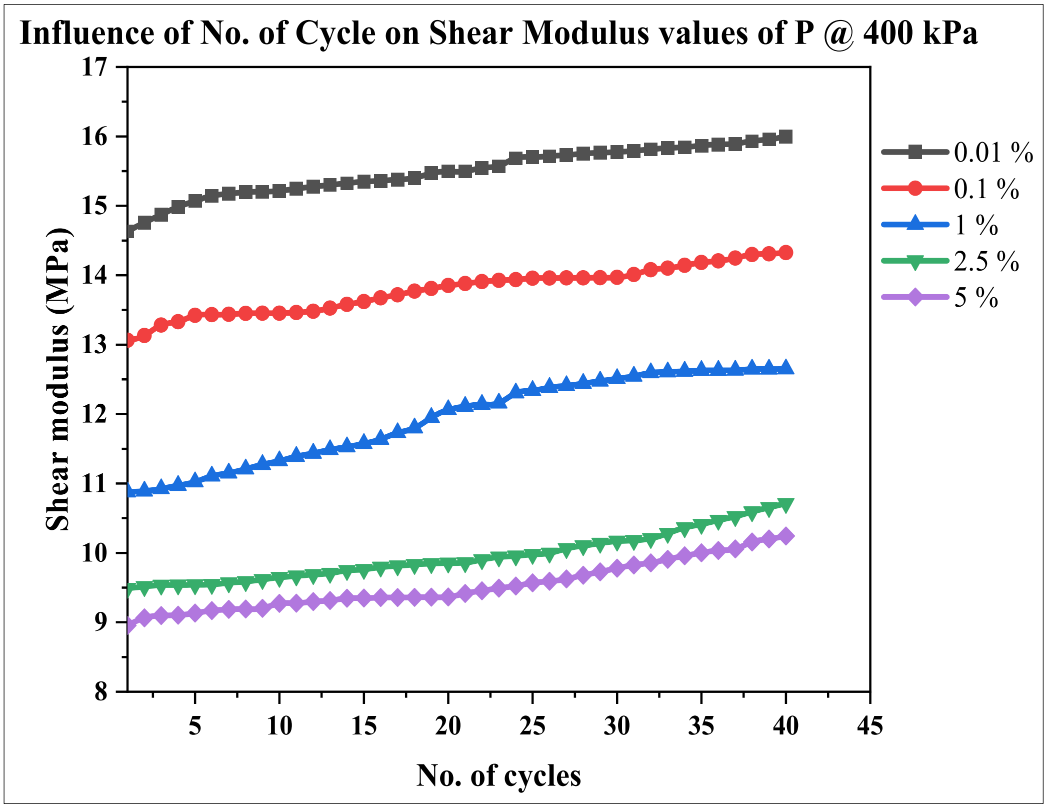

Figure G-5: Influence of number of cycles on shear modulus value of P @ 400 kPa

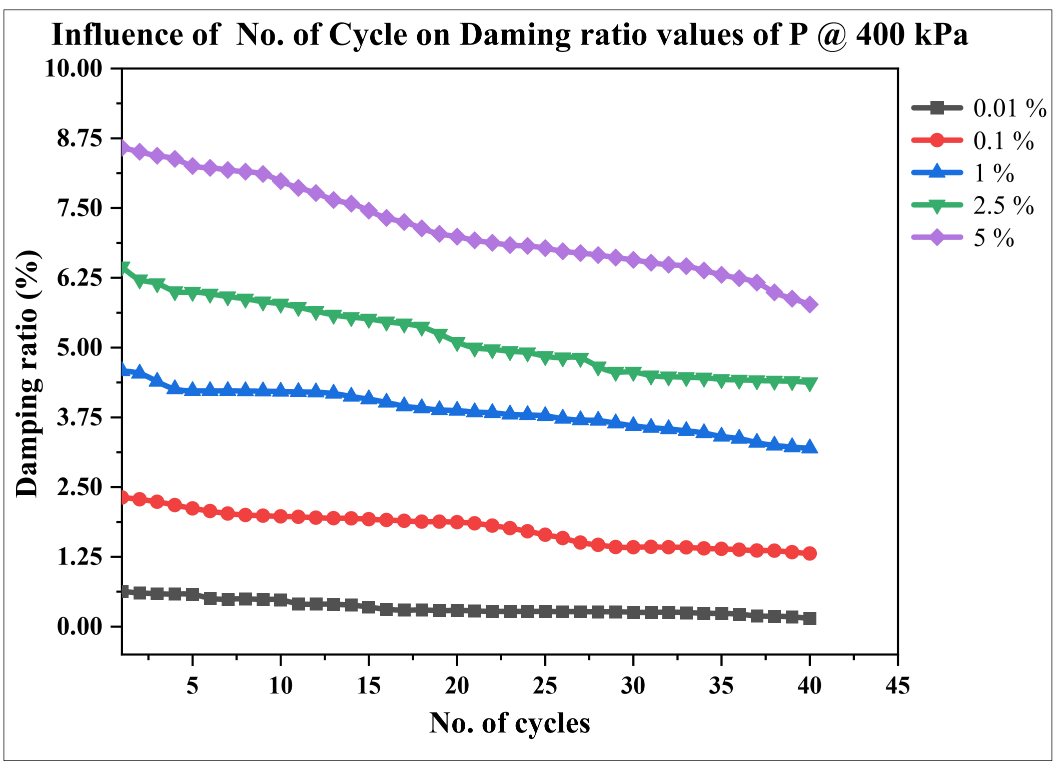

Figure G-6: Influence of number of cycles on damping ratio value of P @ 400 kPa

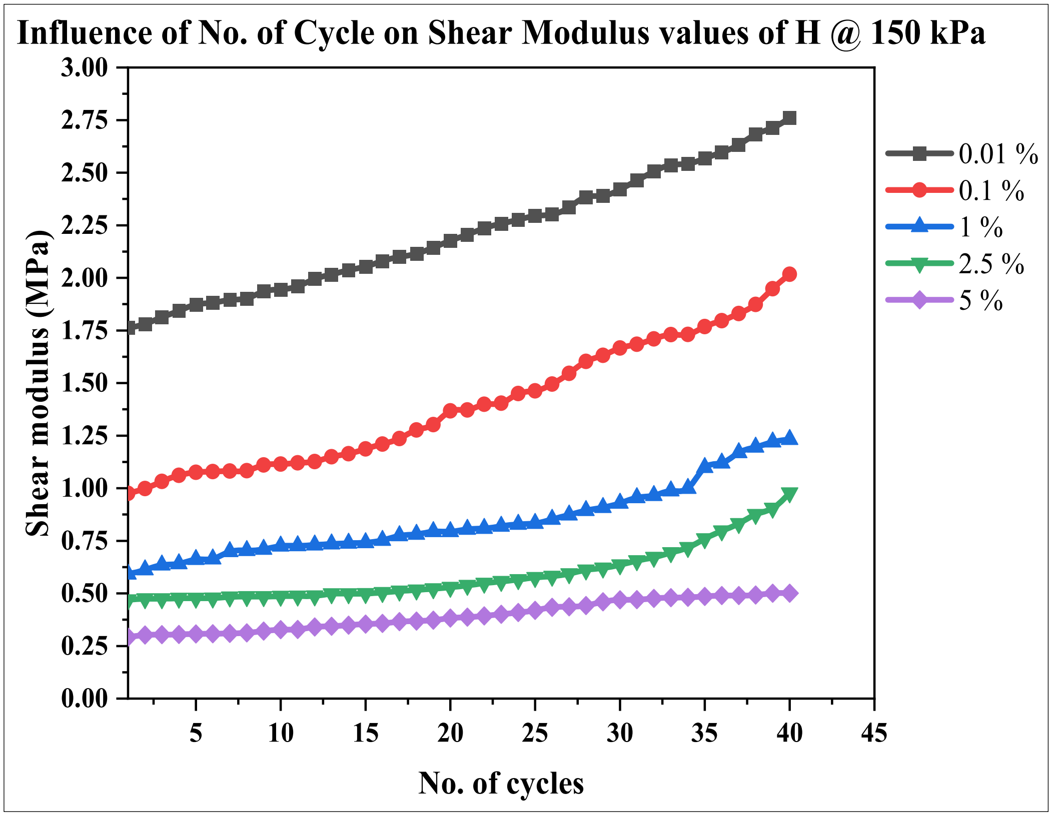

Figure G-7: Influence of number of cycles on shear modulus value of H @ 150 kPa

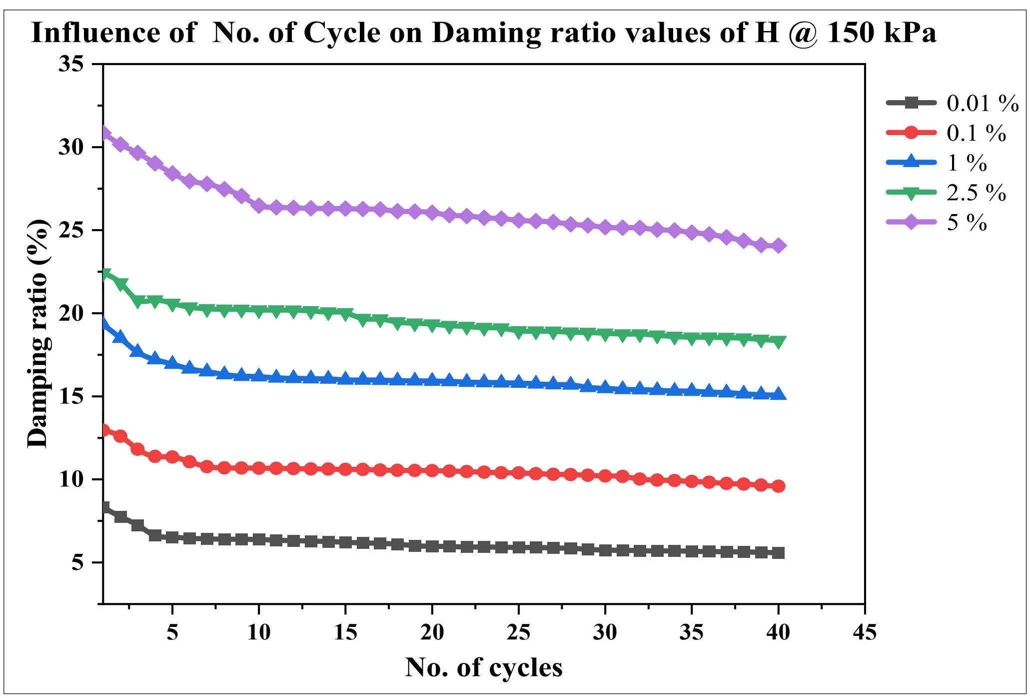

Figure G-8: Influence of number of cycles on damping ratio value of H @ 150 kPa

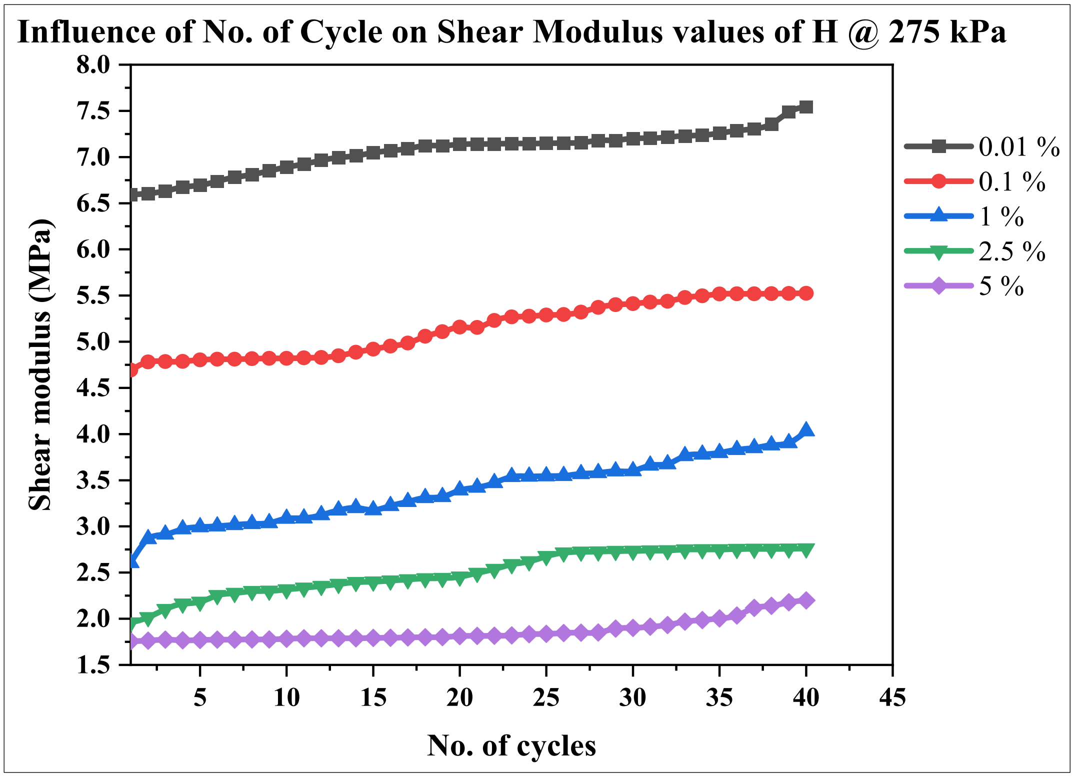

Figure G-9: Influence of number of cycles on shear modulus value of H @ 275 kPa

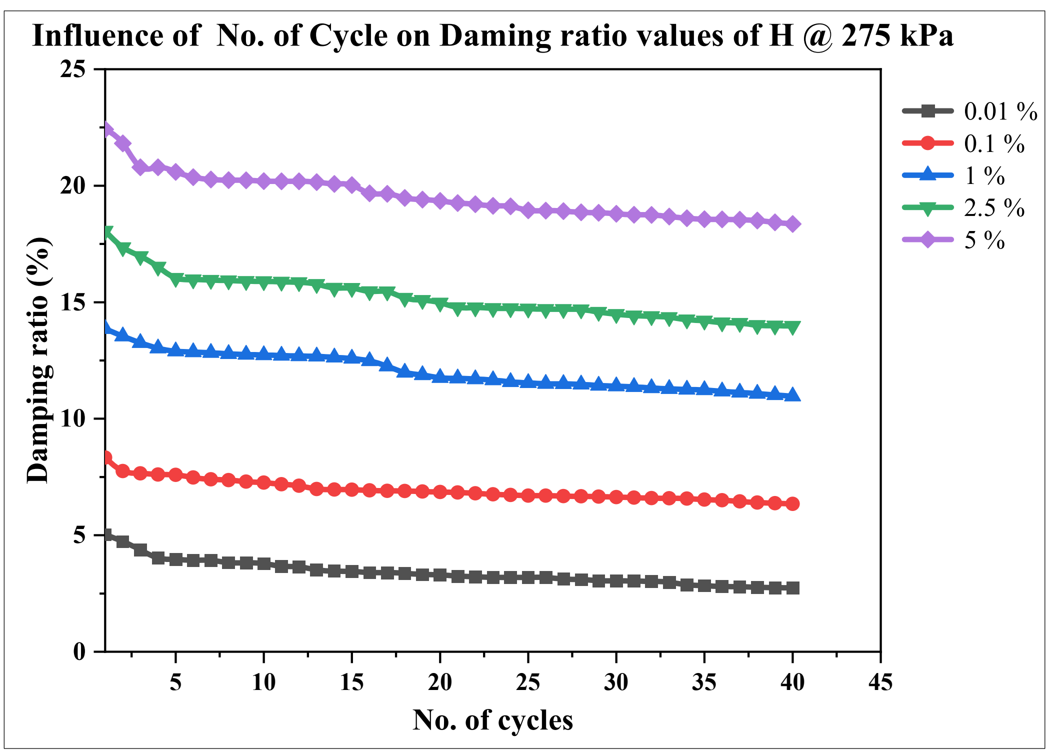

Figure G-10: Influence of number of cycles on damping ratio value of H @ 275 kPa

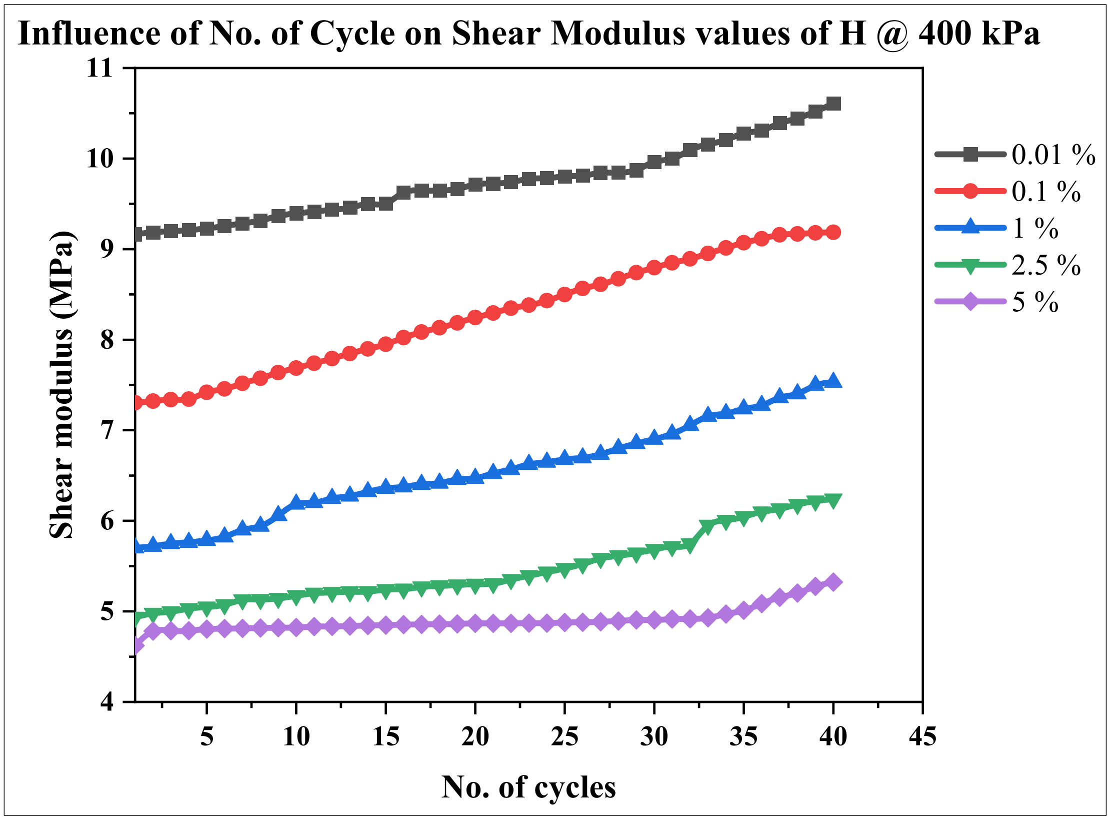

Figure G-11: Influence of number of cycles on shear modulus value of H @ 400 kPa

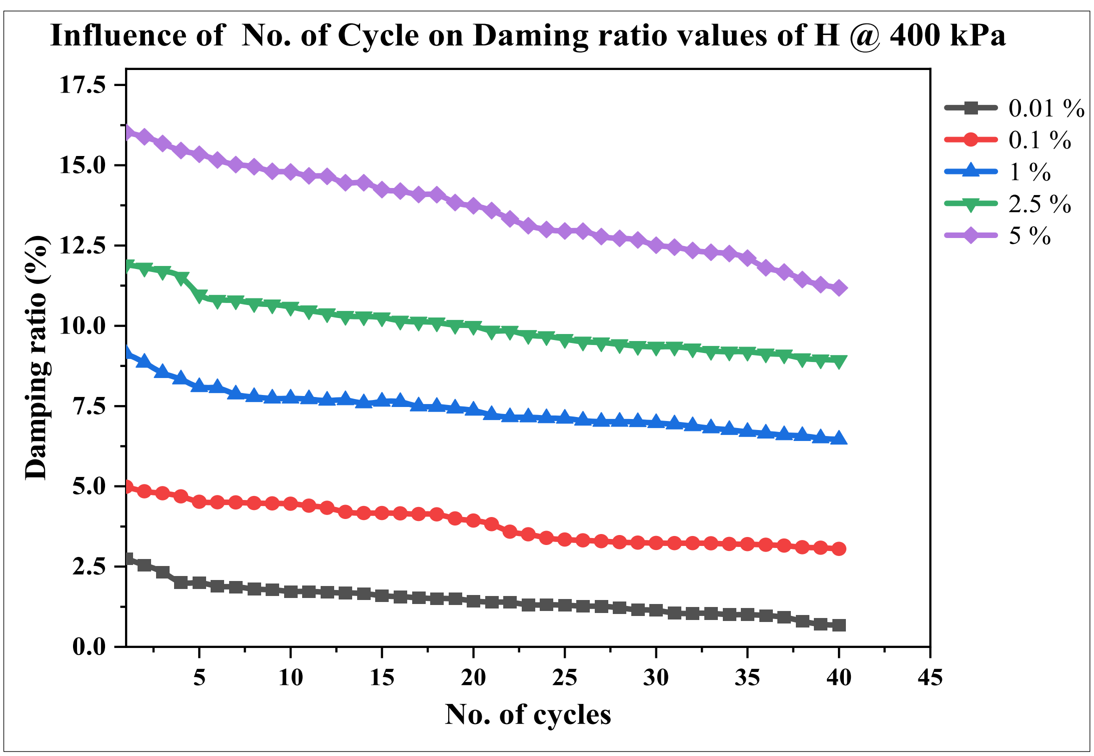

Figure G-12: Influence of number of cycles on damping ratio value of H @ 400 kPa

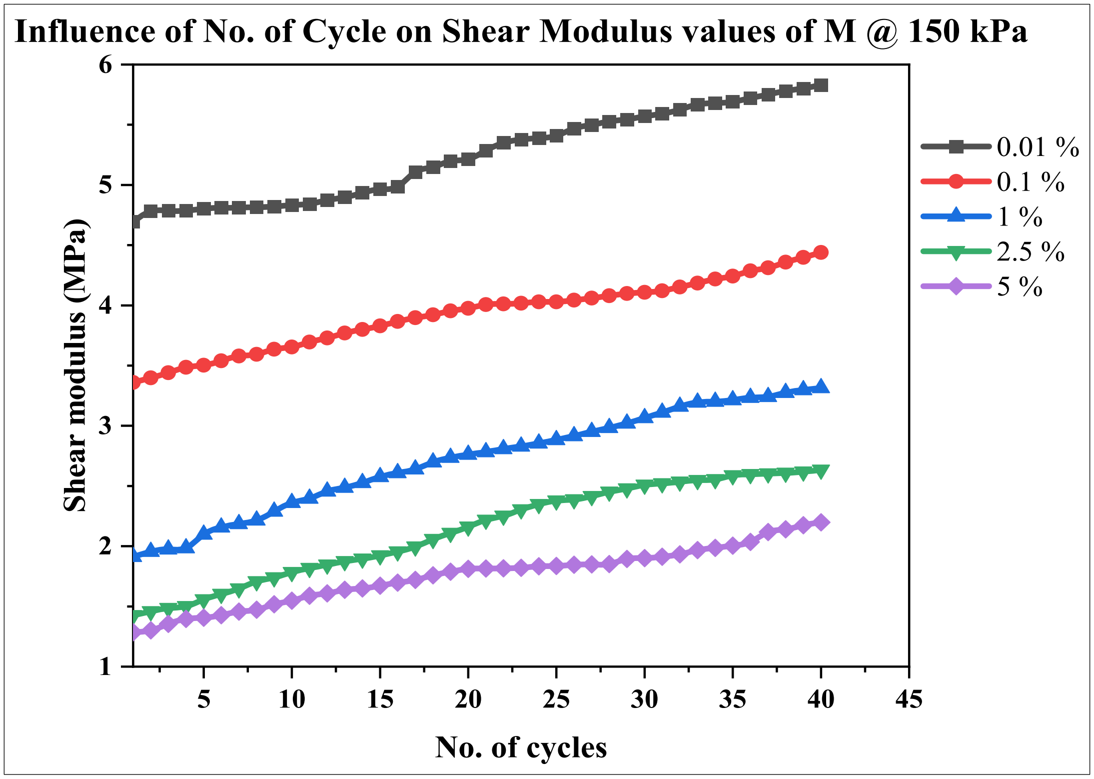

Figure G-13: Influence of number of cycles on shear modulus value of M @ 150 kPa

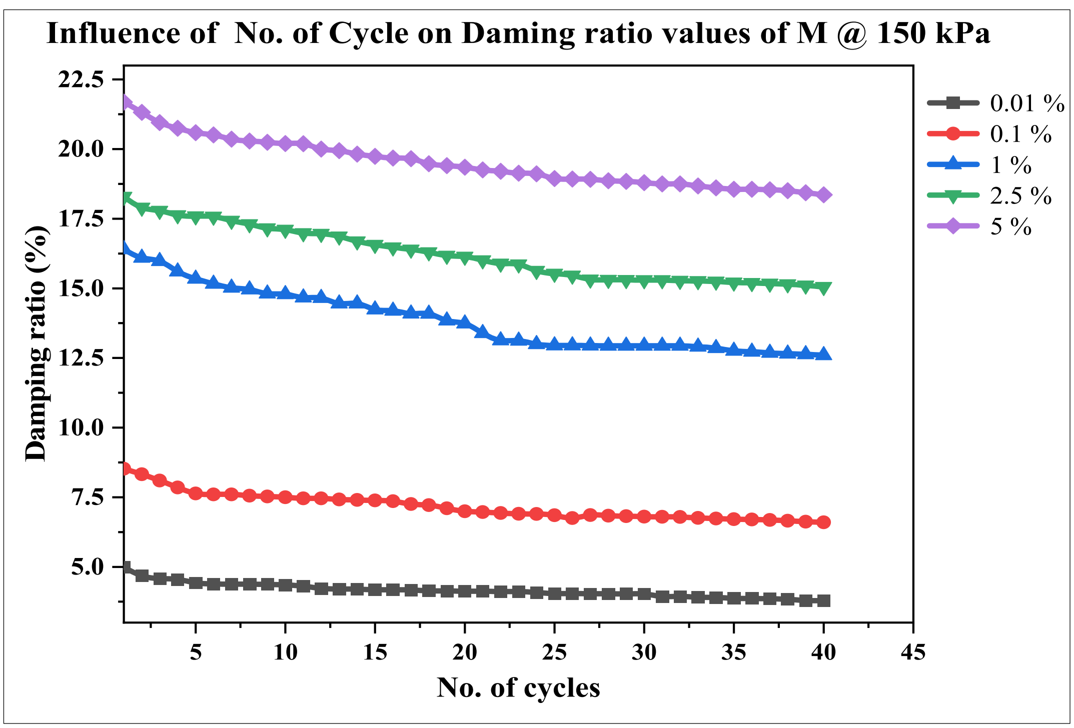

Figure G-14: Influence of number of cycles on damping ratio value of M @ 150 kPa

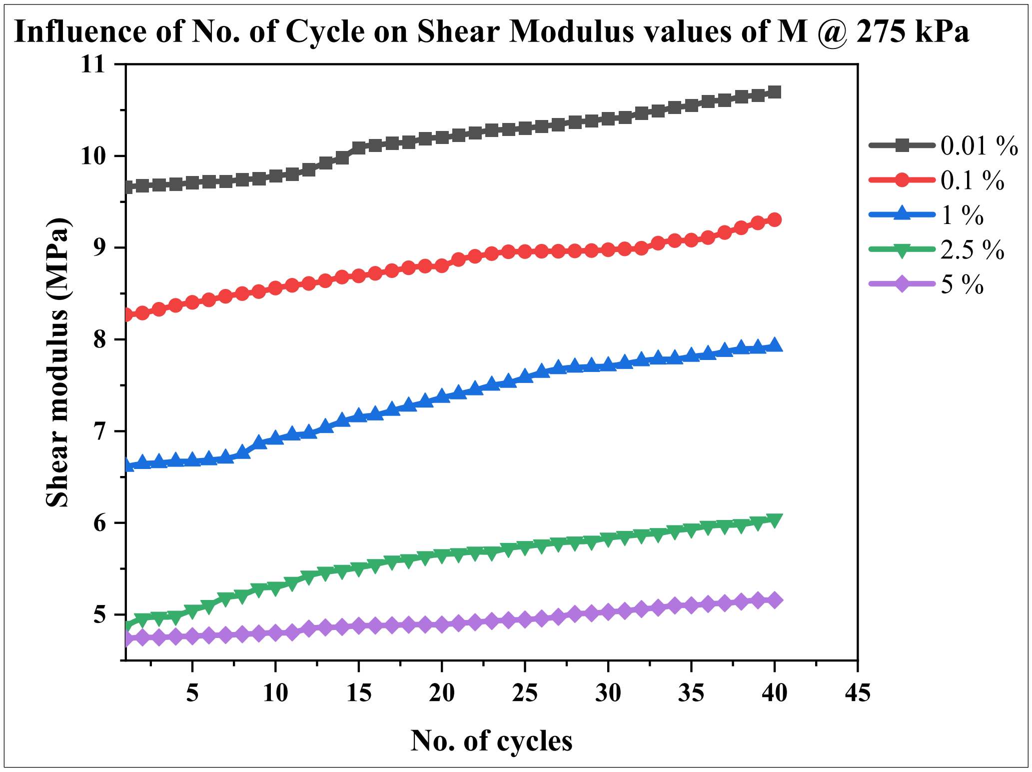

Figure G-15: Influence of number of cycles on shear modulus value of M @ 275 kPa

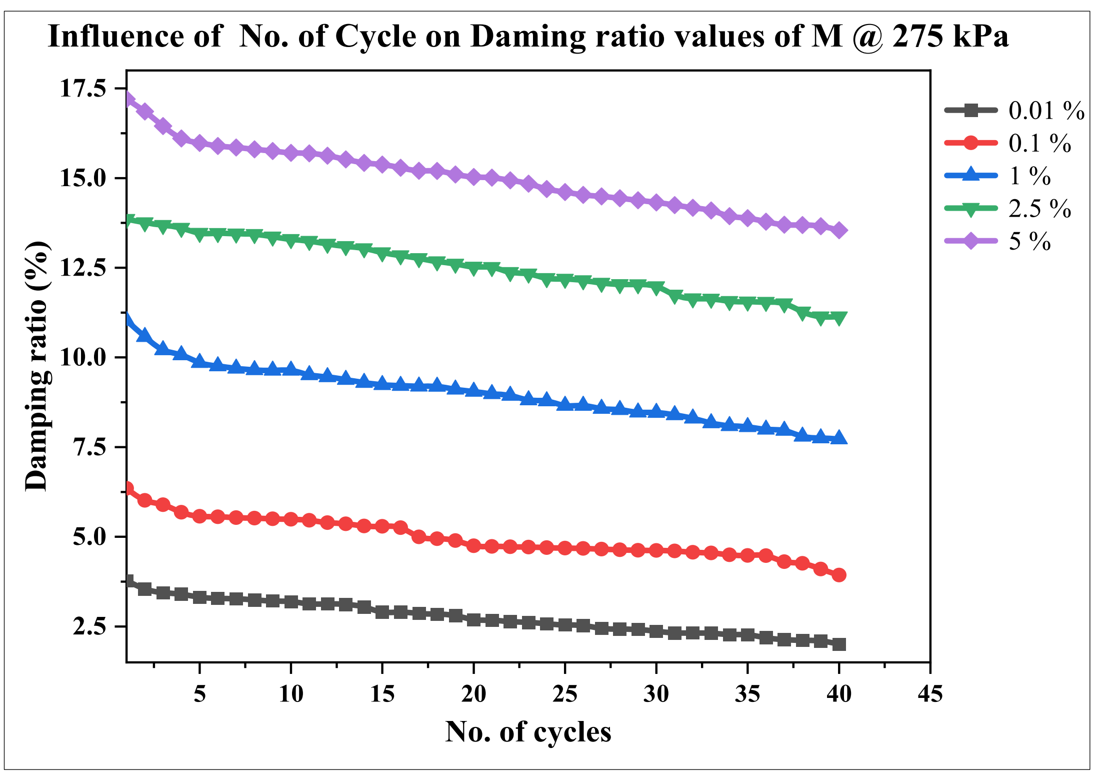

Figure G-16: Influence of number of cycles on damping ratio value of M @ 275 kPa

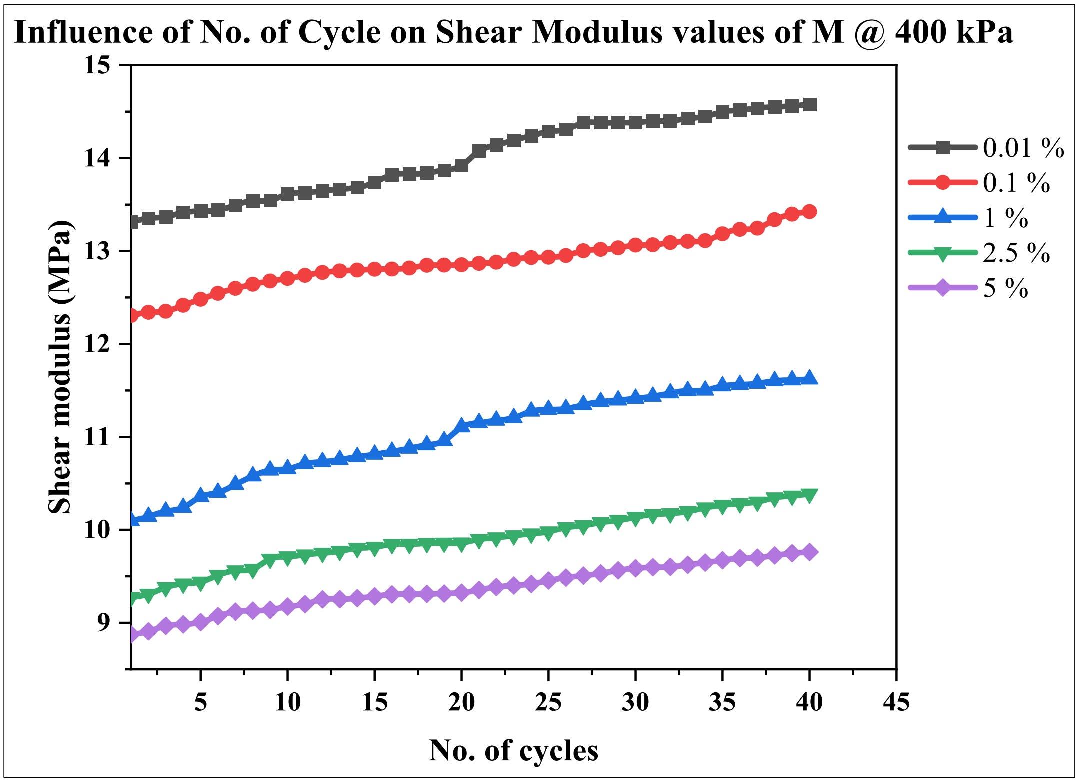

Figure G-17: Influence of number of cycles on shear modulus value of M @ 400 kPa

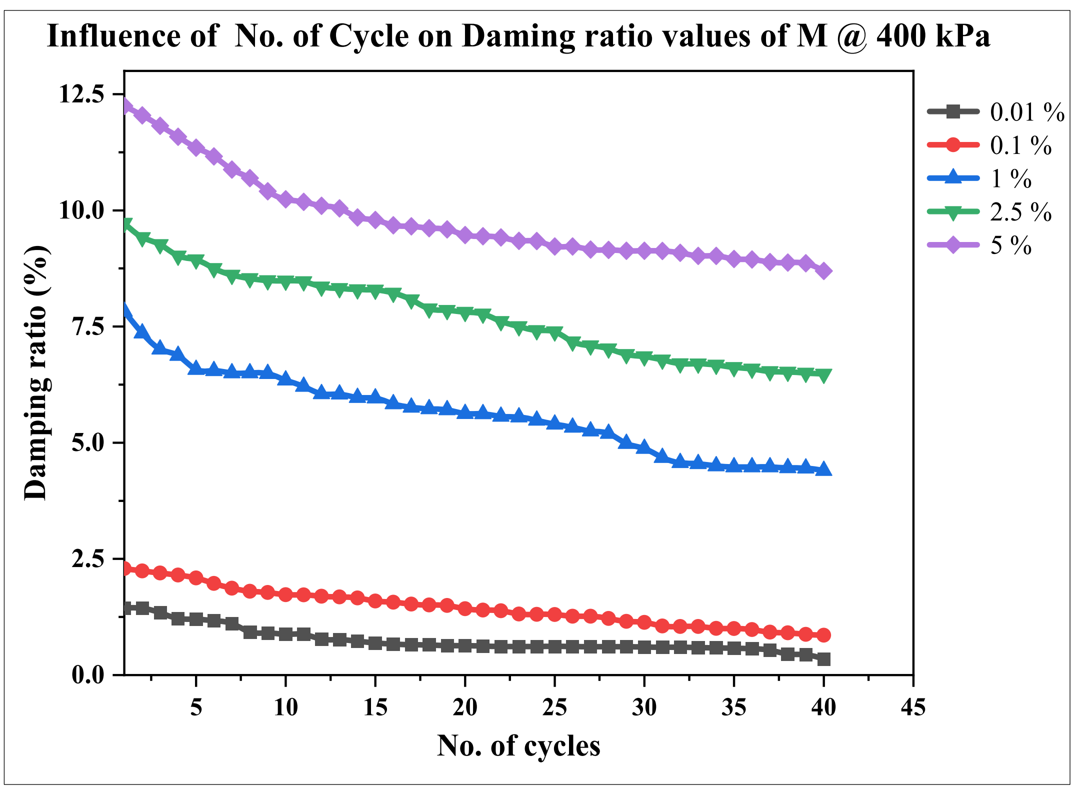

Figure G-18: Influence of number of cycles on damping ratio value of M @ 400 kPa

Appendix - H

Photos Taken During Thesis Work

H.1. Test pits photo

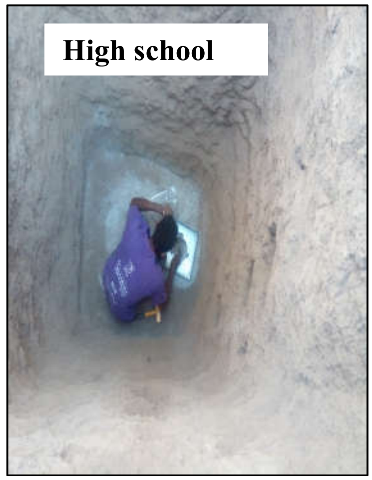

H.2. Field density test

H.3. Sieve analysis (wet)


H.4. Liquied limit



H.5. Plastic limit


H.6. Specific gravity



H.7. Compaction


H.8. 1D – Consolidation



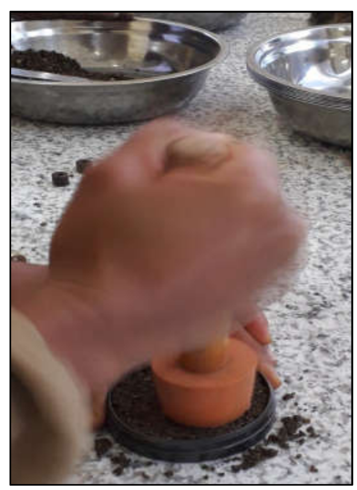

H.9. Cyclic simple shear